

175p



REPORT NO.

NASA-CR-54089

WESTINGHOUSE  
WAED 64.30E

JUNE, 1964

N64-25010

CODE-1 CAT. 17

# RESEARCH AND DEVELOPMENT PROGRAM ON MAGNETIC, ELECTRICAL CONDUCTOR, ELECTRICAL INSULATION, AND BORE SEAL MATERIALS

Third Quarterly Report

by

P. E. Kueser et al

prepared for

NATIONAL AERONAUTICS AND SPACE ADMINISTRATION  
LEWIS RESEARCH CENTER  
UNDER CONTRACT NAS3-4162

OTS PRICE

\$ 12.50 ph

XEROX

MICROFILM \$



**Westinghouse Electric Corporation**  
AEROSPACE ELECTRICAL DIVISION  
LIMA, OHIO

## NOTICE

This report was prepared as an account of Government-sponsored work. Neither the United States nor the National Aeronautics and Space Administration (NASA), nor any person acting on behalf of NASA:

- A) Makes any warranty or representation, expressed or implied, with respect to the accuracy, completeness, or usefulness of the information contained in this report, or that the use of any information, apparatus, method, or process disclosed in this report may not infringe privately-owned rights; or
- B) Assumes any liabilities with respect to the use of, or for damages resulting from the use of any information, apparatus, method or process disclosed in this report.

As used above, "person acting on behalf of NASA" includes any employee or contractor of NASA, or employee of such contractor, to the extent that such employee or contractor of NASA or employee of such contractor prepares, disseminates, or provides access to, any information pursuant to his employment or contract with NASA, or his employment with such contractor.

## AVAILABILITY NOTICE

Qualified requestors may obtain copies of this report from:

National Aeronautics and Space Administration  
Office of Scientific and Technical Information  
Washington 25, D. C.  
Attn: AFSS-A

CASE FILE 0071

1698

Report No. 64. 30E

March 1964

RESEARCH AND DEVELOPMENT PROGRAM ON MAGNETIC,  
ELECTRICAL CONDUCTOR, ELECTRICAL INSULATION,  
AND BORE SEAL MATERIALS

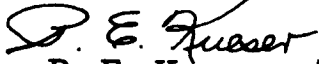
THIRD QUARTERLY REPORT  
(MARCH 1, 1964 - MAY 30, 1964)  
NAS3-4162

sponsored by

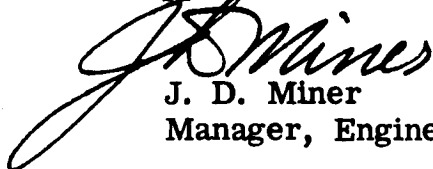
NATIONAL AERONAUTICS AND SPACE ADMINISTRATION  
CONTRACT NAS3-4162

Technical Management  
NASA - Lewis Research Center  
R. A. Lindberg

Prepared by:

  
P. E. Kueser, et al  
Manager, NASA Materials Study  
and Research Program

Approved:

  
J. D. Miner  
Manager, Engineering

Westinghouse Electric Corporation  
Aerospace Electrical Division  
Lima, Ohio

## PREFACE

The work reported here was sponsored by the Nuclear Power Technology Branch of NASA Lewis Research Center under Contract NAS3-4162. Mr. R. A. Lindberg of NASA has provided the Technical Management for the program. The work was accomplished at the Westinghouse Aerospace Electrical Division which is the prime contractor, at the Westinghouse Research and Development Center, and at the Eitel-McCullough Corp., which are both sub-contractors. The latter is conducting the ceramic-metal bore seal investigations. In any project of this type, many skilled engineers and scientists are consulted to provide the desired information. Those who actively participated during the past quarter are recognized below:

<u>Westinghouse Aerospace Electrical Division</u>	<u>Westinghouse Research and Development Center</u>	<u>Eitel-McCullough Corp.</u>
Dr. A. C. Beiler	L. J. Ceschini	D. W. Grobecker
D. H. Lane	W. P. Hughes	R. C. McRae
W. S. Neff	Dr. D. W. Lewis	Dr. Leonard Reed
Dr. D. M. Pavlovic	L. E. Moberly	
R. P. Shumate	A. E. Moredock	
J. W. Toth	R. D. Olson	
	R. N. Sampson	
	J. Sefko	
	E. H. VanAntwerp	
	C. H. Vondracek	



## ABSTRACT

25010

This is the third quarterly report concerning the evaluation of design information on electrical materials suitable for application to space electric power systems. The program data are based upon some literature sources but the majority are based on tests completed in this program.

Mechanical tests have shown that high-saturation materials such as iron-cobalt are not suitable for high-stress applications at elevated temperature. The 50 Co-50 Fe material also undergoes atomic ordering at elevated temperature, thereby increasing the coercive force. Nivco (23 Ni - 1.1 Zr - 1.8 Ti - Co) has the best creep properties of potential rotor materials for temperatures in excess of 900°F.

All conductor materials have been delivered. They include clad and unclad construction. Several new dispersion-strengthened copper conductors have been developed as well as austenitic stainless steel-clad conductors.

Weight-loss tests on insulations in vacuum have shown the importance of prior treatment on material performance since all samples showed a high initial loss rate which later tapered off.

Ceramic-to-metal seals using high purity ceramics and silica-free metalizings appear to be marginal in strength. Emphasis is now being placed on active metal brazing methods for fabricating ceramic-to-metal seals.

Author

## TABLE OF CONTENTS

Section		Page
I	INTRODUCTION .....	1
II	MAGNETIC MATERIALS .....	2
	A. Introduction .....	2
	B. Summary of Effort in This Quarter .....	2
	C. Mechanical and Thermophysical Test Results .....	5
	D. Magnetic Test Results .....	10
III	ELECTRICAL CONDUCTORS .....	71
	A. Introduction .....	71
	B. Summary of Effort in This Quarter .....	72
	C. Mechanical and Thermophysical Test Results .....	73
	D. General Discussion .....	75
IV	ELECTRICAL INSULATION MATERIALS .....	103
	A. Introduction .....	103
	B. Summary of Effort in This Quarter .....	103
	C. Electrical and Thermophysical Test Results .....	104
	D. Material Selection .....	111
V	BORE SEAL MATERIALS .....	127
	A. Introduction .....	127
	B. Summary of Effort in This Quarter .....	127
	C. Discussion .....	129
VI	PROGRAM .....	160
	A. Overall Program Plan .....	160
	B. Fourth Quarter Plan .....	160

## LIST OF FIGURES

<u>Figure</u>	<u>Title</u>	<u>Page</u>
II-1	S-N Diagram of Notched and Unnotched H-11 at 800°F. Stress Ratio = $\infty$ . Tests in Air. ....	31
II-2	S-N Diagram of Notched and Unnotched H-11 at 800°F. Stress Ratio = 0.25. Tests in Air. ....	32
II-3	S-N Diagram of Notched and Unnotched H-11 at 800°F. Stress Ratio = 2.00. Tests in Air. ....	33
II-4	S-N Diagram of Notched and Unnotched H-11 at 1000°F. Stress Ratio = $\infty$ . Tests in Air. ....	34
II-5	S-N Diagram of Notched and Unnotched H-11 at 1000°F. Stress Ratio = 0.25. Tests in Air. ....	35
II-6	S-N Diagram of Notched and Unnotched H-11 at 1000°F. Stress Ratio = 2.00. Tests in Air. ....	36
II-7	S-N Diagram of Notched and Unnotched Nivco at 900°F. Stress Ratio = $\infty$ . Tests in Air. ....	37
II-8	S-N Diagram of Notched and Unnotched Nivco at 900°F. Stress Ratio = 0.25. Tests in Air. ....	38
II-9	S-N Diagram of Notched and Unnotched Nivco at 1000°F. Stress Ratio = $\infty$ . Tests in Air. ....	39
II-10	S-N Diagram of Notched and Unnotched Nivco at 1000°F. Stress Ratio = 0.25. Tests in Air. ....	40
II-11	S-N Diagram of Notched and Unnotched Nivco at 1100°F. Stress Ratio = $\infty$ . Tests in Air. ....	41
II-12	S-N Diagram of Notched and Unnotched Nivco at 1100°F. Stress Ratio = 0.25. Tests in Air. ....	42
II-13	Fatigue Test Arrangement Showing Specimen in Position For Testing .....	43
II-14	Creep, Forged Nivco Tested in Air at 900°F .....	44
II-15	Creep, Forged Nivco Tested in Air at 1100°F .....	45
II-16	Creep, Forged Nivco Tested in Air at 1400°F .....	46
II-17	Creep, Forged Nivco Tested in Air at 1600°F .....	47
II-18	Creep, Forged Hiperco Tested in Air at 700°F .....	48
II-19	Creep, Forged Hiperco 27 Tested in Air at 900°F ....	49
II-20	Creep, Forged Hiperco 27 Tested in Air and Argon at 1100°F .....	50
II-21	Creep, Forged Hiperco 27 Tested in Argon at 1400°F .	51
II-22	Creep, Nivco Sheet 0.025" Thick (Transverse) Tested in Air at 900°F .....	52

# LIST OF FIGURES (Cont.)

<u>Figure</u>	<u>Title</u>	<u>Page</u>
II-23	Creep, Nivco Sheet 0.025" Thick (Transverse) Tested in Air at 1100°F .....	53
II-24	Creep, Nivco Sheet 0.025" Thick (Transverse) Tested in Air at 1400°F .....	54
II-25	Creep, Forged Maraging Steel (15 Percent Nickel) Tested in Air at 900°F .....	55
II-26	Larson-Miller Plot of Forged Bar and Sheet Nivco Creep Data, Tested in Air .....	56
II-27	Creep Test Arrangement Showing Extensometer and Thermocouples Attached to Specimen .....	57
II-28	Tension Test Specimen in Position For Testing, With Extensometer in Place .....	58
II-29	Resistivity Specimen Wrapped on Quartz Mandrel, With Leads and Thermocouples Attached .....	59
II-30	Specific Heat, Forged Hiperco 27 in Vacuum .....	60
II-31	Specific Heat, Cubex in Vacuum .....	61
II-32	Specific Heat, 1% Silicon Iron in Vacuum .....	62
II-33	Specific Heat, Supermendur Rolling Stock in Vacuum .....	63
II-34	Specific Heat Specimen in Evacuated Quartz Capsule.	64
II-35	DC Magnetization Curves for AMS5210 (1% Si-Fe) Casting, Ring 4-7/8 x 3-7/8 x 1/2 inch. Test Atmosphere: Air to 800°F, Argon above 800°F ..	65
II-36	DC Magnetization Curves for AMS5210 (1% Si-Fe) Casting, Ring 4-7/8 x 3-7/8 x 1/2 inch. Test Atmosphere: Air to 800°F, Argon above 800°F ..	66
II-37	DC Magnetization Curves for H-11 Steel Forging, Ring 4-7/8 x 3-7/8 x 1/2 inch. Test Atmosphere: Air to 500°F, Argon above 800°F .....	67
II-38	DC Magnetization Curves for Hiperco 27, Ring Laminations, 0.008 thick. Test Atmosphere: Air to 800°F, Argon above 500°F .....	68
II-39	DC Magnetization Curves for Hiperco 27, Ring Laminations, 0.008 thick. Test Atmosphere: Air to 800°F, Argon above 800°F .....	69
II-40	DC Magnetization Curves for Cubex. Ring Laminations, 0.006 inch thick. Test Atmosphere: Air to 500°F, Argon above 500°F .....	70

# LIST OF FIGURES (Cont.)

<u>Figure</u>	<u>Title</u>	<u>Page</u>
III-1	Tensile Strength, Dispersion Strengthened Copper (CuFo, BeO-Cu) Tests at 800°F and above made in argon, all others in air .....	88
III-2	Tensile Ductility, Dispersion Strengthened Copper (CuFo, BeO-Cu) Tests at 800°F and 1000°F made in argon, all others in air .....	89
III-3	Tensile Strength, 0.100" Diameter 'CuFo' Wire ....	90
III-4	Tensile Strengths, Nickel-Clad Copper. Tests at 800°F and above made in argon, all others in air..	91
III-5	Ductility, Nickel-Clad Copper. Tests at 800°F and above made in argon, all others in air .....	92
III-6	Tensile Strengths, 321 Stainless Steel-Clad Silver. All tests in argon at 800°F and above .....	93
III-7	Ductility, 321 Stainless Steel-Clad Silver. All tests in argon at 800°F and above .....	94
III-8	Thermal Expansion, Nickel-Clad Copper, 10 Gage Wire, Tested in Argon .....	95
III-9	Thermal Expansion, CuFo Dispersion Strengthened Copper, 10 Gage Wire, Tested in Argon .....	96
III-10	Thermal Expansion, Type 321 Stainless Steel-Clad Silver, 10 Gage Wire Tested in Argon.....	97
III-11	Thermal Expansion Specimen in Quartz Tube Dilatometer, Ready For Insertion into Furnace .....	98
III-12	Electrical Resistivity vs. Temperature of Conductors in Vacuum .....	99
III-13	Electrical Resistivity vs. Temperature of Stainless Steel Clad Zirconium Copper in Vacuum.....	100
III-14	321 Stainless Steel Clad Silver .....	101
III-15	Inconel-Clad Dispersion-Strengthened Copper (Cu Fo) With Columbium Barrier Layer.....	102
IV-1	Thermal Expansion, Westinghouse Doryl H17511 in Air .....	114
IV-2	Thermal Expansion, Epoxy-Hysol in Air .....	115
IV-3	Thermal Expansion, 92M in Argon Atmosphere .....	116
IV-4	Thermal Expansion, Sauereisen #8 in Air .....	117
IV-5	Schematic of Weight Loss Apparatus .....	118
IV-6	Weight Loss of 92M Boron Phosphate-Bonded Asbestos Rigid Sheet at 1560°F, 10 <sup>-6</sup> Torr .....	119

# LIST OF FIGURES (Cont.)

<u>Figure</u>	<u>Title</u>	<u>Page</u>
IV-7	Weight Loss of 92M Boron Phosphate-Bonded Asbestos Rigid Sheet at 1560°F, $10^{-3}$ Torr .....	120
IV-8	Weight Loss of 128-50-1 Silicone-Bonded, Glass- backed Mica Flexible Sheet, 932°F and 1112°F, $10^{-5}$ - $10^{-6}$ Torr .....	121
IV-9	Weight Loss of Polyimide H Film, 482°F, $10^{-5}$ - $10^{-6}$ Torr .....	122
IV-10	Weight Loss of Pyre ML-glass-cloth Semi-Flexible 482°F, $10^{-5}$ - $10^{-6}$ Torr .....	123
IV-11	Weight Loss of Doryl H-17511 Rigid Sheet 482°F, $10^{-5}$ - $10^{-6}$ Torr .....	124
IV-12	Weight Loss of Hysol C9-4186-H5-3537 Encapsulating Compound at 302°F, $10^{-5}$ - $10^{-6}$ Torr .....	125
IV-13	Weight Loss of Scotchply 1100 at 482°F, $10^{-5}$ - $10^{-6}$ Torr .....	126
V-1	Dry Box Facility .....	130
V-2	Alkali Metal Facility Plumbing .....	131
V-3	Right Side of Dry Box .....	132
V-4	Dual Vacuum Furnace .....	133
V-5	Overall Schematic of Liquid Metal Loading Arrange- ment .....	134
V-6	Iron Plated Tungsten Metalize Paints on Alumina CLM-15 Pieces .....	143
V-7(a)	W-12 Metalizing on Ei-3-3 Ceramic (600X) .....	144
V-7(b)	20A Metalizing on AD-94 Ceramic (600X) .....	144
V-8	Photomicrographs showing the solution of the columbium-1% zirconium and the attach on the tungsten metalize after penetration of the iron barrier by the nickel braze alloy (200X) .....	146
V-9	Photomicrograph showing a crack in the braze region; such defects seem to be associated with excessive solution of the columbium-1% zir- conium metal by the nickel braze material (X200). .....	147
V-10	Section Through a CLM-15 Test Sample With a Cb-Zr-Be Active Metal Braze Between AD-99 Ceramic and Cb-1Zr .....	154

LIST OF FIGURES (Cont.)

<u>Figure</u>	<u>Title</u>	<u>Page</u>
V-11	Idealized Geometry of First Electroform Seal .....	155
V-12	Alumina to Columbian-1% Zirconium Seal Joined by Electroforming a Sheath in a Sulphamate Nickel Bath .....	156
VI-1	Program Plan - NASA Materials Study and Research Program .....	161

## LIST OF TABLES

<u>Number</u>	<u>Title</u>	<u>Page</u>
II-1	800° and 1000°F Fatigue Test Data For H-11 Un-notched Specimens in Air .....	12
II-2	800° and 1000°F Fatigue Test Data For H-11 Notched Specimens in Air .....	13
II-3	900°, 1000°, and 1100°F Fatigue Test Data For Nivco Unnotched Specimens in Air .....	14
II-4	900°, 1000°, 1100°F Fatigue Test Data For Nivco Notched Specimens in Air .....	15
II-5	Creep Data For Nivco Forging .....	16
II-6	Creep Data For Nivco Forging .....	17
II-7	Creep Data For Hiperco 27 Forging .....	18
II-8	Creep Data For Hiperco 27 Forging .....	19
II-9	Creep Data For Nivco Sheet 0.025" Thick (Transverse) .....	20
II-10	Creep Data For 15 Percent Nickel Maraging Steel ..	21
II-11	Tensile Test Data For Nivco Forging .....	22
II-12	Tensile Test Data For Nivco 0.025" Transverse Sheet Material .....	23
II-13	Tensile Test Data For Hiperco 27 (Investment Cast and Annealed) .....	24
II-14	Electrical Resistivity of Supermendur 2 Mil Ribbon in Vacuum .....	25
II-15	Electrical Resistivity of Supermendur 2 Mil Ribbon in Vacuum .....	26
II-16	DC Magnetic Properties, Hiperco 50, Nivco Alloys .	27
II-17	Core Loss, Hiperco 50 Alloy.....	28
II-18	Core Loss, Hiperco 27 Alloy.....	29
II-19	Core Loss, Cubex Alloy .....	30
III-1	Tensile Test Data For Bare Conductor Wire .....	76
III-2	Tensile Test Data For Clad Conductor Wire .....	77
III-3	Electrical Resistivity, 321 Stainless Steel-Clad Silver Wire in Vacuum .....	78
III-4	Electrical Resistivity, Inconel-Clad 'Cu-Fo' Copper Wire in Vacuum .....	79
III-5	Electrical Resistivity, 'CuFo' Copper Wire in Vacuum .....	80



# LIST OF TABLES (Cont.)

<u>Number</u>	<u>Title</u>	<u>Page</u>
III-6	Electrical Resistivity, 'CuFo' Copper Wire in Vacuum .....	81
III-7	Electrical Resistivity, Inconel-Clad Silver Wire in Vacuum .....	82
III-8	Electrical Resistivity, TD Nickel Wire, in Vacuum..	83
III-9	Electrical Resistivity, 304 Stainless Steel-Clad Zirconium Copper Wire in Vacuum (First Test) ..	84
III-10	Electrical Resistivity 304 Stainless Steel-Clad Zirconium Copper Wire in Vacuum (Second Test)....	85
III-11	Electrical Resistivity, 304 Stainless Steel-Clad Zirconium Copper Wire in Vacuum (First Test) ..	86
III-12	Electrical Resistivity, 304 Stainless Steel-Clad Zirconium Copper Wire in Vacuum (Second Test).	87
IV-1	Tensile Tests on Flexible Sheet Insulation at Room Temperature in Air .....	104
IV-2	Compressive Strength of Various Materials In Air ..	105
IV-3	Flexural Strength and Modulus on Rigid Sheet Insulations In Air .....	106
IV-4	Linear Thermal Expansion for Various Materials ...	106
IV-5	Water Absorption .....	110
V-1	Ceramic Modulus of Rupture Test Data .....	137
V-2	Effect of Surface Preparation on Ceramic-Metal Modulus of Rupture Assemblies .....	138
V-3	Correlation: CLM-15 Tensile Strength vs. Modulus of Rupture Data .....	139
V-4	Correlation: CLM-15 Drum Peel vs. Tab Peel Data .....	140
V-5	Leak Test Results - Tungsten Series Paints Ceramic-Metal Brazed ASTM, CLM-15 Assemblies .....	142
V-6	Sinter Test of Tungsten Metalize on Beryllia Bodies .....	149
V-7	Evaluation of Metalize and Braze on 99.8% Beryllia Bodies .....	150
V-8	Active Metal Braze Alloys .....	152
V-9	Analysis of Potassium and NaK .....	158
V-10	Specimen Distribution for 1600°F Potassium Exposure Evaluation .....	159

## SECTION I

### INTRODUCTION

This is the third quarterly report on magnetic, electrical conductor, electrical insulation, and bore seal materials suitable for application to advanced, space electric power systems. A punched card bibliography was prepared and reported in the first quarterly report (Westinghouse WAED 63.16E). This bibliography now encompasses 900 references with additions during the past quarter. It includes a keyword or descriptor word and a number identifying various chemical, mechanical and thermo-physical properties. The first report also defines the tests which must be accomplished to fill-in the gaps in properties necessary for designing advanced, space electric power systems.

The test program begun during the second quarter has continued into the third quarter. All materials have been received with the exceptions of a few isolated cases. Some additional material is also being processed to clarify anomalies observed during testing.

The magnetic materials under a-c and d-c tests include those for high strength, high saturation, and "square-loop" applications. Both clad and unclad electrical conductors suitable for vacuum, inert gas, and air atmospheres are under evaluation. Organic and inorganic electrical insulations in the form of flexible sheet, rigid sheet, molded shapes, encapsulation compounds, interlaminar films and magnetic and flexible wire coatings are under investigation. Ceramic-to-metal seals for bore seal applications processed by metalizing or by active metal brazing are under study in potassium, NaK, and lithium vapors. The temperature range of interest for all materials is 500°F to 1600°F except for the organic insulation which is -65°F to 1000°F. Vacuum, inert gas, and air represent the test atmospheres.

Three topical reports, one on magnetic materials, one on electrical insulations and conductor materials, and one on bore seal materials will be published at the end of this program. They will incorporate properties obtained from the literature and from this program's test efforts. In reporting the data, curves and tables are credited to the originating source. All data generated by this program are referenced to NAS3-4162.

A technical discussion on the third quarter's effort follows in subsequent sections.

## SECTION II

### MAGNETIC MATERIALS

#### A. INTRODUCTION.

Selection of the magnetic materials for the present program has been based on applications to both solid and laminated rotors where strength is important; to motor and generator stators, electromagnetic pumps and transformers where high induction and low losses at a reasonable magnetizing force are desired; to d-c solenoids; and to saturable reactors where square-loop magnetic properties are desirable. The materials have been further selected for their elevated temperature capabilities and their potential application to advanced, space electric power systems.

#### B. SUMMARY OF EFFORT IN THIS QUARTER.

During the past quarter the following mechanical and thermophysical tests were started or completed:

- 1) 800°F and 1000°F fatigue tests were completed on 25 notched bar and 24 smooth bar specimens of H-11 alloy (5Cr-1Mo-1V-Fe)
- 2) 900°F, 1000°F, and 1100°F fatigue tests were completed on 22 notched bar and 32 smooth bar specimens of Nivco alloy (23Ni-1.1Zr-1.8Ti-Co)
- 3) Elevated temperature creep tests were initiated on the following in air:
  - a) 10 Hiperco 27 (27Co-Fe) specimens
  - b) 18 forged Nivco specimens
  - c) 8 sheet Nivco transverse specimens

- d) 8 sheet H-11 transverse specimens
  - e) 6 forged 15 percent nickel Maraging steel (Almar 15) specimens
  - f) 11 investment cast Hiperco 27 specimens
- 4) Elevated temperature creep tests were started on the following in argon or in vacuum:
- a) 2 forged Nivco specimens (argon)
  - b) 3 forged Hiperco 27 specimens (vacuum)
  - c) 3 forged Nivco specimens (vacuum)
  - d) 4 forged H-11 specimens (vacuum)
- 5) Room and elevated temperature tensile tests were completed on the following:
- a) 10 forged Nivco specimens
  - b) 10 investment cast Hiperco 27 specimens
  - c) 12 sheet Cubex (3Si-Fe) longitudinal and transverse specimens
  - d) 12 sheet Hiperco 50 specimens
  - e) 10 sheet Nivco transverse specimens
- 6) Room and elevated temperature compression tests were completed on a total of 9 sheet Cubex transverse and longitudinal specimens.
- 7) The electrical resistivity of Supermendur (49Co-2V-Fe) tape (0.002 inch) was measured to 1150 °F.
- 8) Specific heat as a function of temperature was measured on the following:
- a) Hiperco 27 (forged bar)
  - b) Cubex (TIG welded sheet)

c) Iron - 1 percent silicon (investment cast)

d) Supermendur rolling stock

Magnetic testing has been completed on the following:

- 1) Cubex laminations, 0.012 inch thick
- 2) Cubex 0.002 inch, tape-wound toroid, field annealed
- 3) Hiperco 27 Casting
- 4) Hiperco 27 laminations, 0.008 inch thick
- 5) Hiperco 50 laminations, 0.004 and 0.008 inch thick
- 6) Nivco forging and laminations, 0.014 and 0.025 inch thick
- 7) AMS5210 casting (1Si-Fe)
- 8) H-11 forging

Testing has been partially completed on:

- 1) Cubex 0.002 inch, tape-wound toroid, stress-relief annealed
- 2) Cubex 0.006 inch lamination toroid, field annealed
- 3) Cubex laminations, 0.006 inch thick
- 4) Supermendur 0.002 inch, tape-wound toroid
- 5) Hiperco 27 laminations, 0.004 inch thick

Material preparation:

A complete description of the material preparation was contained on pages 17 thru 20 of the Second Quarterly Report, WAED64. 14E.

## C. MECHANICAL AND THERMOPHYSICAL TEST RESULTS.

### 1. Fatigue Testing

All completed fatigue test data are presented in Tables II-1 through II-4 and are plotted in Figures II-1 through II-12. As indicated in previous reports, nearly all fatigue tests run on this program were to be made in an air atmosphere. The decision to air test the H-11 and Nivco was made when the literature failed to provide master air-atmosphere fatigue data on both the above alloys. A large amount of inert-gas atmosphere, fatigue data has been obtained for other alloys by Westinghouse on the Maritime Gas Cooled Reactor Program<sup>1</sup>. These data showed a modest effect of atmosphere purity on the fatigue life of various nickel and iron-base, high-temperature alloys. However, both beneficial and adverse effects of the purified test atmosphere on the alloys studied were noted. In general, effects were found to be a function of grain size, alloy composition, and test atmosphere purity. A comprehensive study like that performed on the MGCR Program is beyond the scope of this program. It was decided to obtain the best possible base-line, air-atmosphere data from which a detailed atmosphere test program could be planned if such data became a design necessity. Several high-purity atmosphere tests are planned, however, to check the alloys of interest in this program for this sensitivity, and to alert the designer of these trends. This check had been done early in the creep program with no significant differences observed.

An analysis of the fatigue data plots shows that the notched 1000°F fatigue life of H-11 (Figure II-5) and the 900°F and 1000°F fatigue life of Nivco (Figures II-8 and II-10) are noticeably improved (nearly equal to smooth bar data) when the cyclic or fatigue stress is one quarter of the maximum applied stress ( $A = 0.25$ , ratio of maximum stress to static stress). In this situation, the stresses acting on the sample are primarily static and tend to lessen the effects of cyclic loading. It has been observed during creep tests that neither Nivco nor H-11 are notch sensitive. The classic notched-unnotched fatigue pattern existed on all other tests with the notched materials failing at a much lower stress. This is shown by the 800°F H-11 (Figure II-3) data in which a difference

<sup>1</sup>Wall, F. J., "Metallurgical Development for 1500°F MGCR Gas Turbine", Maritime Gas Cooled Reactor Project Engineering Report, Westinghouse Electric Corp., Lester, Pa., February, 1964.

in endurance and/or strength was observed between all the notched and unnotched H-11 samples. These particular data on H-11 and Nivco are presented graphically in Figures II-2, II-5, II-8 and II-10.

All fatigue specimen notch geometry was calculated to give a stress concentration factor ( $K_t$ ) of three. Figure II-13 has been included which shows a fatigue specimen mounted in a set of bolted grips. These are then clamped in a Sonntag Model SF-1U fatigue machine. The furnace has been removed to provide a better view of the specimen. A thermocouple attached to the center of the specimen records the specimen temperature.

## 2. Creep Testing

Creep test data for all completed tests are given in Tables II-5 through II-10 and are plotted as creep strain-time curves in Figures II-14 through II-25. The two tests on Nivco forgings in an argon atmosphere, while still incomplete, indicate that air may have a deleterious effect at 1600° and perhaps at 1400°F. These temperatures, though, are well above the maximum-use temperatures of the alloy. New tests are being made at 900°F and 1100°F because stresses above the yield strength were found necessary to produce the 0.2 and 0.4 percent creep strain in 1000 hours; creep testing above the yield strength introduces scatter not encountered when testing at stresses below the yield strength. In general, these creep data would favor forged Nivco over all other solid rotor materials at temperatures of 900°F and above. Creep data obtained on other programs would suggest H-11 to 800°F<sup>2</sup>.

All creep data obtained on this and other programs will be integrated with magnetic properties in the final topical reports to be prepared at the end of the present program.

Initial creep data (see Table II-9 and Figures II-22, 23, and 24) on sheet Nivco (0.025" thick) were disappointing. It was found the 0.2 and 0.4 percent creep strains could be produced in 0.025 inch thick transverse sheet specimens of Nivco alloy at stresses which were much lower than that required to produce equivalent

<sup>2</sup>1963 Annual SPUR Generator Development Report, WAED 64.2E, Westinghouse Electric Corp., Aerospace Electrical Division, Lima, Ohio, Prepared for the AiResearch Mfg. Co., Division of the Garrett Corp. under Contract No. AF33(657)10922.

deformations in forged-bar samples. The creep data for the two forms of this alloy are compared in a Larson-Miller plot in Figure II-26.

It was reasonable to assume that the low creep strength of the sheet Nivco was somehow connected with the cold finishing operation used on Nivco sheet after solution annealing.

Shop practice for making magnetic alloy sheet usually requires the materials to be cold finished. The Nivco used for this program was bought in the cold finished condition. Initially, the Nivco rolling stock consisted of 1 inch thick sheet bar which had been forged from a 5 x 5 square and was subsequently hot rolled to 0.100 inch. After hot rolling, the material was water quenched from 1725°F and cold rolled with successive re-solution anneals to near the desired finish size. Final processing consisted of one final anneal, a water quench, a pickling treatment and the cold finishing process. Test samples were cut, rough machined, aged in dry hydrogen at 1225°F for 25 hours, finish machined, and tested.

A comparison of all the tensile (Tables II-11, II-12) and creep data for both sheet and forged Nivco (Tables II-5, II-6, II-9) shows the large disparity between the tensile and short-time creep data for the sheet materials. The sheet possessed extremely good transverse yield and tensile strength, but extremely poor creep strength. The fact that creep is a function of the fourth power of the stress for any given temperature makes the high-creep rates difficult to understand. However, these data can probably be rationalized in a qualitative manner as follows: It is known that all materials have different deformation mechanisms which are operative over certain ranges of strain rates and at any particular temperature. When a material is cold finished, large amounts of energy are "locked" into those deformation systems which are normally operative at the relatively high-strain rates used for cold rolling. Since there are now certain specific areas of the bulk material at a fairly high level of retained energy, the strengthening phase will precipitate preferentially in those areas leaving other areas of lower retained energy depleted of strengthening phase. It is these "other areas" that probably comprise the operative deformation mechanisms during slow straining processes such as creep. Since these other areas are poor in the strengthening phase, there is only token resistance to the passage or movement of dislocations and other lattice defects resulting in abnormally high creep rates.

The solution to the problem of high creep rate in Nivco sheet appears obvious. Reheat treat the sheet in pure dry hydrogen after



the cold finishing operation at a temperature (1900°F) which will cause recrystallization of the material and the elimination of high energy areas. Several test samples are being reheat treated at this writing to test the validity of the foregoing rationalization. The reheat treated test samples will be creep tested at stresses close to those used on longitudinal bar samples of Nivco alloy.

The balance of the creep data presented in this report is fairly straight forward and does not require further explanation at this time. Detailed analysis of all creep data is in progress and will be presented with several types of design type curves in the final topical reports.

Figure II-27 shows a typical creep specimen with extensometer attached in an air creep machine ready for heating and loading.

### 3. Tensile Testing

Tensile data for tests completed during this period are given in Tables II-11 through II-13.

The arrangement for making tension tests at elevated temperatures is shown in Figure II-28. An extensometer attached directly to the specimen gage length is used for reproducing the stress-strain curve.

### 4. Electrical Resistivity Testing

Electrical resistivity data for 0.002 inch Supermendur tape (field annealed) are given in Tables II-14 and II-15. Because room temperature measurements had shown that the resistivity of the ribbon might vary as much as three percent from the end of the reel to the center, complete tests were made on specimens from both locations. The change in resistivity with temperature was found to be essentially the same in both. The specimen was wound on a quartz mandrel in the same way that the wire specimen shown in Figure II-29 was made. All resistivity tests were made at a pressure in the  $10^{-6}$  torr range.

### 5. Specific Heat Measurements

Specific heat data for Hiperc 27, Cubex, 1% silicon iron, and Supermendur alloys are plotted in Figures II-30 to II-33 respectively. The curve for Hiperc 27 shows that the specific heat increases gradually up to about 1100°F, then increases rapidly; the other three materials exhibit a constant specific heat up to about 700°F and then show a rapid increase. The inflection points on these

curves are indicative of changes occurring within the alloy. In the case of Supremendur, 750°F corresponds to the order-disorder temperature of the alloy. The change in the slope of the curves for the other alloys have not been explained.

Oxidation is prevented by sealing the specific heat specimens in evacuated quartz capsules. During normal testing, the specimen temperature is measured with a platinum-rhodium thermocouple mounted in a quartz well which is inserted halfway down the center of the specimen. A specimen in an evacuated quartz tube with the thermocouple in the well is shown in Figure II-34. Since quartz is not as good a heat conductor as the metal specimen, it was necessary to determine the difference in temperature between the quartz well and the specimen. To do this, a 1/16 inch diameter hole was drilled in a copper specimen to within 3/16 inch of the quartz well, and thermocouples were positioned in both the specimen and the quartz well. Temperatures were recorded at both locations as the specimen was taken through a complete test. The quartz cover on the bottom of the specimen was left out in the test to facilitate the placement of the thermocouple in the specimen. The results show that the temperatures in the quartz well and in the specimen were within 1% except at 1500°F where they differ by about 1.5%. This means that the thermocouple in the quartz well measures the specimen temperature with good accuracy over the entire testing temperature range.

#### D. MAGNETIC TEST RESULTS.

A considerable amount of test data has been collected and is currently being analyzed. Examples of these data will be presented and discussed for solid rings of AMS 5210 (1% Si-Fe), H-11, and Nivco (Figures II-35, 36, 37 and Table II-16) and ring laminations of Hiperco 27, Hiperco 50, and Cubex (Figures II-38, 39, 40 and Tables II-16, 17, 18, 19).

The magnetic properties of all materials tested follow the pattern expected at high temperatures, i. e. as the temperature increases, the magnetization curves rise more quickly at lower fields, and then flatten out and saturate at lower inductions. In addition, coercive force, residual induction, and core losses decrease with increasing temperature.

Exposure to high temperatures brought about structural changes in some materials. In Nivco (Table II-16) and H-11 steel (Figure II-37) where precipitation of one or several new phases makes a major contribution to high temperature strength, changes in room temperature properties were observed after the samples had been exposed to 1400°F or 1100°F respectively. This occurs at high temperatures when the precipitates go back into solution thus removing the obstacles to the movement of domain walls, as well as decreasing the amount of non-magnetic substance in the alloy. As a result, the coercive force decreased and the high-field induction increased. Both Nivco and H-11 steel also show a considerable decrease in the coercive force at high temperatures. At 1400°F the coercive force of Nivco decreased by over 250%; at that temperature the high-field induction of Nivco decreased by only 18%. Unfortunately, the dissolution of precipitates affects the mechanical strength, hence both magnetic and mechanical properties will have to be considered for a complete evaluation of the merits of high-temperature structural changes.

Of the cobalt iron alloys, Hiperco 50 (Tables II-16 and II-17) shows a considerable increase in the room temperature coercive force after exposure to 1400°F. This may be associated with the strain or with a new arrangement in the atom positions, both brought about by an atomic-ordering reaction which for 50% Co-Fe occurs at temperatures up to 1350°F. The ordering region does not extend to 27% cobalt iron (Figures II-38 and II-39, Table II-18); this alloy shows a considerable decrease in room temperature coercive force after exposure to 1400°F. This could have been brought about by strain relief effects of the high-temperature anneal. The strain relief also appears to be responsible for the slight improvement of the room temperature coercive force of Cubex (Figure II-40) and AMS 5210 (Figures II-35 and II-36) after exposure to 1100°F.

Both Hiperco 27 (Table II-18) and Hiperco 50 (Table II-17) show a decrease in core loss for various frequencies at temperatures up to 800-

1100°F but a large increase at 1400°F. After exposure to 1400°F, room temperature core loss shows a large increase at all frequencies over the original room temperature losses. From the improvement in d-c room temperature properties, and the marked deterioration in the core loss, it may be concluded that the interlaminar insulation on these samples had broken down at the elevated temperature. This conclusion will be checked by additional tests. Cubex (Table II-19) core losses decreased with increasing temperatures as expected.

It may be of interest from the application standpoint to mention that at 1100°F and in a field of 300 oersteds, Hiperco 50 laminations reached a flux density of 21.4 kilogausses, AMS 5210 casting reached about 17.2 kilogausses and H-11 and Nivco forgings 14 and 11 kilogausses, respectively. At 1400°F, a temperature at which iron and its alloys (except cobalt-iron) are non-magnetic, Hiperco 27 and Hiperco 50 reached an induction of 18 and 18.5 kilogausses respectively and Nivco that of about 10 kilogausses, all in a field of 300 oersteds.

TABLE II-1. 800° and 1000°F Fatigue Test Data For H-11  
Unnotched Specimens in Air  
See Figures II-1, 2, 3, 4, 5 and 6

Test: ASTM STP91 - Frequency 3600 cpm

Specimen No.	Test Temp. °F	Stress Ratio (A) <sup>(1)</sup>	Max. Stress (Psi)	Cycles to Failure
100	800	∞	89,600	1,130,000
101	800	∞	110,000	19,000
102	800	∞	100,000	60,000
103	800	∞	84,100	4,680,000
104	800	∞	94,000	138,000
111	800	∞	82,000	1,332,000
107	800	0.25	175,150	2,000
109	800	0.25	179,600	12,047,000
112	800	0.25	175,150	4,000
113	800	0.25	172,450	186,000
115	800	0.25	171,350	922,000
117	800	2.00	120,050	572,000
108	800	2.00	112,250	1,213,000
119	800	2.00	124,932	190,000
122	800	2.00	115,016	1,386,000
123	800	2.00	108,866	628,000
133	800	2.00	135,000	166,000
124	800	2.00	108,866	1,155,000
130	800	2.00	97,995	10,000,000*
106	1000	∞	75,000	5,171,000
110	1000	∞	90,000	783,000
114	1000	∞	110,000	3,000
116	1000	∞	100,000	33,000
118	1000	∞	82,000	663,000
128	1000	∞	80,000	1,566,000
125	1000	0.25	170,000	2,000
134	1000	0.25	160,750	15,000
127	1000	0.25	152,000	29,000
126	1000	0.25	140,000	58,000
129	1000	0.25	130,000	5,634,000
136	1000	2.0	129,000	394,000
137	1000	2.0	120,000	826,000
131	1000	2.0	144,000	5,000
135	1000	2.0	114,000	1,600,000

(1)  $A = \frac{\text{Maximum Stress}}{\text{Static Stress}}$

\*No failure

(Reference: NAS3-4162)

TABLE II-2. 800° and 1000°F Fatigue Test Data For H-11  
Notched (2) Specimens in Air  
See Figures II-1, 2, 3, 4, 5 and 6

Test: ASTM STP91 - Frequency 3600 cpm

Specimen No.	Test Temp. °F	Stress Ratio (A) <sup>(1)</sup>	Max. Stress (Psi)	Cycles to Failure
203	800	∞	40,000	7,761,000
207	800	∞	60,000	7,000
206	800	∞	50,000	35,000
202	800	∞	46,000	12,245,000
208	800	∞	44,000	14,000,000*
215	800	∞	50,000	24,000,000*
211	800	∞	65,000	4,000
222	800	∞	55,800	15,000
221	800	0.25	125,250	9,656,000
223	800	0.25	131,250	5,100,000
225	800	0.25	135,750	396,000
227	800	0.25	140,400	92,000
231	800	0.25	147,000	75,000
220	800	2.00	52,500	50,000
228	800	2.00	65,000	13,000
237	800	2.00	44,000	7,873,000
240	800	2.00	47,000	10,000,000*
217	1000	∞	37,000	30,000
219	1000	∞	34,600	127,000
226	1000	∞	32,000	5,272,000
224	1000	∞	41,000	8,000
218	1000	∞	33,600	14,955,000
239	1000	∞	33,000	10,000,000*
235	1000	0.25	103,950	13,733,000*
234	1000	0.25	129,950	1,040,000
236	1000	0.25	140,000	958,000
232	1000	0.25	110,000	1,145,000
229	1000	0.25	120,300	570,000
233	1000	0.25	126,500	914,000
230	1000	2.0	35,100	10,221,000*
238	1000	2.0	50,100	1,380,000

(1)  $A = \frac{\text{Maximum Stress}}{\text{Static Stress}}$

(2) Stress Concentration Factor,  $K_T = 3$

\*No failure

(Reference: NAS3-4162)

TABLE II-3. 900°, 1000°, and 1100°F Fatigue Test Data For  
Nivco Unnotched Specimens in Air  
See Figures II-7, 8, 9, 10, 11 and 12

Test: ASTM STP91 - Frequency 3600 cpm

Specimen No.	Test Temp. °F	Stress Ratio (A) <sup>(1)</sup>	Max. Stress (Psi)	Cycles to Failure
300	900	∞	100,000	1,500
304	900	∞	80,000	84,000
305	900	∞	70,000	662,000
325	900	∞	65,000	3,194,000
327	900	∞	60,000	2,415,000
307	900	0.25	150,000	23,000
310	900	0.25	135,000	18,000,000*
312	900	0.25	142,000	4,532,000
316	900	0.25	146,250	10,000
315	900	0.25	143,750	204,000
306	1000	∞	69,750	3,639,000
308	1000	∞	90,000	7,000
309	1000	∞	80,000	96,000
311	1000	∞	66,000	7,250,000
313	1000	∞	74,000	563,000
318	1000	0.25	143,750	553,000
320	1000	0.25	150,000	6,000
302	1000	0.25	135,900	828,000
322	1000	0.25	146,250	8,000
321	1000	0.25	128,000	12,474,000
332	1000	0.25	129,950	4,488,000
314	1100	∞	74,000	200,000
317	1100	∞	82,000	31,000
319	1100	∞	70,000	722,000
303	1100	∞	62,000	8,690,000
323	1100	∞	66,000	4,500,000
324	1100	0.25	134,750	28,000
326	1100	0.25	120,000	716,000
328	1100	0.25	110,000	9,830,000*
329	1100	0.25	125,800	299,000
330	1100	0.25	129,950	159,000
331	1100	0.25	115,500	637,000

(1)  $A = \frac{\text{Maximum Stress}}{\text{Static Stress}}$

\*No failure

(Reference: NAS3-4162)

TABLE II-4. 900°, 1000°, 1100°F Fatigue Test Data For Nivco  
Notched (2) Specimens in Air  
See Figures II-7, 8, 9, 10 and 11

Test: ASTM STP91 - Frequency 3600 cpm

Specimen No.	Test Temp. °F	Stress Ratio (A) <sup>(1)</sup>	Max. Stress (Psi)	Cycles to Failure
400	900	∞	55,000	18,000
402	900	∞	50,000	23,000
409	900	∞	40,000	10,330,000*
406	900	∞	45,000	62,000
404	900	∞	42,500	108,000
410	900	0.25	135,000	10,000,000*
413	900	0.25	150,000	121,000
420	900	0.25	139,750	8,790,000
416	900	0.25	145,000	148,000
438	900	0.25	165,000	17,000
435	1000	∞	49,750	12,000
425	1000	∞	40,000	56,000
403	1000	∞	30,000	9,729,000*
408	1000	∞	35,000	9,791,000
412	1000	∞	37,500	10,045,000*
439	1000	0.25	145,000	240,000
427	1000	0.25	152,000	33,000
422	1000	0.25	134,000	955,000
414	1100	∞	35,000	2,419,000
437	1100	∞	45,000	16,000
433	1100	∞	30,000	10,000,000*
424	1100	∞	40,000	36,000
434	1100	∞	37,000	12,250,000

(1)  $A = \frac{\text{Maximum Stress}}{\text{Static Stress}}$

(2) Stress Concentration Factor  $K_T = 3$

\*No failure

(Reference: NAS3-4162)



TABLE II-5. Creep Data For Nivco Forging  
See Figures II-14, 15 and 16

Test: ASTM E139

Temperature (°F)	1400	1100	900
Stress (psi)	7000	90000	95000
Duration of Test (hours)	214	70.9**	1204
Total Creep Strain (percent)	0.1920	0.9756	0.263
Time to Cause 0.2 percent Creep Strain (hours)	217.0*	1.3	96
Time to Cause 0.4 percent Creep Strain (hours)	***	32.2	***
Plastic Strain obtained on loading specimen (percent)	None	0.0588	0.118
Test Atmosphere	Air	Air	Air
See Strain-Time Plot in Figure	II-16	II-15	II-14
*Extrapolated			
**Notch failure			
***Testing not complete		(Reference: NAS3-4162)	

TABLE II-6. Creep Data For Nivco Forging  
See Figures II-16 and 17

Test: ASTM E139

Temperature (°F)	1400	1400	1400	1400	1600	1600	1600
Stress (psi)	22000	18000	11000	11000	6000	6000	2000
Duration of Test (hours)	48	120	240	1.75	20.7	119	
Total Creep Strain (percent)	2.35	1.18	0.47	7.37	5.91	1.43	
Time to Cause 0.2 percent Creep Strain (hours)	7.2	23	87.5	0.05	0.4	7.6	
Time to Cause 0.4 percent Creep Strain (hours)	16	51	202	0.09	1.25	21.6	
Plastic Strain obtained on loading specimen (percent)	0	0	0	0	0	0	
Test Atmosphere	Air	Air	Air	Air	Air	Air	
See Strain-Time Plot in Figure	II-16	II-16	II-16	---	II-17	II-17	

(Reference: NAS3-4162)

TABLE II-7. Creep Data For Hipercro 27 Forging  
See Figures II-18 and 19

Test: ASTM E139

Temperature (°F)	900	900	900	700	700
Stress (psi)	46000	44000	48000	70000	65000
Duration of Test (hours)	447	622	143	548	1516
Total Creep Strain (percent)	0.5190	0.4848	0.4525	0.4489	0.457
Time to Cause 0.2 percent Creep Strain (hours)	94	202	28.0	36.0	372
Time to Cause 0.4 percent Creep Strain (hours)	303	511	118.0	276.0	1230
Plastic Strain obtained on loading specimen (percent)	0.0050	0.0201	0.0187	0.092	0.029
Test Atmosphere	Air	Air	Air	Air	Air
See Strain-Time Plot in Figure	II-19	II-19	II-19	II-18	II-18

(Reference: NAS3-4162)

TABLE II-8. Creep Data For Hipercro 27 Forging  
See Figures II-19, 20 and 21

Test: ASTM E139

Temperature (°F)	900	1100	1100	1100	1100	1400
Stress (psi)	42000	12000	9000	7000	3000	800
Duration of Test (hours)	617	186.6	257.4	332	1024	56
Total Creep Strain (percent)	0.494	0.84	0.52	0.337	0.236	0.587
Time to Cause 0.2 percent Creep Strain (hours)	108	76	127	182	755	14.7
Time to Cause 0.4 percent Creep Strain (hours)	482	122	213	---	---	34.8
Plastic Strain obtained on loading specimen (percent)	0	0	0	0	0	0
Test Atmosphere	Air	Argon	Argon	Argon	Air	Argon
See Strain-Time Plot in Figure	II-19	II-20	II-20	II-20	II-20	II-21

(Reference: NAS3-4162)

TABLE II-9. Creep Data For Nivco Sheet 0.025" Thick (Transverse)  
See Figures II-22, 23 and 24

Test: ASTM E139

Temperature (°F)	900	1100	1100	1100	1400
Stress (psi)	40000	30000	25000	65000	2000
Duration of Test (hours)	116	146	143	2.4	72.0
Total Creep Strain (percent)	0.444	6.04	6.6	4.02	7.83
Time to Cause 0.2 percent Creep Strain (hours)	13.8	0.47	0.59	0.0	0.92
Time to Cause 0.4 percent Creep Strain (hours)	89.5	3.19	2.5	0.02	2.14
Plastic Strain obtained on loading specimen (percent)	None	0.0462	None	0.125	None
Test Atmosphere	Air	Air	Air	Air	Air
See Strain-Time Plot in Figure	II-22	II-23	II-23	II-23	II-24

(Reference: NAS3-4162)

TABLE II-10. Creep Data For 15 Percent Nickel Maraging Steel  
See Figure II-25

Test: ASTM E139

Temperature (°F)	900	900
Stress (psi)	90000	80000
Duration of Test (hours)	140	261
Total Creep Strain (percent)	0.6432	0.521
Time to Cause 0.2 percent Creep Strain (hours)	19.5	42
Time to Cause 0.4 percent Creep Strain (hours)	68.5	155
Plastic Strain obtained on loading specimen (percent)	None	None
Test Atmosphere	Air	Air
See Strain-Time Plot in Figure	II-25	II-25

(Reference: NAS3-4162)

TABLE II-11. Tensile Test Data For Nivco Forging

Test: ASTM E21 - Strain Rate: 0.005 in/in-min and 0.05 in/in-min

Spec. No.	Dia. (In.)	Hardness BHN (3000 KG)	Test Temp. (°F)	0.02 Per- cent Offset Yield Str. (Psi)	0.2 Per- cent Offset Yield Str. (Psi)	Ultimate Strength (Psi)	Elongation 1.4 inches (percent)	Reduction of Area (percent)
5	0.357	316	R. T.	104,700	112,400	166,350	31.3	44.9
6	0.357	316	R. T.	99,900	112,400	164,350	30.1	42.4
1	0.358	336	900	83,150	91,750	136,300	21.4	43.6
7	0.357	302	900	66,950	86,600	131,350	20.7	43.7
2	0.358	331	1100	84,500	94,150	127,850	24.6	45.2
8	0.358	316	1100	69,500	85,650	121,400	24.0	48.9
3	0.358	321	1400	22,600	29,000	43,700	47.9Q	73.9
9	0.357	321	1400	40,350	43,550	54,650	37.4	68.9
4	0.358	326	1600	12,950	15,750	20,800	57.6	94.3
10	0.357	321	1600	12,400	16,200	23,150	90.2	93.9
Q - Quarterbreak								
All tests made in air.								
(Reference: NAS3-4162)								

TABLE II-12. Tensile Test Data For Nivco 0.025" Transverse Sheet Material

Test: ASTM E21 - Strain Rate: 0.005 in/in-min and 0.05 in/in-min

Mark	Test Temp. (°F)	0.02 Percent Offset Yield Stress (Psi)	0.2 Percent Offset Yield Stress (Psi)	Ultimate Strength (Psi)	Elongation in 2 Inches (percent)
26 T	80	103200	151900	A	A
4 T	80	155300	171900	180950	2.7
30 T	900	73700	109750	126450	12.2
31 T	900	71900	105950	125300	9.8 Q
32 T	1100	54100	79100	101200	10.1
33 T	1100	B	B	107550	13.2
27 T	1400	23250	34950	44150	25.0 Q
34 T	1400	25400	35350	43550	35.0
35 T	1600	10000	13950	20000	52.4
36 T	1600	9450	14100	19950	64.1

A = Broke in grips.  
 B = Curve unreliable. Extensometer slipped on specimen.  
 Q = Quarterbreak.  
 All tests made in air.

(Reference: NAS3-4162)



TABLE II-13. Tensile Test Data For Hipercro 27 (Investment Cast and Annealed)

Test: ASTM E21 - Strain Rate: 0.005 in/in-min and 0.05 in/in-min

Spec. No.	Dia. (In.)	Hardness BHN (3000 KG)	Test Temp. (°F)	0.02 Percent Offset Yield Str. (Psi)	0.2 Percent Offset Yield Str. (Psi)	Ultimate Strength (Psi)	Elongation 1.4 inches (percent)	Reduction of Area (percent)
1	0.250	149	R. T.	33,800	43,200	65,800	2.4Q	1.6
2	0.250	166	R. T.	37,800	44,600	62,750	1.5Q	0
4	0.249	153	500	26,500	35,300	73,300	27.0	59.1
5	0.250	153	500	27,900	31,550	71,900	29.2Q	48.7
6	0.250	153	700	31,250	34,100	67,400	14.4Q	28.1
7	0.251	156	700	32,850	40,000	72,200	21.5Q	39.5
8	0.250	166	1000	31,050	36,450	66,700	8.8Q	21.8
9	0.251	159	1000	26,450	31,300	55,950	9.3Q	21.8
10	0.251	159	1400	9,700	11,700	12,100	35.6Q	60.4
11	0.250	163	1400	8,850	10,850	12,300*	48.8Q	79.6

NOTE: BHN Converted from R<sub>B</sub> hardness readings

Q - Quarterbreak

\* - Tested in argon atmosphere. All others tested in air.

(Reference: NAS3-4162)

TABLE II-14. Electrical Resistivity of Supermendur 2 Mil Ribbon  
in Vacuum ( $10^{-5}$  torr)

Test: ASTM A344

Specimen No. 1, Continuous Heating		
Width - 0.250 inches, Thickness - 0.002 inches, Length - 12.96 inches		
Temp. (°F)	Resistance (Ohms)	Resistivity (Microhm-Cm)
79	0.4673	45.79
200	0.4741	46.46
300	0.4825	47.28
400	0.4943	48.44
500	0.5104	50.01
600	0.5300	51.94
710	0.5545	54.34
810	0.5796	56.80
907	0.6061	59.39
1000	0.6336	62.09
1100	0.6690	65.56
950	0.6230	61.05
750	0.5675	55.61
550	0.5245	51.40
350	0.4932	48.32
150	0.4713	46.18
(Reference: NAS3-4162)		

TABLE II-15. Electrical Resistivity of Supremendur 2 Mil Ribbon  
in Vacuum ( $10^{-5}$  torr)

Test: ASTM A344

Specimen No. 2, Continuous Heating		
Width - 0.250 inches, Thickness - 0.002 inches, Length - 11.39 inches		
Temp. (°F)	Resistance (Ohms)	Resistivity (Microhm-Cm)
77	0.4199	46.818
200	0.4268	47.59
300	0.4361	48.63
400	0.4800	49.95
500	0.4618	51.49
600	0.4780	53.30
703	0.4972	55.44
803	0.5205	58.03
900	0.5450	60.77
1000	0.5707	63.63
1100	0.6016	67.08
946	0.5580	62.22
746	0.5095	56.81
550	0.4702	52.43
350	0.4422	49.31
150	0.4230	47.16
(Reference: NAS3-4162)		

TABLE II-16. DC Magnetic Properties  
Test Atmosphere: Air to 500°F, Argon at 800°F and above

Test: ASTM A341

	R. T.	500°F	800°F	1100°F	1400°F	R. T. after 1400°F
<u>Hiperco 50 (50% Co-Fe) Ring Laminations, 0.004 inch thick</u>						
Coercive Force* (oersteds)	0.616	0.576	0.490	0.314	0.478	1.73
Residual Induction* (Kilogausses)	10.9	8.9	7.4	10.2	10.8	4.8
Induction (B <sub>tip</sub> ) for H = 300 oersteds (Kilogausses)	24.0	23.4	22.0	21.4	18.5	24.0
<u>Nivco (23 Ni-1.1 Zr-1.8 Ti-Co) Ring Forging</u>						
Coercive Force* (oersteds)	11.5	9.56	8.43	6.31	4.29	8.91
Residual Induction* (Kilogausses)	5.1	4.9	4.6	4.4	4.7	8.7
Induction (B <sub>tip</sub> ) for H = 200 oersteds (Kilogausses)	12.0	11.6	11.3	11.0	9.75	13.05
*Taken from B <sub>tip</sub> for H = 100 oersteds. (Reference: NAS3-4162)						

TABLE II-17. Core Loss

Hiperco 50 (50% Co-Fe) Ring Laminations, 0.004 inch thick  
 Test Atmosphere: Air to 500°F, Argon at 800°F and above

Test: ASTM A343

		Core Loss (Watts per pound)				
		R. T.	500°F	800°F	1100°F	1400°F
		R. T. after 1400°F				
Induction (kilogausses)		400 cps				
		1600 cps				
12		6.03	5.6	5.04	4.03	9.28
14		7.65	7.14	6.33	4.81	11.29
16		9.55	8.74	7.63	5.6	13.34
18		11.46	10.37	8.88	6.5	16.77
6		11.58	---	9.5	9.8	---
8		18.57	---	15.4	14.5	---
10		26.9	---	22.6	19.8	---
12		36.6	---	30.9	25.6	---

(Reference: NAS3-4162)

TABLE II-18. Core Loss

Hiperco 27 (27% Co-Fe) Ring Laminations, 0.008 inch thick  
 Test Atmosphere: Air to 500°F, Argon at 800°F and above

Test: ASTM A343

		Core Loss (Watts per pound)				
		R. T.	500°F	800°F	1100°F	1400°F R. T. after 1400°F
<u>Induction (kilogausses)</u>		<u>400 cps</u>				
18	30.9	24.97	21.0	20.57	31.4	46.1
12	17.3	14.2	11.86	11.6	14.5	22.5
				<u>800 cps</u>		
12	43.7	---	28.6	31.54	53.65	64.7
				<u>1600 cps</u>		
12	117	---	73.0	94.25*	183*	204.5*
				<u>3200 cps</u>		
8	106	---	100	141*	295*	283*

\*Interlaminar insulation probably damaged. Samples being reinsulated.

(Reference: NAS3-4162)

TABLE II-19. Core Loss

Cubex, Ring Laminations, 0.006 inch thick  
 Test Atmosphere: Air to 500°F, Argon at 800°F and above

Test: ASTM A343

Core Loss (Watts per pound)							
	R. T.	300°F	500°F	800°F	1100°F	R. T. after 1100°F	
<u>Induction (kilogausses)</u>	15 10	9.2 4.3	8.5 3.85	7.8 3.6	<u>400 cps</u>		
					6.9	---	9.24
					3.0	2.3	4.22
	10	11.7	---	9.5	<u>800 cps</u>		
					---	6.17	---
	10	32.4	---	26.5	<u>1600 cps</u>		
					---	18.14	---
	8	62.3	---	51.1	<u>3200 cps</u>		
					---	43.6	---
	(Reference: NAS3-4162)						

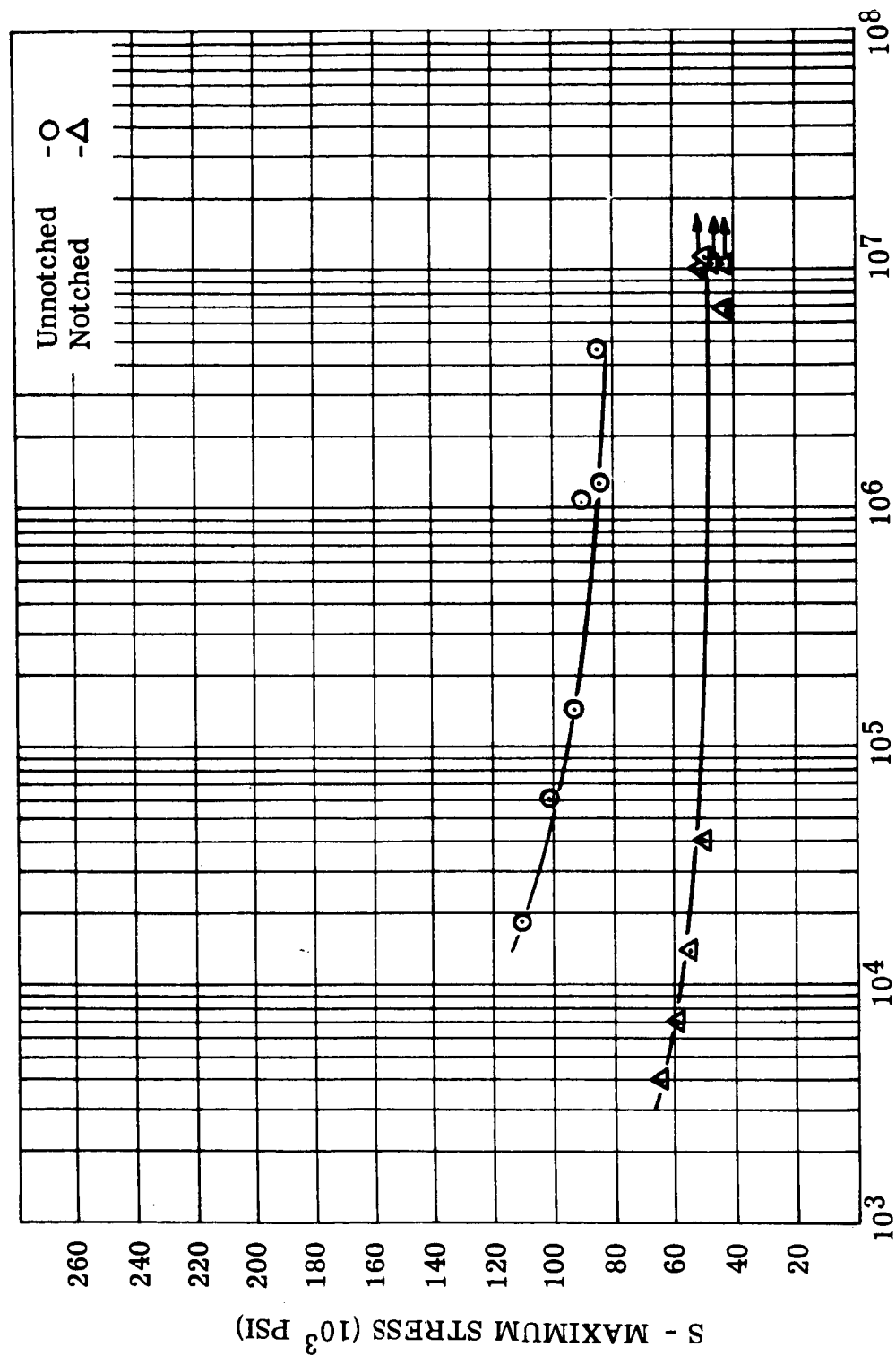


Figure II-1. Fatigue - H-11

FIGURE II-1. S-N Diagram of Notched and Unnotched H-11 at 800°F.  
Stress Ratio A = ∞. Tests Made in Air. (See Data  
Tables II-1, II-2)(Reference: NAS3-4162)



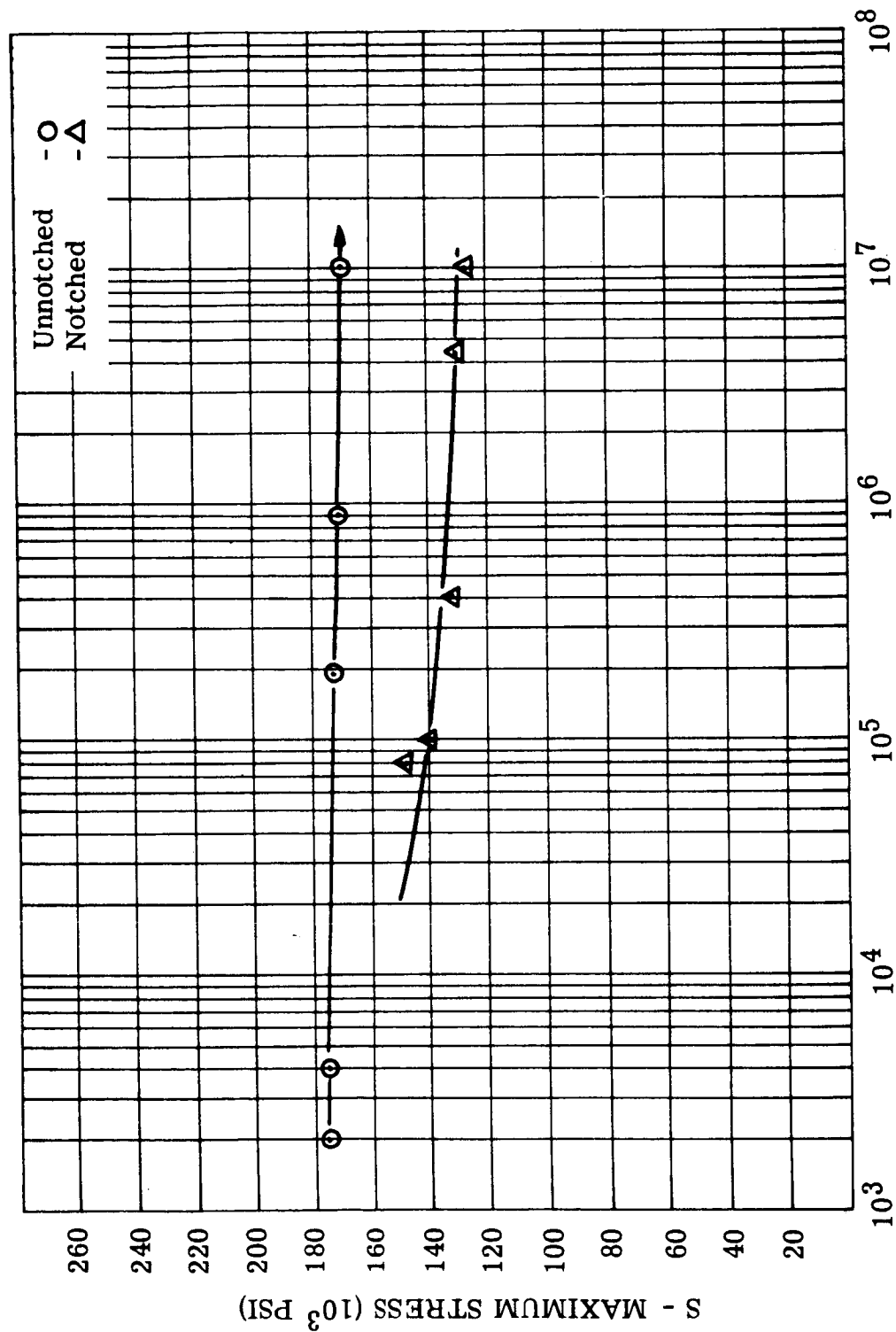
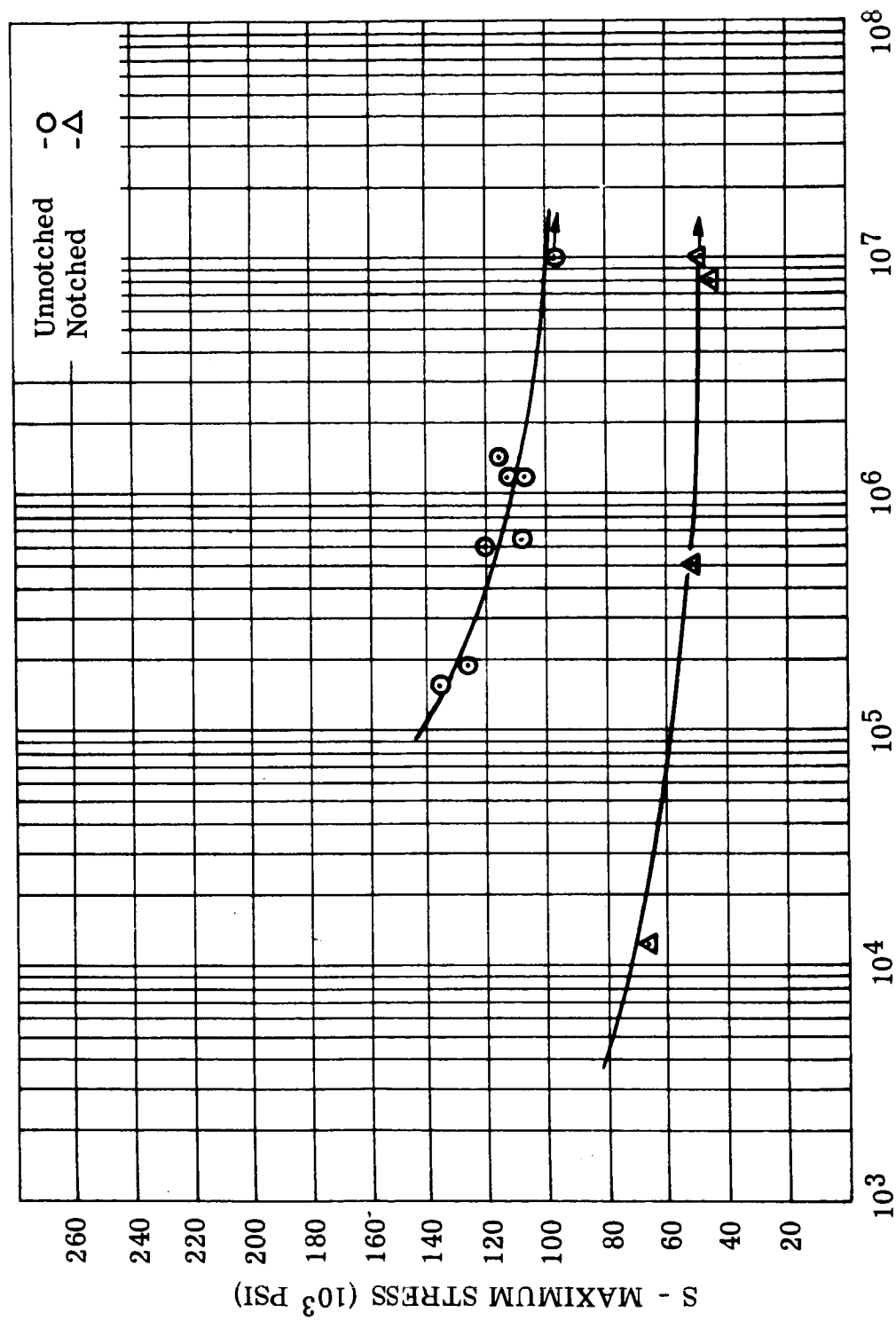


FIGURE II-2. S-N Diagram of Notched and Unnotched H-11 at 800°F.  
 Stress Ratio = 0.25. Tests Made in Air. (See Data  
 Tables II-1, II-2)(Reference: NAS3-4162)

Figure II-2. Fatigue - H-11

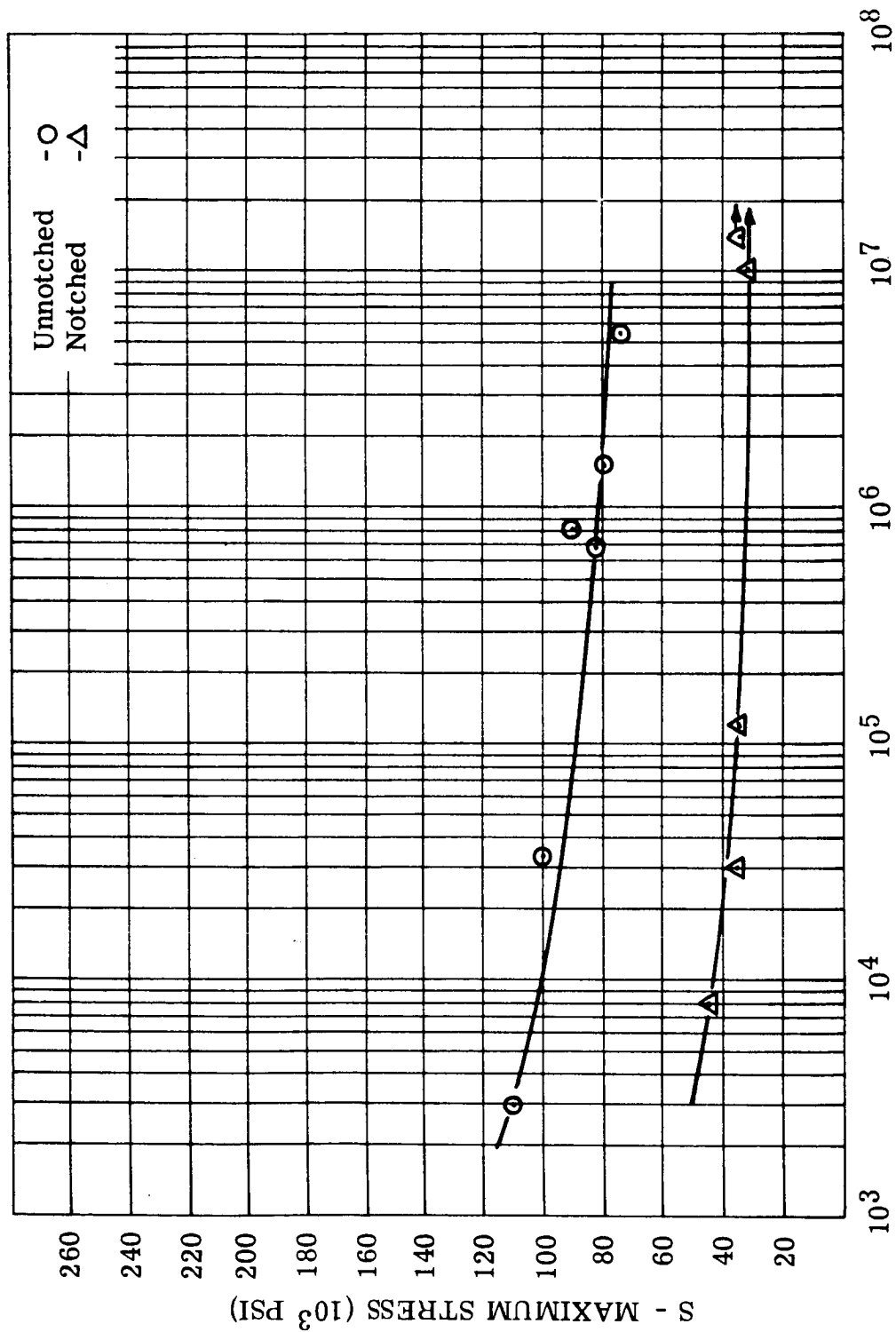


N - CYCLES TO FAILURE

FIGURE II-3. S-N Diagram of Notched and Unnotched H-11 at 800°F.  
Stress Ratio = 2.00. Tests Made in Air. (See Data  
Tables II-1, II-2)(Reference: NAS3-4162)

Figure II-3. Fatigue - H-11

WAED64. 30E-33

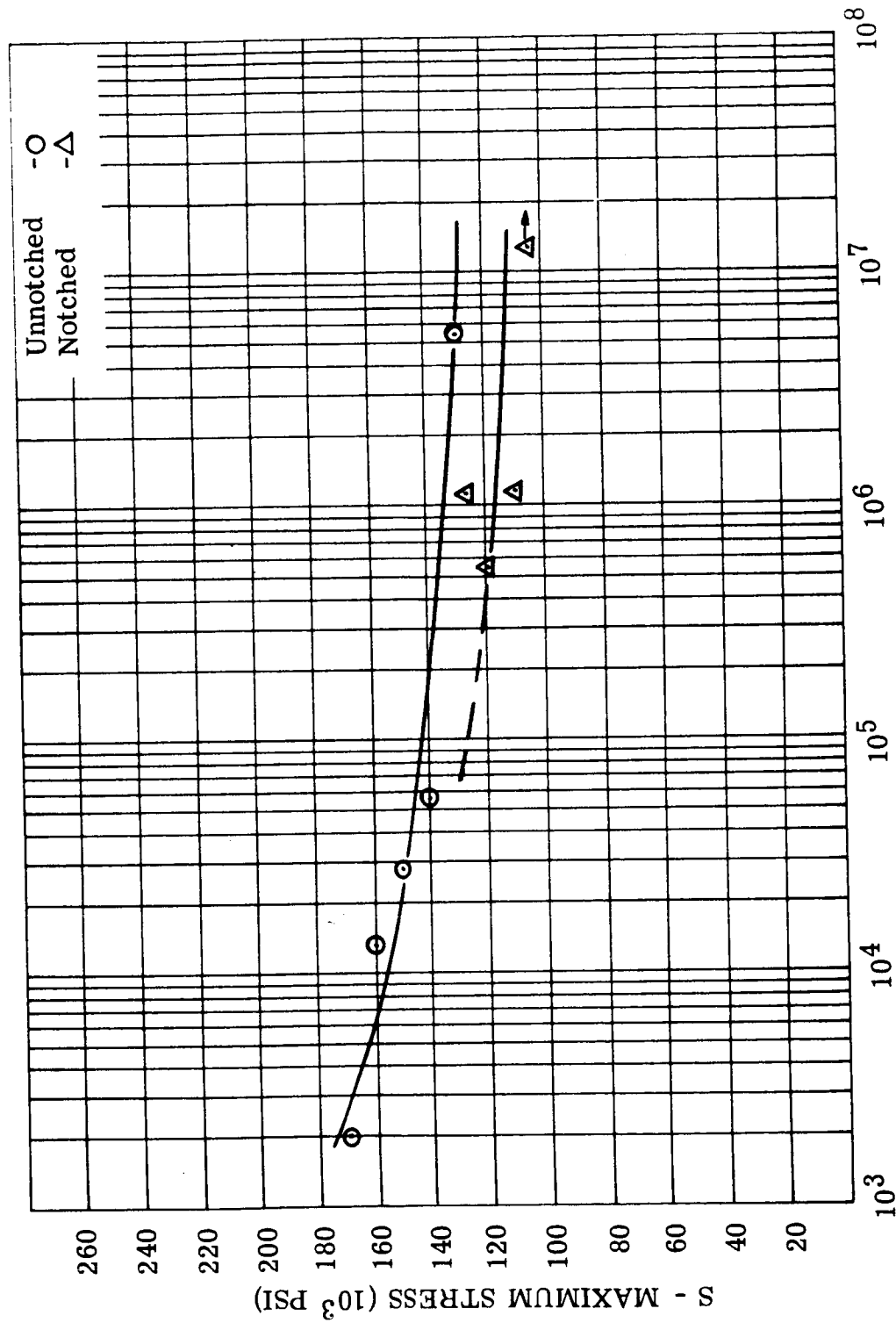


N - CYCLES TO FAILURE

FIGURE II-4. S-N Diagram of Notched and Unnotched H-11 at 1000°F.  
Stress Ratio = ∞ . Tests Made in Air. (See Data  
Tables II-1, II-2)(Reference: NAS3-4162)

Figure II-4. Fatigue - H-11

WAED64. 30E-34



N - CYCLES TO FAILURE

FIGURE II-5. S-N Diagram of Notched and Unnotched H-11 at 1000°F. Stress Ratio = 0.25. Tests Made in Air. (See Data Tables II-1, II-2)(Reference: NAS3-4162)

Figure II-5. Fatigue - H-11

WAED64. 30E-35

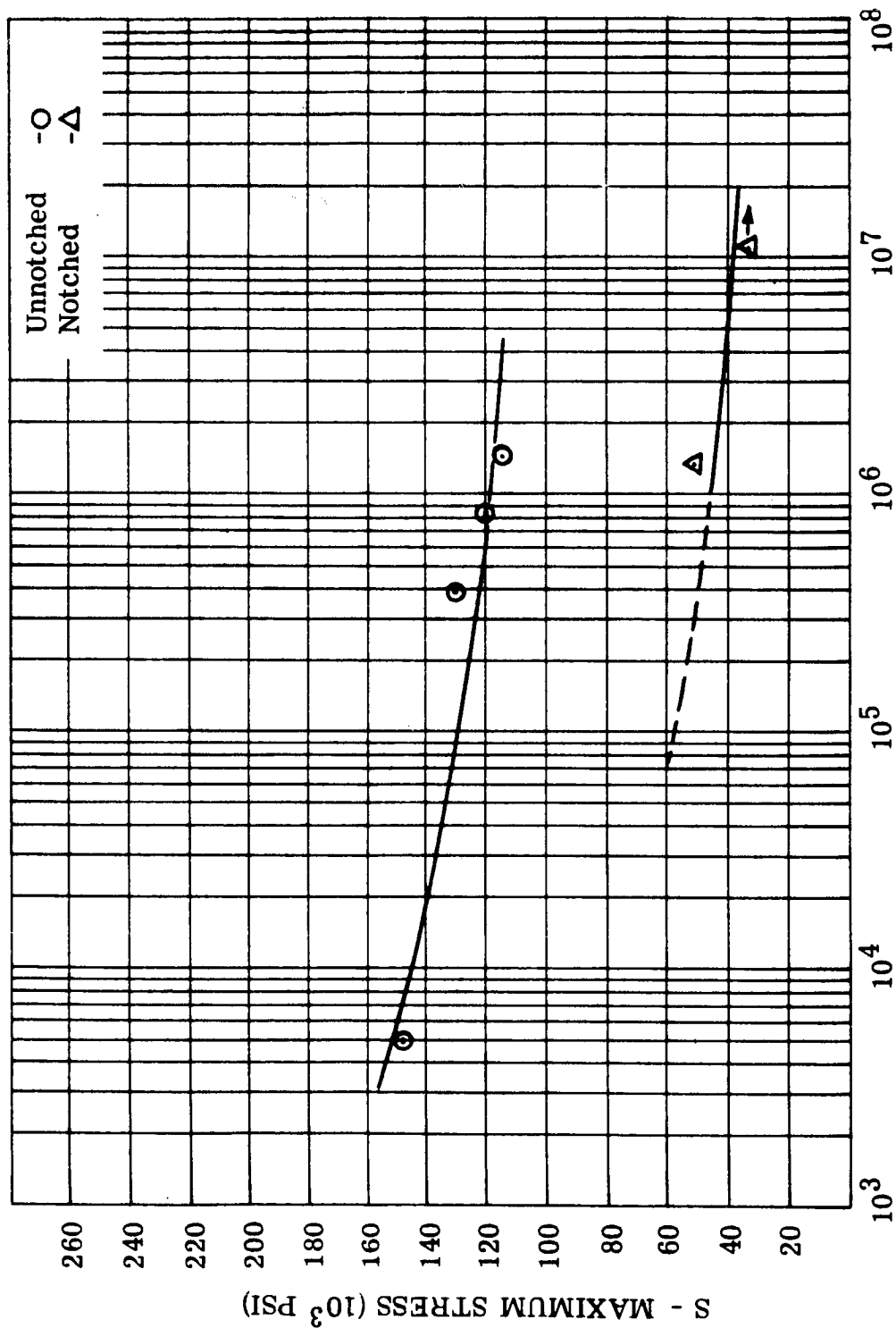
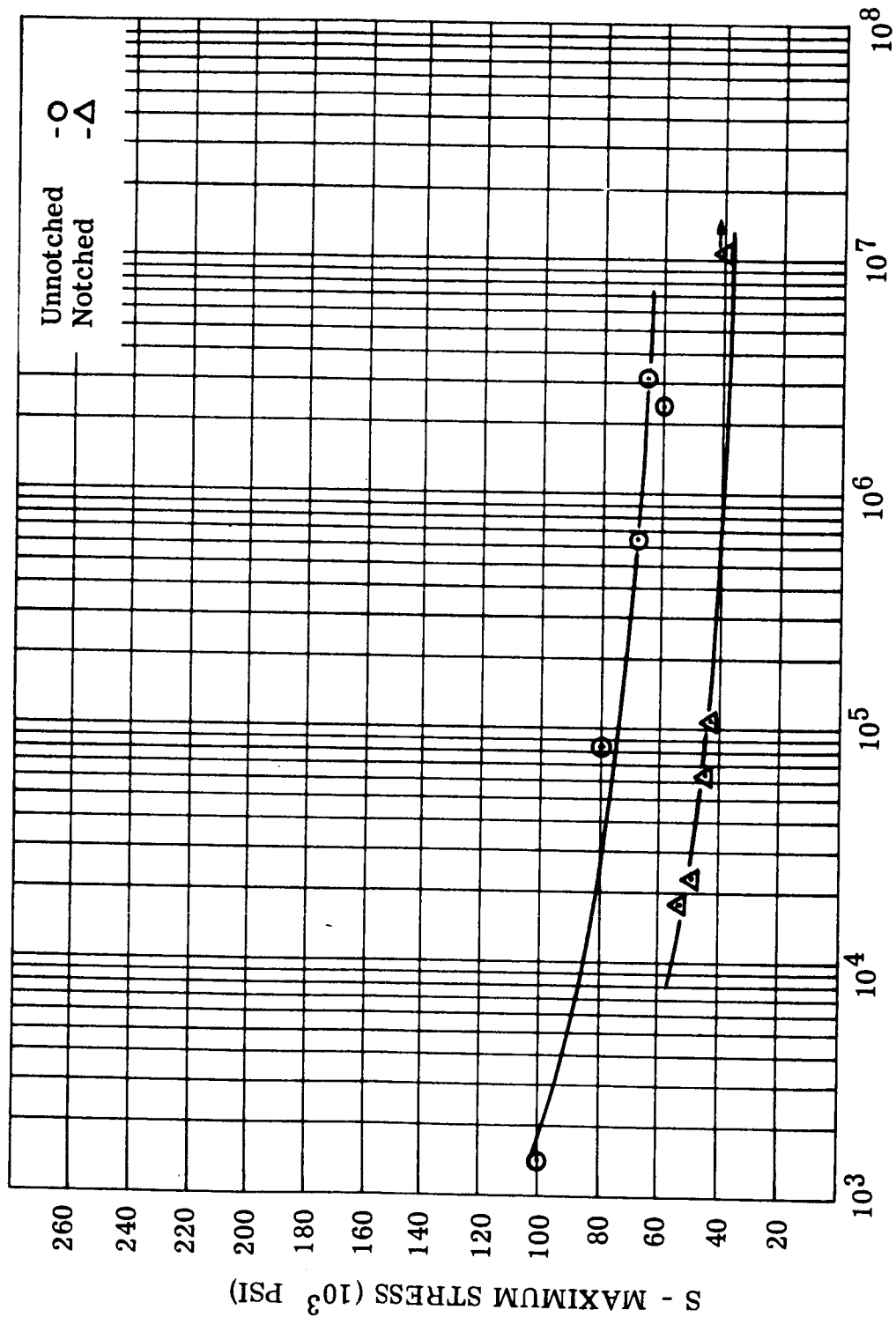


Figure II-6. Fatigue - H-11

N - CYCLES TO FAILURE

FIGURE II-6. S-N Diagram of Notched and Unnotched H-11 at 1000°F. Stress Ratio = 2.00. Tests Made in Air. (See Data Tables II-1, II-2)(Reference: NAS3-4162)



N - CYCLES TO FAILURE

FIGURE II-7. S-N Diagram of Notched and Unnotched Nivco at 900°F.  
Stress Ratio = ∞. Tests Made in Air. (See Data  
Tables II-3, II-4)(Reference: NAS3-4162)

Figure II-7. Fatigue - Nivco

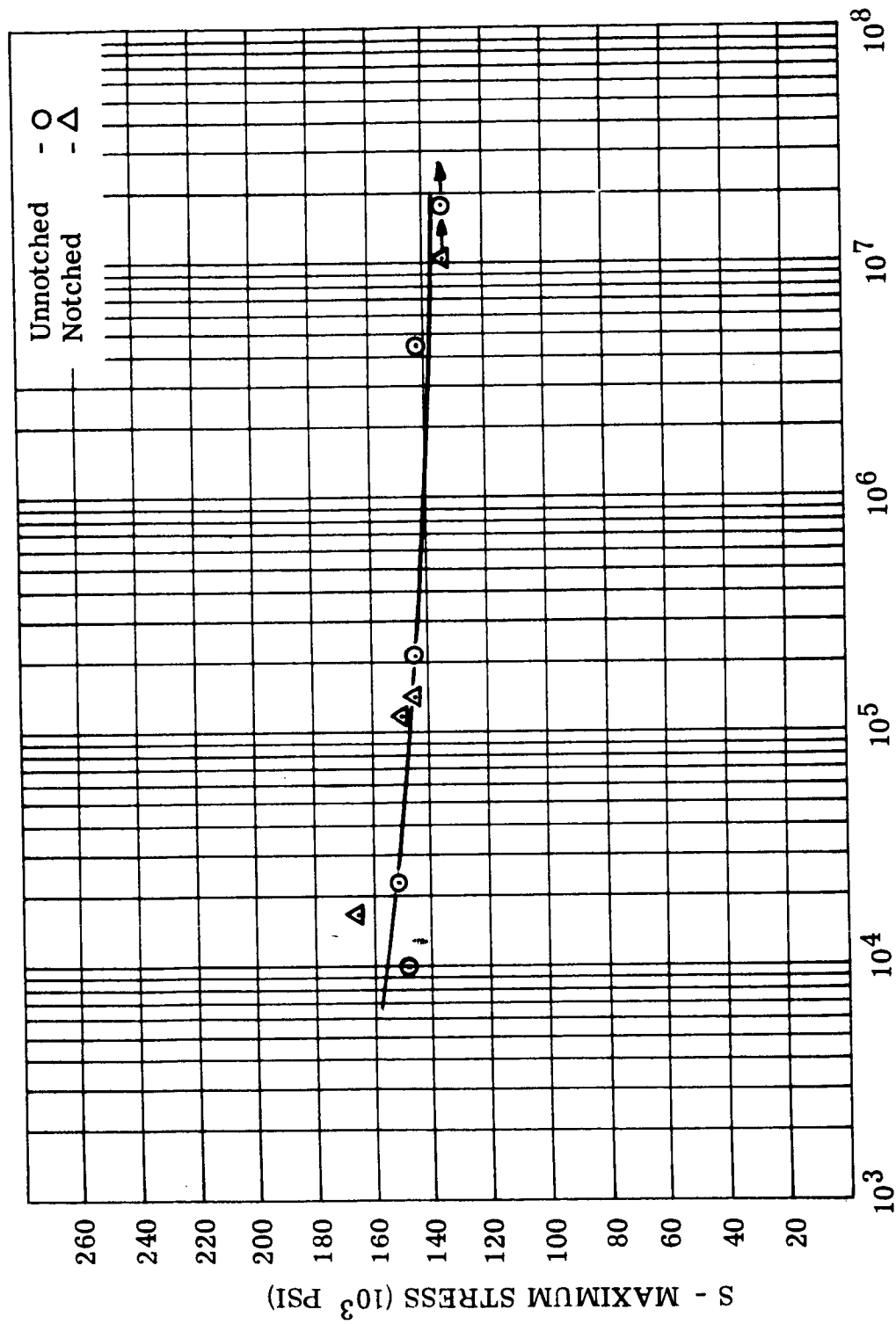
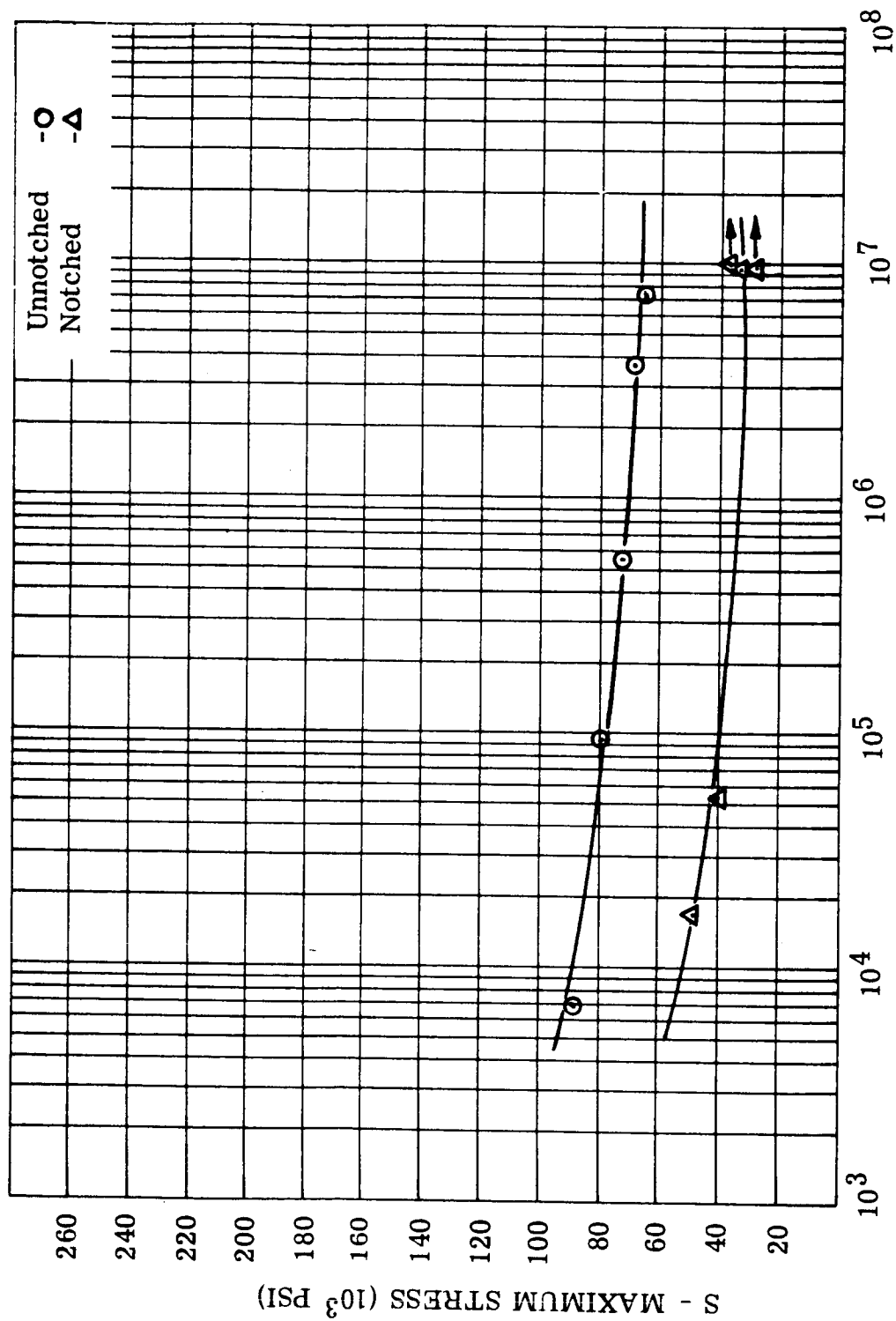


Figure II-8. Fatigue - Nivco

FIGURE II-8. S-N Diagram of Notched and Unnotched Nivco at 900°F.  
Stress Ratio = 0.25. Tests Made in Air. (See Data  
Tables II-3, II-4)(Reference: NAS3-4162)



N - CYCLES TO FAILURE

FIGURE II-9. S-N Diagram of Notched and Unnotched Nivco at 1000°F. Stress Ratio = ∞. Tests Made in Air. (See Data Tables II-3, II-4)(Reference: NAS3-4162)

Figure II-9. Fatigue - Nivco



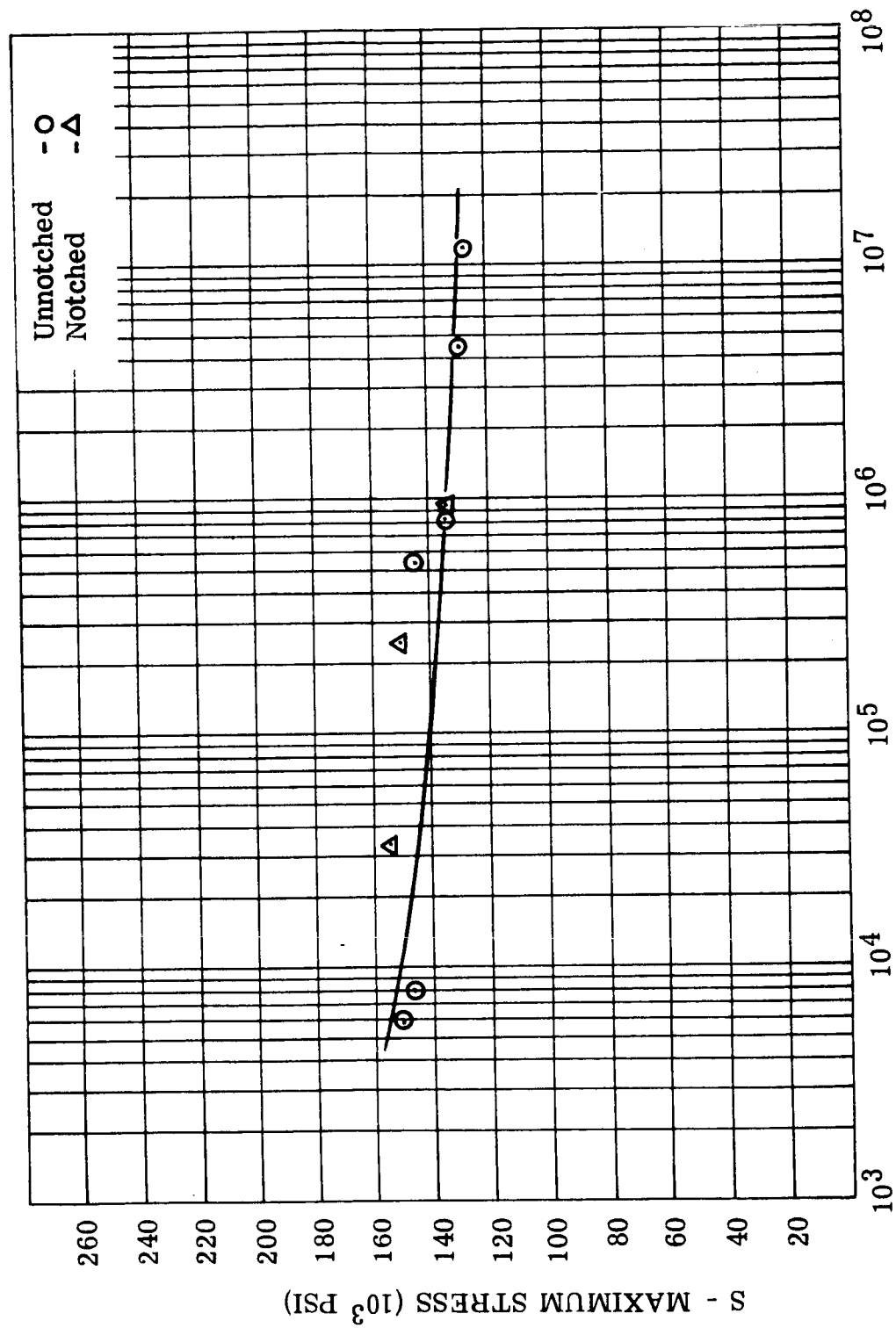


Figure II-10. Fatigue - Nivco

N - CYCLES TO FAILURE

FIGURE II-10. S-N Diagram of Notched and Unnotched Nivco at 1000°F.  
Stress Ratio = 0.25. Tests Made in Air. (See Data  
Tables II-3, II-4)(Reference: NAS3-4162)

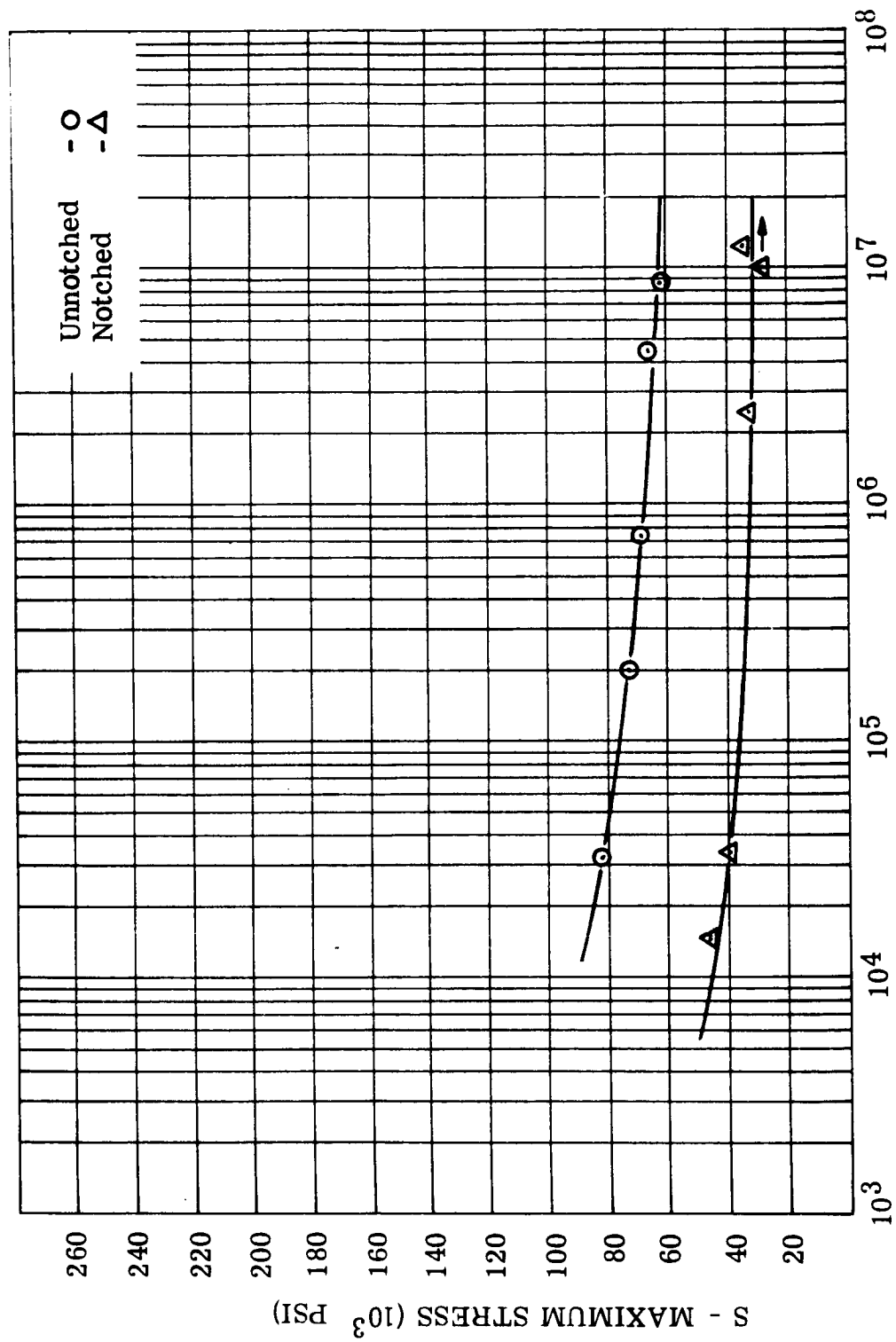


Figure II-11. Fatigue - Nivco

FIGURE II-11. S-N Diagram of Notched and Unnotched Nivco at 1100°F.  
 Stress Ratio =  $\infty$ . Tests Made in Air. (See Data  
 Tables II-3, II-4)(Reference: NAS3-4162)

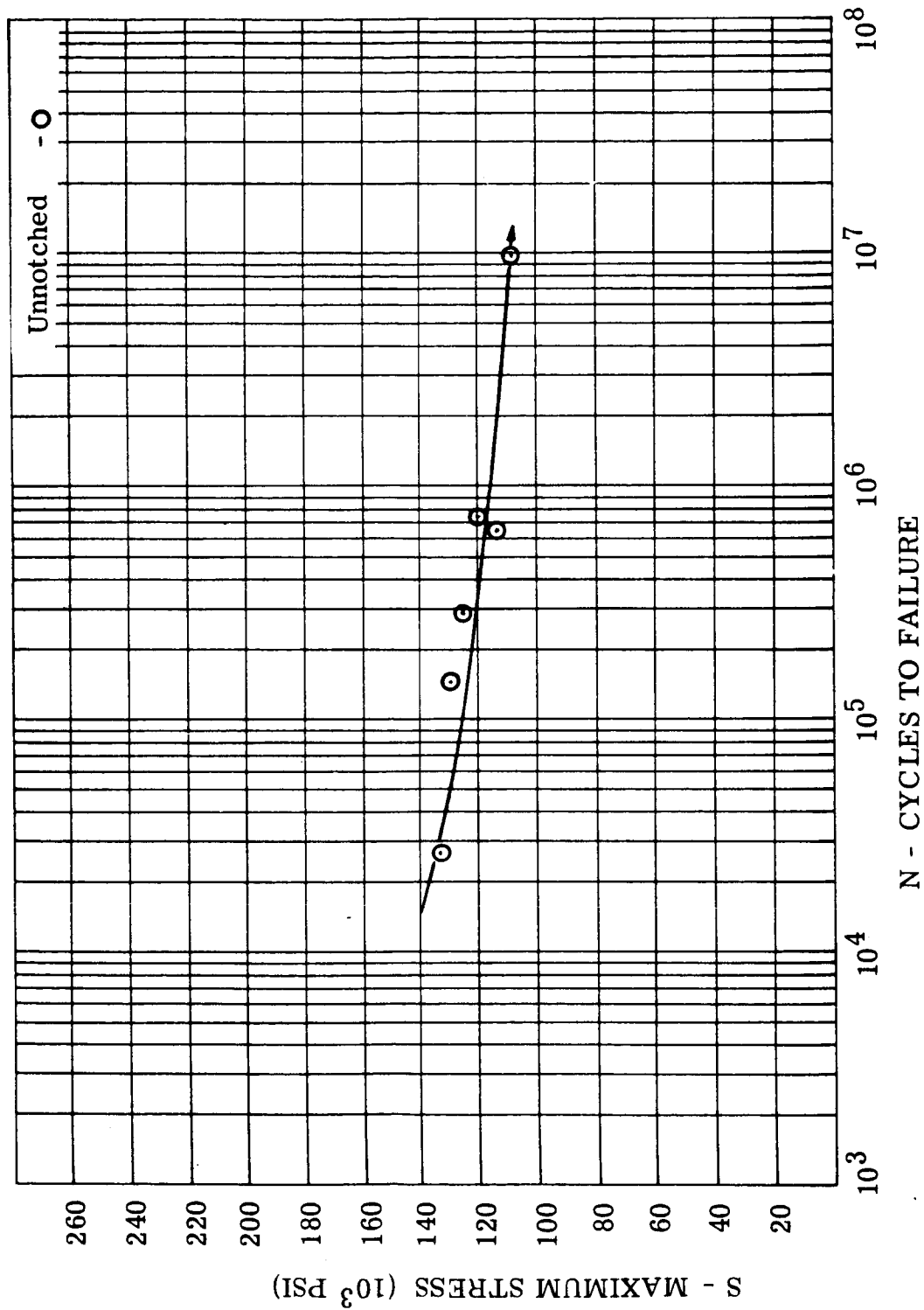


Figure II-12. Fatigue - Nivco

FIGURE II-12. S-N Diagram of Notched and Unnotched Nivco at 1100°F.  
Stress Ratio = 0.25. Tests Made in Air. (See Data Table II-3) (Reference: NAS3-4162)

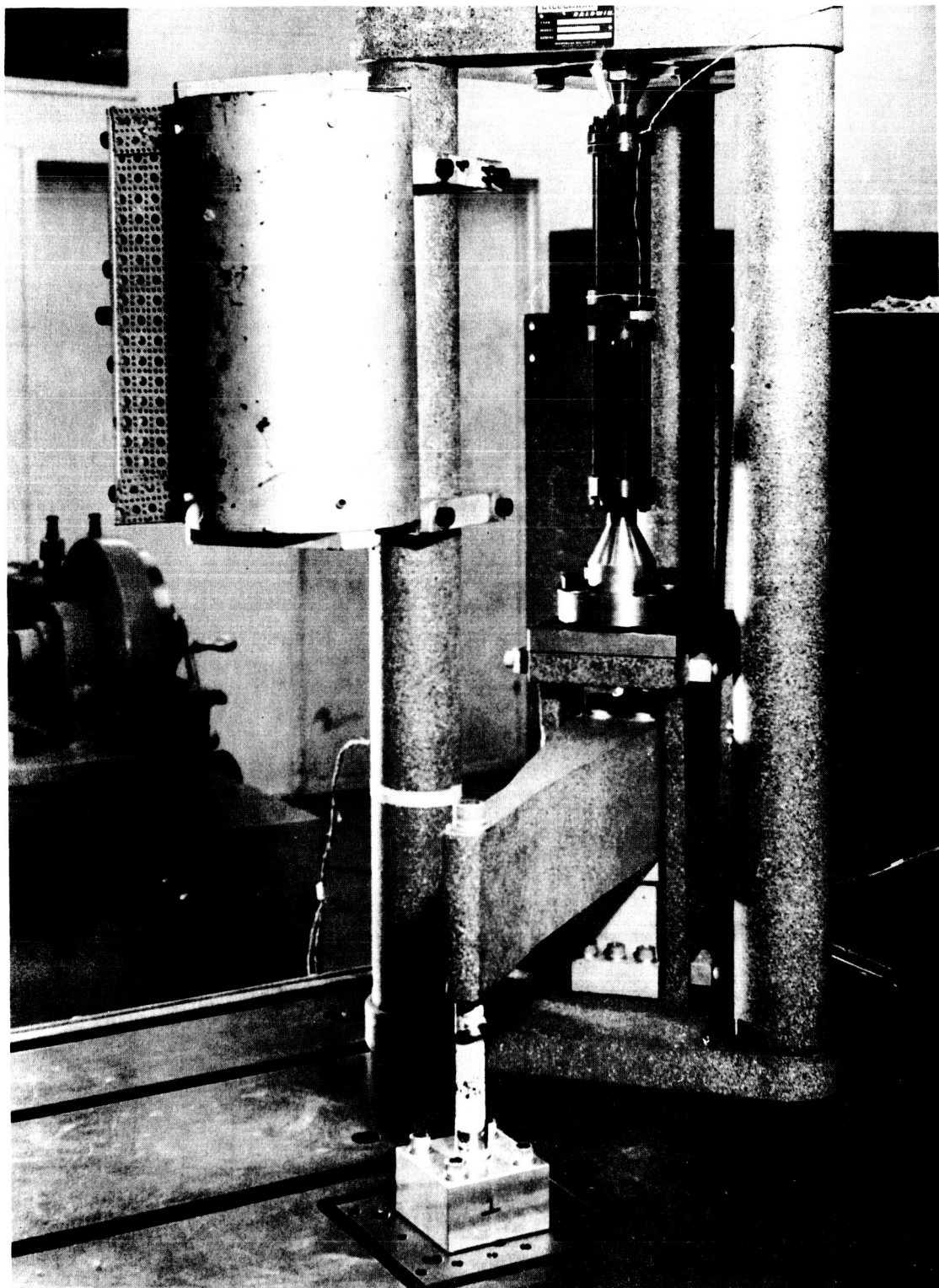


FIGURE II-13. Fatigue Test Arrangement Showing Specimen  
in Position For Testing

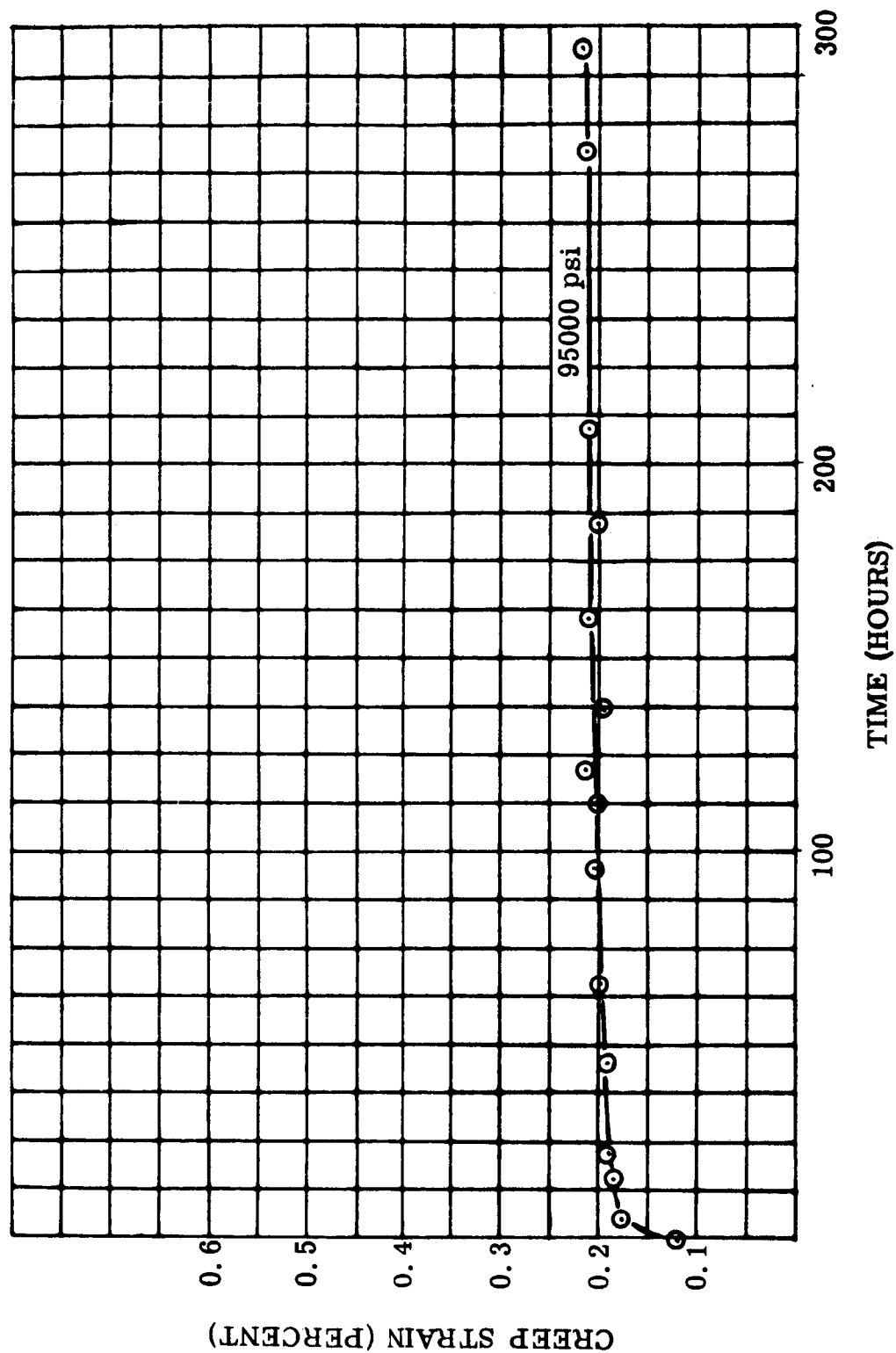


FIGURE II-14. Creep, Forged Nivco Tested in Air at 900°F. See Data Table II-5. (Reference: NAS3-4162)

Figure II-14. Creep - Nivco Bar

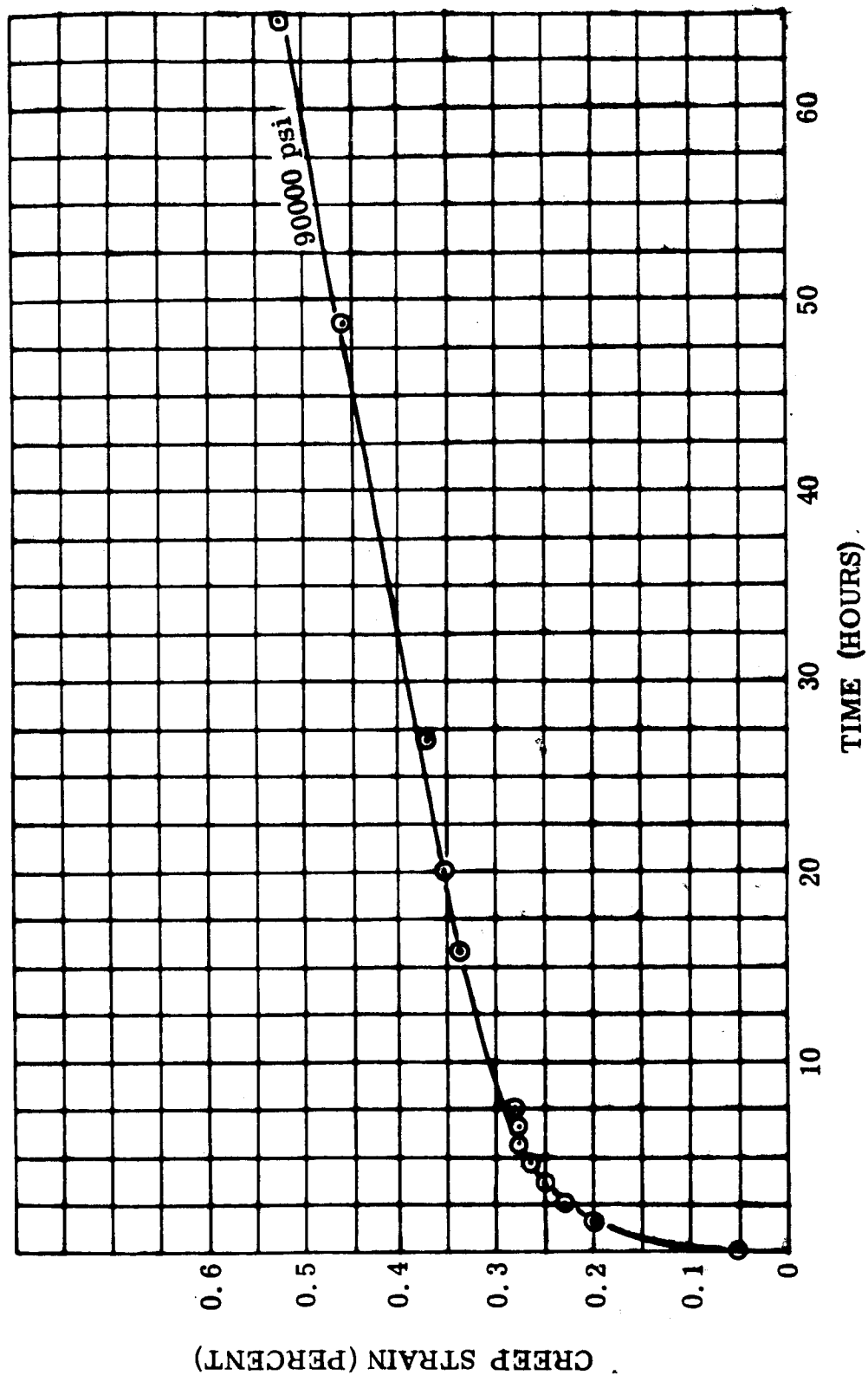


FIGURE II-15. Creep, Forged Nivco Tested in Air at 1100°F. See Data Table II-5. (Reference: NAS3-4162)

Figure II-15. Creep - Nivco Bar

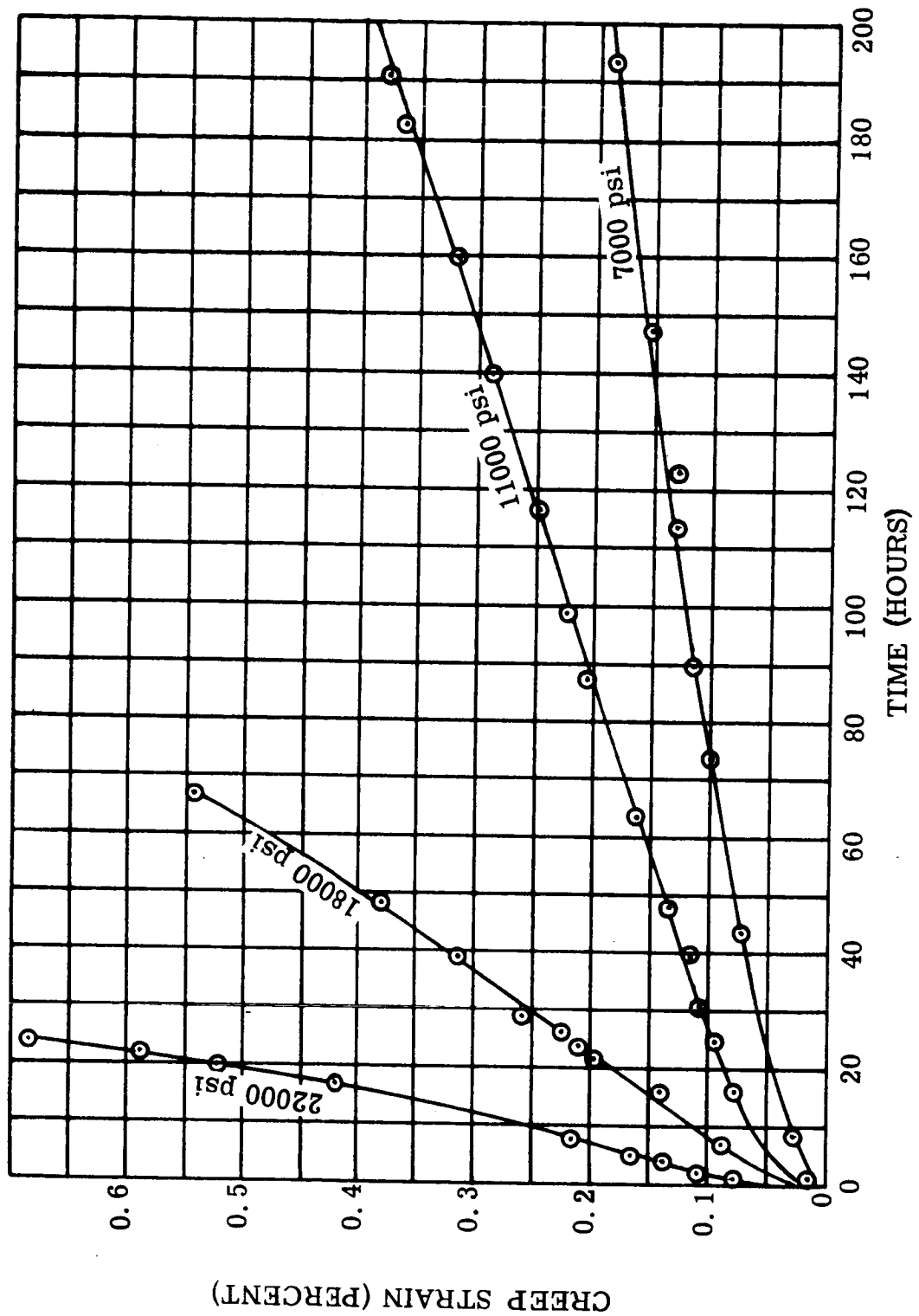


FIGURE II-16. Creep, Forged Nivco Tested in Air at 1400°F. See Data Tables II-5 and II-6. (Reference: NAS3-4162)

Figure II-16. Creep - Nivco Bar

WAED64.30E-46

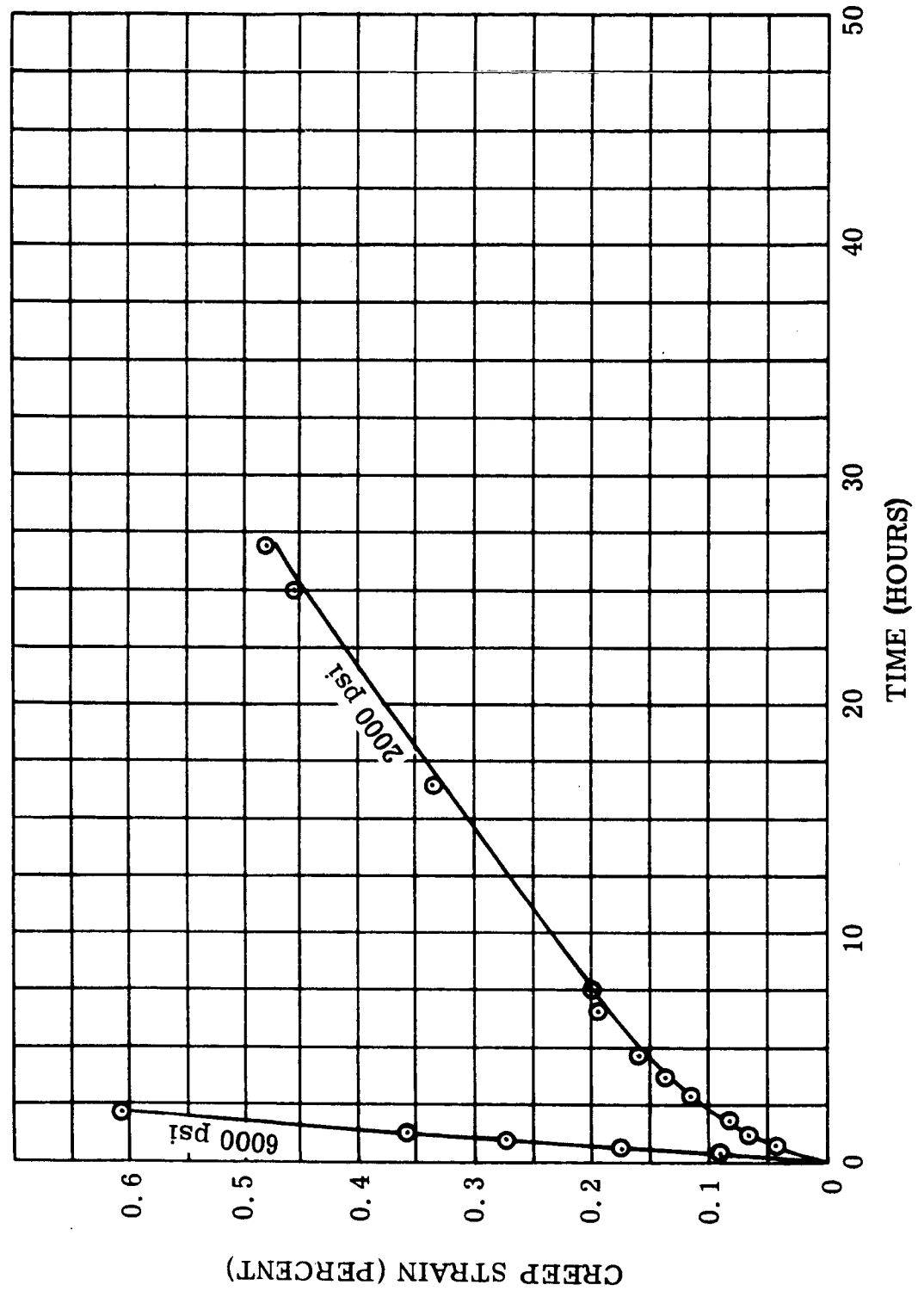


FIGURE II-17. Creep, Forged Nivco Tested in Air at 1600°F. (See Data Table II-6)(Reference: NAS3-4162)

Figure II-17. Creep - Nivco Bar



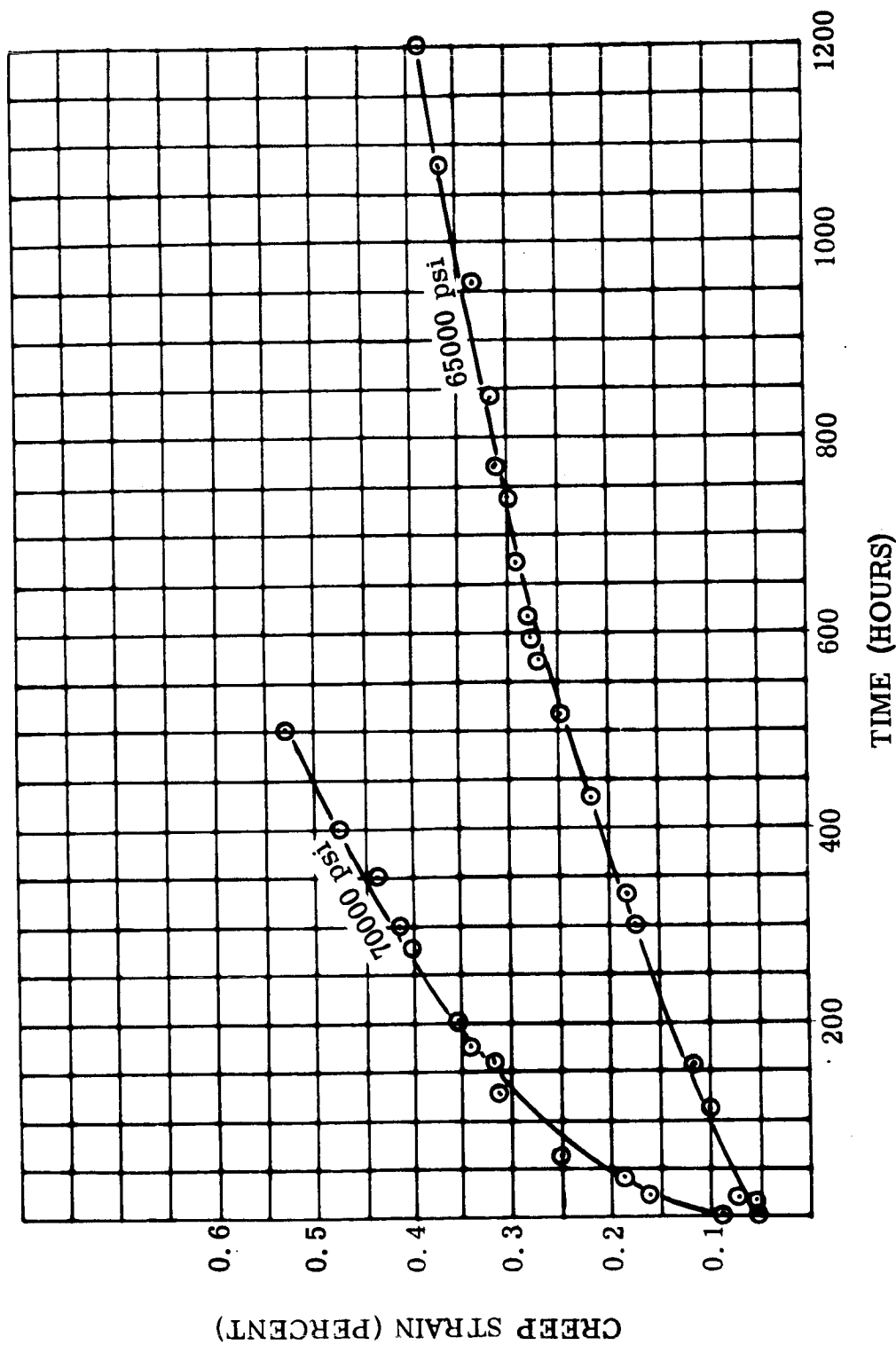


FIGURE II-18. Creep, Forged Hipercro 27 Tested in Air at 700°F  
(See Data Table II-7) (Reference: NAS3-4162)

Figure II-18. Creep - Hipercro 27

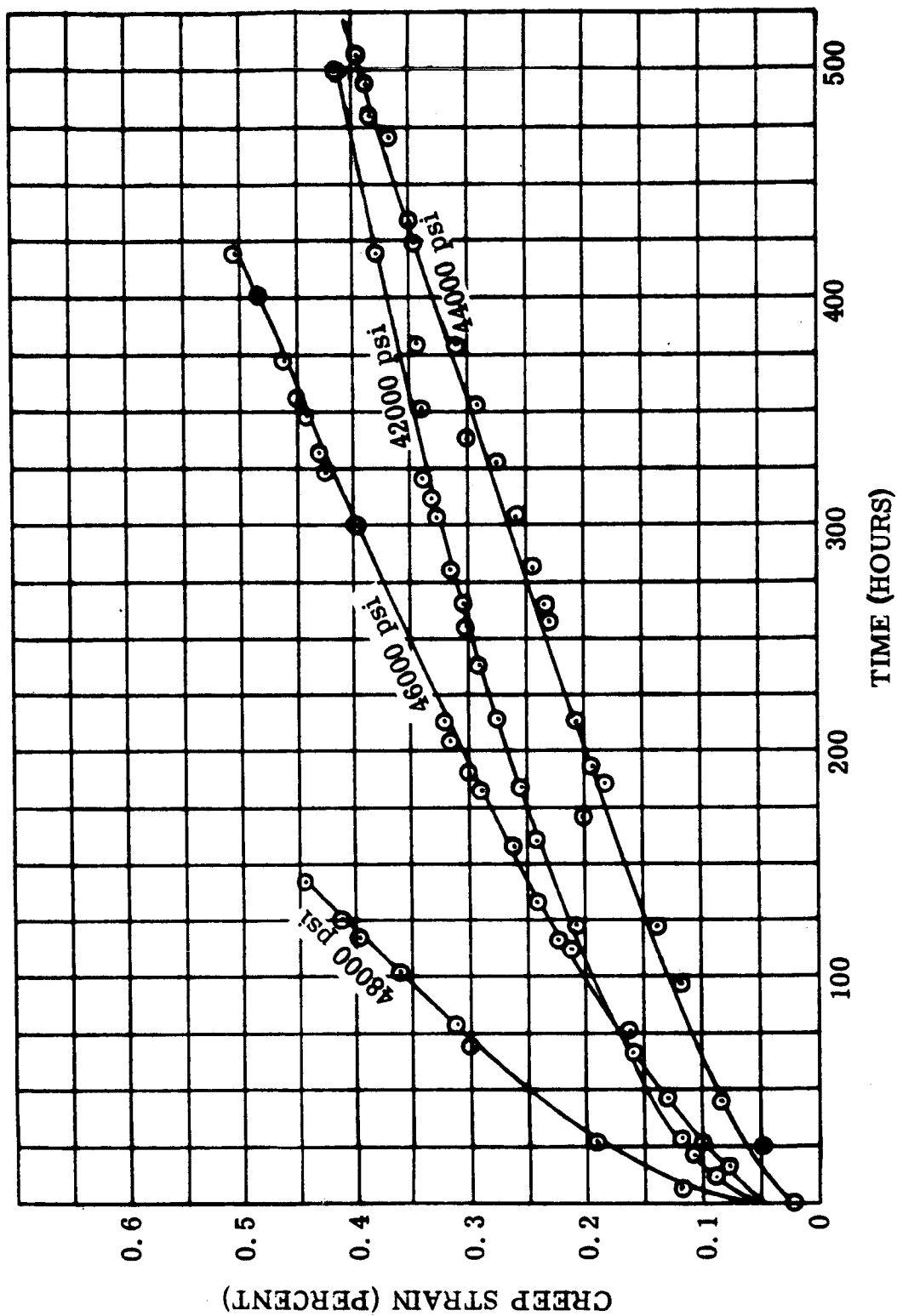


FIGURE II-19. Creep, Forged Hipercro 27 Tested in Air at 900°F (See Data Tables II-7 and II-8)(Reference NAS3-4162)

Figure II-19. Creep - Hipercro 27

WAED64. 30E-49

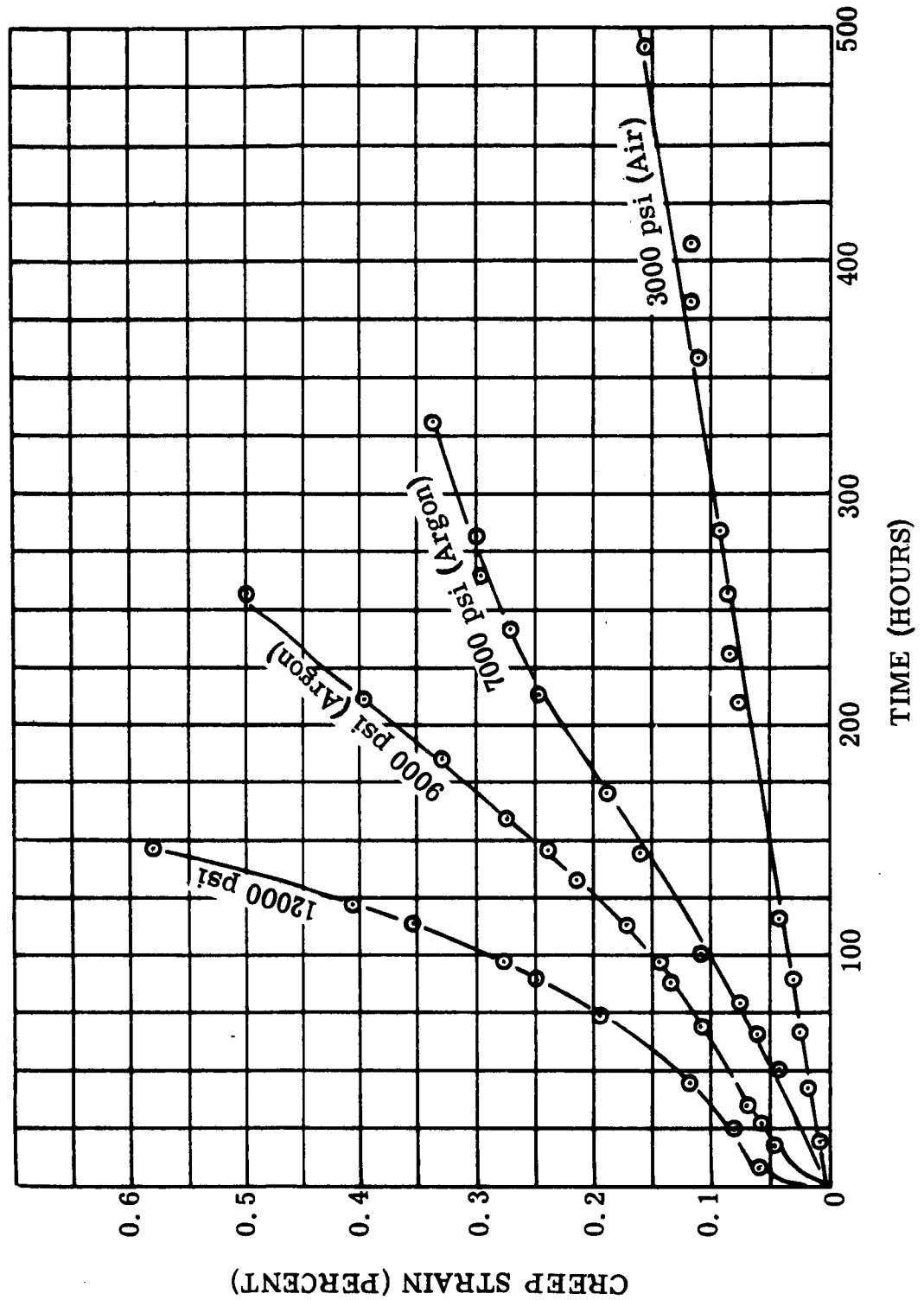


FIGURE II-20. Creep, Forged Hipercro 27 Tested in Air and Argon at 1100°F. See Data Table II-8. (Reference:NAS3-4162)

Figure II-20. Creep - Hipercro 27

WAED64. 30E-50

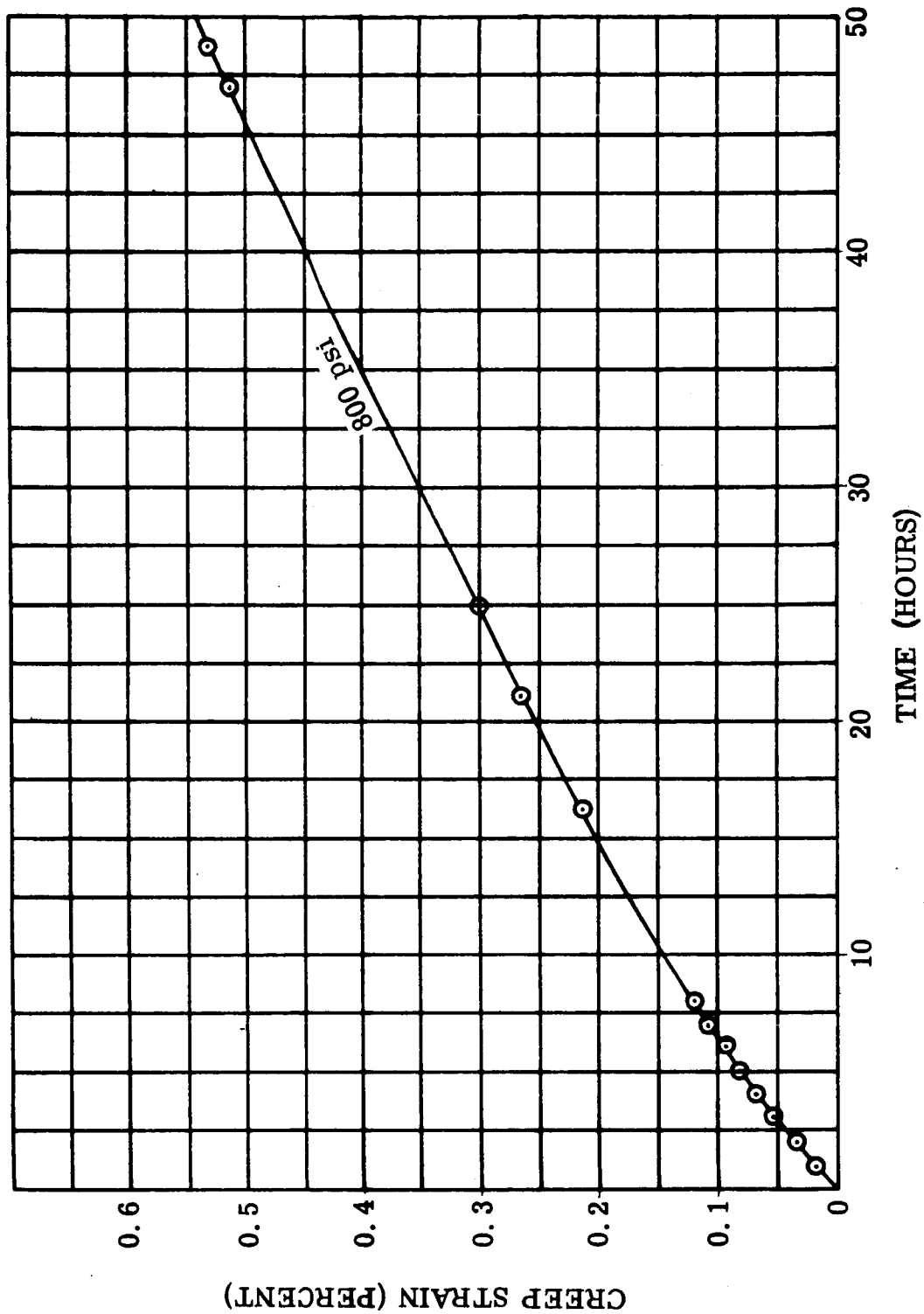


FIGURE II-21. Creep, Forged Hipercro 27 Tested in Argon at 1400°F.  
See Data Table II-8. (Reference: NAS3-4162)

Figure II-21. Creep - Hipercro 27

WAED64. 30E-51

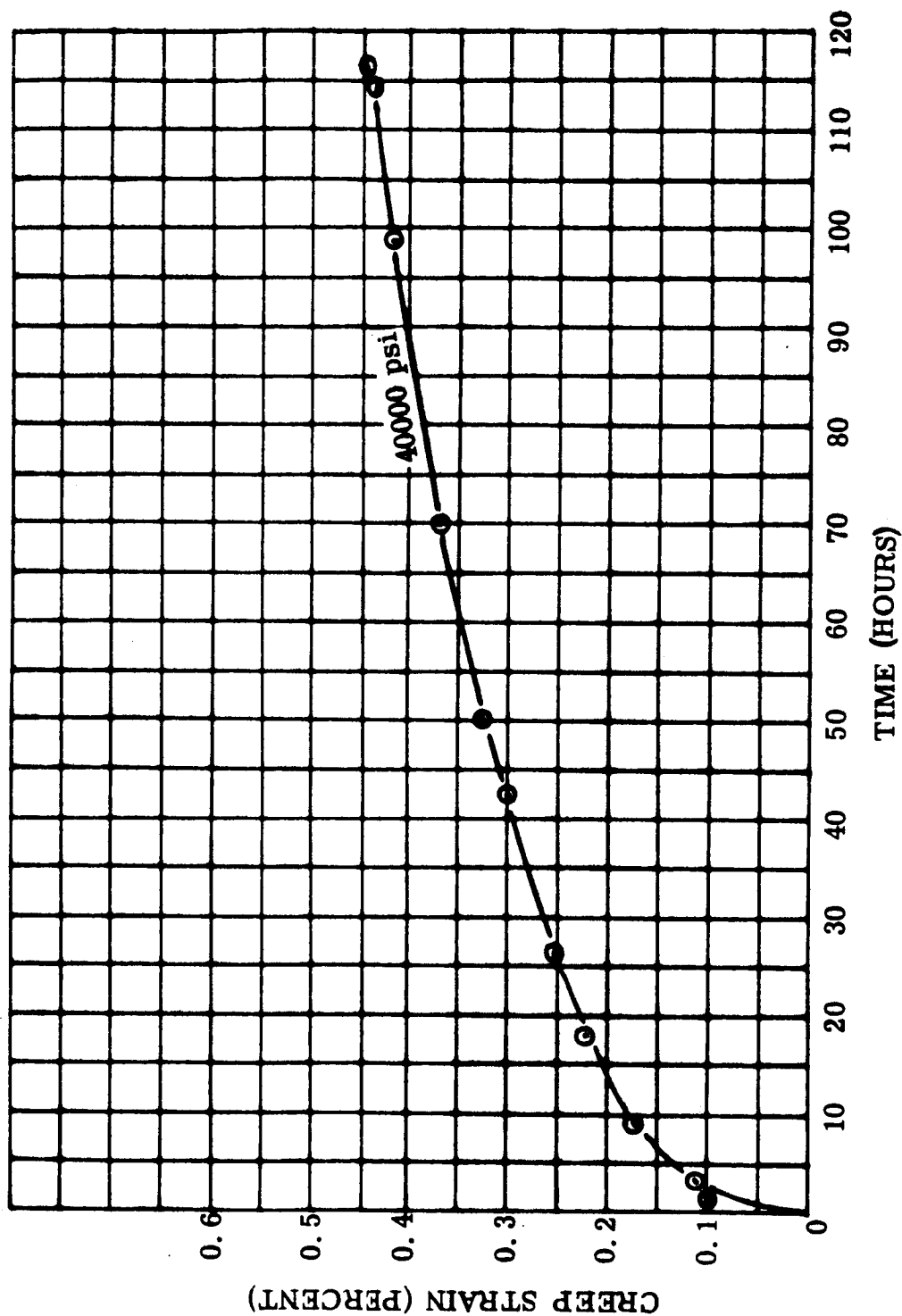


FIGURE II-22. Creep, Nivco Sheet 0.025 inch Thick (Transverse) Tested in Air at 900°F. See Data Table II-9. (Reference: NAS3-4162)

Figure II-22. Creep - Nivco Sheet

WAED64.30E-52

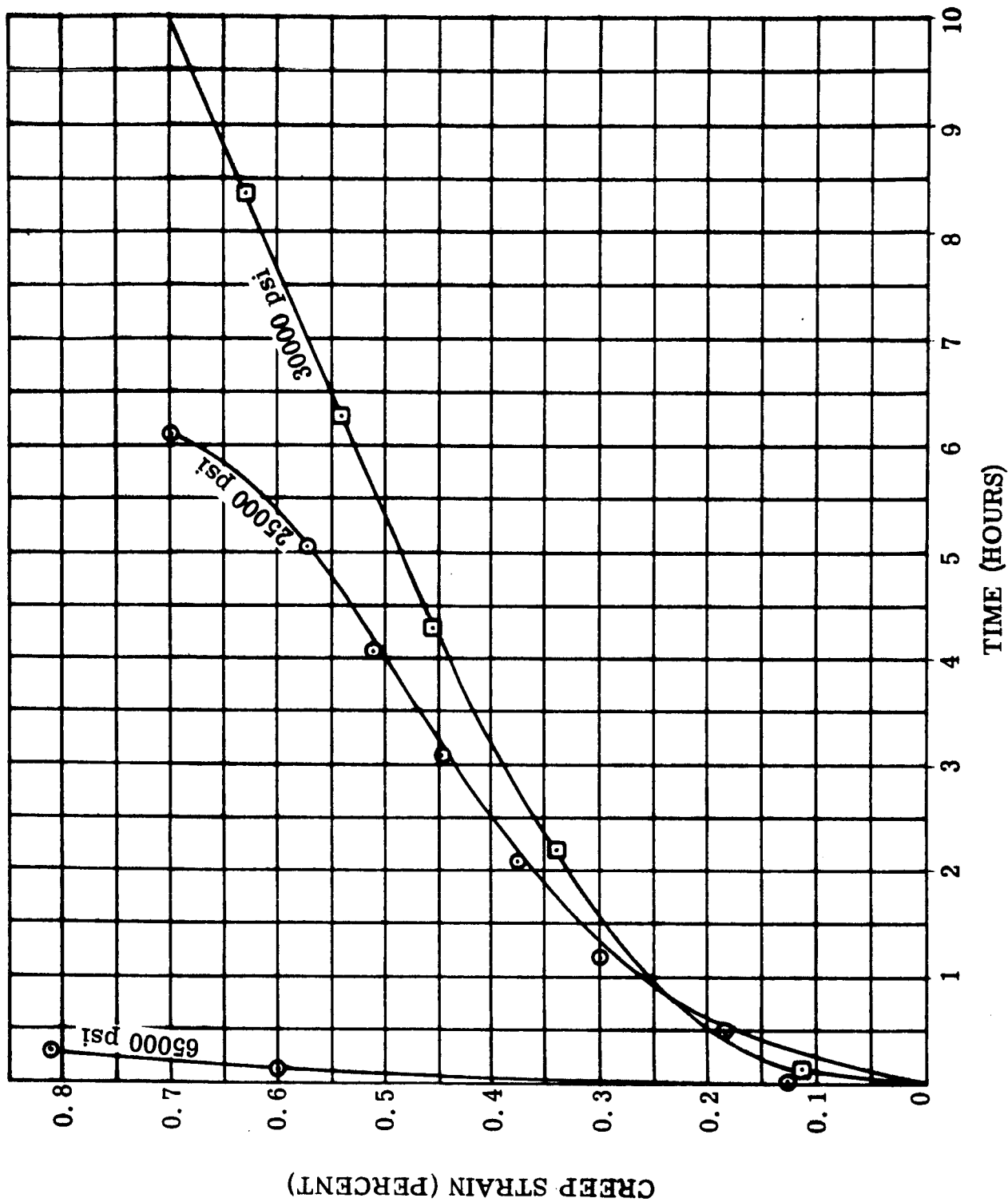


FIGURE II-23. Creep, Nivco Sheet 0.025 inch Thick (Transverse) Tested in Air at 1100°F. See Data Table II-9. (Reference: NAS3-4162)

Figure II-23. Creep - Nivco Sheet

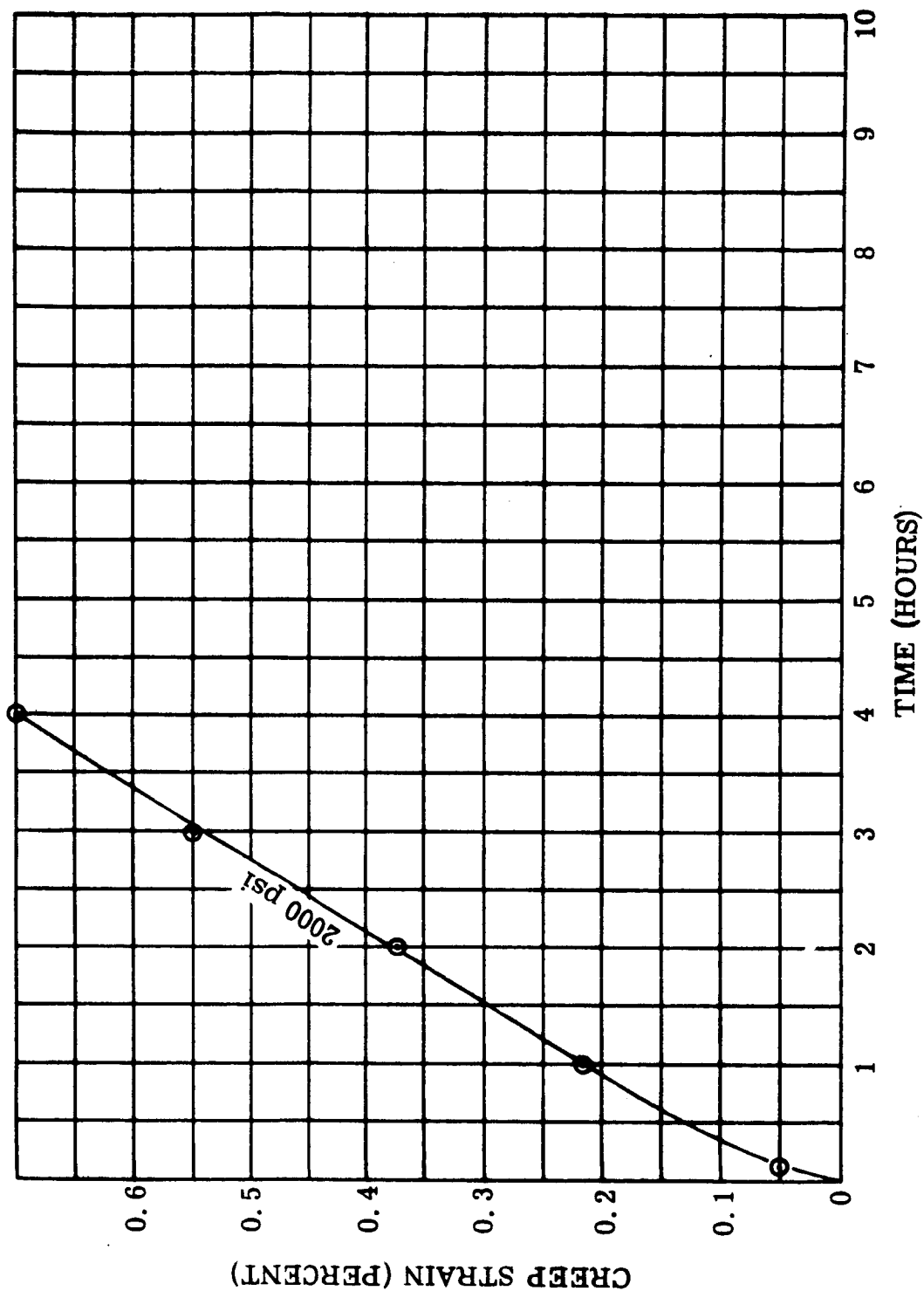


FIGURE II-24. Creep, Nivco Sheet 0.025 inch Thick (Transverse) Tested in Air at 1400°F. See Data Table II-9. (Reference: NAS3-4162)

Figure II-24. Creep - Nivco Sheet

WAED64. 30E-54

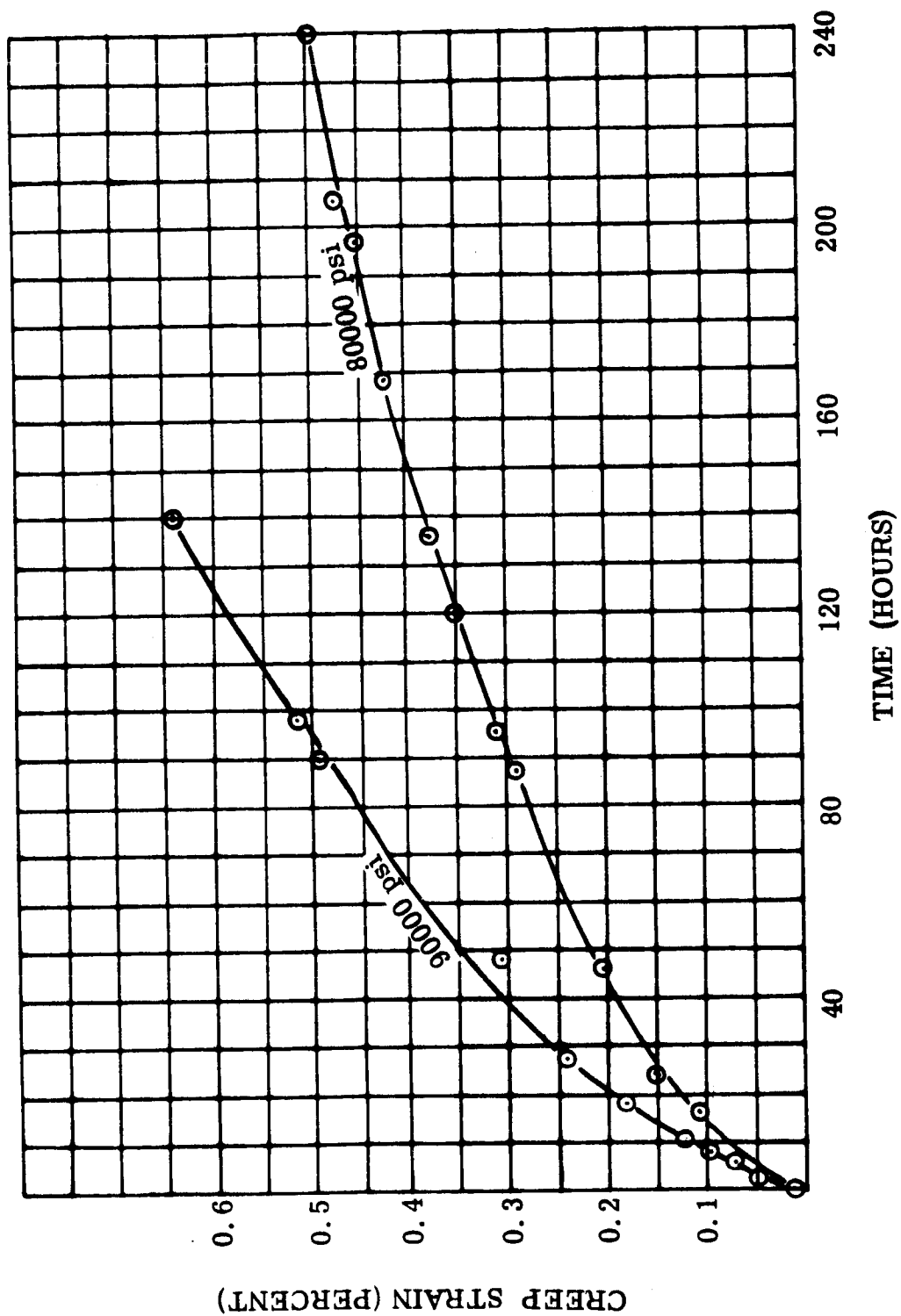


FIGURE II-25. Creep, Forged Maraging Steel (15 Percent Nickel) Tested in Air at 900°F. See Data Table II-10. (Reference: NAS3-4162)

Figure II-25. Creep - Maraging Steel



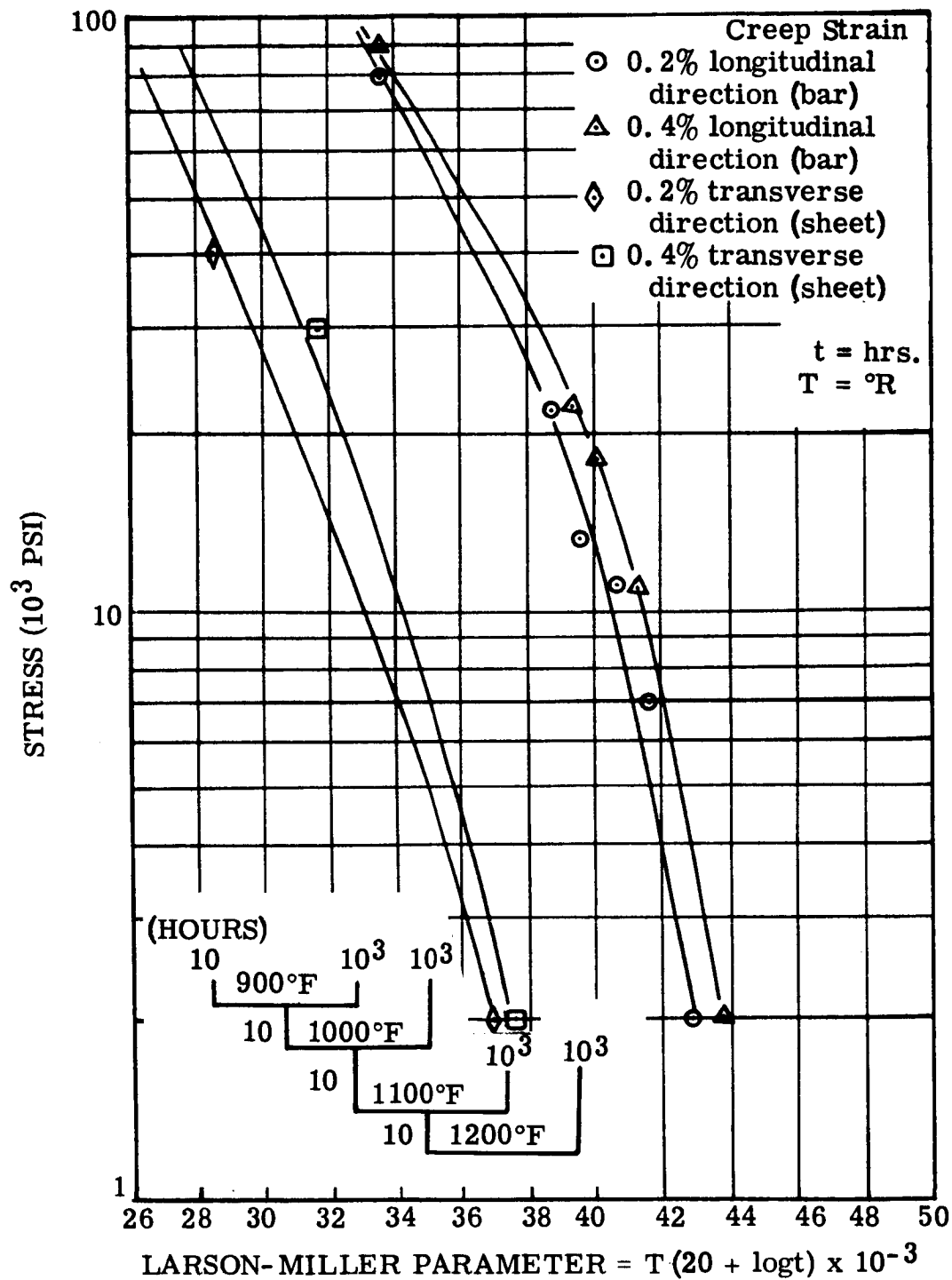


FIGURE II-26. Larson-Miller Plot of Forged Bar and Sheet Nivco Creep Data, Tested in Air. (Reference: NAS3-4162)

Figure II-26. Creep - Larson-Miller Plot - Nivco

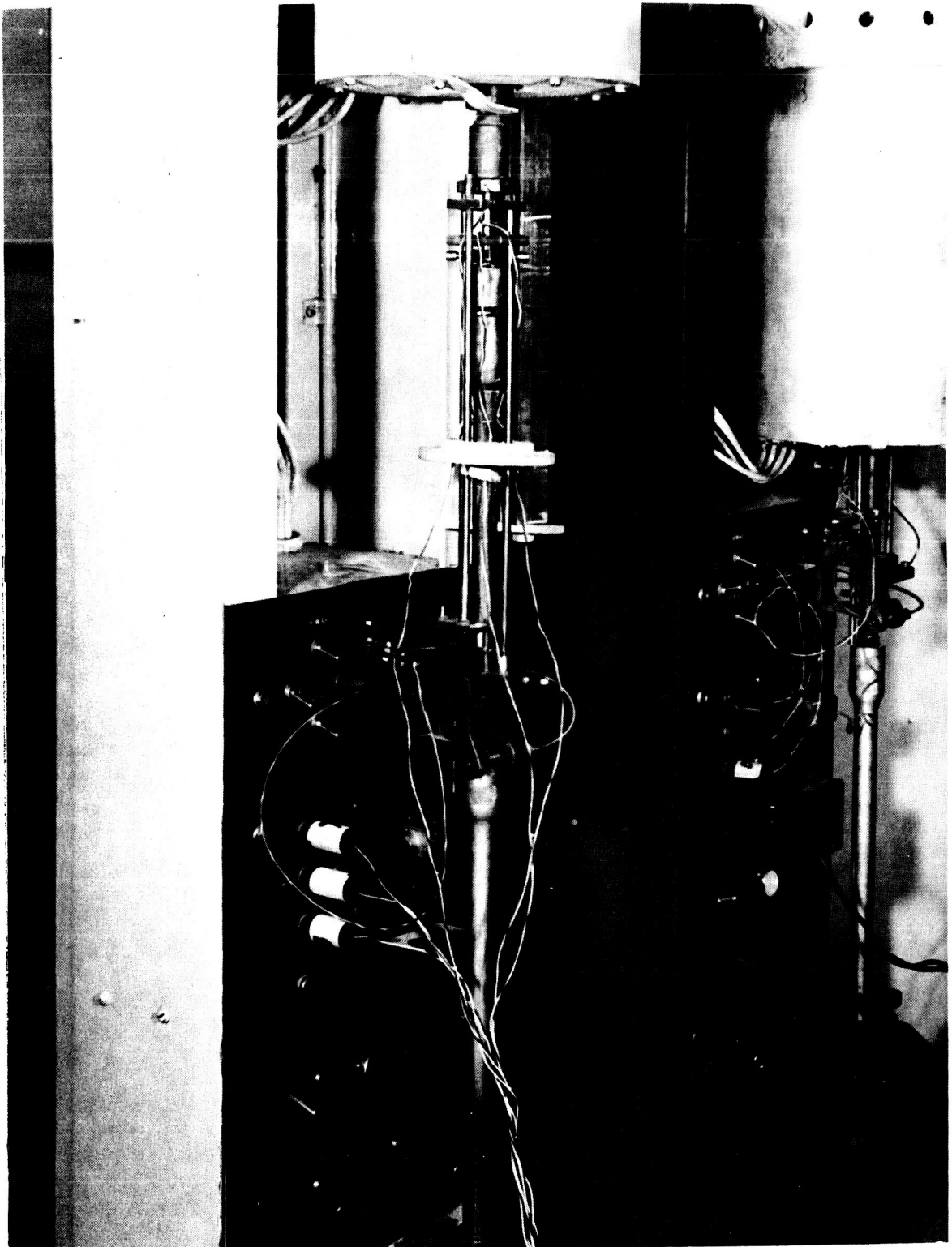


FIGURE II-27. Creep Test Arrangement Showing Extensometer and Thermocouples Attached to Specimen

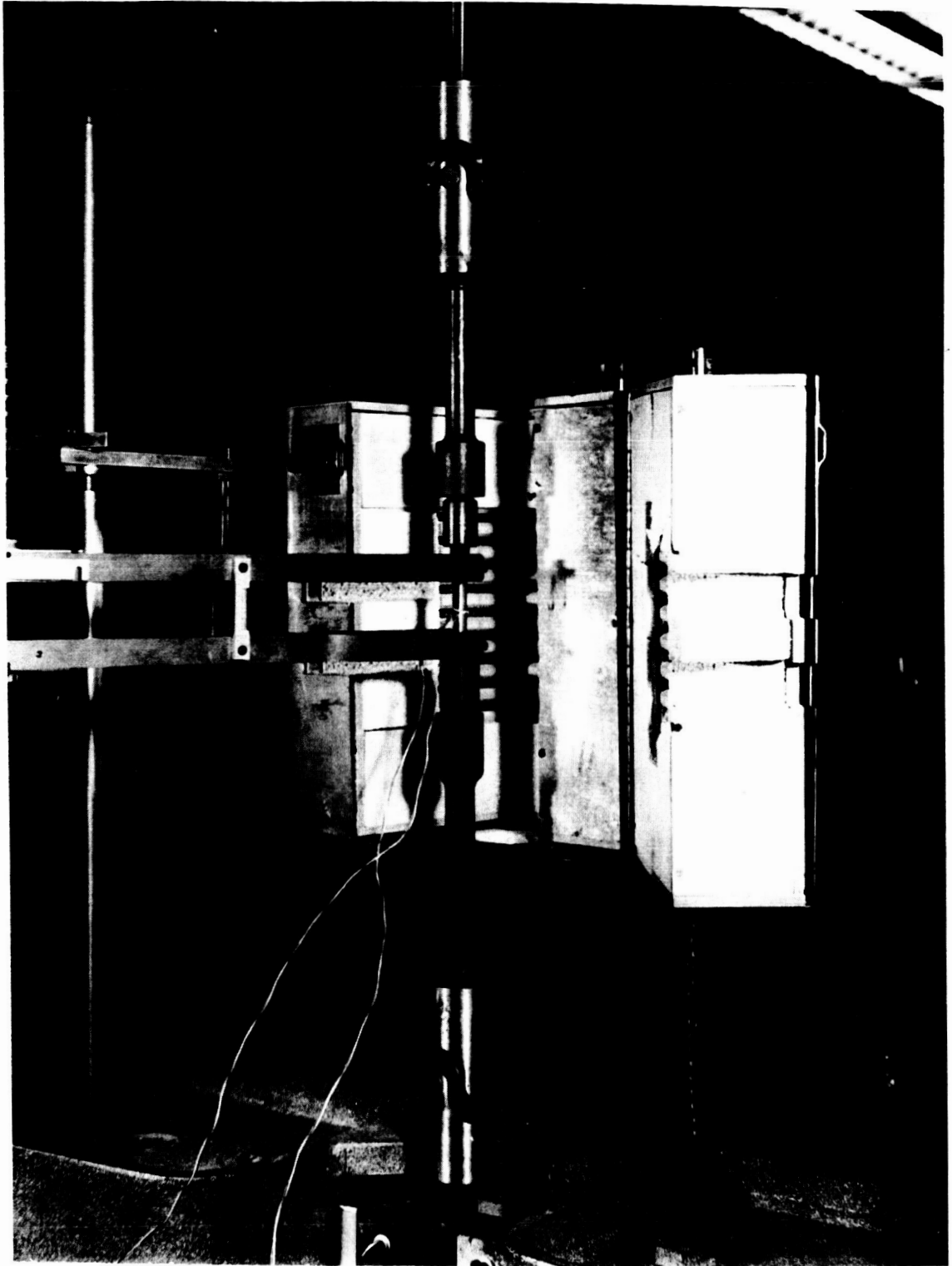


FIGURE II-28. Tension Test Specimen in Position For Testing,  
With Extensometer in Place

WAED64. 30E-58

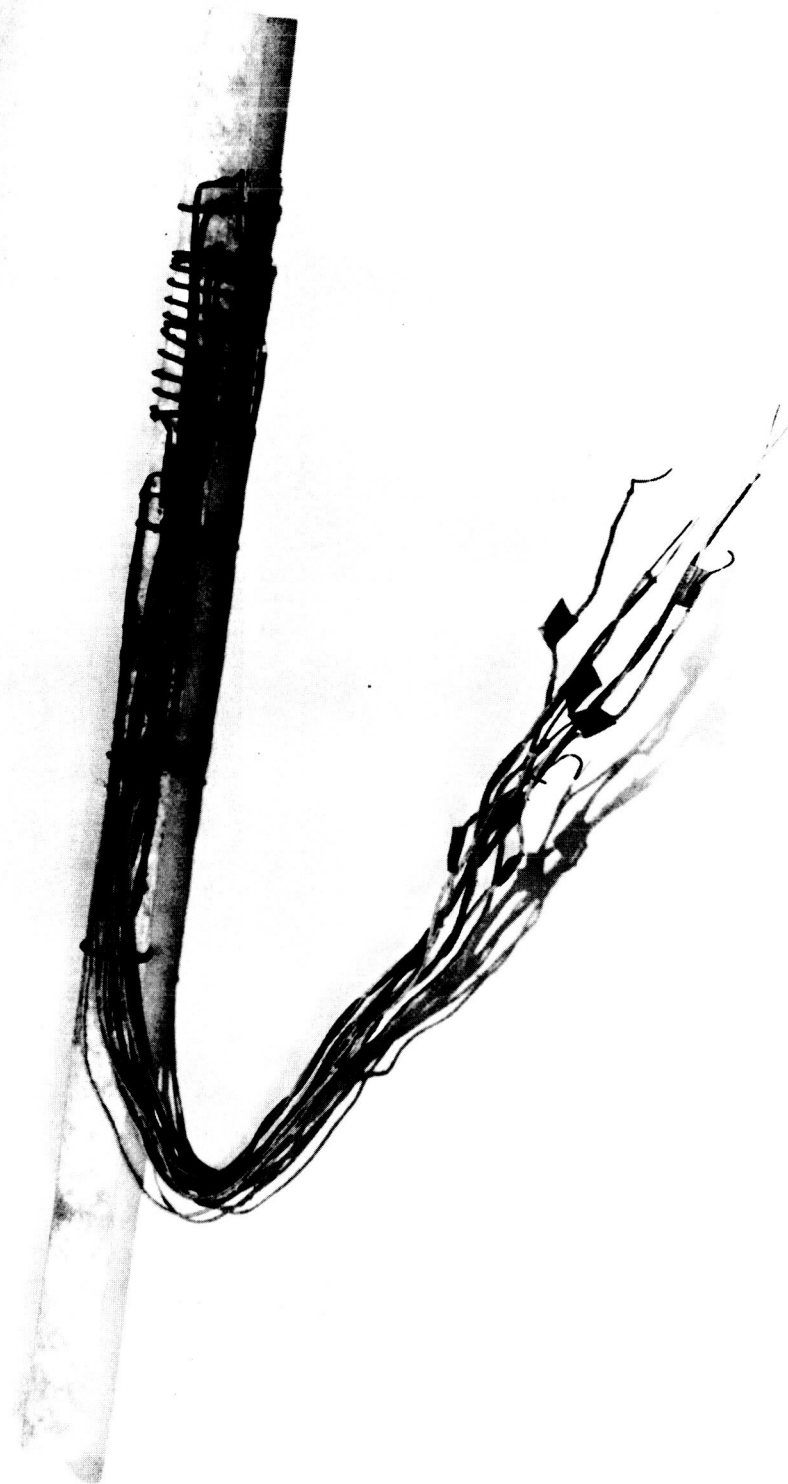


FIGURE II-29. Resistivity Specimen Wrapped on Quartz Mandrel,  
With Leads and Thermocouples Attached

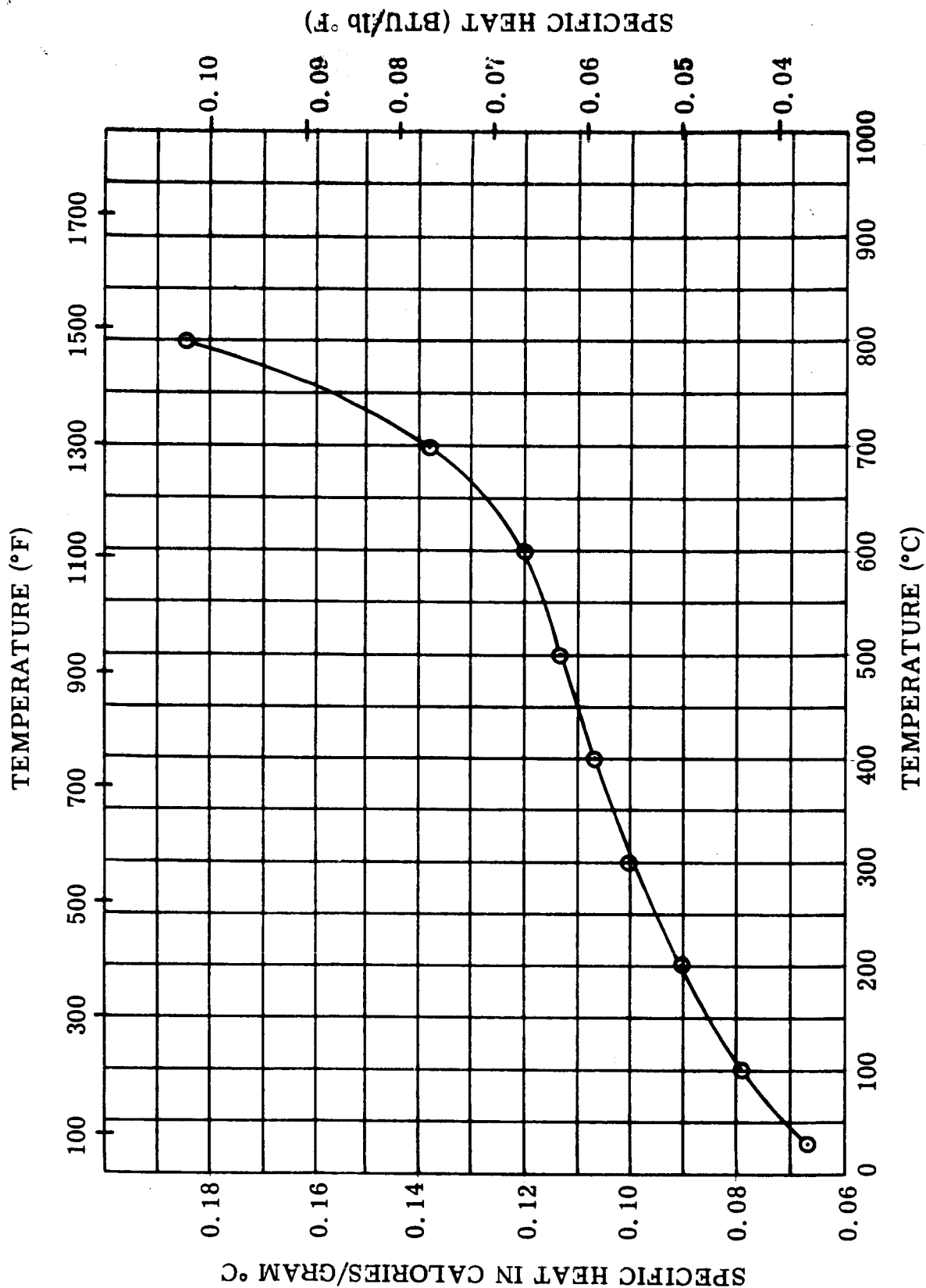


Figure II-30. Specific Heat - Hipercó 27

FIGURE II-30. Specific Heat, Forged Hipercó 27 in Vacuum (10<sup>-5</sup> torr) (Reference: NAS3-4162)

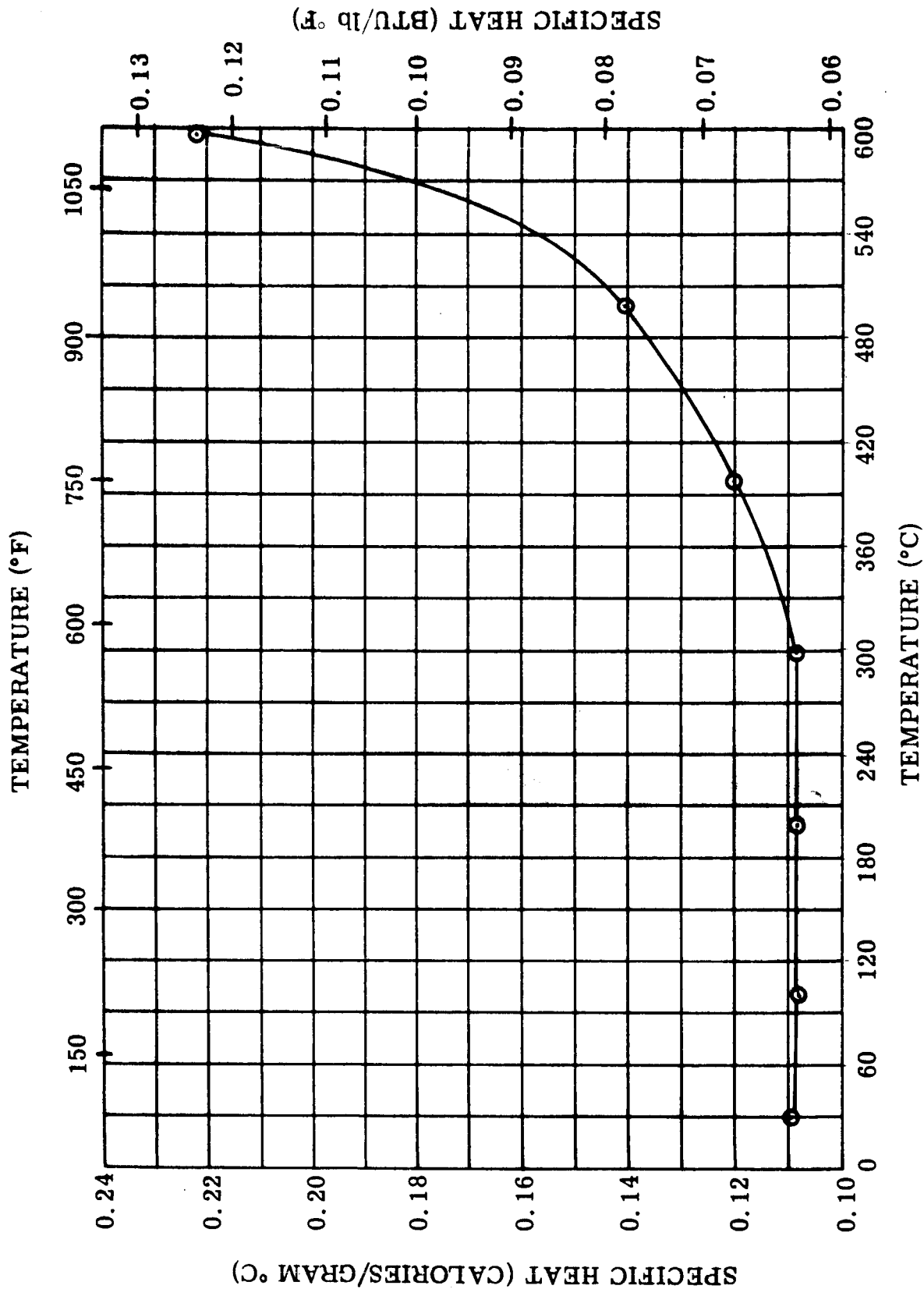


FIGURE II-31. Specific Heat, Cubex in Vacuum (10<sup>-5</sup> torr) (Reference: NAS3-4162)

Figure II-31. Specific Heat - Cubex

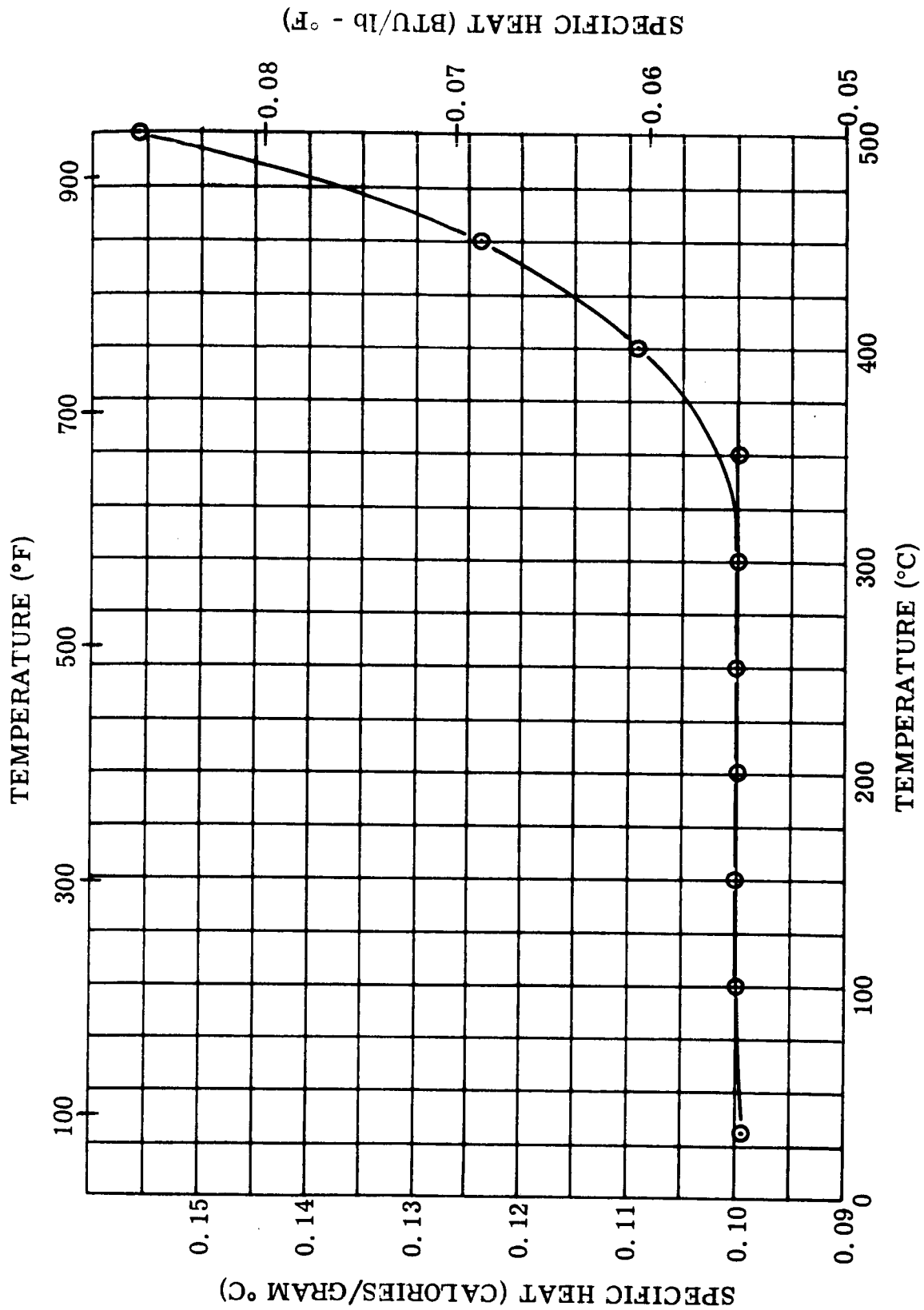


FIGURE II-32. Specific Heat, 1% Silicon Iron in Vacuum ( $10^{-5}$  torr)  
(Reference: NAS3-4162)

Figure II-32. Specific Heat Investment Cast Silicon Iron

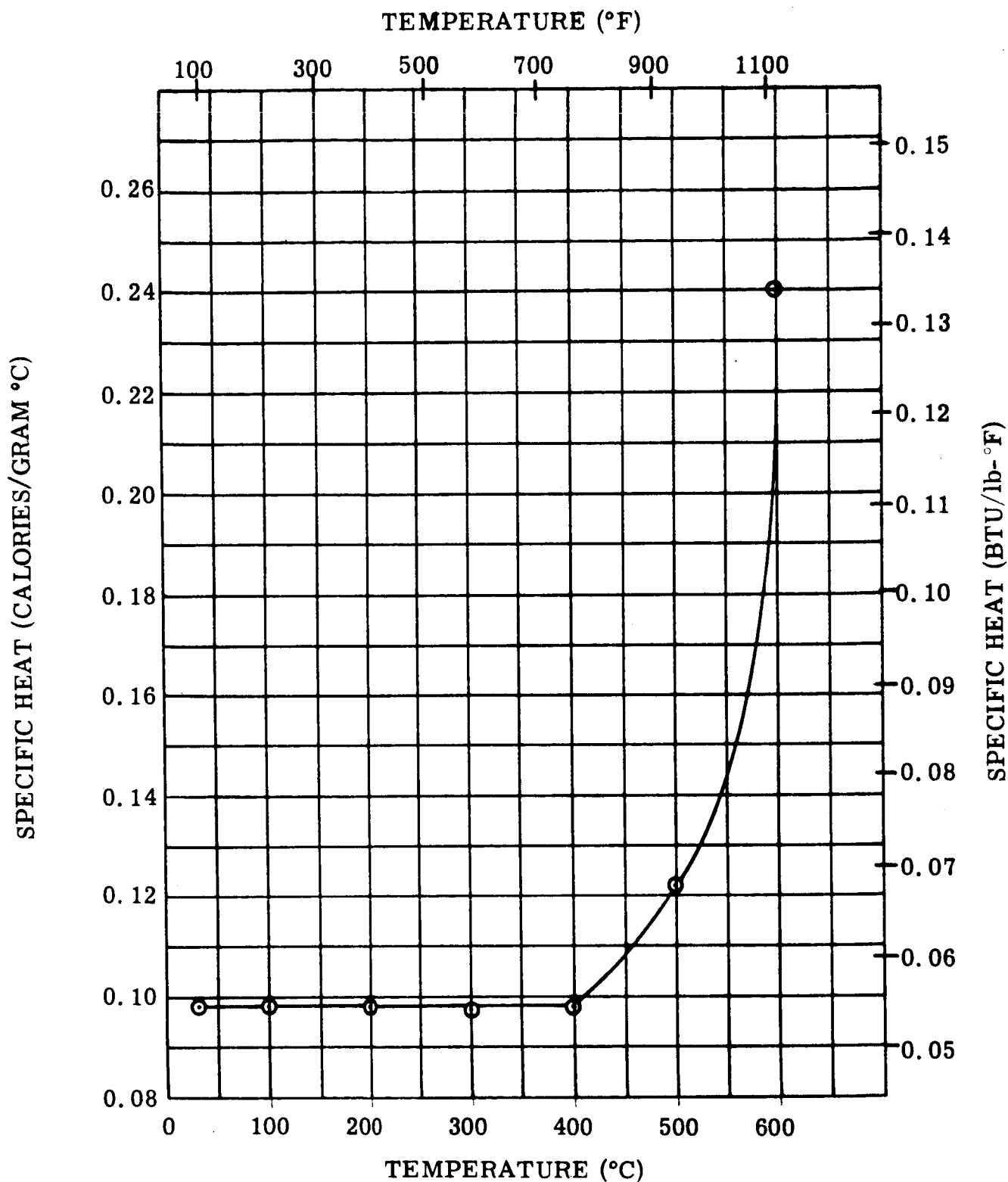


FIGURE II-33. Specific Heat, Supermendur Rolling Stock in Vacuum ( $10^{-5}$  torr) (Reference: NAS3-4162)

Figure II-33. Specific Heat - Supermendur



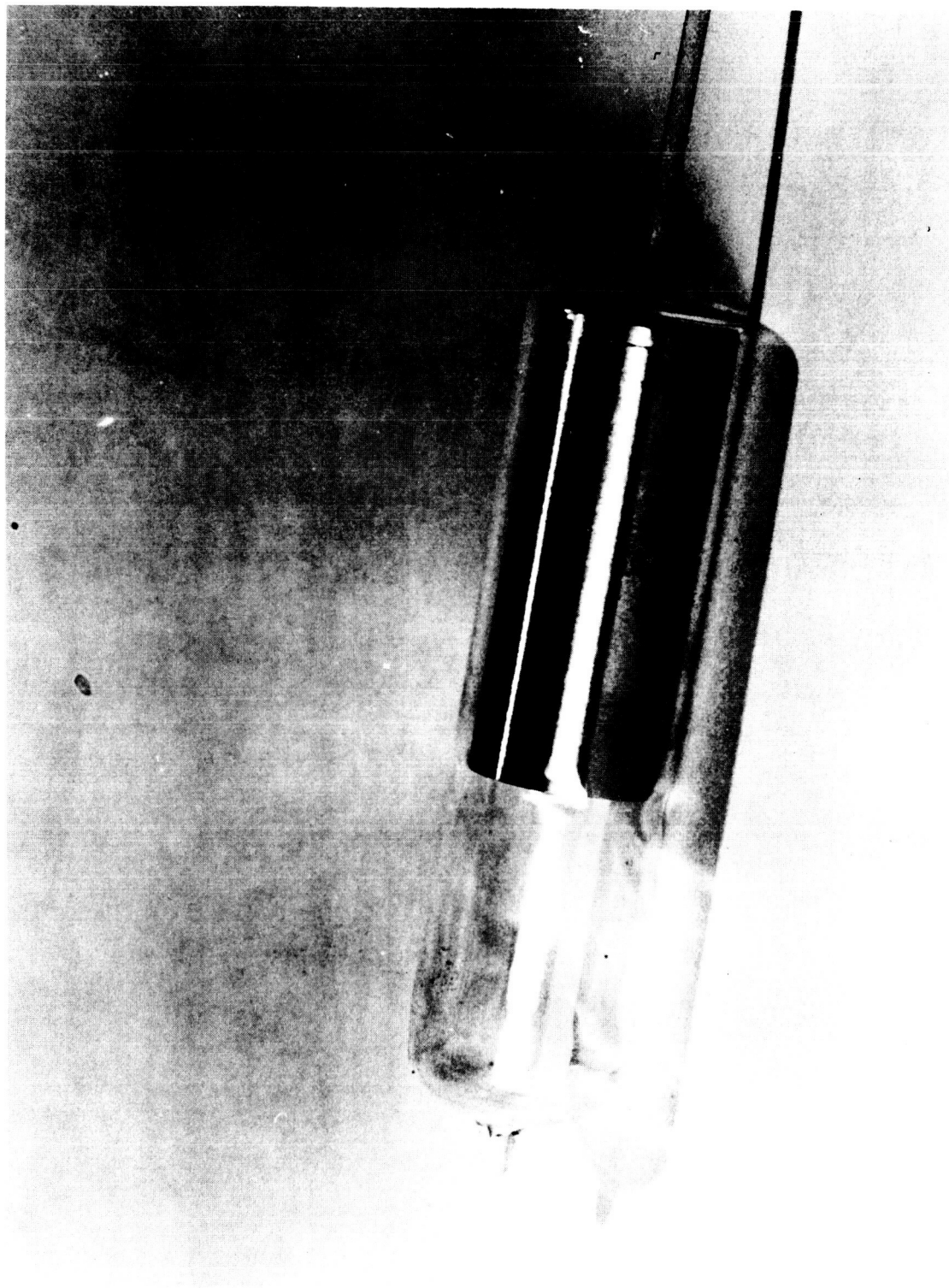


FIGURE II-34. Specific Heat Specimen in Evacuated Quartz Capsule.  
Insulated Thermocouple is Inserted in Well at Right.  
The Specimen is  $1\frac{1}{16}$ " Diameter By  $2\frac{1}{2}$ " Long.

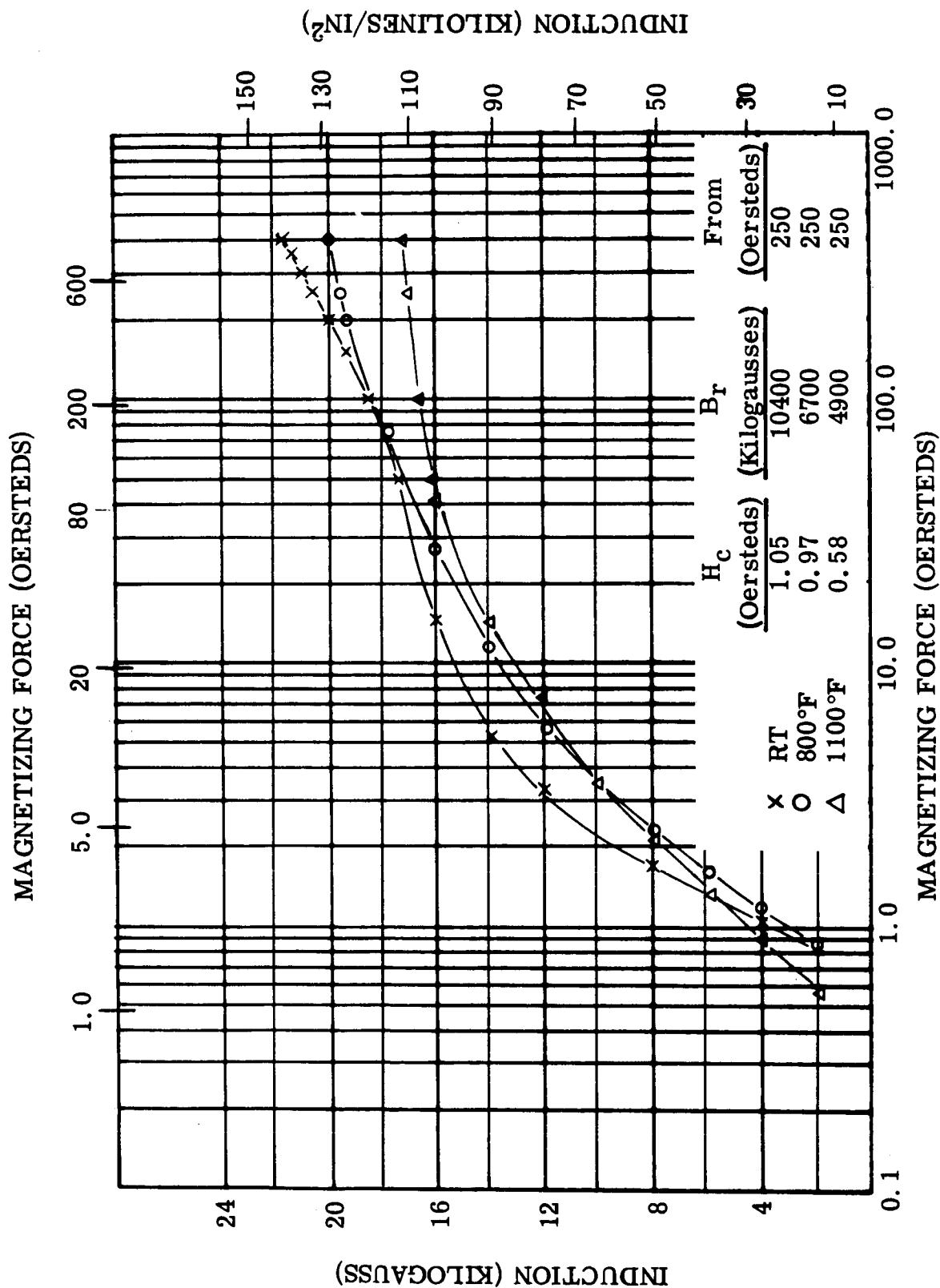


FIGURE II-35. DC Magnetization Curves for AMS5210 (1% Si-Fe) Casting, Ring 4-7/8 x 3-7/8 x 1/2 inch. Test Atmosphere: Air to 800°F, Argon above 800°F. (Reference: NAS3-4162)

Figure II-35. DC Magnetization - AMS5210

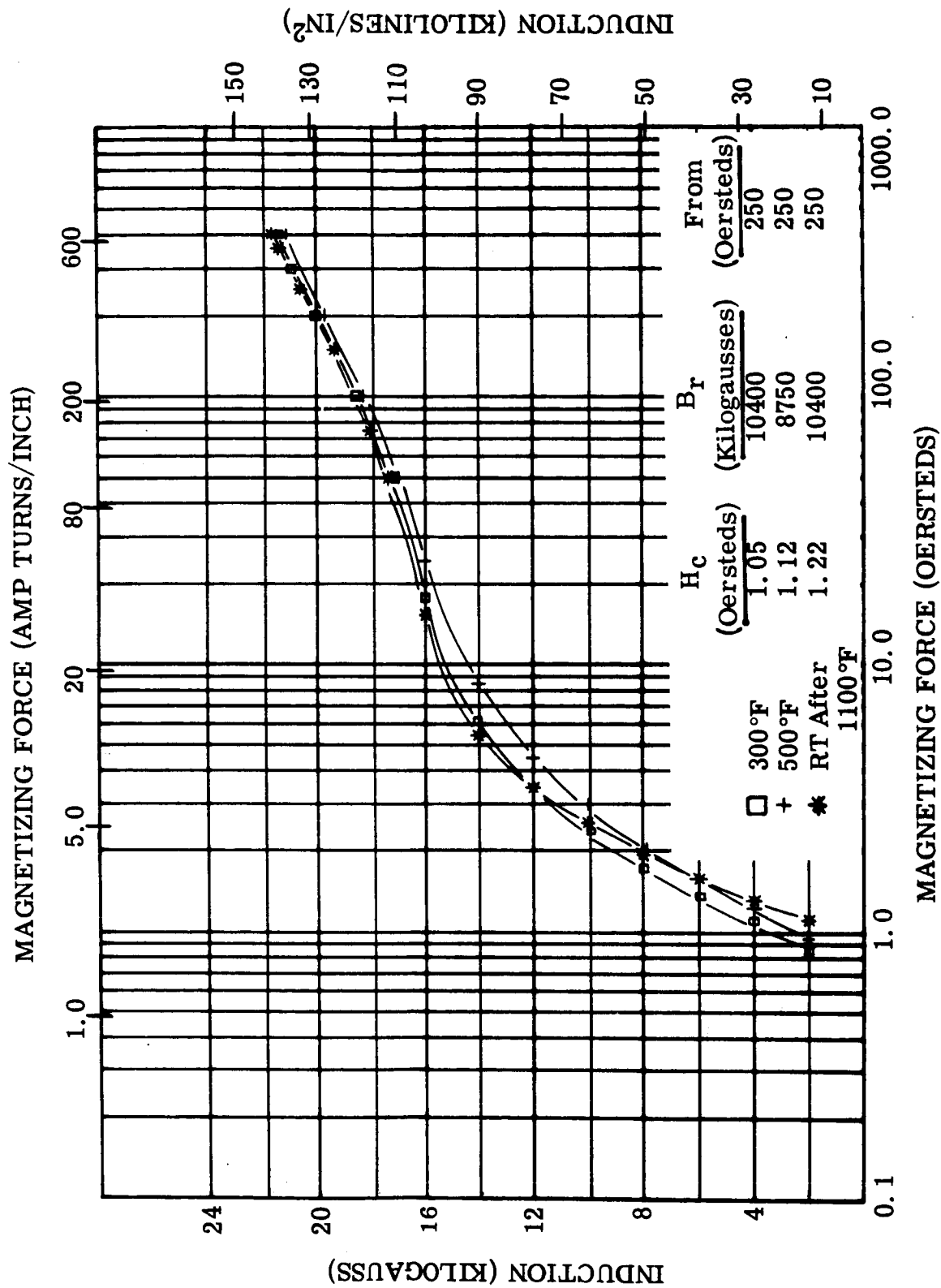


Figure II-36. DC Magnetization - AMS5210 Casting

FIGURE II-36. DC Magnetization Curves for AMS5210 (1% Si-Fe) Casting, Ring 4-7/8 x 3-7/8 x 1/2 inch. Test Atmosphere: Air to 800°F, Argon above 800°F. (Reference: NAS3-4162)

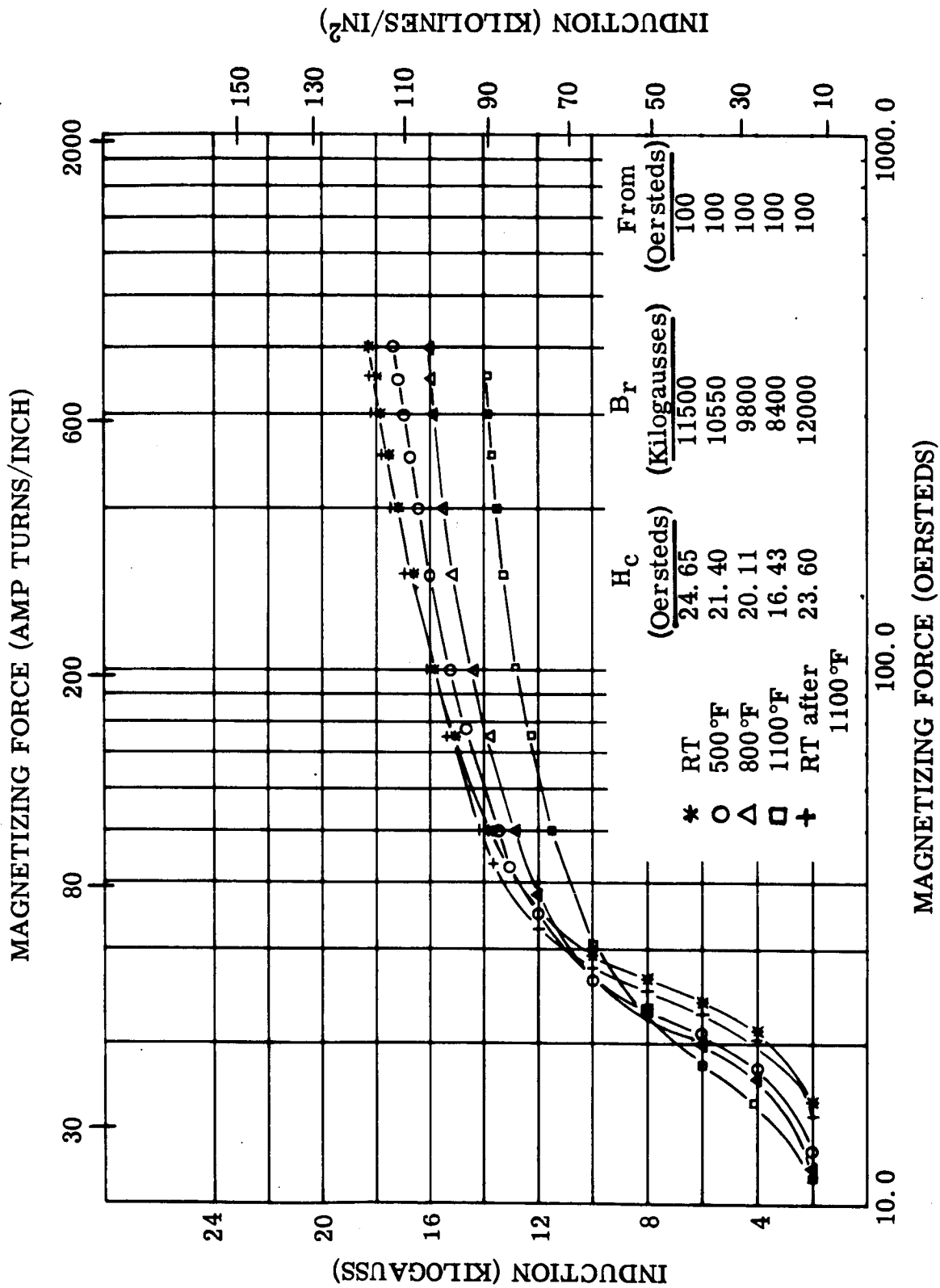


Figure II-37. DC Magnetization - H-11 Steel Forging

FIGURE II-37. DC Magnetization Curves for H-11 Steel Forging, Ring 4-7/8 x 3-7/8 x 1/2 inch. Test Atmosphere: Air to 500° F, Argon above 500°F (Reference: NAS3-4162)

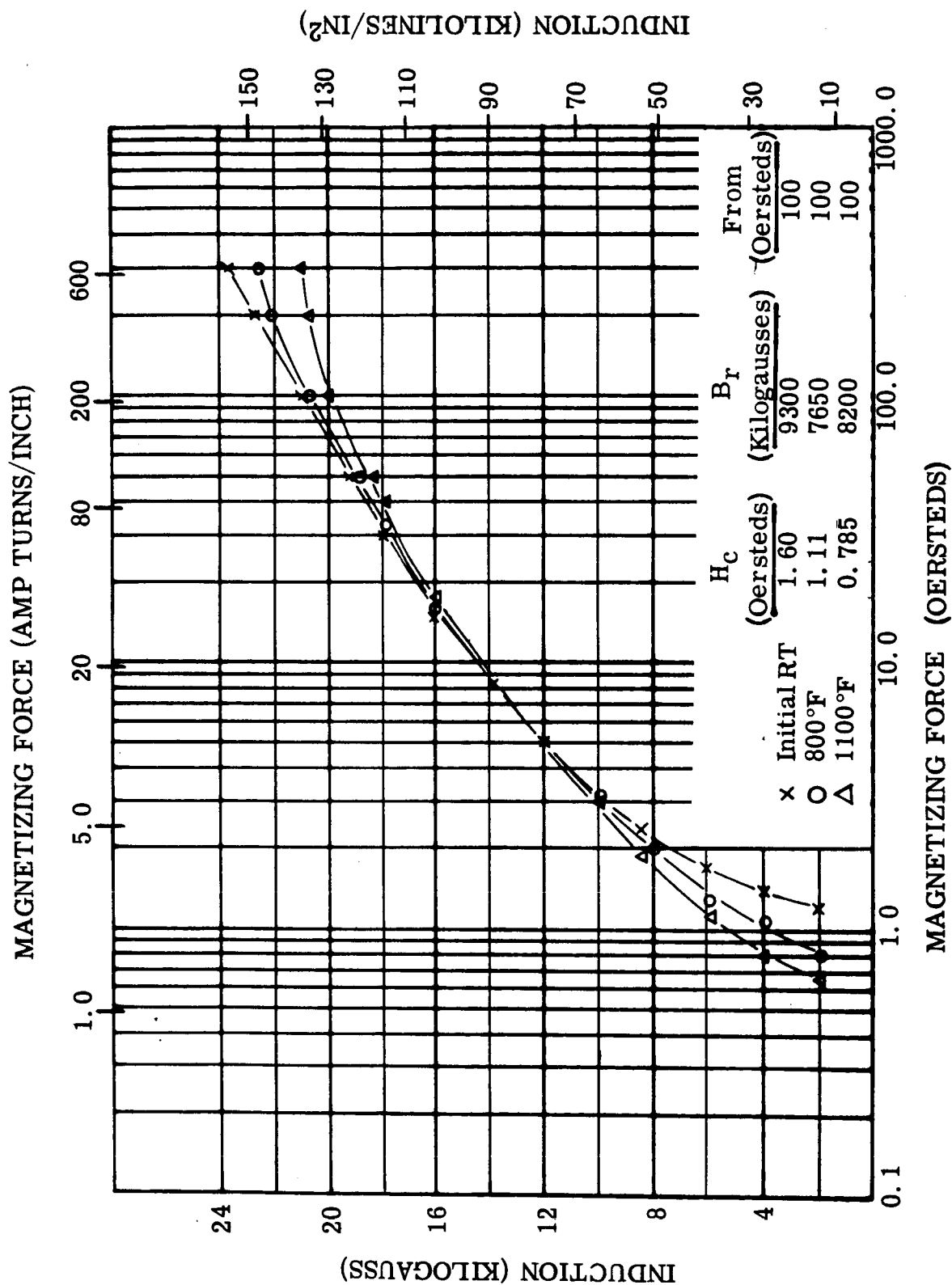


Figure II-38. DC Magnetization - Hiperco 27 Laminated Ring

FIGURE II-38. DC Magnetization Curves for Hiperco 27, Ring Laminations, 0.008 inch thick. Test Atmosphere: Air to 800°F, Argon above 800°F (Reference: NAS3-4162)

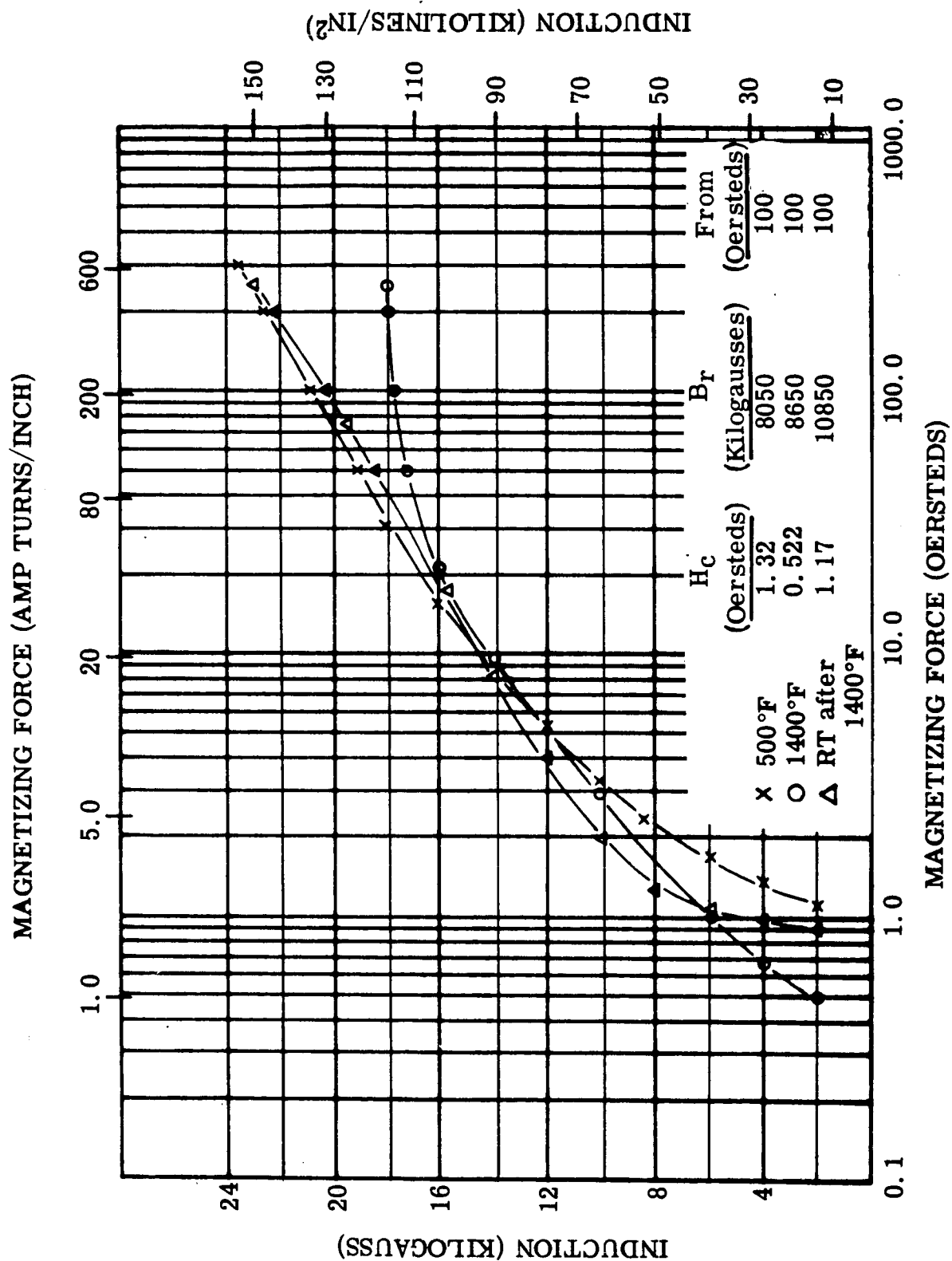


Figure II-39. DC Magnetization - Hipercro 27 Laminated Ring

FIGURE II-39. DC Magnetization Curves for Hipercro 27, Ring Laminations, 0.008 inch thick. Test Atmosphere: Air to 800°F, Argon above 800°F (Reference: NAS3-4162)

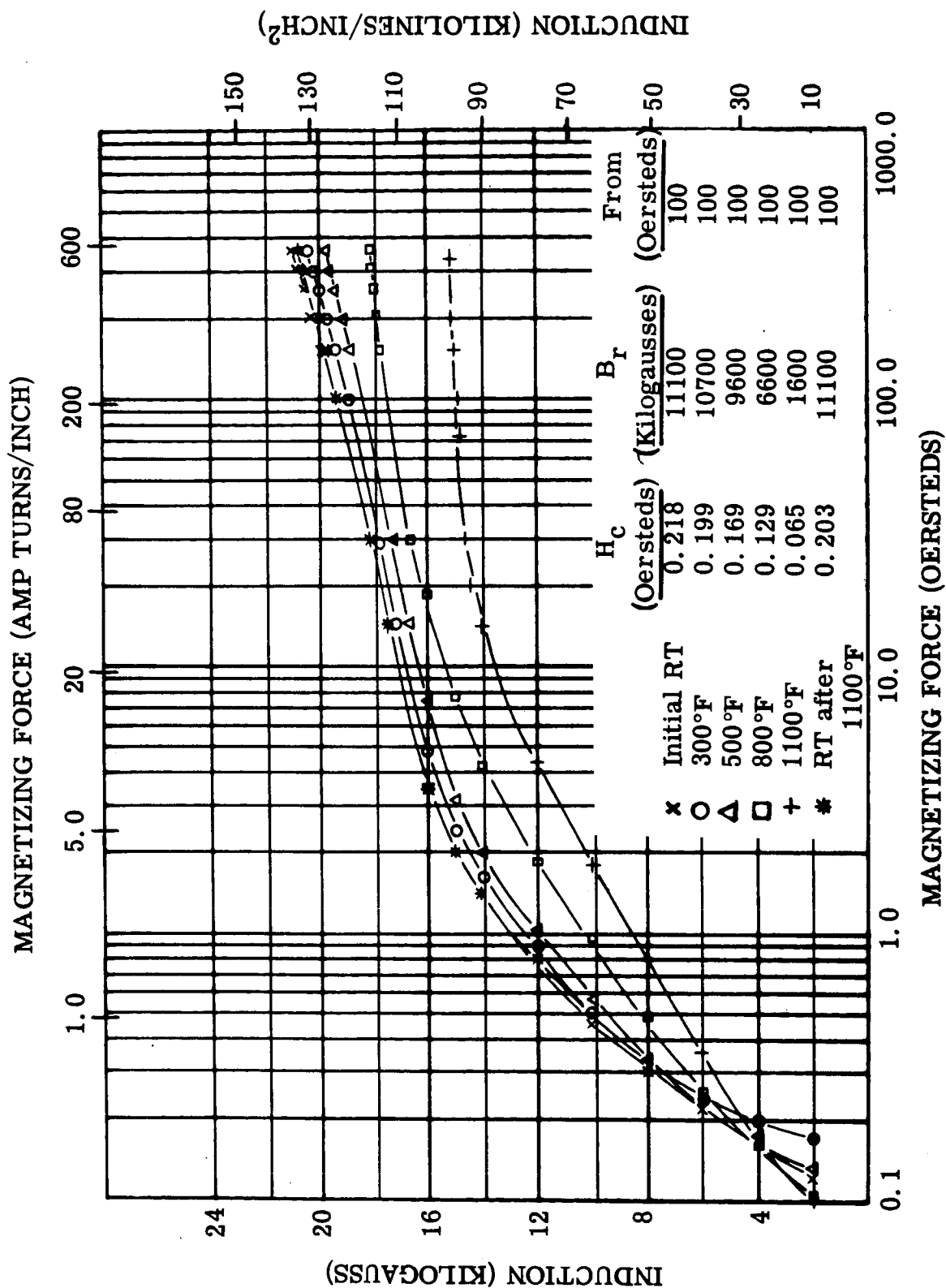


Figure II-40. DC Magnetization - Cubex Laminated Ring

FIGURE II-40. DC Magnetization Curves for Cubex. Ring Laminations, 0.006 inch thick. Test Atmosphere: Air to 500°F, Ar-gon above 500°F (Reference: NAS3-4162)

## SECTION III

### ELECTRICAL CONDUCTORS

#### A. INTRODUCTION.

During the previous quarter, the balance of the conductor materials developed for this program were received from Sylvania Electric Products Corporation. Samples from these wires are now being evaluated electrically, mechanically, and thermophysically.

The electrical conductors selected remain the same as reported in the second quarterly report (WAED 64. 14E).

#### B. SUMMARY OF EFFORT IN THIS QUARTER.

- 1) Creep testing
  - a) 3 samples of beryllia dispersion-strengthened copper 10-gage wire were placed on test.
- 2) Tensile testing at room and elevated temperature were completed on the following:
  - a) 11 samples of 10-gage nickel-clad copper wire
  - b) 12 samples of 10-gage bare dispersion-strengthened copper wire
  - c) 15 samples of 10-gage Type 321 stainless steel-clad silver wire
- 3) Thermal expansion measurements were completed on the following:
  - a) Type 321 stainless steel-clad silver wire



- b) Bare dispersion-strengthened copper wire
  - c) Nickel-clad copper wire
- 4) Electrical resistivity measurement were completed on the following:
- a) Type 321 stainless steel-clad silver wire
  - b) Inconel-clad over columbium-clad over dispersion-strengthened copper wire
  - c) Bare dispersion-strengthened copper wire
  - d) Inconel-clad silver wire
  - e) Thoria dispersion-strengthened nickel wire
  - f) Type 304 stainless steel-clad zirconium copper wire
- 5) All conductors were placed on thermo stability test.

## C. MECHANICAL AND THERMOPHYSICAL TEST RESULTS.

### 1. Creep

Sufficient test data are not yet available to warrant a discussion in this report.

### 2. Tensile Tests at Room and Elevated Temperatures

All tensile data obtained during the past quarter are presented in Tables III-1 and III-2 and in Figures III-1 to III-7. These data are straight forward and do not require comment at this time. Figure III-3 is worthy of note since it compares data obtained on this program with the dispersion-strengthened material CuFo (BeO-Cu) data published by Handy and Harman<sup>1</sup>. It shows not only the accuracy of the published information but the uniformity of the commercial product. The Handy and Harman data represents an average of several lots of material and the agreement between the two sets of data is indicative of a uniform product.

### 3. Thermal Expansion Measurements

The thermal expansion of three conductors; nickel-clad copper, CuFo, and 321 stainless steel-clad silver are presented in Figures III-8, III-9, and III-10. These data show nothing unexpected. The curves are replots from data recorded on an autographic recorder, and have been corrected for expansion of the quartz rod and tube. A thermal expansion specimen assembled in the dilatometer and ready for insertion into the furnace is shown in Figure III-11.

### 4. Electrical Resistivity Measurements

Electrical resistivity data for all tests completed during this period are given in Tables III-3 to III-12 and are plotted in Figures III-12 and III-13.

Wherever possible, the two electric current carrying and two measuring lead wires are resistance welded to the specimen to assure a good connection. In the case of the bare dispersion-strengthened copper, CuFo; however, resistance-welded leads separated from the specimen at about 1550°F, terminating the test.

<sup>1</sup> Handy and Harman product literature (CuFo) January 1964.

These data are shown in Table III-5 but were not plotted. To overcome this problem, small holes (0.020 inch diameter) were drilled through the 0.040 inch diameter wire at the proper locations near the ends of the test specimen, 0.020 inch chromel lead wire inserted through the holes, and the holes peened closed. Joints made in this manner have provided excellent tests up to the maximum test temperature of 1600°F.

The electrical resistivity data are plotted together on Figure III-12. The tests on Specimen No. 2 of the stainless steel-clad, zirconium-copper (Table III-11 and 12) are not plotted for curve clarity since these data are essentially the same as that of the first specimen. The data are included for informational purposes only.

An aging effect was noted in the data for stainless steel-clad, zirconium-copper which is shown in the inflection point on Curve 1 of Figure III-13. A second run was made on the same specimen (see Curve 2 Figure III-13) which did not show the change in slope of Curve 2, indicating the zirconium-copper core was in an equilibrium condition due to the heating required when obtaining the first curve.

D. GENERAL DISCUSSION.

Sylvania Electric Products Corporation supplied a series of photomicrographs of the conductors made by them. Two of these are included in Figures III-14 and III-15. The quality of these developmental wires is evident by the uniformity of the columbium cladding on the Inconel-columbium clad dispersion-strengthened copper.

TABLE III-1. Tensile Test Data For Bare Conductor Wire

Test: ASTM E21 - Strain Rate : 0.005 in/in-min and 0.05 in/in-min

Material	Spec. No.	Dia. (in.)	Test Temp. (°F)	0.02 Percent Offset Yield Str. (Psi)	0.2 Percent Offset Yield Str. (Psi)	Ultimate Strength (Psi)	Elongation in 2 inches (percent)	Reduction of Area (percent)
'CuFo' Dispersion Strengthened Copper (BeO-Cu) (See Figures III-1 through III-3)	1	0.1002	R. T.	40950	62850	80600	14.4	62.9
	2	0.1002	R. T.	41300	62000	80750	8.7	33.0
	3	0.1003	500	38550	54350	66850	6.2	33.2
	4	0.1005	500	41000	56600	67800	8.6	36.6
	5	0.1005	800	40650	50950	53950	1.4	0.5 D
	6	0.1005	800	43150	50550	50550	1.5	6.8 D
	7	0.1003	1000	35900	42350	52350	1.6	17.7 D
	8	0.1003	1000	27800	B	40450	1.5	4.6 D
	9	0.1003	1400	28500	B	30400	0.5	0.6
	10	0.1003	1400	24450	B	27450	0.3	0.4
	11	0.1003	1600	20750	B	24300	0.3	0.6
	C 12	0.1003	1600	-	-	-	-	-

B = Specimen failed before 0.2 percent offset yield was reached.

C = Specimen slipped in grips and on rerun broke in grips. No additional materials available.

D = Argon atmosphere. All others tested in air.

(Reference: NAS3-4162)

TABLE III-2. Tensile Test Data For Clad Conductor Wire. Cladding is 28% of Conductor Area

Test: ASTM E21 - Strain Rate: 0.005 in/in-min and 0.05 in/in-min

Material	Spec. No.	Dia. (in.)	Test Temp. (°F)	0.02 Per-cent Offset Yield Str. (Psi)	0.2 Per-cent Offset Yield Str. (Psi)	Ultimate Strength (Psi)	Elongation in 2 inches (percent)	Reduction of Area (percent)
321 S. S. - Clad Silver (See Figures III-6 and III-7)	1	0.1010	R. T.	12500	18350	48700	27.9	59.8
	2	0.1006	R. T.	7550	14400	47900	34.4	58.2
	3	0.1006	R. T.	12800	17100	47100	27.2	58.2
	4	0.1003	500	9600	14800	32000	15.7	12.2
	5	0.1005	500	9500	13800	30950	13.8	12.5
	6	0.1000	500	9550	14500	30300	13.9	22.5
	7	0.1010	800	7850	12400	26450	18.6	34.1 D
	8	0.1010	800	7950	12500	26200	17.7	32.5 D
	9	0.1009	1000	8500	12200	22900	20.3	41.7 D
	10	0.1005	1000	7800	11350	21050	21.3	42.7 D
	11	0.1006	1400	4950	6350	10700	27.3	92.8 D
	12	0.1010	1400	A	A	10500	27.4	93.9 D
	13	0.1006	1400	4900	6800	10450	28.3	92.8 D
	14	0.1010	1600	1500	2350	4350	68.4	92.3 D
	15	0.1009	1600	1150	1900	3550	66.3	96.9 D
Ni-Clad Copper (See Figures III-4 and III-5)	1	0.1019	R. T.	6400	10450	40000	35.4	66.5
	2	0.1016	R. T.	8150	9900	40050	34.6	84.5
	3	0.1015	R. T.	9400	11100	40800	36.3	74.8
	4	0.1018	500	5300	8250	32100	31.6	54.1
	5	0.1019	500	6850	9700	30650	33.1	56.7
	6	0.1016	800	8250	10100	25700	27.6	51.2 D
	7	0.1020	800	6250	7350	24500	30.1	47.4 D
	8	0.1018	800	7750	9400	24250	31.4	61.7 D
	9	0.1018	1000	4800	6500	13550	31.4	68.7 D
	10	0.1019	1000	4950	6750	14250	31.0	61.8 D
	11	0.1015	1000	5350	7850	14850	32.7	63.9 D

A = Curve unreliable. Extensometer slipped.  
D = Argon atmosphere. All others tested in air.

(Reference: NAS3-4162)

TABLE III-3. Electrical Resistivity, 321 Stainless Steel-Clad (28% of Area)  
Silver Wire in Vacuum ( $10^{-5}$  torr)  
See Figure III-12

Test: ASTM B193

Specimen No. 1, Continuous Heating				
Wire Diameter - 0.040 Inches, Test Length - 23.24 Inches				
Temp. (°F)	Resistance (Ohms)	Resistivity (Ohms Cir Mil/Ft)	Resistivity (Microhm-Cm)	Conductivity (percent IACS)
76	0.01782	14.722	2.45	71.63
200	0.02005	16.564	2.75	63.67
300	0.02271	18.762	3.12	56.21
400	0.02824	23.330	3.88	45.20
500	0.03141	25.949	4.31	40.64
600	0.03574	29.526	4.91	35.72
708	0.03938	32.534	5.41	32.42
821	0.04365	36.062	5.99	29.24
918	0.04674	38.614	6.42	27.31
1017	0.05004	41.341	6.87	25.51
1100	0.05430	44.860	7.46	23.51
1200	0.05800	47.917	7.97	22.01
1300	0.06200	51.221	8.51	20.59
1408	0.06650	54.939	9.13	19.20
1500	0.06981	57.674	9.59	18.29
1600	0.07570	62.540	10.40	16.86
1541	0.07320	60.474	10.05	17.44
1449	0.06919	57.162	9.50	18.45
1292	0.06176	51.024	8.48	20.67
1100	0.05526	45.654	7.59	23.10
900	0.04771	39.416	6.55	26.76
700	0.04008	33.112	5.50	31.85
500	0.03250	26.850	4.46	39.28
300	0.02580	21.315	3.54	49.48
200	0.02198	18.158	3.02	58.08
76	0.01776	14.672	2.44	71.88

(Reference: NAS3-4162)

TABLE III-4. Electrical Resistivity, Inconel-Clad (28% of Area),  
Columbium-Clad (8% of Area), 'CuFo' Copper Wire  
in Vacuum ( $10^{-5}$  torr)  
See Figure III-12

Test: ASTM B193

Specimen No. 1, Continuous Heating				
Wire Diameter - 0.0405 Inches, Test Length - 23.47 Inches				
Temp. (°F)	Resistance (Ohms)	Resistivity (Ohms Cir Mil/Ft)	Resistivity (Microhm-Cm)	Conductivity (percent IACS)
76	0.02423	20.320	3.38	51.90
200	0.02835	23.776	3.95	44.36
300	0.03280	27.507	4.57	38.34
400	0.03710	31.114	5.17	33.90
505	0.04170	34.971	5.81	30.16
610	0.04631	38.838	6.46	27.16
703	0.05031	42.192	7.01	24.99
800	0.05440	45.622	7.58	23.12
900	0.05880	49.312	8.20	21.39
1008	0.06340	53.170	8.84	19.84
1100	0.06785	56.902	9.46	18.54
1200	0.07250	60.802	10.11	17.35
1300	0.07740	64.911	10.79	16.25
1400	0.08230	69.020	11.47	15.28
1500	0.08755	73.423	12.21	14.36
1600	0.09250	77.574	12.90	13.60
1450	0.08515	71.410	11.87	14.77
1250	0.07560	63.401	10.54	16.64
1050	0.06628	55.585	9.24	18.97
850	0.05720	47.970	7.97	21.99
650	0.04853	40.700	6.77	25.91
450	0.03970	33.294	5.53	31.68
250	0.03152	26.434	4.39	39.90
150	0.02775	23.272	3.87	45.32
76	0.02298	19.272	3.20	54.73

(Reference: NAS3-4162)



TABLE III-5. Electrical Resistivity, 'CuFo' Copper Wire  
in Vacuum ( $10^{-5}$  torr)  
Not Plotted - See Table III-6

Test: ASTM B193

Specimen No. 1, Continuous Heating				
Wire Diameter - 0.040 Inches, Test Length - 23.23 Inches				
Temp. (°F)	Resistance (Ohms)	Resistivity (Ohms Cir Mil/Ft)	Resistivity (Microhm-Cm)	Conductivity (percent IACS)
77	0.01509	12.472	2.07	84.39
100	0.01537	12.703	2.11	82.86
200	0.01740	14.381	2.39	73.19
300	0.01980	16.364	2.72	64.32
400	0.02253	18.621	3.10	56.52
523	0.02560	21.158	3.52	49.74
600	0.02790	23.059	3.83	45.64
700	0.03000	24.795	4.12	42.45
800	0.03344	27.638	4.59	38.08
900	0.03631	30.010	4.99	35.07
1000	0.03920	32.398	5.39	32.48
1114	0.04290	35.456	5.89	29.68
1200	0.04600	38.019	6.32	27.68
1300	0.04960	40.994	6.81	25.67
1400	0.05309	43.878	7.29	23.98
1528	0.05747	47.498	7.90	22.16
NOTE: 1. Test leads separated from the specimen at 1550°F. This test repeated using a better technique to attach the leads to the specimen.				
(Reference: NAS3-4162)				

TABLE III-6. Electrical Resistivity, 'CuFo' Copper Wire  
in Vacuum ( $10^{-5}$  torr)  
See Figure III-12

Test: ASTM B193

Specimen No. 2, Continuous Heating				
Wire Diameter - 0.040 Inches, Test Length - 23.24 Inches				
Temp. (°F)	Resistance (Ohms)	Resistivity (Ohms Cir Mil/Ft)	Resistivity (Microhm-Cm)	Conductivity (percent IACS)
76	0.01485	12.269	2.04	86.06
200	0.01808	14.937	2.48	70.69
307	0.02044	16.887	2.81	62.53
400	0.02350	19.415	3.23	54.39
500	0.02640	21.811	2.63	48.41
600	0.02920	24.124	4.01	43.77
700	0.03200	26.437	4.39	39.94
800	0.03489	28.825	4.79	36.63
907	0.03800	31.394	5.22	33.63
1000	0.04095	33.831	5.62	31.21
1100	0.04400	36.351	6.04	29.05
1200	0.04706	38.879	6.46	27.16
1319	0.05040	41.638	6.92	25.36
1400	0.05390	44.530	7.40	23.71
1500	0.05734	47.372	7.88	22.29
1600	0.06131	50.652	8.42	20.85
1450	0.05630	46.513	7.73	22.70
1250	0.04937	40.788	6.78	25.89
1050	0.04295	35.484	5.90	29.76
850	0.03676	30.370	5.05	34.77
650	0.03102	25.627	4.26	41.20
432	0.02525	20.861	3.47	50.62
250	0.01995	16.482	2.74	64.06
150	0.01711	14.136	2.35	74.70

(Reference: NAS3-4162)

TABLE III-7. Electrical Resistivity, Inconel-Clad (28% of Area)  
Silver Wire in Vacuum ( $10^{-5}$  torr)  
See Figure III-12

Test: ASTM B193

Specimen No. 1, Continuous Heating				
Wire Diameter - 0.040 Inches, Test Length - 23.41 Inches				
Temp. (°F)	Resistance (Ohms)	Resistivity (Ohms Cir Mil/Ft)	Resistivity (Microhm-Cm)	Conductivity (percent IACS)
77	0.01787	14.656	2.44	72.10
200	0.02096	17.191	2.86	61.47
300	0.02480	20.340	3.38	51.95
400	0.02828	23.194	3.86	45.56
500	0.03186	26.130	4.34	40.44
600	0.03548	29.099	4.84	36.31
700	0.03907	32.044	5.33	32.98
800	0.04257	34.914	5.80	30.27
902	0.04637	38.031	6.32	27.79
1000	0.04982	40.860	6.79	25.86
1100	0.05365	44.002	7.31	24.01
1200	0.05750	47.159	7.84	22.41
1300	0.06155	50.481	8.39	20.93
1400	0.06565	53.844	8.95	19.63
1500	0.06971	57.173	9.50	18.48
1600	0.07489	61.422	10.21	17.20
1450	0.06850	56.181	9.34	18.81
1250	0.06040	49.538	8.24	21.33
1050	0.05275	43.264	7.19	24.42
850	0.04523	37.096	6.17	28.49
650	0.03777	30.977	5.15	34.11
450	0.02965	24.318	4.04	43.45
250	0.02397	19.659	3.27	53.75
171	0.02100	17.223	2.86	61.35
77	0.01747	14.328	2.38	73.75

(Reference: NAS3-4162)

TABLE III-8. Electrical Resistivity, TD Nickel Wire, in Vacuum  
(10<sup>-5</sup> torr)  
See Figure III-12 (Continuous Heating Data Not Plotted)

Test: ASTM B193

Specimen No. 1, Continuous Heating				
Wire Diameter - 0.040 Inches, Test Length - 23.02 Inches				
Temp. (°F)	Resistance (Ohms)	Resistivity (Ohms Cir Mil/Ft)	Resistivity (Microhm-Cm)	Conductivity (percent IACS)
76	0.05460	45.539	7.57	23.14
100	0.05701	47.549	7.90	22.16
205	0.07255	60.510	10.06	18.35
300	0.09100	75.898	12.62	13.88
400	0.1141	95.165	15.82	11.07
504	0.1420	118.435	19.69	8.99
600	0.1730	144.290	23.99	7.30
700	0.2135	178.069	29.80	5.92
800	0.2351	196.085	32.60	5.37
900	0.2505	208.929	34.73	5.04
1000	0.2640	220.189	36.60	4.79
1100	0.2770	231.031	38.41	4.56
1224	0.2917	243.292	40.44	4.33
1321	0.3029	252.633	41.99	4.17
1441	0.3170	264.894	44.04	3.98
Wire Soaked at Test Temperature Before Measurement				
Wire Diameter - 0.040 Inches, Test Length - 23.16 Inches				
75	0.05462	45.279	7.53	23.26
321	0.1000	82.900	13.78	12.71
463	0.1372	113.738	18.91	9.26
695	0.2212	183.374	30.48	5.74
980	0.2655	220.099	36.59	4.79
1291	0.3023	250.606	41.66	4.20
1600	0.3320	275.228	45.75	3.83
1375	0.3076	255.000	42.39	4.13
874	0.2496	206.918	34.40	5.09
593	0.1796	148.888	24.75	7.08
314	0.1032	85.552	14.22	12.31
75	0.05471	45.354	7.54	23.21
NOTE: 1. In the continuous heating test, leads separated from the test specimen between 1450 and 1500°F.				
(Reference: NAS3-4162)				

TABLE III-9. Electrical Resistivity, 304 Stainless Steel-Clad (28% of Area)  
Zirconium Copper Wire in Vacuum ( $10^{-5}$  torr)(First Test)  
See Figures III-12 and 13

Test: ASTM B193

Specimen No. 1, Continuous Heating				
Wire Diameter - 0.0405 Inches, Test Length - 23.48 Inches				
See Plots Figures III-12 and 13				
Temp. (°F)	Resistance (Ohms)	Resistivity (Ohms Cir Mil/Ft)	Resistivity (Microhm-Cm)	Conductivity (percent IACS)
77	0.02954	24.763	4.12	42.66
200	0.03390	28.418	4.72	37.17
307	0.03790	31.771	5.28	33.25
400	0.04125	34.579	5.75	30.55
500	0.04525	37.933	6.31	27.85
600	0.04894	41.026	6.82	25.75
700	0.05260	44.094	7.33	23.96
809	0.05590	46.860	7.79	22.54
900	0.05754	48.235	8.02	21.90
975	0.05728	48.017	7.98	21.99
1000	0.05736	48.084	7.99	21.97
1102	0.05980	50.130	8.33	21.07
1202	0.06445	54.028	8.98	19.55
1300	0.06926	58.060	9.65	18.19
1400	0.07444	62.402	10.37	16.93
1500	0.07930	66.476	11.05	15.89
1600	0.08595	72.051	11.98	14.66
1450	0.07760	65.051	10.81	16.24
1240	0.06690	56.081	9.32	18.84
1050	0.05855	49.082	8.16	21.52
986	0.05580	46.776	7.78	22.58
950	0.05435	45.561	7.57	23.18
910	0.05268	44.161	7.34	23.92
834	0.04965	41.621	6.92	25.38
650	0.04224	35.409	5.89	29.83
450	0.03455	28.963	4.81	36.47
250	0.02675	22.424	3.73	47.11
150	0.02279	19.105	3.18	55.29
79	0.01986	16.648	2.77	63.77

(Reference: NAS3-4162)

TABLE III-10. Electrical Resistivity 304 Stainless Steel-Clad (28% of Area)  
Zirconium Copper Wire in Vacuum ( $10^{-5}$  torr)(Second Test)  
See Figure III-13

Test: ASTM B193

Specimen No. 1, Continuous Heating				
Wire Diameter - 0.0405 Inches, Test Length - 23.48 Inches				
Temp. (°F)	Resistance (Ohms)	Resistivity (Ohms Cir Mil/Ft)	Resistivity (Microhm-Cm)	Conductivity (percent IACS)
79	0.01986	16.648	2.77	63.77
203	0.02425	20.328	3.38	52.22
319	0.02900	24.310	4.04	43.67
402	0.03230	27.077	4.50	39.21
500	0.03630	30.430	5.06	34.89
611	0.04015	33.657	5.60	31.54
707	0.04440	37.220	6.19	28.52
800	0.04815	40.364	6.71	26.30
900	0.05225	43.801	7.28	24.24
1000	0.05592	46.877	7.79	22.65
1113	0.06055	50.758	8.44	20.91
1200	0.06430	53.902	8.96	19.70
1300	0.06880	57.674	9.59	18.41
1400	0.07420	62.201	10.34	17.07
1500	0.07986	66.946	11.13	15.86
1603	0.08725	73.141	12.16	14.51
1450	0.07814	65.504	10.89	16.21
1238	0.06675	55.956	9.30	18.97
1043	0.05865	49.166	8.17	21.59
850	0.05049	42.325	7.04	25.08
650	0.04253	35.652	5.93	29.78
450	0.03474	29.122	4.84	36.45
250	0.02617	21.938	3.65	48.39
170	0.02350	19.700	3.27	53.89
77	0.02045	17.143	2.85	61.69

(Reference: NAS3-4162)

TABLE III-11. Electrical Resistivity, 304 Stainless Steel-Clad (28% of Area)  
Zirconium Copper Wire in Vacuum ( $10^{-5}$  torr)  
(First Test)

Test: ASTM B193

Specimen No. 2, Continuous Heating				
Wire Diameter - 0.0405 Inches, Test Length - 23.47 Inches				
Temp. (°F)	Resistance (Ohms)	Resistivity (Ohms Cir Mil/Ft)	Resistivity (Microhm-Cm)	Conductivity (percent IACS)
77	0.02907	24.379	4.05	43.41
200	0.03258	27.323	4.54	38.74
300	0.03683	30.887	5.13	34.27
405	0.04060	34.049	5.66	31.08
515	0.04501	37.747	6.28	28.04
600	0.04828	40.490	6.73	26.14
700	0.05194	43.559	7.24	24.30
805	0.05526	46.344	7.70	22.84
900	0.05731	48.063	7.99	22.02
950	0.05741	48.147	8.00	21.98
1000	0.05754	48.256	8.02	21.93
1100	0.05950	49.899	8.30	21.21
1300	0.06945	58.244	9.68	18.17
1400	0.07500	62.898	10.46	16.83
1505	0.08055	67.553	11.23	15.67
1600	0.08709	73.038	12.14	14.49
1450	0.07794	65.364	10.87	16.19
1250	0.06750	56.609	9.41	18.70
1044	0.05842	48.994	8.14	21.60
840	0.04995	41.890	6.96	25.27
650	0.04245	35.600	5.92	29.73
450	0.03480	29.185	4.85	36.27
250	0.02694	22.593	3.76	46.85
150	0.02306	19.339	3.21	54.73

(Reference: NAS3-4162)

TABLE III-12. Electrical Resistivity, 304 Stainless Steel-Clad  
(28% of Area) Zirconium Copper Wire in Vacuum  
(10<sup>-5</sup> torr)(Second Test)

Test: ASTM B193

Specimen No. 2, Continuous Heating				
Wire Diameter - 0.0405 Inches, Test Length - 23.47 Inches				
Temp. (°F)	Resistance (Ohms)	Resistivity (Ohms Cir Mil/Ft)	Resistivity (Microhm-Cm)	Conductivity (percent IACS)
79	0.01998	16.756	2.79	63.36
200	0.02320	19.457	3.23	54.56
300	0.02825	23.692	3.94	44.81
400	0.03220	27.004	4.49	39.31
500	0.03642	30.543	5.08	34.76
614	0.04070	34.133	5.67	31.10
711	0.04470	37.487	6.23	28.32
800	0.04829	40.498	6.73	26.21
905	0.05275	44.155	7.34	24.04
1000	0.05607	47.023	7.28	22.58
1100	0.05980	50.151	8.34	21.17
1200	0.06480	54.344	9.03	19.53
1300	0.06945	58.244	9.68	18.23
1400	0.07494	62.848	10.45	16.89
1500	0.08080	67.763	11.27	15.67
1600	0.08762	73.482	12.22	14.45
1450	0.07904	66.287	11.02	16.01
1246	0.06830	57.279	9.52	18.53
1050	0.05902	49.497	8.23	21.45
850	0.05064	42.469	7.06	25.00
644	0.04270	35.810	5.95	29.65
450	0.03519	29.512	4.91	35.97
250	0.02700	22.643	3.76	46.88
150	0.02327	19.515	3.24	54.40

(Reference: NAS3-4162)



Figure III-1. Tensile Strength - CuFo Dispersion Strengthened Copper

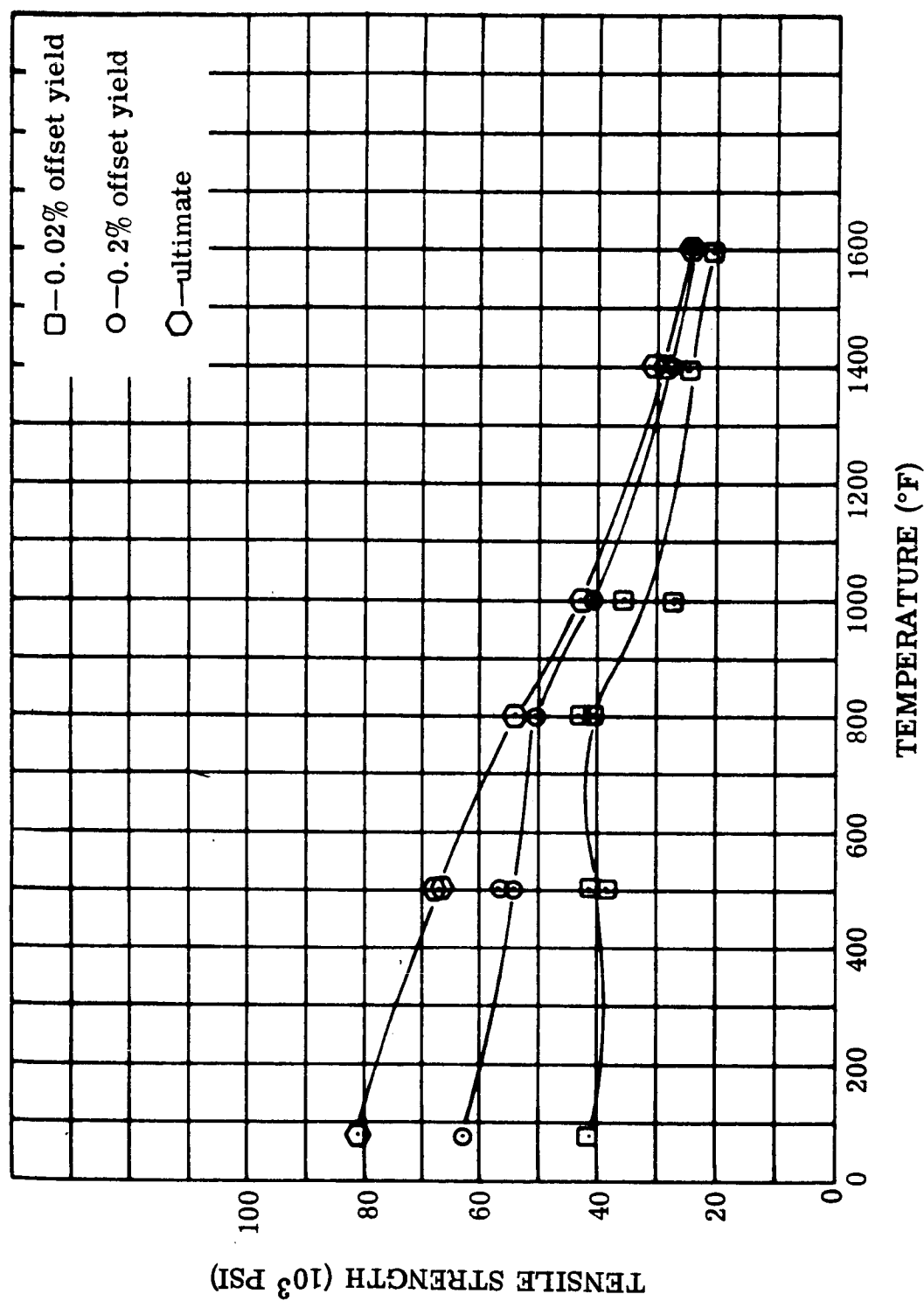


FIGURE III-1. Tensile Strength, Dispersion Strengthened Copper Wire (CuFo, BeO-Cu)  
 Tests at 800 $^{\circ}$ F and above made in argon, all others in air.  
 Strain Rate: 0.005 in/in-min and 0.05 in/in-min  
 (Reference: NAS3-4162)

ELONGATION AND REDUCTION OF AREA (PERCENT)

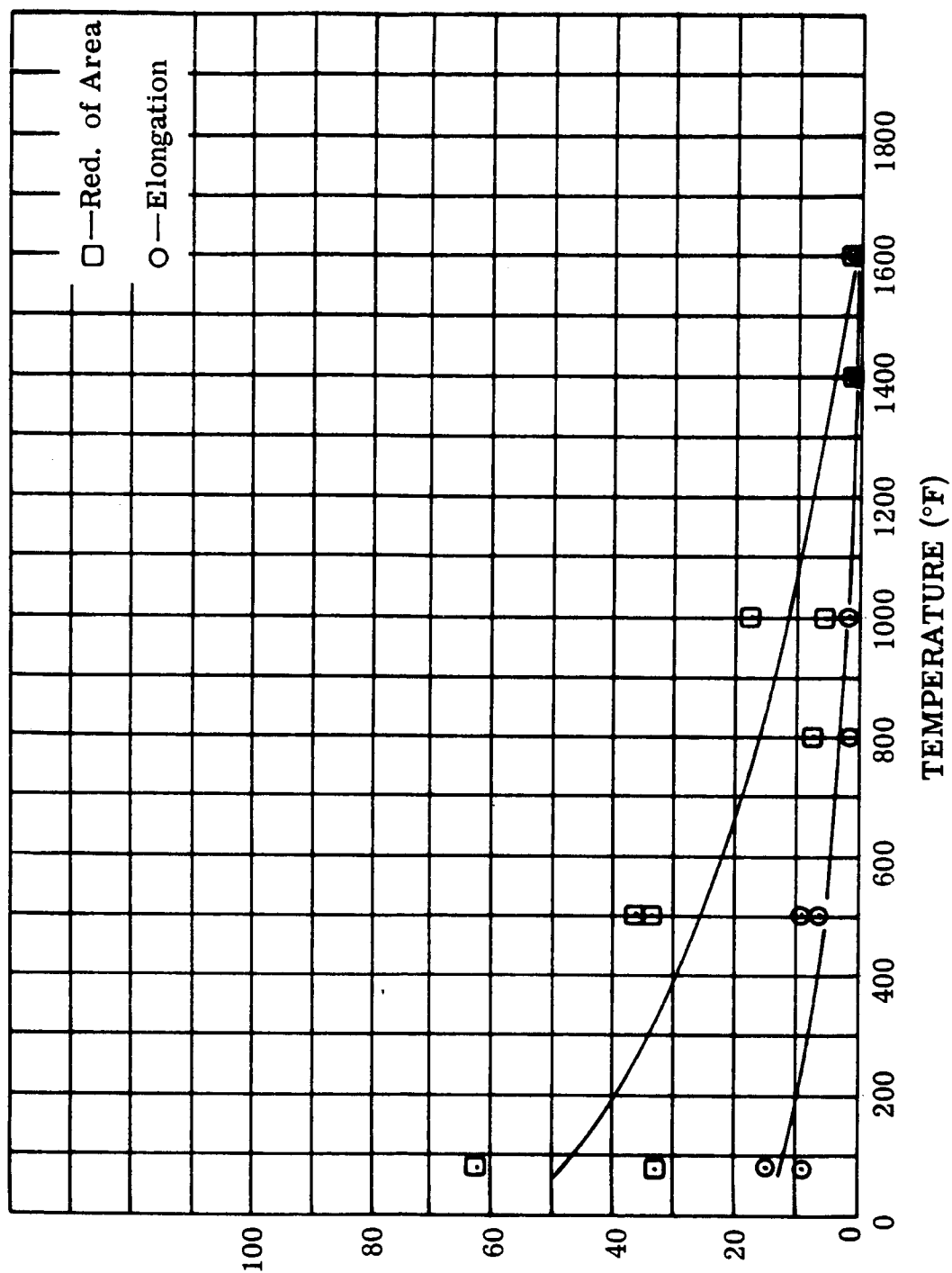


FIGURE III-2. Tensile Ductility, Dispersion Strengthened Copper Wire (CuFo-BeO-Cu). Tests at 800°F and 1000°F made in argon; all others in air. (Reference: NAS3-4162)

Figure III-2. Ductility - CuFo Dispersion Strengthened Copper

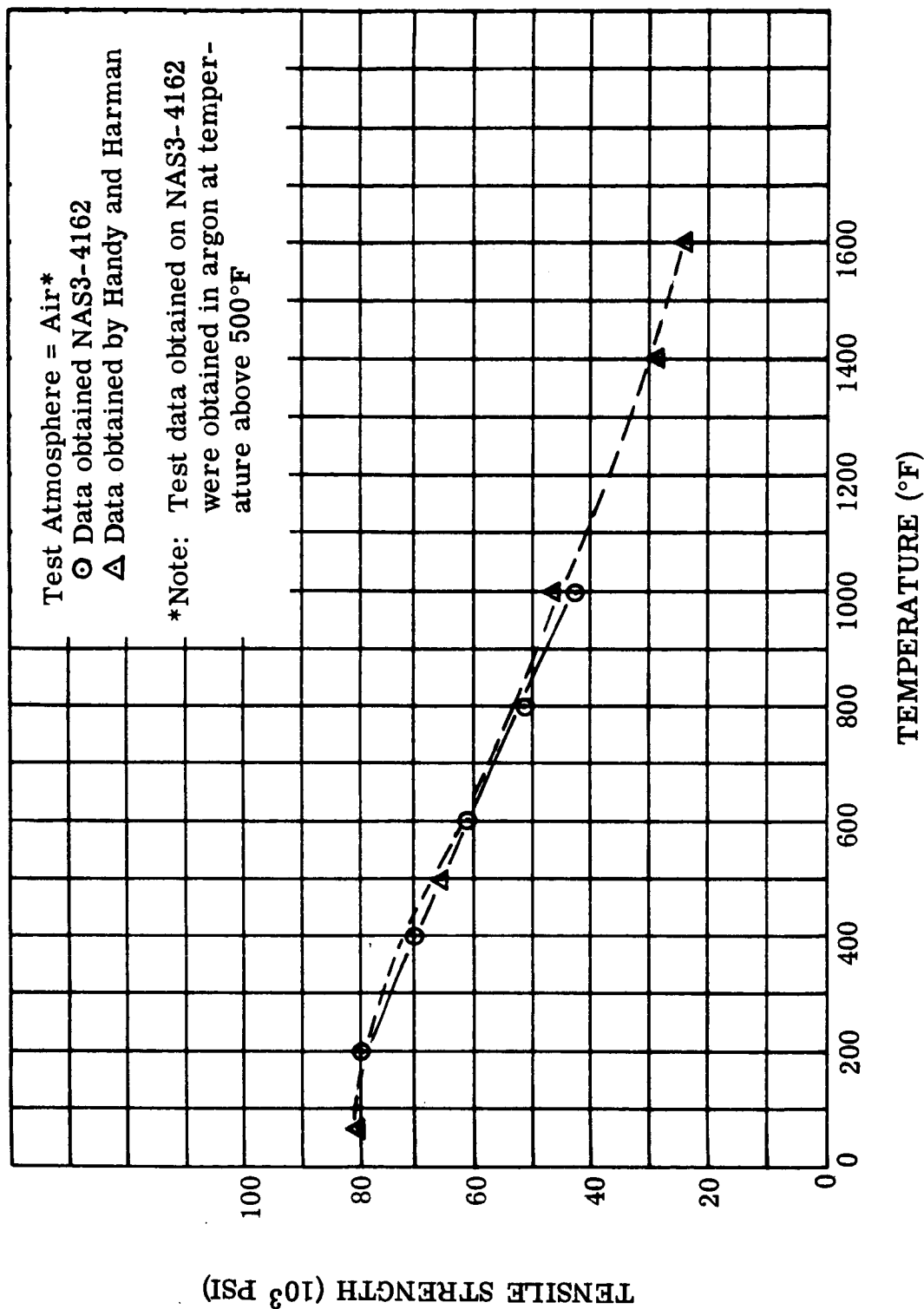


FIGURE III-3. Tensile Strength, 0.100 inch Diameter 'CuFo' Wire. Strain Rate: 0.005 in/in-min and 0.05 in/in-min (Reference: Handy and Harman Product Literature and NAS3-4162)

Figure III-3. Tensile Strength - CuFo (Copper-BeO)

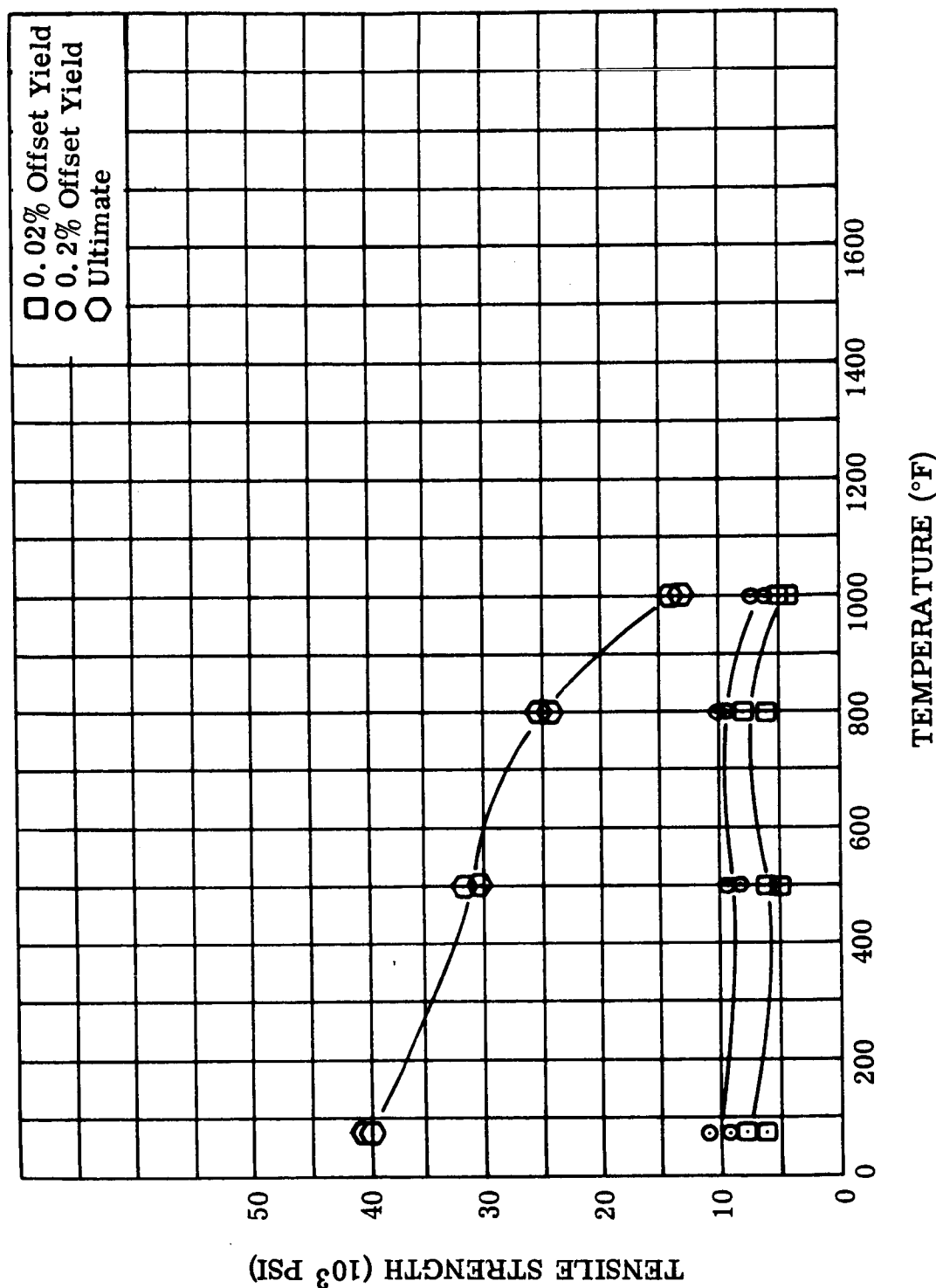


FIGURE III-4. Tensile Strengths, 0.100 inch Diameter Nickel-Clad (28% of Area) Copper Wire. Tests at 800°F and above made in argon; all others in air. Strain Rate: 0.005 in/in-min and 0.05 in/in-min (Reference: NAS3-4162)

Figure III-4. Tensile Strength - Nickel Clad Copper

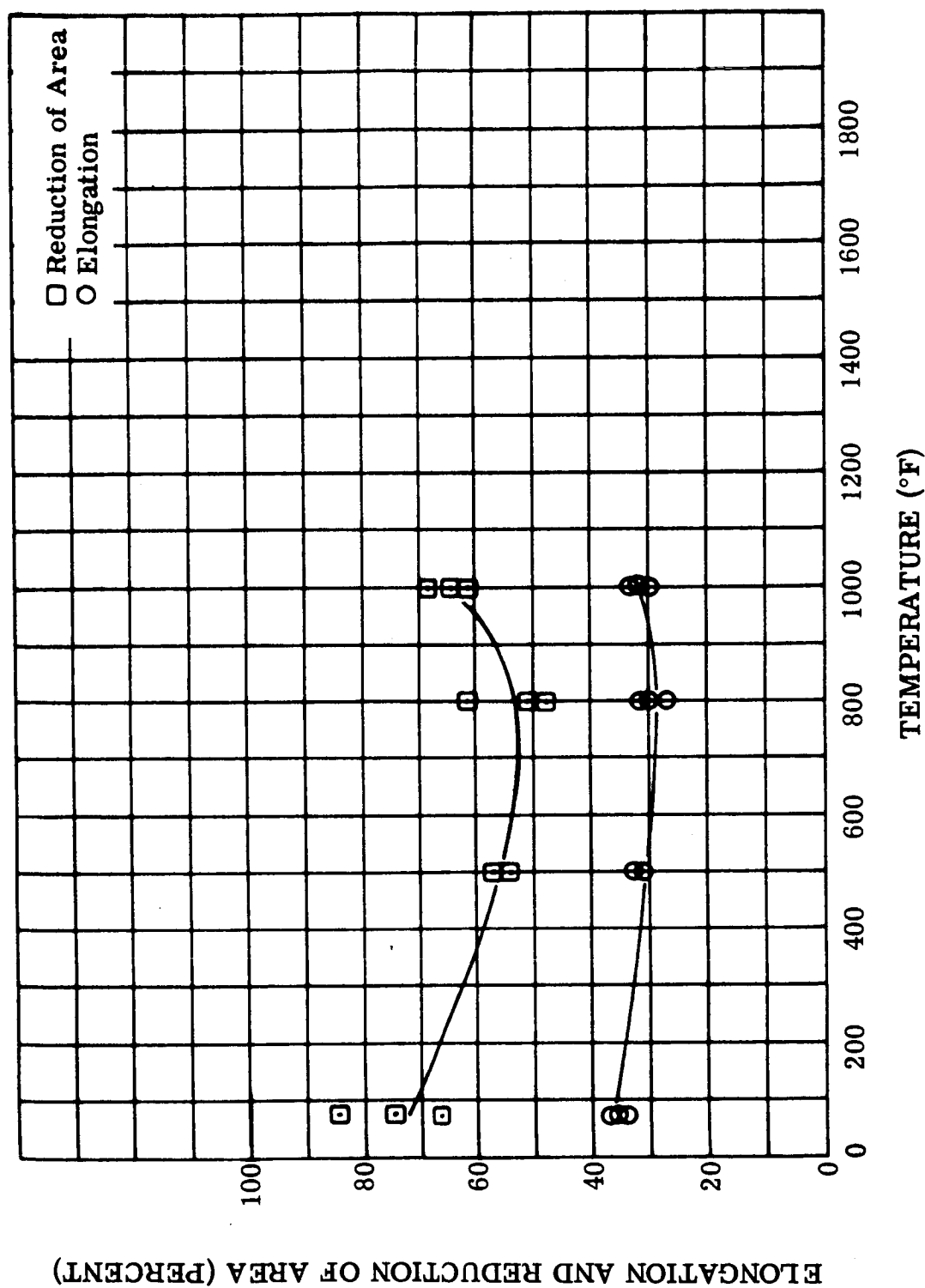


Figure III-5. Ductility - Nickel Clad Copper

WAED64. 30E-92

FIGURE III-5. Ductility, 0.100 inch Diameter Nickel-Clad (28% of Area) Copper Wire. Tests at 800°F and above made in argon, all others in air. (Reference: NAS3-4162)

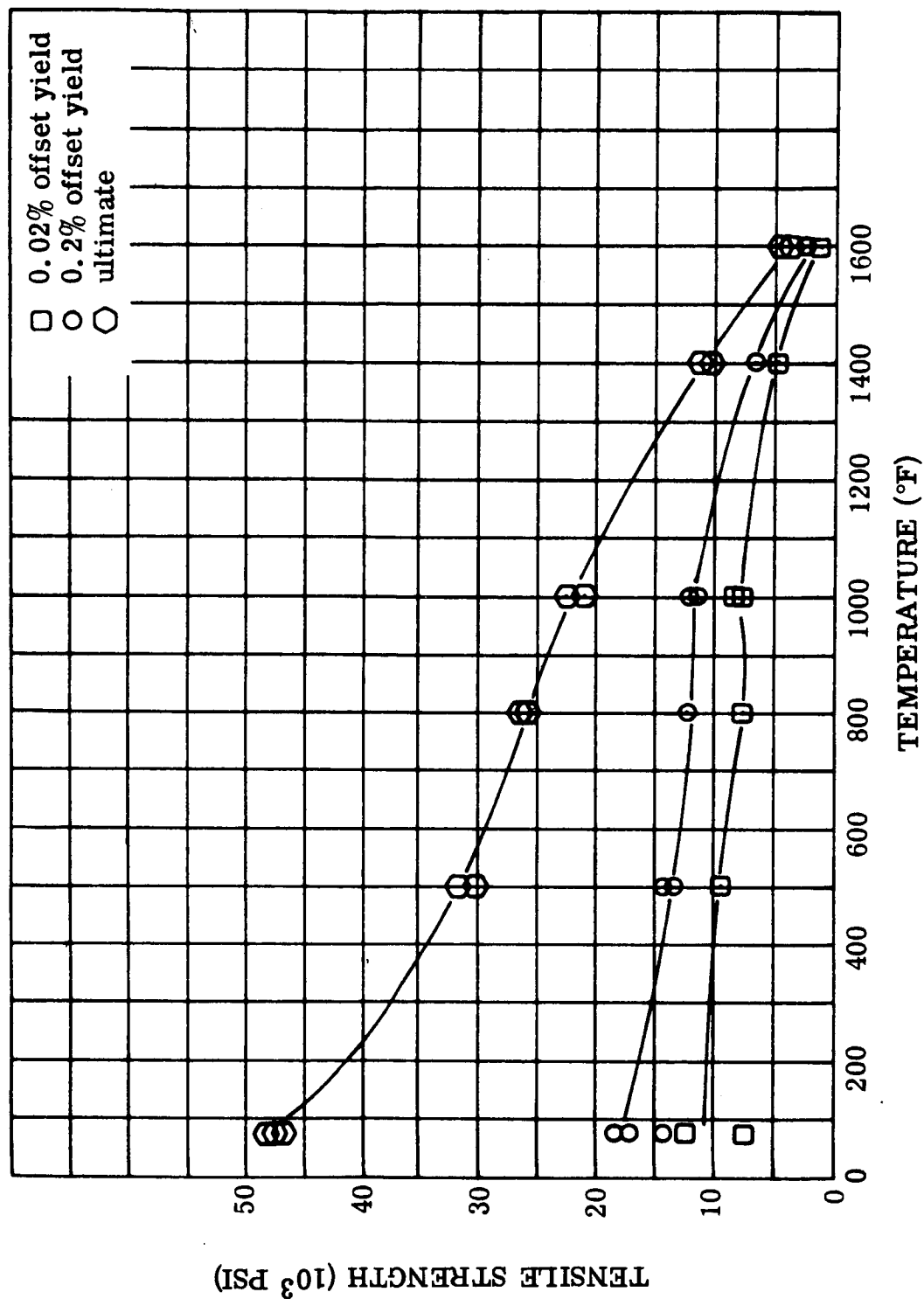


FIGURE III-6. Tensile Strengths, 0.100 inch Diameter 321 Stainless Steel-Clad (28% of Area) Silver Wire. All tests in argon at 800°F and above. (Reference: NAS3-4162)

Figure III-6. Tensile Strength - Stainless Steel Clad Silver

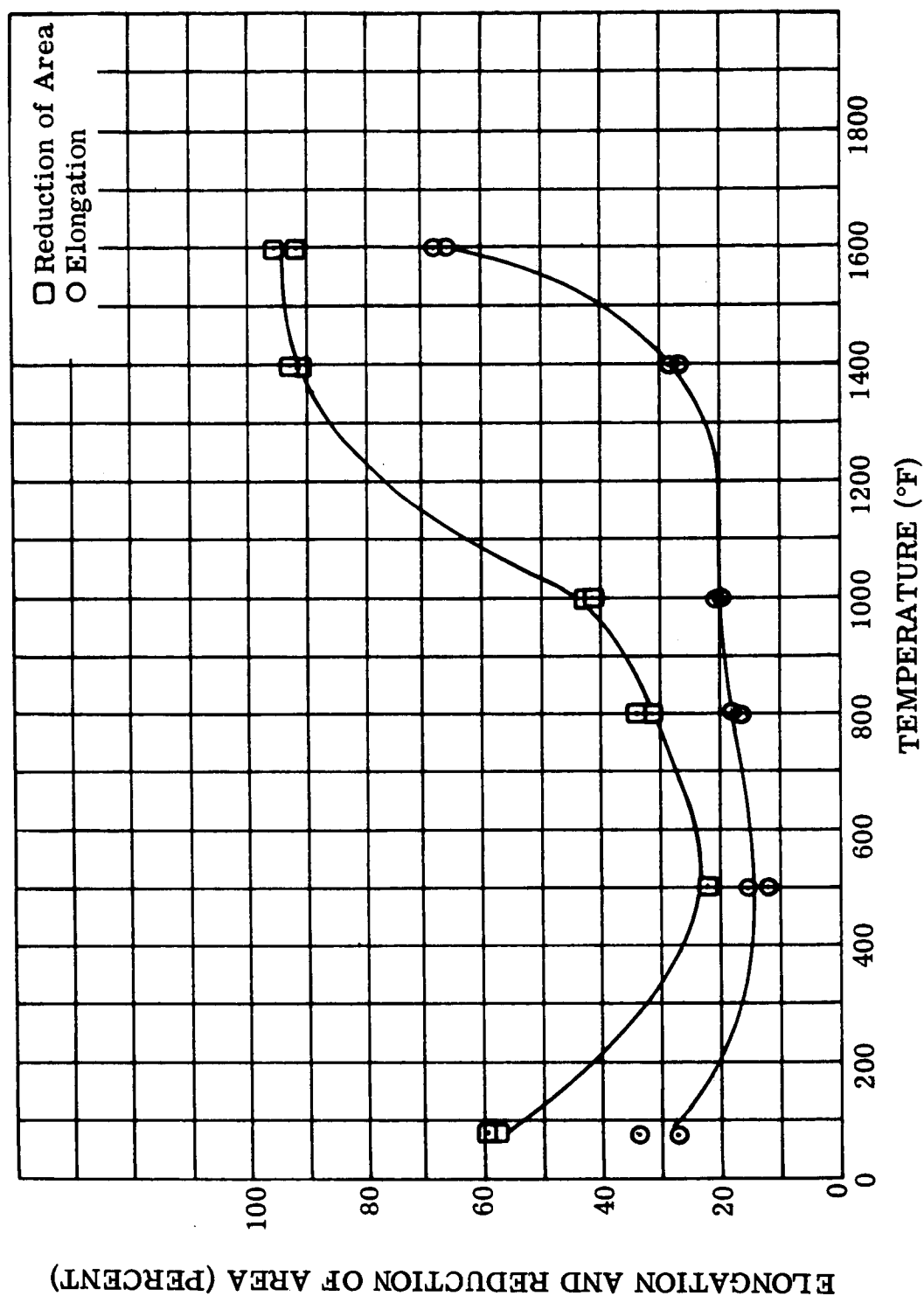


FIGURE III-7. Ductility, 0.100 inch Diameter 321 Stainless Steel-Clad (28% of Area) Silver Wire. All tests in argon at 800°F and above. (Reference: NAS3-4162)

Figure III-7. Ductility - Stainless Steel Clad Silver

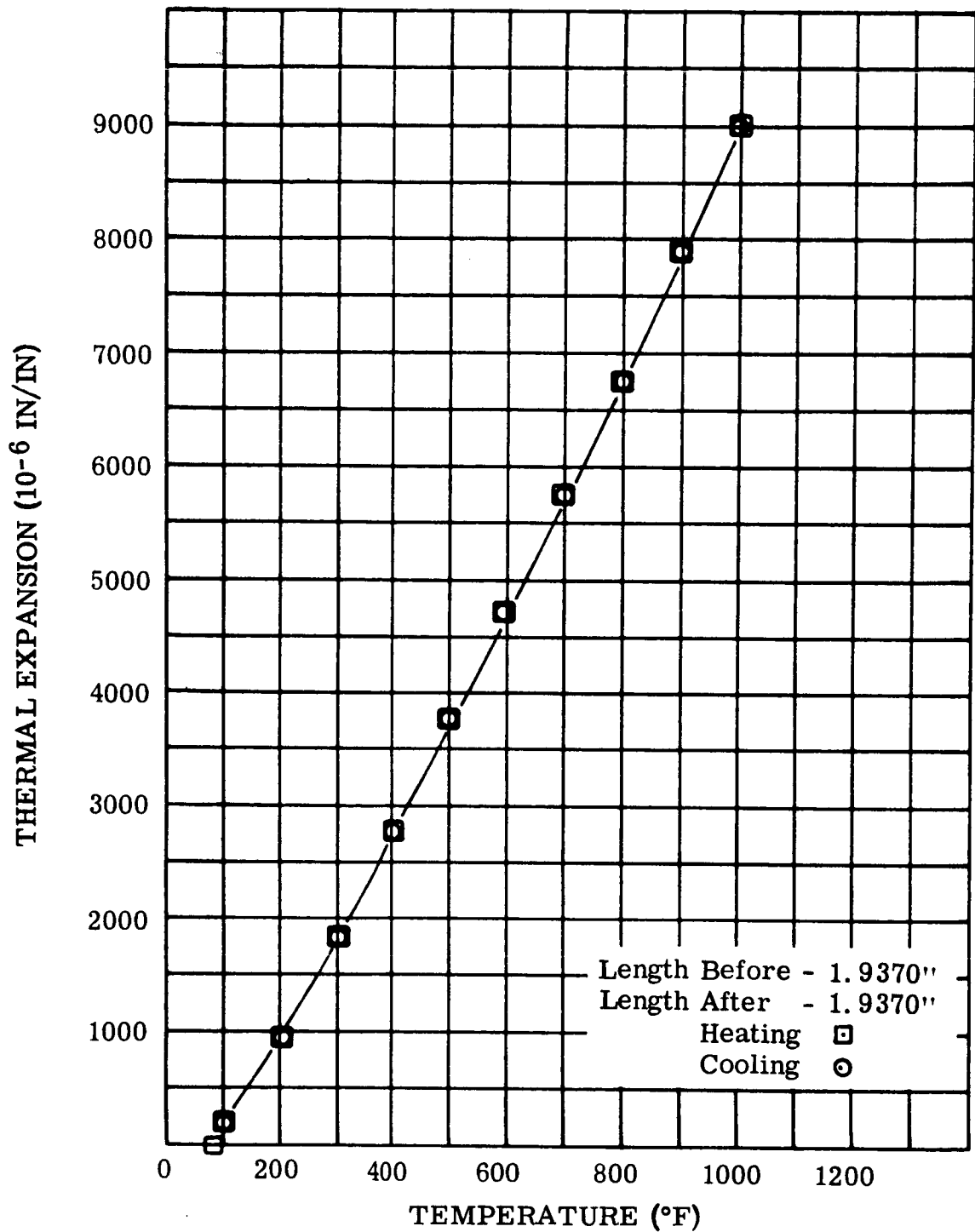


FIGURE III-8. Thermal Expansion, Nickel-Clad (28% of Area) Copper, 10 Gage Wire, Tested in Argon (Reference: NAS3-4162)

Figure III-8. Thermal Expansion - Nickel Clad Copper



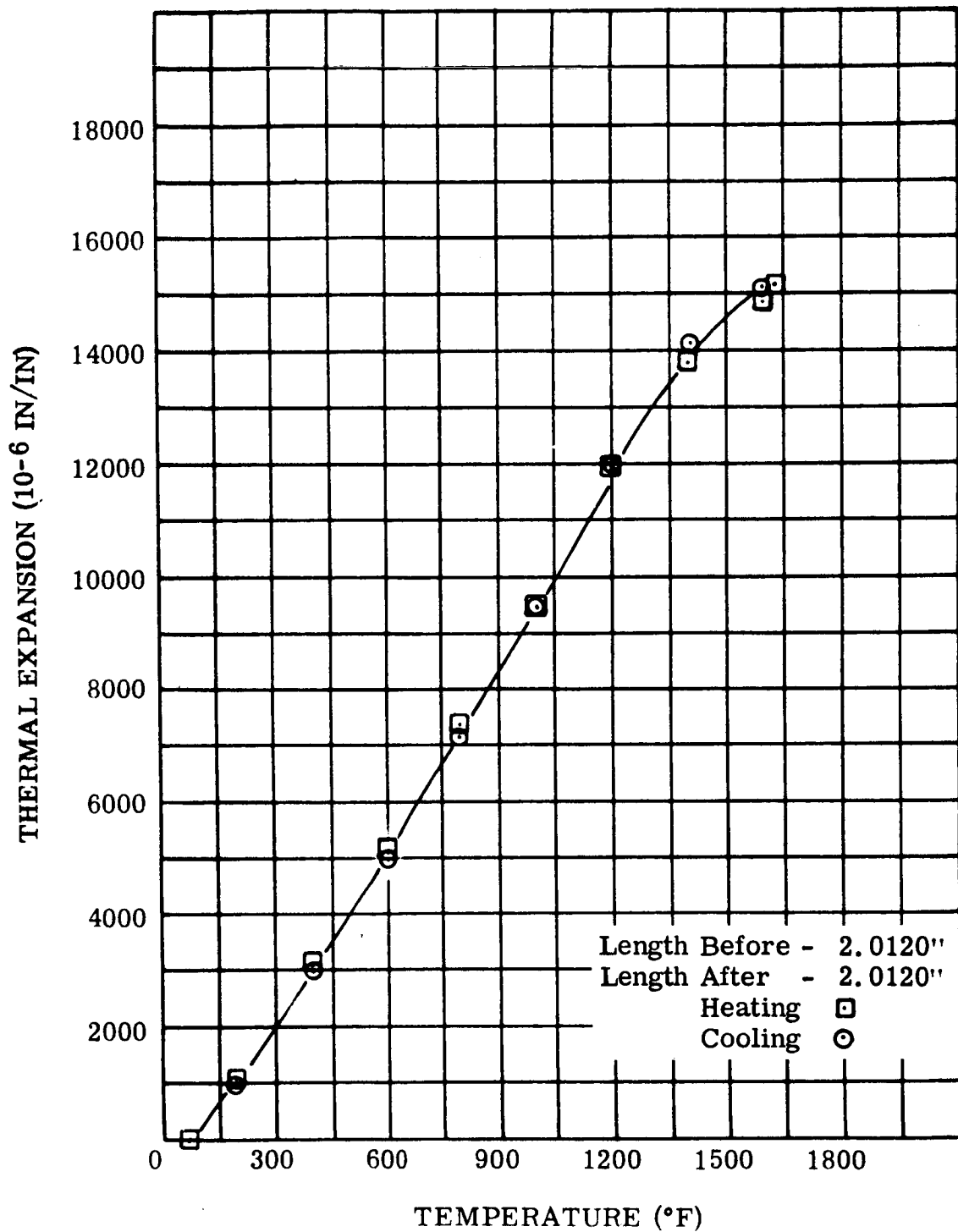


FIGURE III-9. Thermal Expansion, CuFo Dispersion Strengthened Copper, 10 Gage Wire, Tested in Argon (Reference: NAS3-4162)

Figure III-9. Thermal Expansion - CuFo Dispersion Strengthened Copper

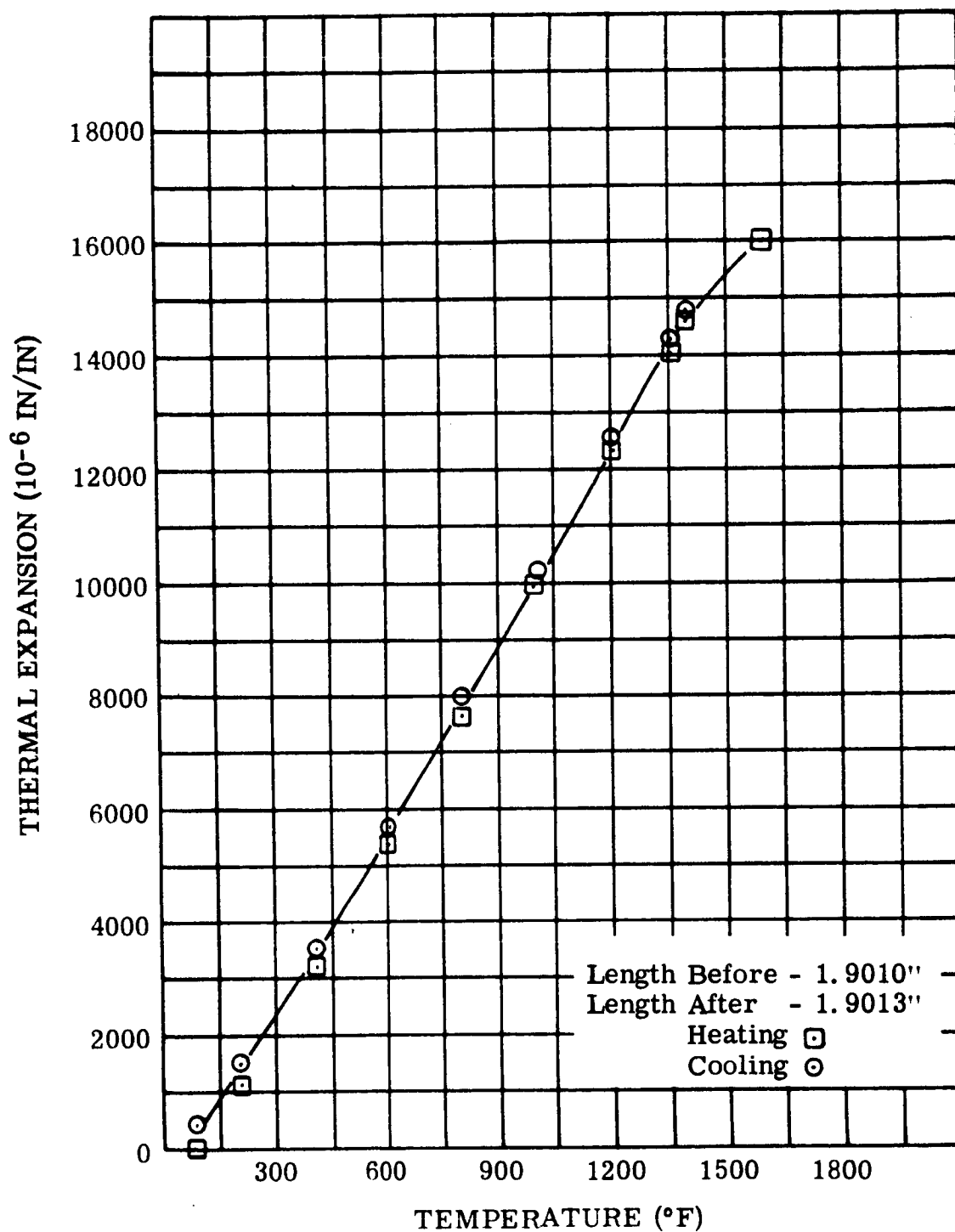


FIGURE III-10. Thermal Expansion, Type 321 Stainless Steel-Clad (28% of Area) Silver, 10 Gage Wire Tested in Argon (Reference: NAS3-4162)

Figure III-10. Thermal Expansion-Stainless Clad Silver

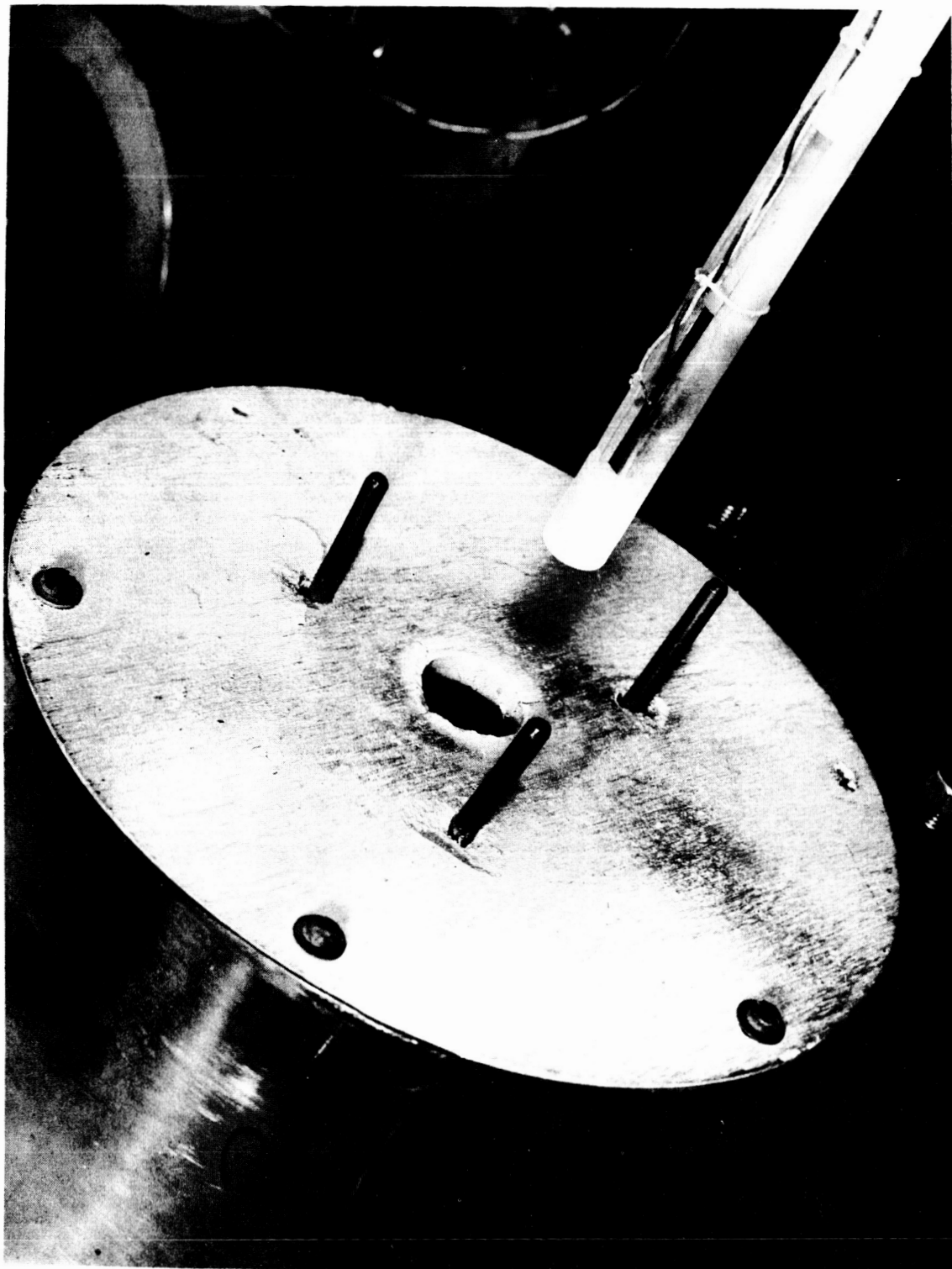


FIGURE III-11. Thermal Expansion Specimen in Quartz Tube Dilatometer,  
Ready For Insertion Into Furnace

Figure III-12. Electrical Resistivity - Conductors

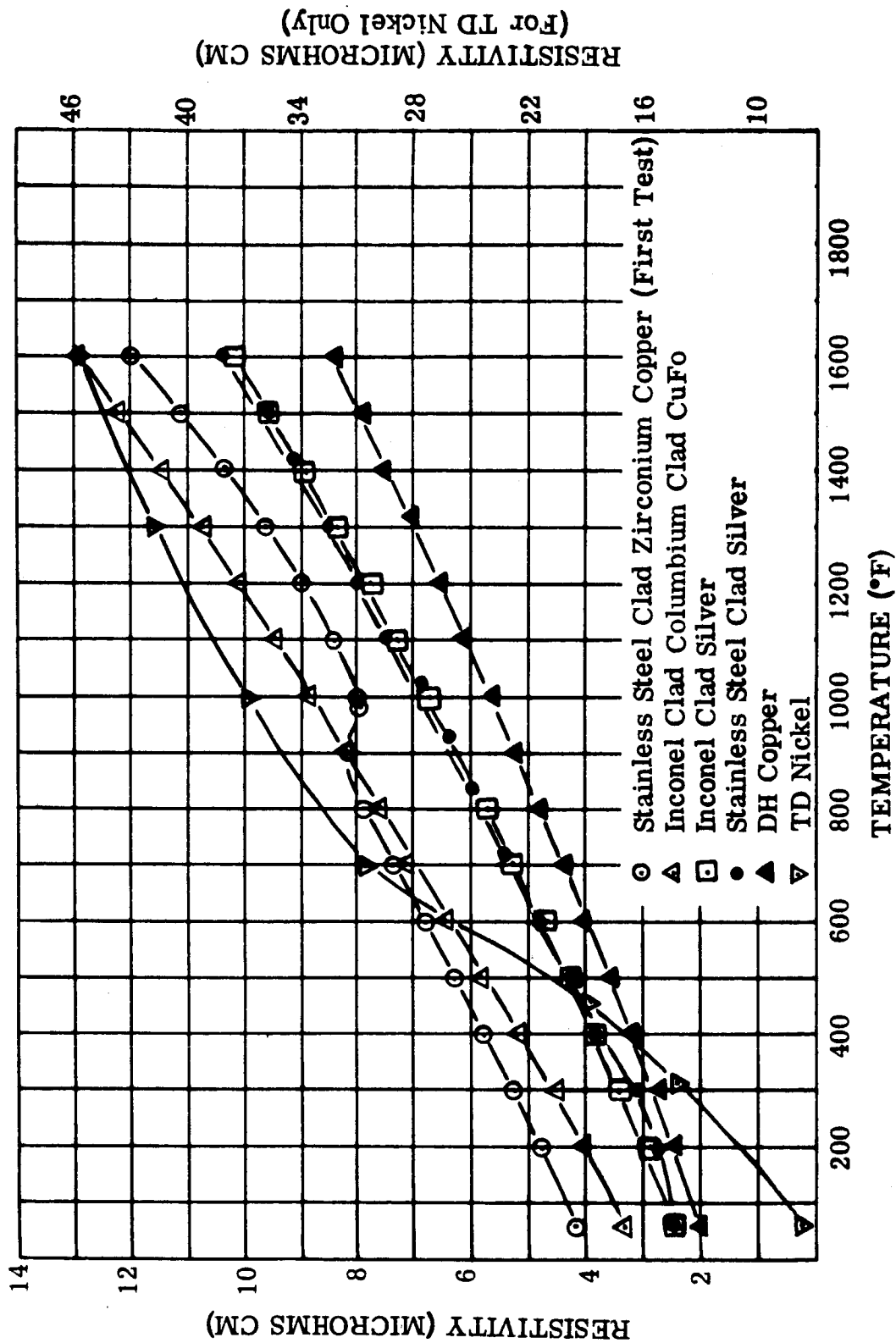


FIGURE III-12. Electrical Resistivity vs. Temperature of Conductors in Vacuum.  
See Tables III-3, III-4, III-6, III-7, III-8 and III-9  
(Reference: NAS3-4162)

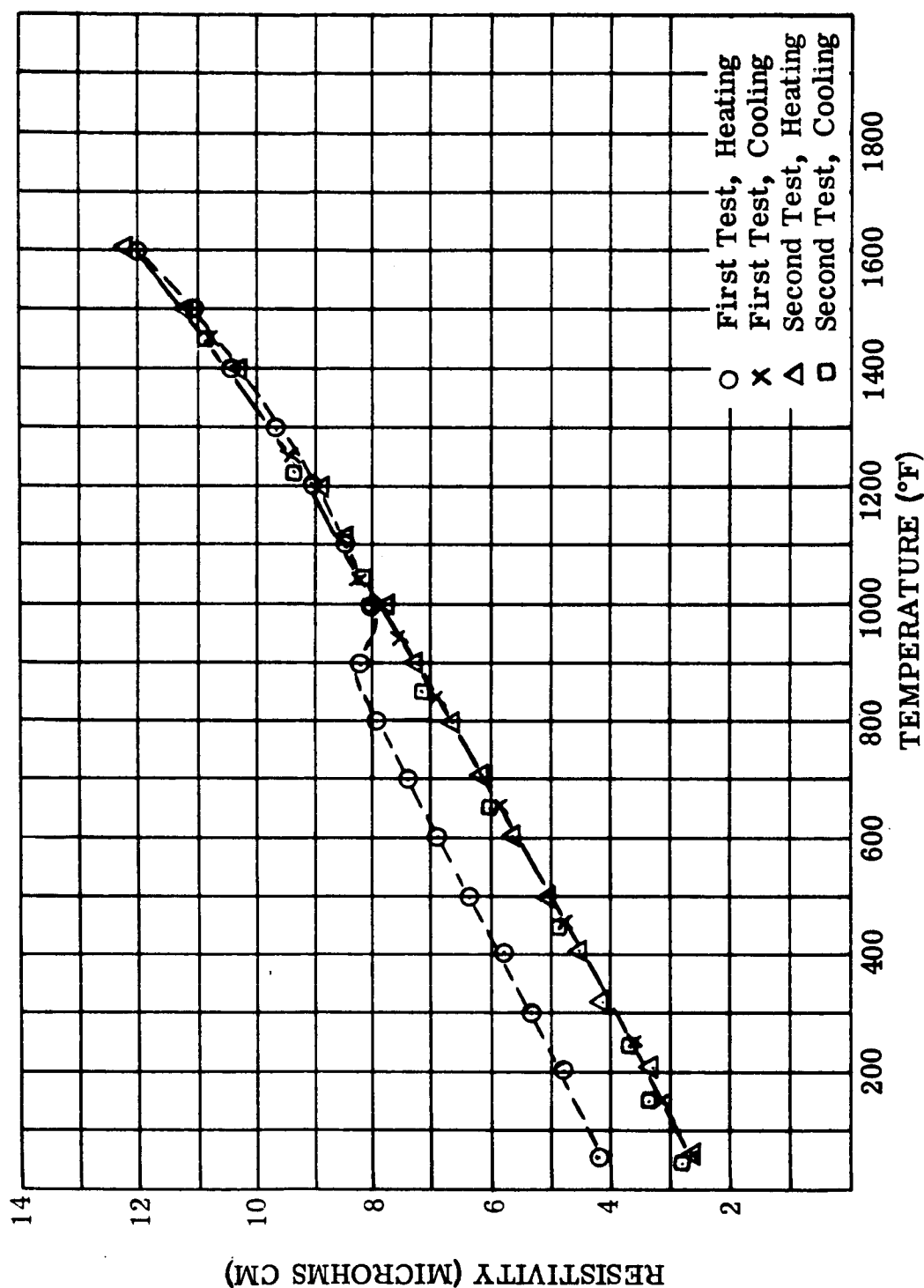
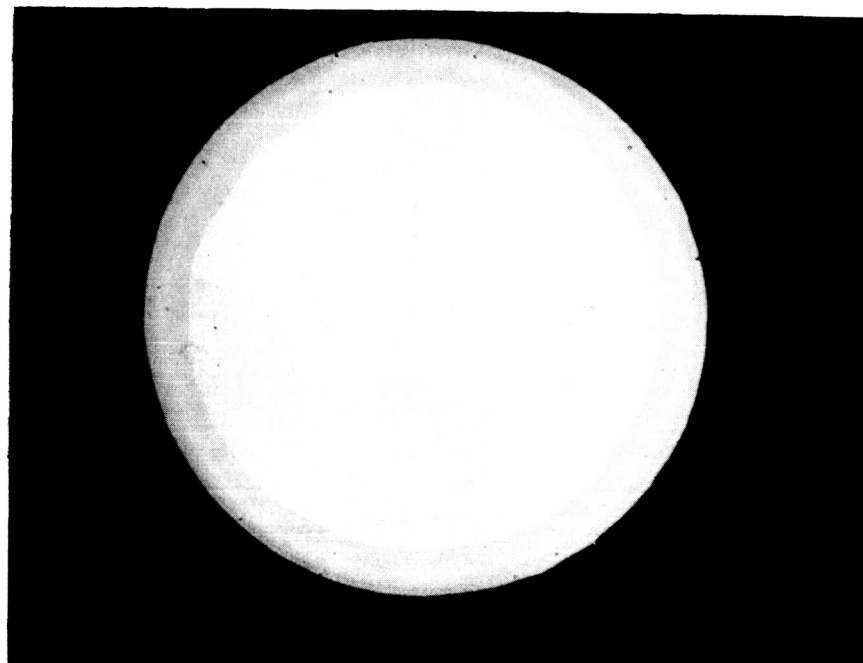


FIGURE III-13. Electrical Resistivity vs. Temperature of Stainless Steel-Clad Zirconium Copper in Vacuum. See Tables III-9 and III-10. (Reference: NAS3-4162)

Figure III-13. Electrical Resistivity - SS-Clad Zr Copper

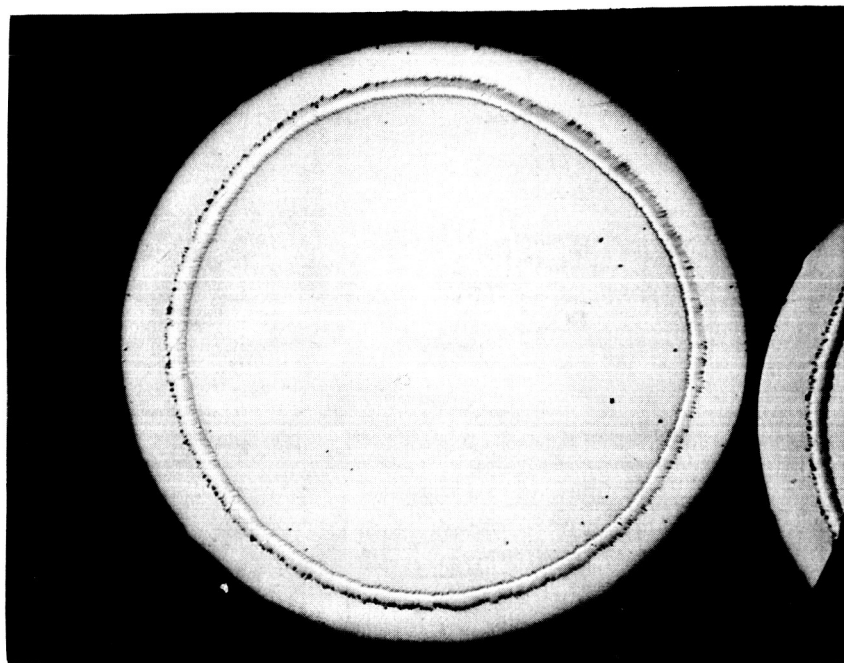


Unetched

Mag. 75X

Typical cross section of 0.040 inch diameter wire as supplied.

FIGURE III-14. 321 Stainless Steel-Clad (28% of Area) Silver



Unetched

Mag. 85X

Typical 0.040 inch diameter wire section illustrating relative thicknesses of outer and inner sheaths and core. These proportions remain constant during drawing.

FIGURE III-15. Inconel-Clad (28% of Area) Dispersion-Strengthened Copper (CuFo) With Columbium Barrier Layer (8% of Area)

## SECTION I V

### ELECTRICAL INSULATION MATERIALS

#### A. INTRODUCTION.

Determination and interpretation of data on the mechanical, physical and electrical properties are in progress on organic and inorganic electrical materials. The forms examined in this program include wire insulation, flexible sheet, laminate, molded, and cast insulations. The composition of the materials selected are given on pages 81 and 82 of the Second Quarterly Report WAED64.14E.

#### B. SUMMARY OF EFFORT IN THIS QUARTER.

During the third quarter of the program, compilation and interpretation of the collected data have continued. The materials selected during the earlier portion of the study are being subjected to tests suitable for evaluation of each category. These tests have been described and submitted to NASA in test book form. The materials needed for the tests have been acquired and the preparation of test specimens is about 95 percent complete. The testing phase itself is approximately 50 percent complete. The degree of completion is as follows: The physical testing program is approximately 40 percent completed. This includes tensile strength data for six flexible sheet insulations, compressive strength data for three rigid sheet insulations and two encapsulants, and flexural strengths and modulus for two rigid sheet insulations. Values were obtained at all required temperatures. In the electrical test program, a total of 107 categories of materials and tests are required in the program. Out of this number, 29 have been 100 percent completed, 2 are 75 percent complete, 3 are 50 percent complete, and 8 are 20 percent complete. Of the total of 28 different insulating materials in the program, 12 have been evaluated for weight loss in vacuum at the required temperatures.



## C. ELECTRICAL AND THERMOPHYSICAL TEST RESULTS.

### 1. Electrical Testing

Electrical testing has been purposely delayed until all testing specimens are prepared. This program is now proceeding rapidly. No data are reported here as it is believed a more meaningful and logical presentation will result after a larger portion of this effort is completed.

### 2. Physical Testing

#### a. Tensile Strength

Tensile strength data for sheet insulation are shown in Table IV-1. The tensile strengths of the organic flexible sheet insulation are higher than the inorganic, reflecting the high strength of the glass cloth base. Of the two types of Pyre-ML, the flexible variety has the lower strength because incomplete wetting of the fibers by the resin has been utilized as a means to gain flexibility. Tensile strength of Fiberfrax is very low, as expected, showing the need for careful handling of this material. All tensile tests on sheet material have been completed.

TABLE IV-1. Tensile Tests on Flexible Sheet Insulation  
at Room Temperature in Air

Test: ASTM D902 (Average of 3 samples)

Sample	Thickness (mils)	Breaking Strength (lbs per inch of width)
Pyre-ML-flexible grade	9.6	138
Pyre-ML-semi-flexible grade	9.9	338
AB1 PM	3.9	27.6
128-50-1	3.7	33.4
Fiberfrax	17.3 (nominal 20 mil)	0.416
Synthetic Mica, CM-1	10.2	8.6

**TABLE I V-2. Compressive Strength of Various  
Materials in Air**

Test: ASTM 759 (Average of 3 Samples)

<u>Material</u>	<u>Type</u>	<u>Test Temperature (°F)</u>	<u>Compressive Strength (psi)</u>
Doryl H17511	Rigid Sheet	350	56,500
Epoxy H2497	Rigid Sheet	75	74,100
Epoxy H2497	Rigid Sheet	350	46,350
92M	Rigid Sheet	75	44,400
92M	Rigid Sheet	932	37,800
92M	Rigid Sheet	1112	23,850
Epoxy-Hysol	Encapsulant	75	26,300
Epoxy-Hysol	Encapsulant	300	12,350
W-839	Encapsulant	75	12,750
W-839	Encapsulant	932	20,200

**b. Compressive Strength**

Compressive strength determinations for several materials have been completed. The data obtained to date are tabulated in Table I V-2. The rather low values obtained at room temperature for the W-839 encapsulant are unexpected and appear unreasonable. Since fabrication techniques may have damaged the test specimens these values will be rechecked.

**c. Flexural Strength and Flexural Modulus**

Tests for determining flexural strength and modulus have been completed on the two materials listed in Table I V-3.

TABLE IV-3. Flexural Strength and Modulus on Rigid Sheet Insulations in Air

Test: ASTM D790 (Average of 3 Samples)

Material	Test Temp. (°F)	Flexural Strength (psi)	Flexural Modulus (psi)
Doryl H17511	75	67,250	$3.06 \times 10^6$
	350	59,650	$2.64 \times 10^6$
	400	42,700	$2.29 \times 10^6$
Epoxy H2497	75	72,650	$3.20 \times 10^6$
	350	17,050	$1.22 \times 10^6$
	400	11,900	$0.94 \times 10^6$

TABLE IV-4. Linear Thermal Expansion for Various Materials

Test: ASTM C372

Material	Type	Temp. Range (°F)	Coefficient of Thermal Expansion (°F) <sup>-1</sup>
Doryl	Rigid Sheet	75-350	$6.9 \times 10^{-6}$ (Figure IV-1)
Hysol Epoxy	Encapsulant	75-200	$23.6 \times 10^{-6}$ (Figure IV-2)
		200-320	$33.3 \times 10^{-6}$
92M	Rigid Sheet	75-570	$2.85 \times 10^{-6}$ (Figure IV-3)
		570-1110	$3.8 \times 10^{-6}$
Sauereisen #8	Encapsulant	75-700	$2.4 \times 10^{-6}$ (Figure IV-4)
		700-1600	$3.6 \times 10^{-6}$

#### d. Thermal Expansion

Linear thermal expansion was measured on four different materials over their recommended use temperature range. In a plot of the total expansion versus temperature data, a curve was generated rather than a straight line relationship. In Table I V-4 the characteristics have been broken down into two temperature ranges to show the higher expansion rates at the higher temperatures. Exact expansion rates for any desired point or temperature range can be taken from the actual expansion curves given in Figures I V-1, I V-2, I V-3, and I V-4.

#### 3. Weight-Loss Tests in Vacuum

A schematic drawing of the apparatus used in the weight-loss tests is shown in Figure I V-5. A magnetic balance is incorporated into the vacuum system which allows a continuous following of weight-loss without breaking the vacuum to remove and reweigh the sample. A loss in weight of the sample is reflected and measured by measuring the decreased coil current required to keep the balance at equilibrium. A very sensitive variable leak has been built into the system to allow determinations to be made at various pressures and in any desired atmosphere. The use of two liquid nitrogen traps in conjunction with the forepump and diffusion pump have produced a vacuum of  $5 \times 10^{-7}$  torr in this system.

The amount of water or other solvent absorbed on a sample is greatly dependent not only on the extent of cure it has received, but also on its storage history. For this reason, the weight-loss "zero point" of all inorganic samples was taken after they had been heated overnight at 212°F under vacuum in the test apparatus. The temperature was then raised to that required in the test. The sample was held at test temperature for at least 21 hours or until a definite weight-loss trend was established. Most of the loss took place within the first three hours.

Weight-loss determinations have been made on two insulated magnet wires, four flexible sheets, three rigid sheets and three potting compounds. Some chipping and loss of insulation from the magnet wires took place during the measurement. This was due to the combined effects of very sharp bends made in forming the sample coil and the method of suspending it from the balance. These tests will be repeated.

The results of the weight-loss tests are plotted in the accompanying figures as milligrams-lost-per-square-centimeter of sample surface versus time-in-hours at stated temperature and pressure. Most of the measurements were made at pressures in the  $10^{-5}$  to  $10^{-6}$  torr range.

One insulation, 92M rigid sheet, was run at  $10^{-6}$  and also in a helium atmosphere of  $10^{-3}$  torr to determine if there is any significant difference in weight-loss at these two pressures. These curves are shown in Figures IV-6 and 7. The similarity of the amount of weight-loss at these two pressures, at  $1562^{\circ}\text{F}$ , indicates that reducing the pressure any further would have little or no effect on the weight-loss. This similarity in weight-loss is to be expected since even at room temperature and  $10^{-3}$  torr, the molecular population density is very low. At these conditions, the average distance which an escaping molecule travels before encountering another molecule is of the order of centimeters. At  $10^{-4}$  and  $10^{-5}$  torr this distance increases to 50 and 500 centimeters, respectively. At higher temperatures, this distance is even greater. So, for all practical purposes, a molecule leaving the surface at  $10^{-5}$  is as lost to the insulation body as it would be at pressures encountered in deep space. Because of these considerations, no measurements will be made at pressures lower than  $10^{-6}$  torr.

In a tubular chamber such as this unit, the wall temperature becomes a factor. Cold walls collect the molecules given off. However, walls at temperatures higher than the specimen temperature reject most of the outgassed molecules which strike the hot wall. The molecules then either are carried off to the pump, or to the cold wall zone, or return to the specimen. The molecular collection capacity represented by the sum of the large area of cold wall plus the pumping volume is many times larger than the capacity to return outgassed molecules to the specimen as represented by the hot wall area. Thus, the error induced by the limited hot wall area in this assembly is negligible for weight-loss studies of this time duration.

Flexible sheet, 128-50-1, a silicone bonded, glass-fabric backed mica was heated in vacuum to  $932^{\circ}\text{F}$  for 22.5 hours and then for 48 hours at  $1112^{\circ}\text{F}$ . The results are shown in Figure IV-8. These data show the need for extended pre-baking and outgassing of resin-bonded high temperature systems.

The weight-loss testing of the organic materials required some modification of the test device. To guard against possible contamination of the vacuum balance during weight-loss measurements of or-

ganic insulations, the original apparatus was redesigned and re-assembled. In the final assembly, shown in Figure I V-5, the condensing surface between the sample and the balance has been increased and the vacuum take-off has been moved from the area of the upper condensing surface to the lowest point in the system. The more thermally stable organic materials, polyimide H film, Pyre ML semi-flexible sheet and Doryl laminate, were run at 482°F and  $10^{-5}$  to  $10^{-6}$  torr. These were first dried at 167°F under vacuum before increasing to 482°F. Conventional organics such as the cast epoxy 4186/H5-3537 were dried at 122°F in the vacuum system before measuring their weight loss at intended operating temperatures. One epoxy, Scotchply 1100, was run at 482°F to determine the order of weight loss expected of such materials which may be exposed to this high temperature.

The results of the above determinations are presented in Figures I V-9, 10, 11, 12 and 13. These data and their implications will be fully discussed in the concluding topical report when complete test results are collected.

#### 4. Water Absorption

The water absorption of three organic materials had been completed. Determination of the values for the other organic and inorganic compositions are in progress. The values are reported in Table I V-5.

TABLE IV-5. Water Absorption

Test: ASTM D57

Material	% Absorbed	Average
Epoxy-Glass (H-2497) Laminate	0.075	0.088
	0.093	
	0.096	
Epoxy Encapsulation (C9-4186, H5-3537)	0.25	0.26
	0.26	
	0.28	
Diphenyl Oxide (H-17511) Glass Laminate	0.33	0.35
	0.36	
	0.37	

#### D. MATERIAL SELECTION.

Several materials have been withdrawn from further test effort for a number of reasons. The materials and the discussion is presented below.

- 1) A change in the type of synthetic mica paper to be used has been made from CM-2 to CM-1. The new mica paper is a synthetic mica and is 100 percent mica instead of 80 percent as in CM-2. Tests by Westinghouse indicate this new selection should be better electrically, will have a lower space factor, and will resist abrasion and handling better.
- 2) Sauereisen Cement #29 was dropped as an encapsulating compound because of low insulation resistance at temperatures above 1000°F. Despite other good properties this would severely limit its temperature capability as an insulator. A suitable replacement has not been found since most of the potential candidates contain similar alkaline silicate binders and thus are limited by electrical performance to about 1000°F. These include Sauereisen numbers 8, 31, and 32.
- 3) Plasma sprayed alumina insulation for conductors is not readily available as a commercial item. The technology of construction is well defined but application of the insulation is limited to preformed shapes. Although the high-temperature capabilities of this wire exceed those of the other insulations, studies on this form are in progress under Contracts AF33(657)10701 and AF33(615)1360 and need not be duplicated.
- 4) The relative advantage of the two flexible sheet insulations made from phlogopite mica were considered in view of intended use requirements. The essential difference between the 128-50-1 and the ABIPM are very much better winding and handling properties of the former and the better bond strength after curing of the latter. The electrical properties are similar after final curing. Because of this, information on the cured 128-50-1 should apply to ABIPM. This suggests any test on cured ABIPM would be a duplication and will be eliminated.
- 5) A review of the glass-bonded mica materials, Micalex 620 and 620BB indicate two deficiencies. One is lower temperature capability than for alumina bodies, and the other is the



possibility of lead sublimation from the glass phase. A major advantage of both of these materials is suitability of metal inserts. However, in foreseeable applications, metal inserts would not be needed and the material has too small an area of application to merit further consideration.

- 6) During the winding of samples of high-temperature magnet wire, Anaconda magnet wire, Anacote, was found deficient in adherence. The wires were wound around 1-1/4 inch ceramic cores. Non-uniform flaking of the coating from Anacote occurred. This adhesion deficiency led to withdrawal of the material from further testing.
- 7) Imidite 1850 rigid sheet laminate has been eliminated due to difficulty in procurement of samples and also on the basis that although initial properties are quite good, these deteriorate rapidly with aging at high temperature.
- 8) CTL91LD, rigid sheet laminate, shows no area of advantage over the other materials in this class, i. e. the whole application range is covered by epoxy laminate, diphenyl oxide laminate, and the polyimide laminate.
- 9) Considerable information is available from DuPont on Polymer SP molding compound. Due to difficulties of cost and availability in procuring special test specimens, only available data will be used in this program. Also, since the polymer is the same as that used in H film and Pyre-ML, it is expected that complete tests on these materials will eliminate the need for further testing of Polymer SP.
- 10) Urethane foam, Carthane 1008, has been excluded as it is no longer available. On the basis that only one organic foam material need be selected, it is believed that silicone foam will be preferred over other available materials in this class for thermal stability reasons.
- 11) Due to the limited applicability of organic molded parts in a space generation system, it has been decided to limit the collection of data on the epoxy compound, Scotchply 1100, to physical properties only. This material had originally been suggested to the program as a substitute for the no longer available PMDA-containing epoxy compound. Because of meager information concerning the substitute epoxy material, a polyester material has been selected as a preferred molding compound and will be used for the program. The choice of polyester materials fell between Plaskon 452 and Plaskon

751. On the basis of easier fabrication and better retention of electric strength with aging at 400°F, Plaskon 751 has been selected for the program.

751. On the basis of easier fabrication and better retention of electric strength with aging at 400°F, Plaskon 751 has been selected for the program.

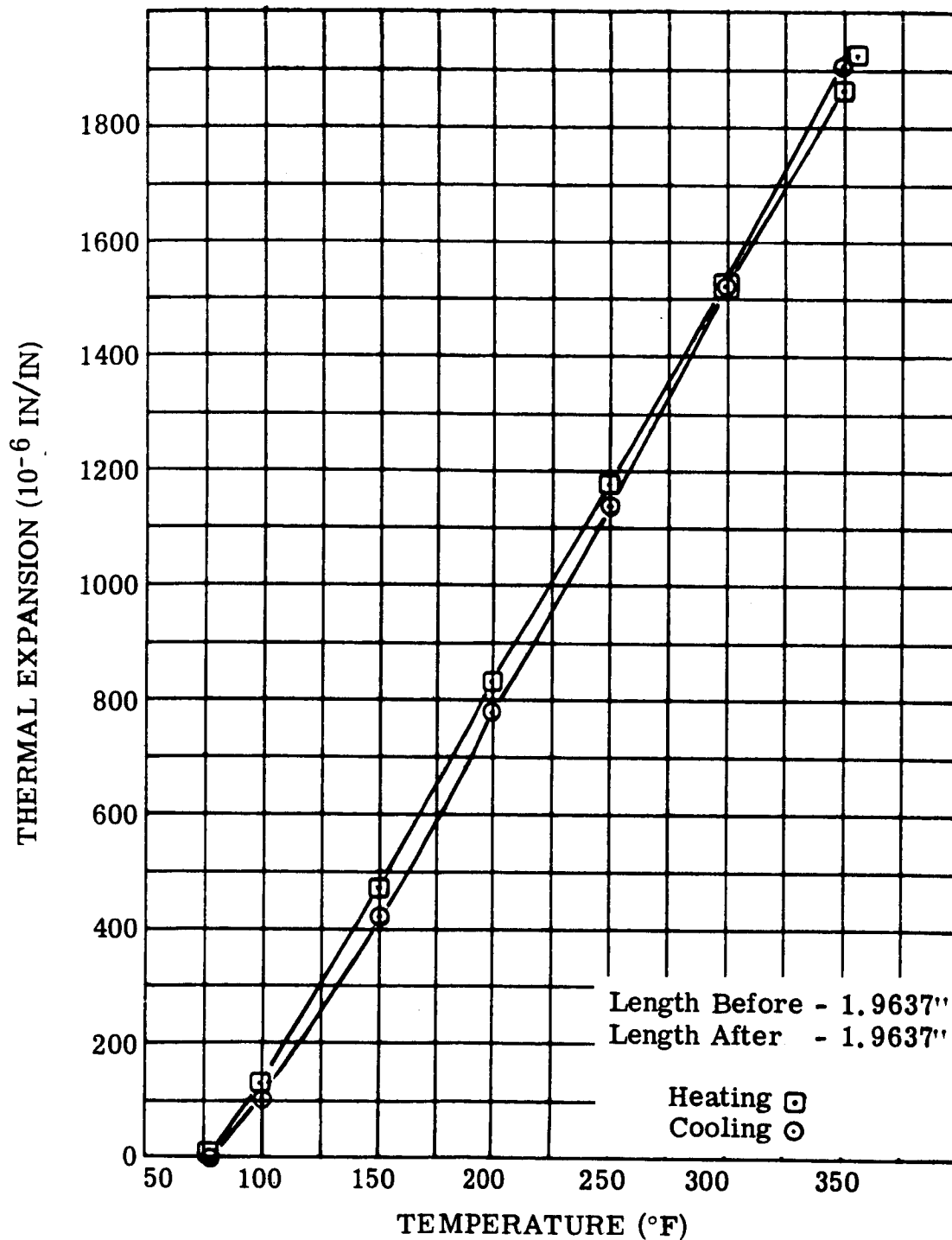


FIGURE I V-1. Thermal Expansion, Westinghouse Doryl H17511  
in Air (Reference: NAS3-4162)

Figure I V-1. Thermal Expansion - Doryl H17511

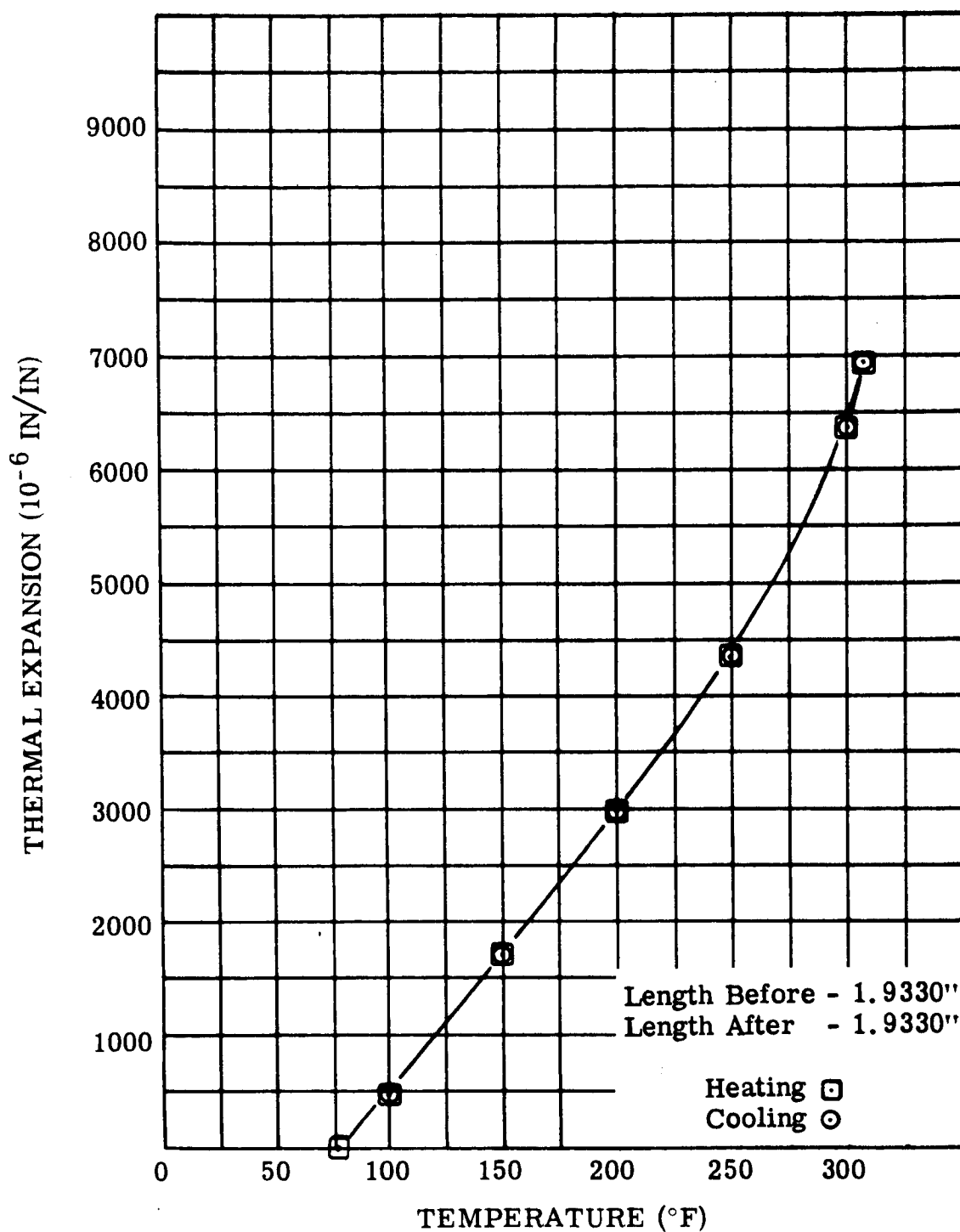


FIGURE I V-2. Thermal Expansion, Epoxy-Hysol in Air  
(Reference: NAS3-4162)

Figure I V-2. Thermal Expansion - Epoxy Hysol

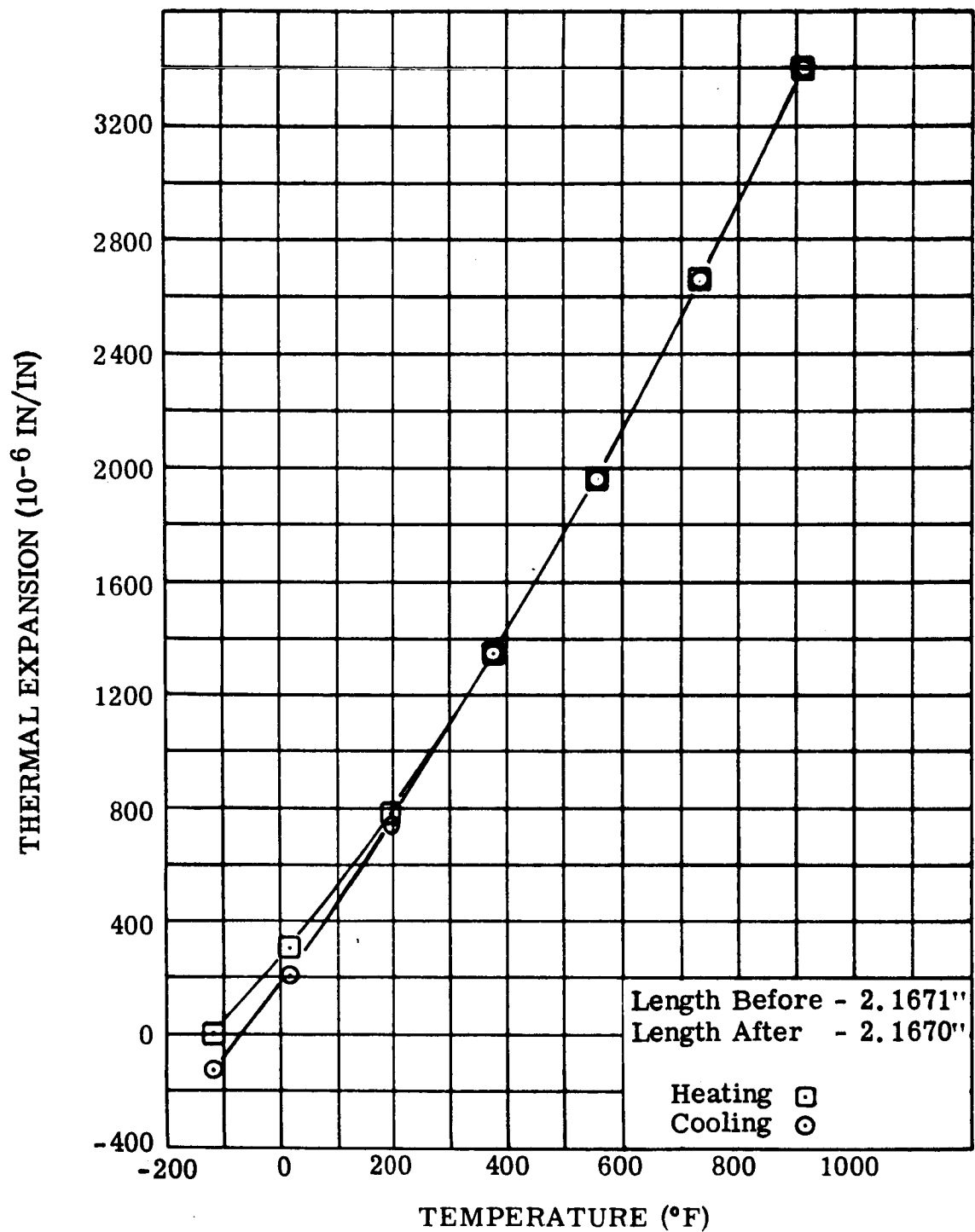


FIGURE IV-3. Thermal Expansion, 92M in Argon Atmosphere  
(Reference: NAS3-4162)

Figure IV-3. Thermal Expansion - 92M

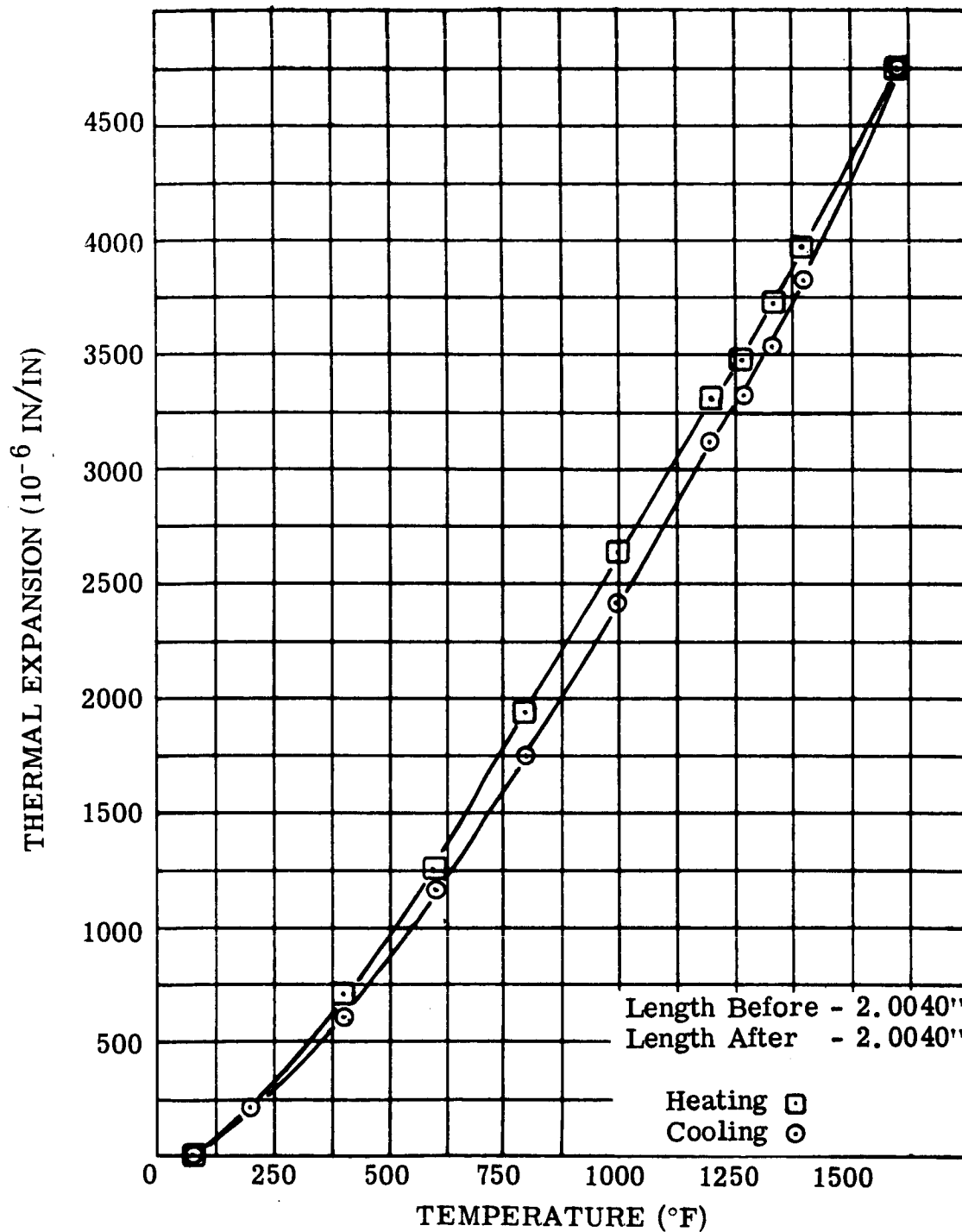


FIGURE IV-4. Thermal Expansion, Sauereisen #8 in Air  
(Reference: NAS3-4162)

Figure IV-4. Thermal Expansion - Sauereisen #8

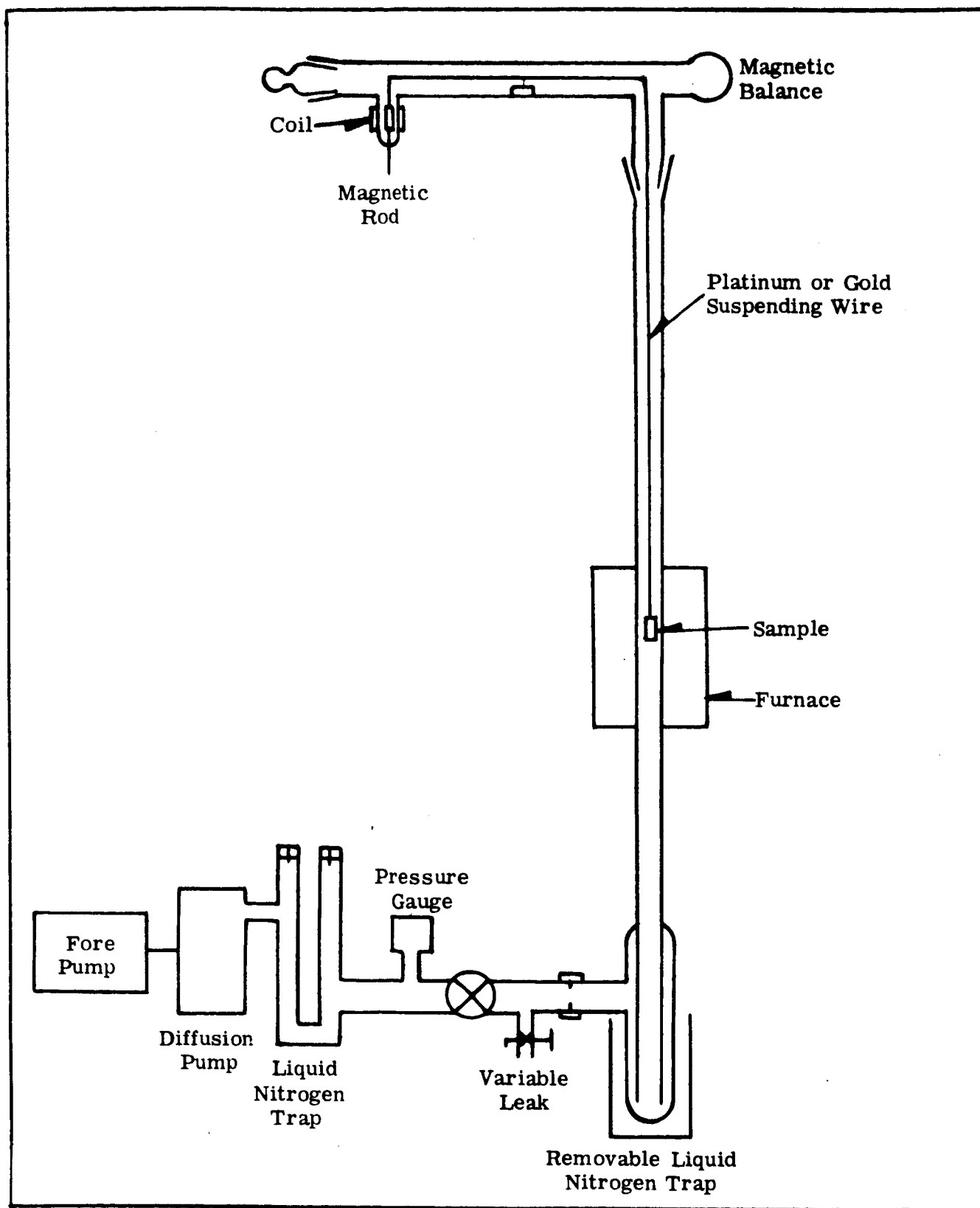


FIGURE IV-5. Schematic of Weight Loss Apparatus



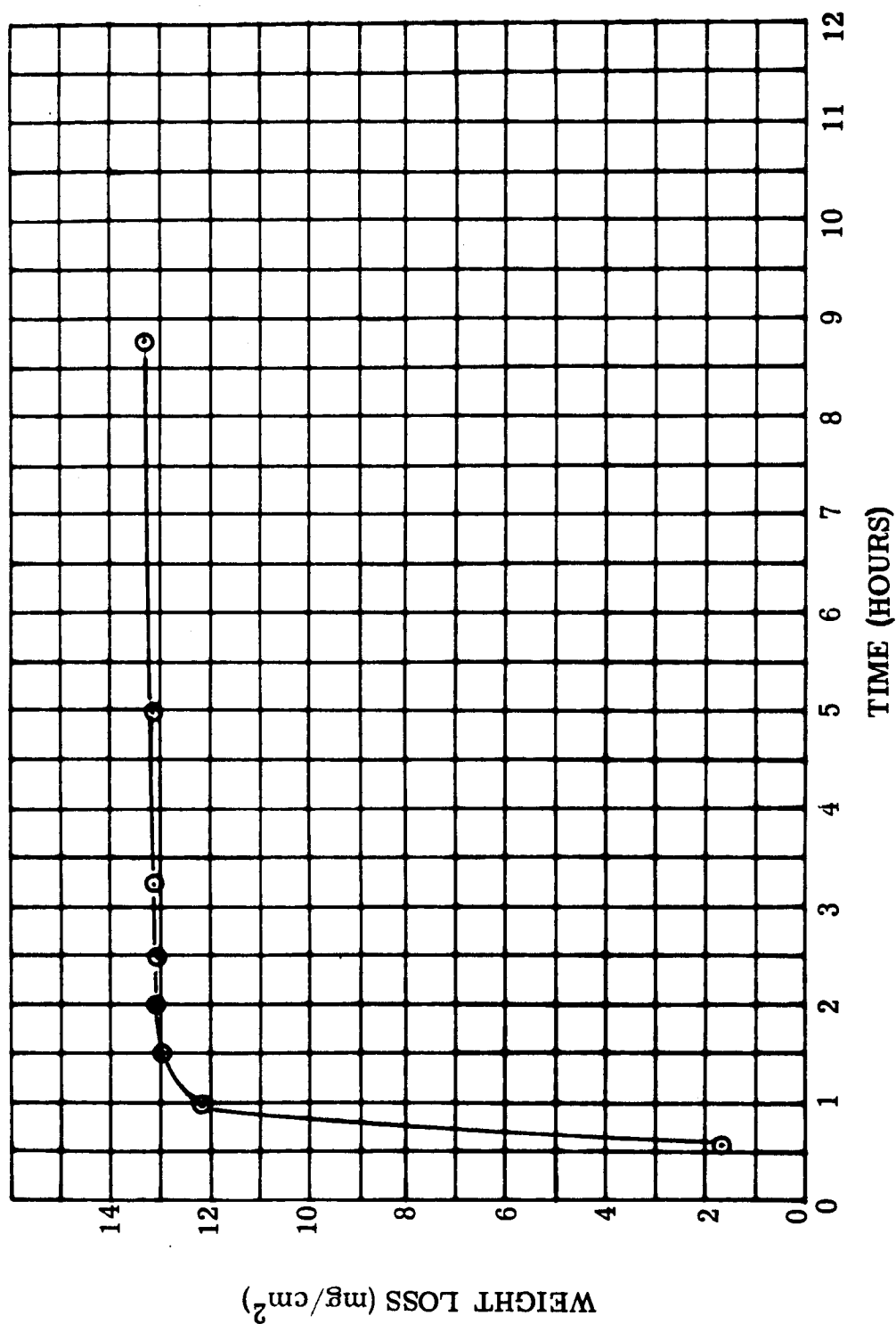


FIGURE I V-6. Weight Loss of 92M Boron Phosphate-Bonded Asbestos Rigid Sheet at 1560°F, 10<sup>-6</sup> Torr (Reference: NAS3-4162)

Figure I V-6. Weight Loss - Rigid Sheet - BPO<sub>4</sub> - Asbestos

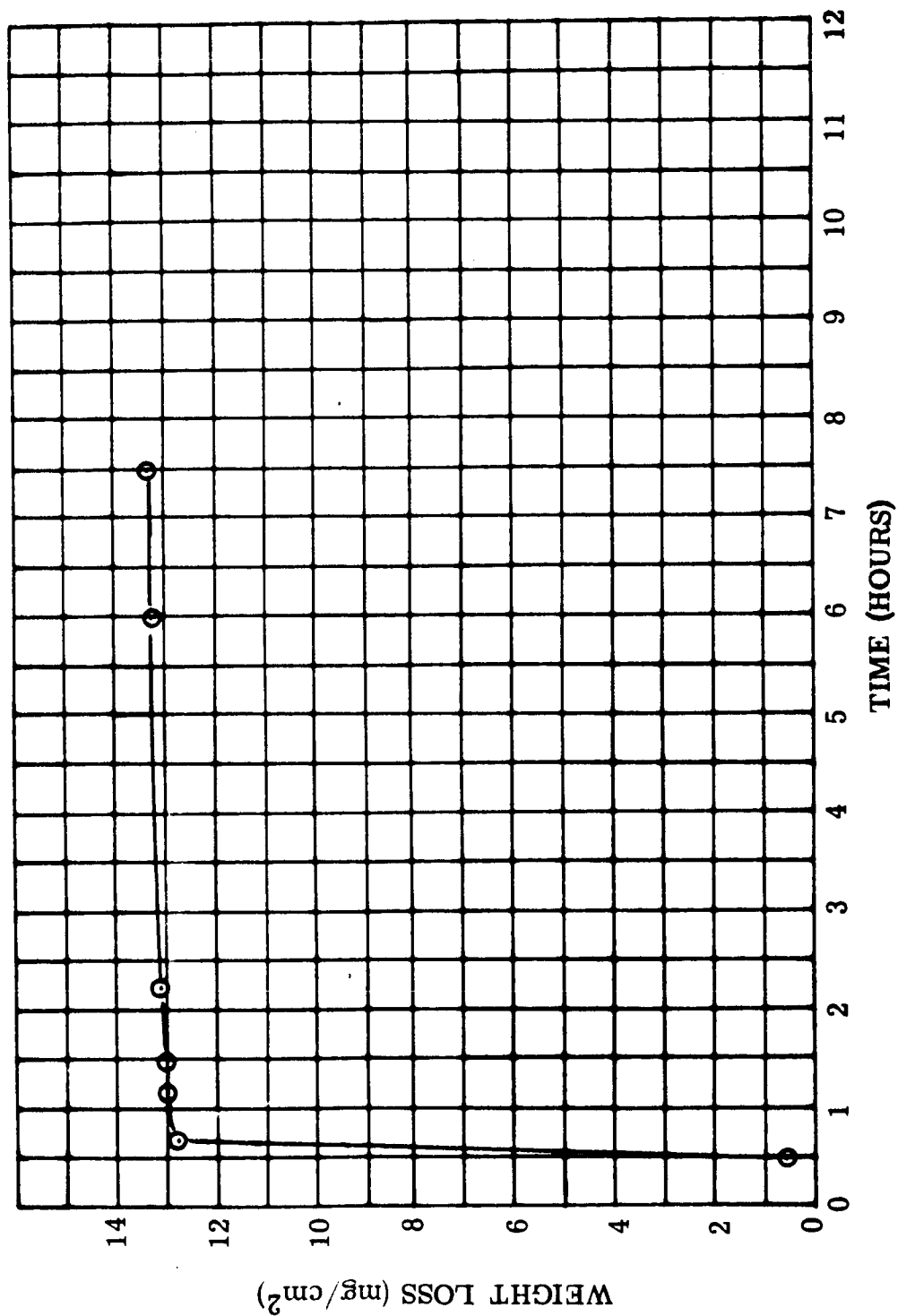


FIGURE IV-7. Weight Loss of 92M Boron Phosphate-Bonded Asbestos Rigid Sheet at 1560°F,  $10^{-3}$  Torr (Reference NAS3-4162)

Figure IV-7. Weight Loss - Rigid Sheet - BPO<sub>4</sub> - Asbestos

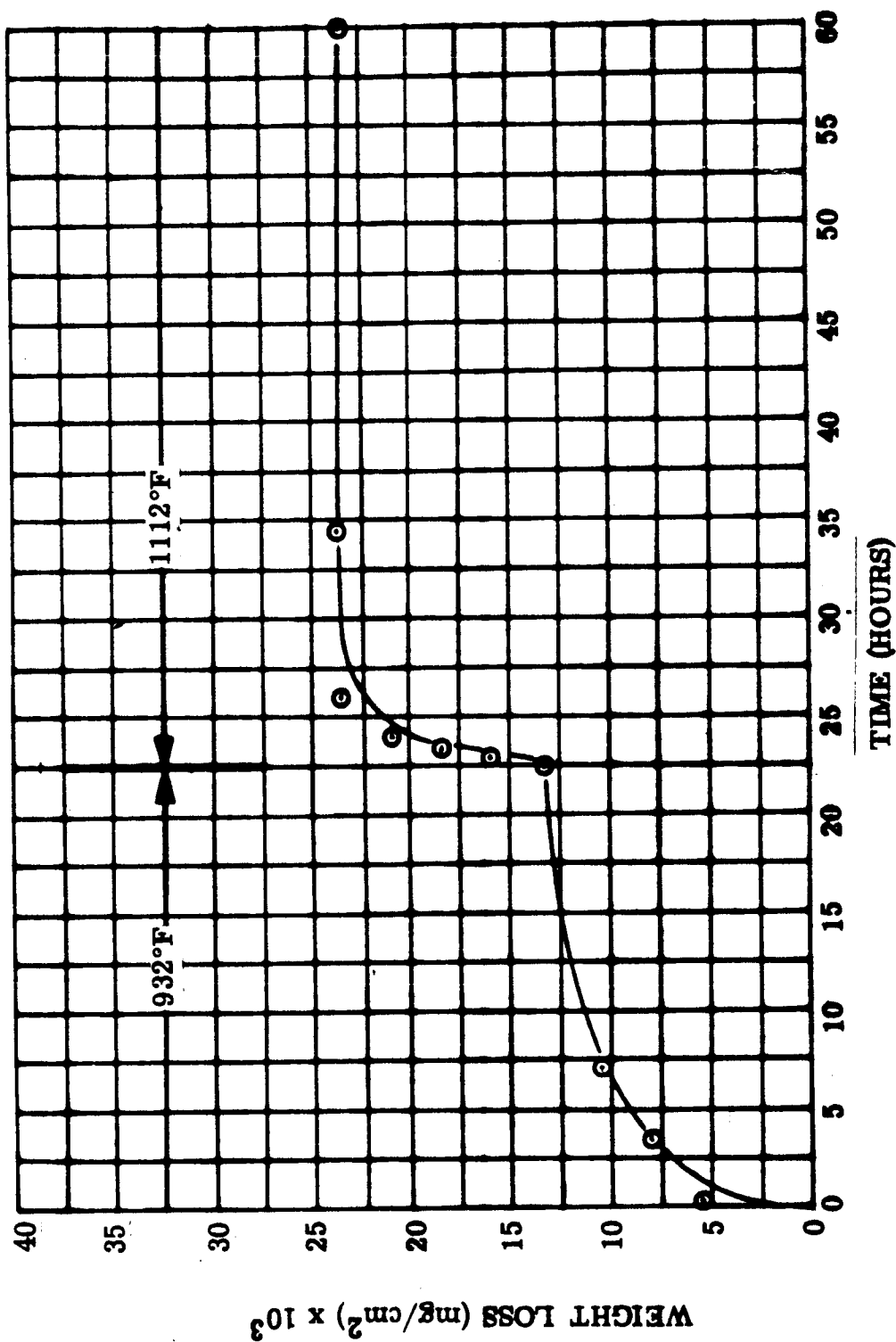


FIGURE IV-8. Weight Loss of 128-50-1 Silicone-bonded, Glass-backed Mica Flexible Sheet, 932°F and 1112°F,  $10^{-5}$  -  $10^{-6}$  Torr (Reference: NAS3-4162)

Figure IV-8. Weight Loss - Flex Sheet - Glass Mica

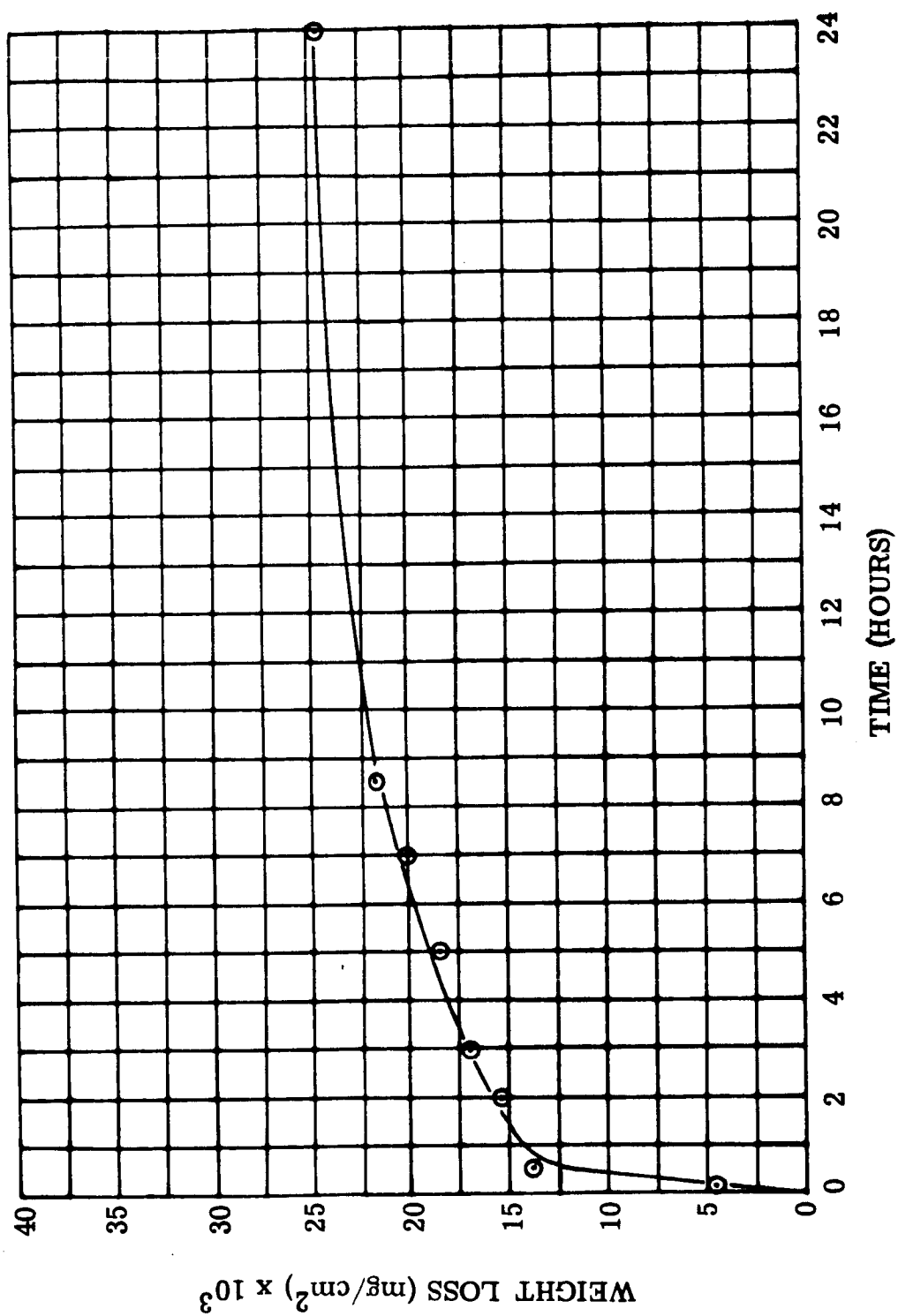


FIGURE I V-9. Weight Loss of Polyimide H Film, 482°F,  $10^{-5}$  -  $10^{-6}$  Torr  
(Reference: NAS3-4162)

Figure I V-9. Weight Loss - Polyimide Film

WAED64. 30E-122

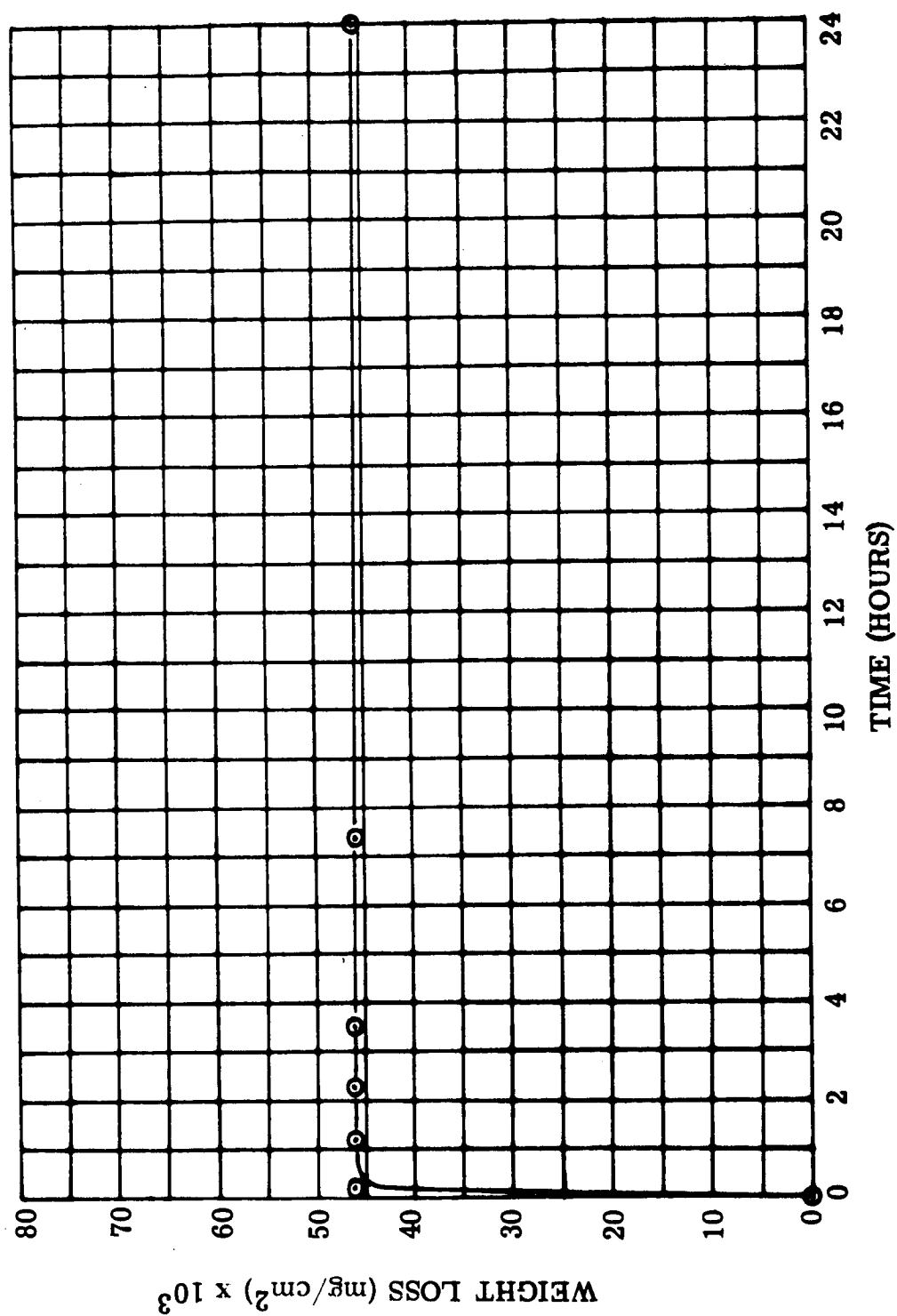


FIGURE I V-10. Weight Loss of Pyre ML-glass-cloth Semi Flexible Sheet  
482°F, 10<sup>-5</sup> - 10<sup>-6</sup> Torr (Reference: NAS3-4162)

Figure I V-10. Weight Loss - Polyimide Glass

WAED64. 30E-123

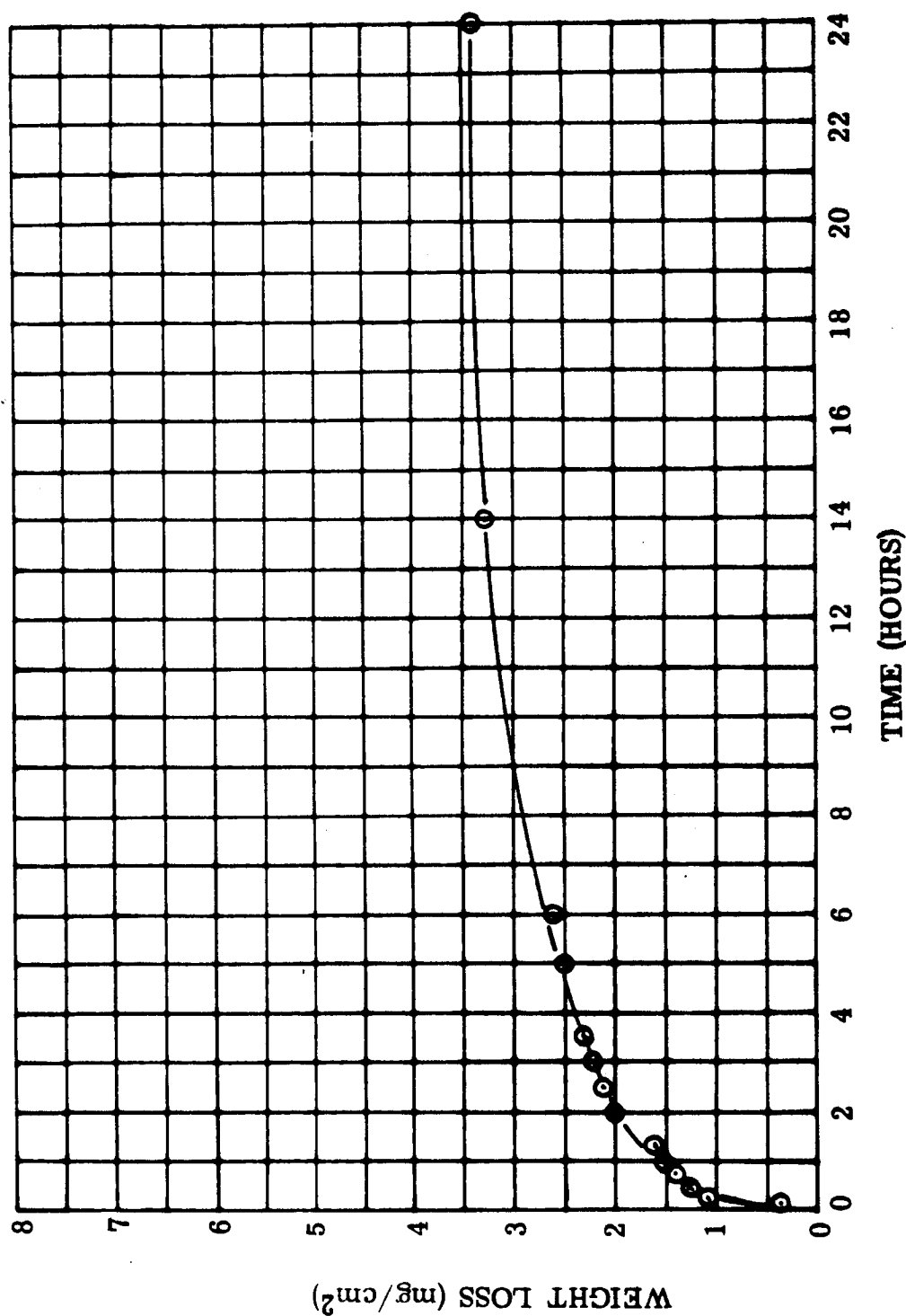


FIGURE IV-11. Weight Loss of Doryl H-17511 Rigid Sheet 482°F, 10-5 - 10-6 Torr. (Reference: NAS3-4162)

Figure IV-11. Weight Loss - Diphenyl Oxide Laminate

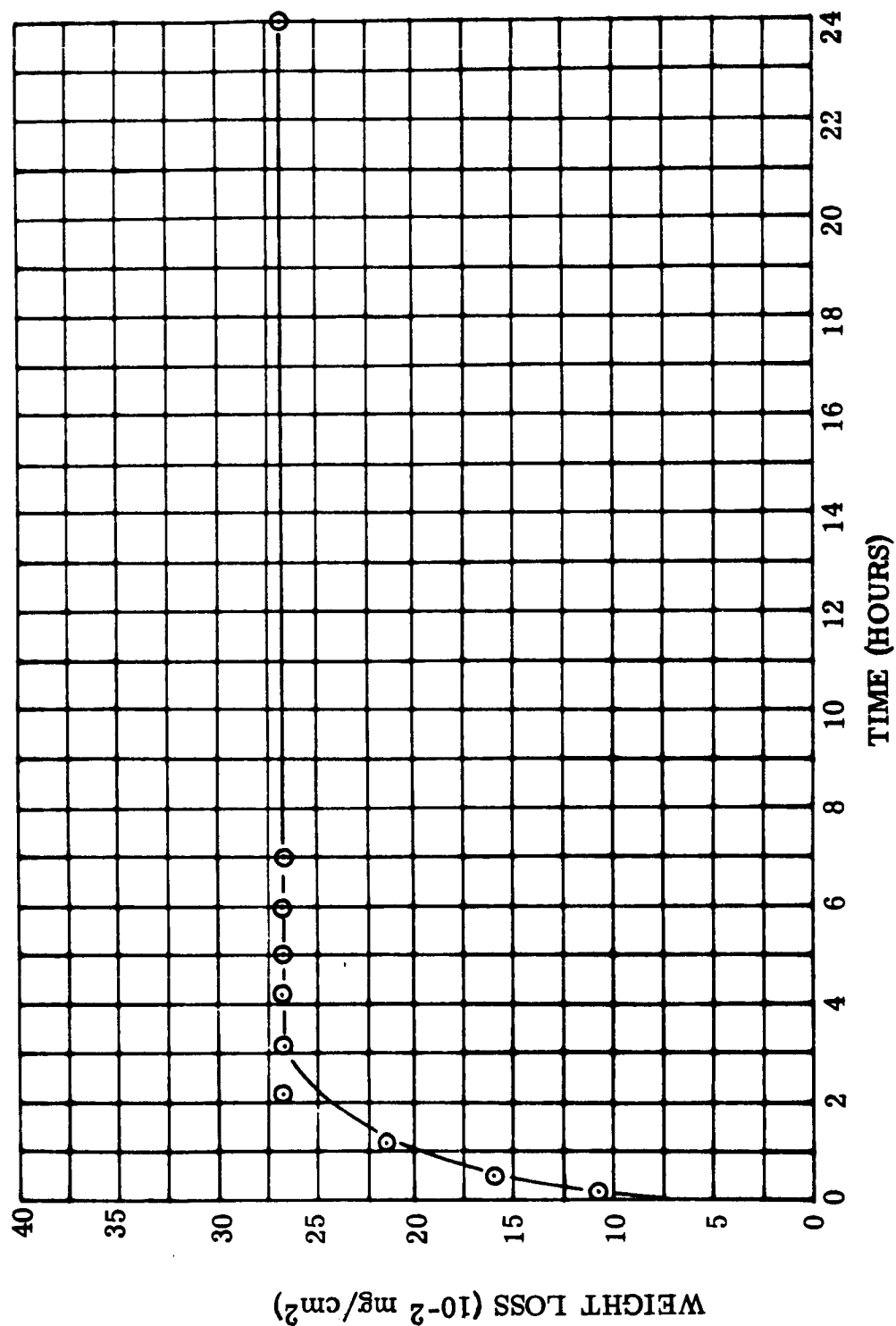


FIGURE IV-12. Weight Loss of Hysol C9-4186-H5-3537 Encapsulating Compound at 302°F, 10<sup>-5</sup> - 10<sup>-6</sup> Torr. (Reference: NAS3-4162)

Figure IV-12. Weight Loss - Epoxy Encapsulant

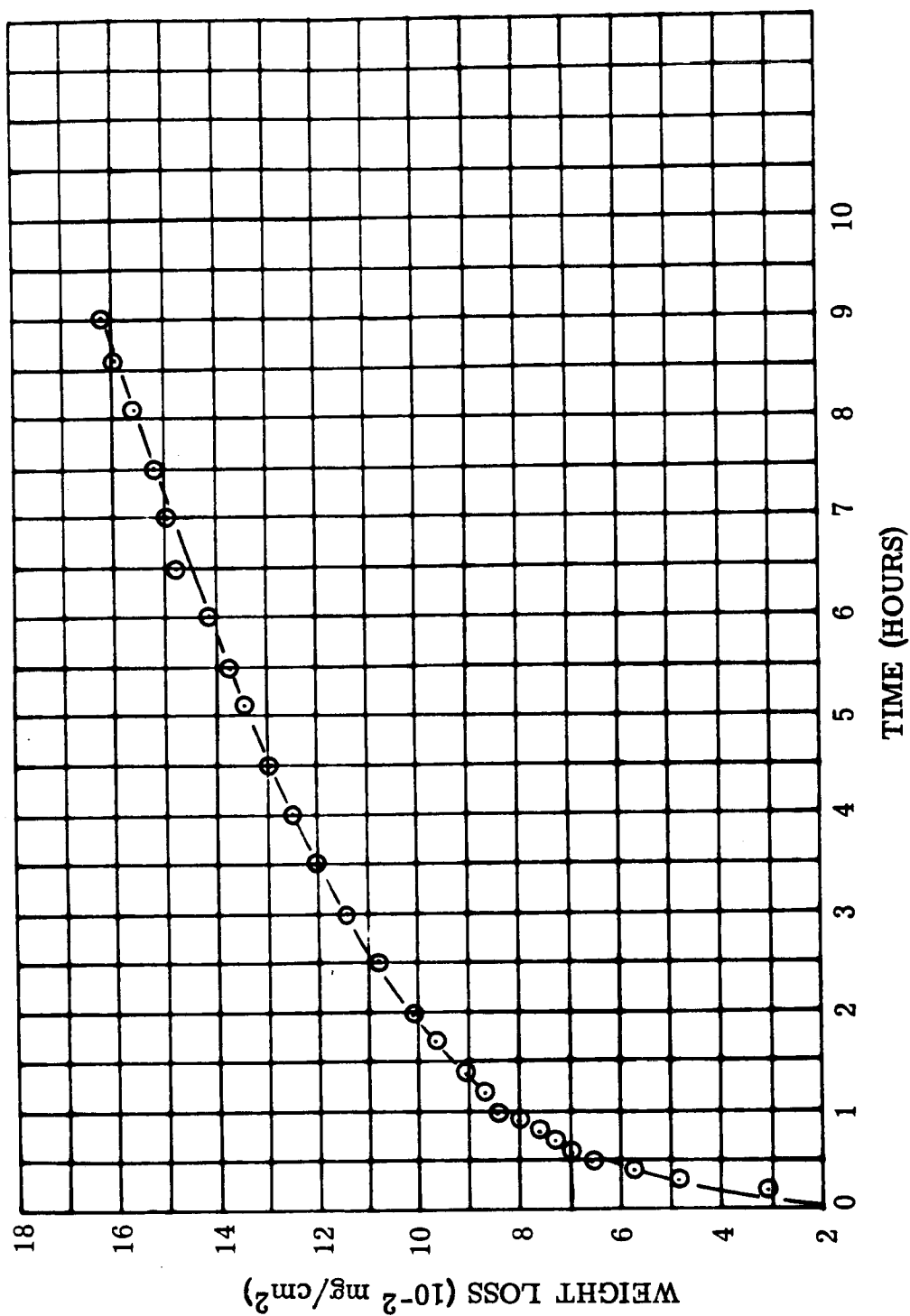


FIGURE IV-13. Weight Loss of Scotchply 1100 at 482°F, 10<sup>-5</sup> - 10<sup>-6</sup> Torr  
(Reference: NAS3-4162)

Figure IV-13. Weight Loss - Epoxy Molding Compound



## SECTION V

### BORE SEAL MATERIALS

#### A. INTRODUCTION.

The bore seal provides a hermetic division between the vulnerable portions of electric generators and motors and the alkali metal working fluids used in advanced space power systems. The objective of this program is to identify properties of bore seal material systems which are capable of long life at 1000°F and 1600°F when exposed to potassium, sodium-potassium eutectic and selectively to lithium.

The candidate materials for this program were selected on the basis of expected environmental compatibility, physical and mechanical properties and fabricability.

Static capsule tests will be used in the present program to determine alkali-metal corrosion effects. High-purity materials are being used in this study. The determination and control of the purity of alkali metals in the test capsules is being stressed, particularly in regard to oxygen contamination.

#### B. SUMMARY OF EFFORT IN THIS QUARTER.

- 1) The capsule loading facility and environmental test furnaces were completed and then operation was initiated.
- 2) Geometry correlation between ASTM CLM-15 and modulus of rupture assemblies was completed.
- 3) Metalizing, braze, thin film metalizing and electroformed seal work were completed.
- 4) All ceramic, metal, and braze materials required for the balance of the program were received.

- 5) Active braze alloy work was expanded and  $\text{Al}_2\text{O}_3$  and BeO seals to Cb-1%Zr metal achieved.
- 6) Five ceramic materials and one active alloy braze ceramic-metal sealing system were prepared in the form of modulus of rupture assemblies for the first 1600°F potassium exposure test.

## C. DISCUSSION.

### 1. Capsule Loading and Environmental Test Facility

The general facility details and tentative capsule loading procedures were discussed in the Second Quarterly Report WAED 64. 14E. Photographs of the overall setup and closeups of specific features are found in the accompanying Figures V-1 through V-4.

Two items which have been revised from the time of the Second Quarterly Report are: (a) position of liquid metal hot trap container during loading, and (b) an effluent gas trap was added to the dry box to prevent backstreaming. The hot-trap liquid metal container has been relocated external to the dry box to facilitate changing from potassium to sodium-potassium eutectic without opening the dry box. The hot-trap containers are too large to fit entirely into the entry vestibule and would necessitate opening both inner and outer door simultaneously for changing, with attendant contamination of the dry-box atmosphere. The new arrangement is shown schematically in Figure V-5. With this setup the "fill line" is evacuated and back filled with purified argon through the dry box. The line is then flushed by extruding the liquid metal through the heated line by pressurizing the hot trap container with valve E closed. A metered amount of liquid metal is then extruded by opening valve E and forcing the liquid metal in the vertical section of pipe out through the capillary needle N. The diameter of needle N is such that the liquid metal will not flow through it except under pressure.

### 2. Studies of Materials and Seals

#### a. Correlation Tests

A program was carried out to correlate existing ASTM tensile and drum peel test data with the modulus of rupture (M-of-R) and tab peel configurations. The new test shapes were selected to permit quantitative evaluation of the ceramic itself as well as the ceramic-metal seal and were designed to be small enough to fit in the 1/2 inch diameter by 4 inch deep test capsules for exposure to alkali metal vapor. Such quantitative data was not obtained on the ceramic portion of a seal in previous corrosion studies because of the limitations of the CLM-15 geometry.

The design of the modulus of rupture and tab-peel test pieces was shown in Figure V-6 of the Second Quarterly Report

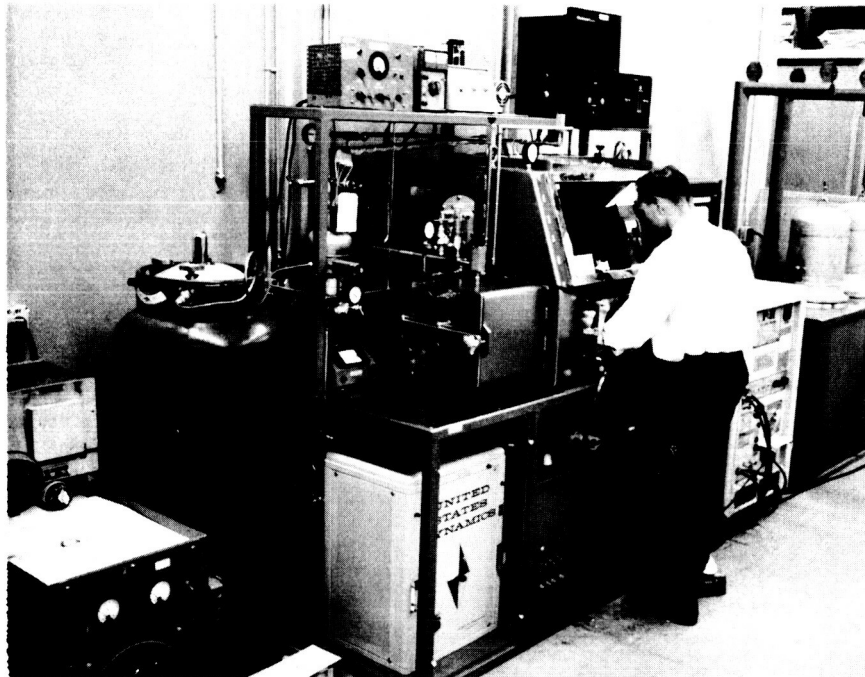


FIGURE V-1. Dry Box Facility

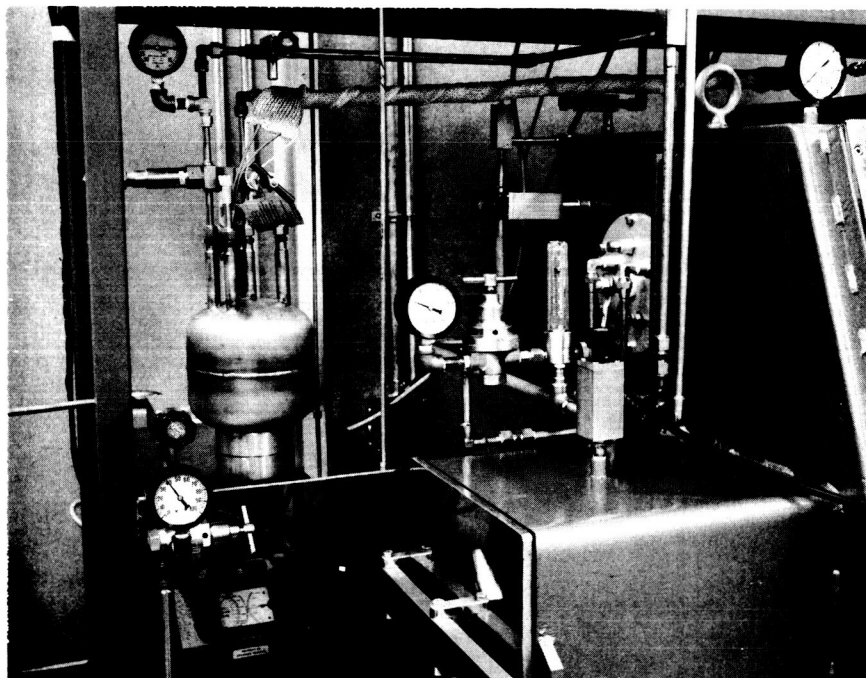


FIGURE V-2. Alkali Metal Facility Plumbing

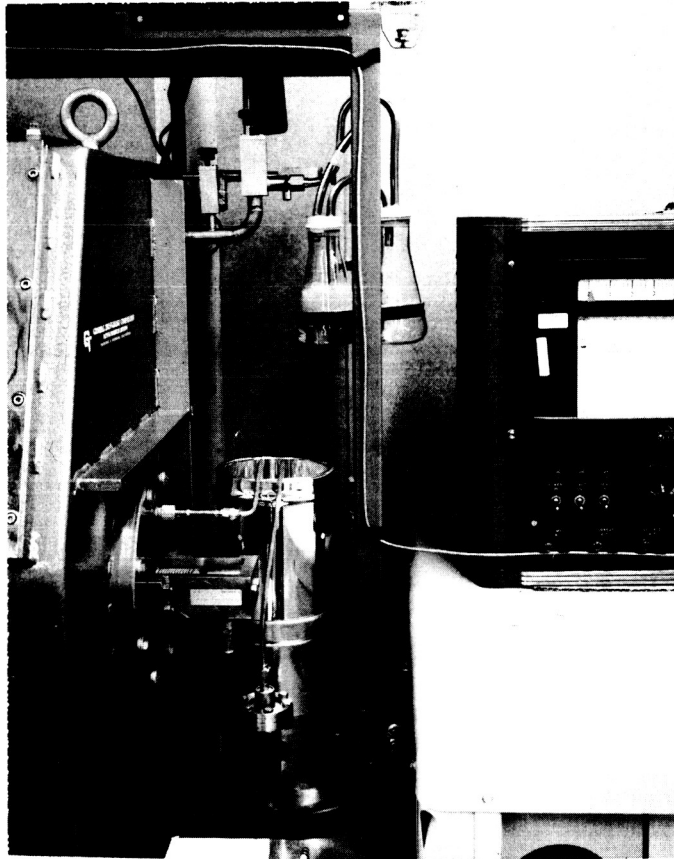


FIGURE V-3. Right Side of Dry Box

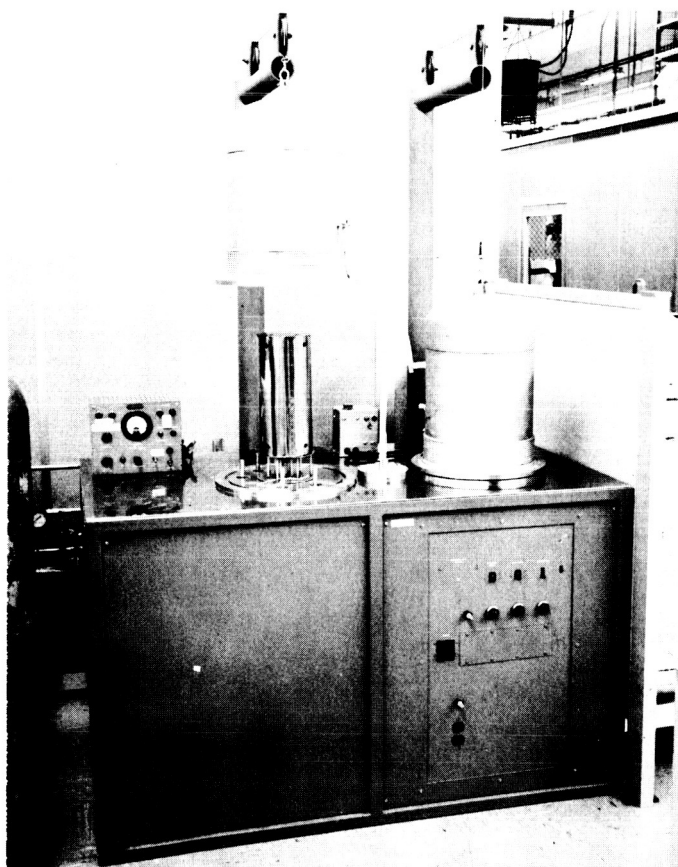


FIGURE V-4. Dual Vacuum Furnace

WAED64. 30E-133

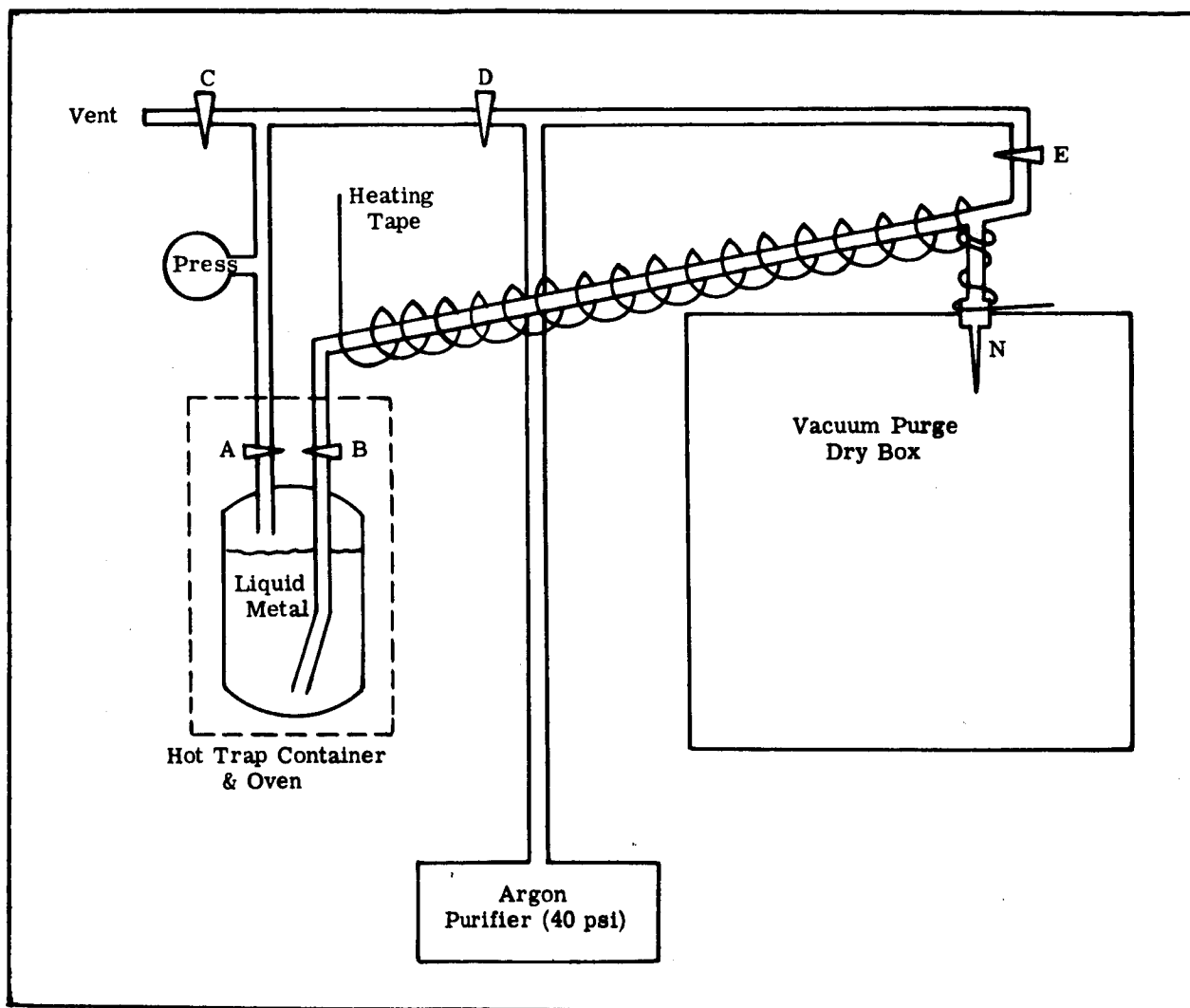


FIGURE V-5. Overall Schematic of Liquid Metal Loading Arrangement



WAED 64.14E. The test fixtures were shown in Figure V-8 and Figure V-9 of the same report. Two ceramic-to-metal braze systems were used in order to establish a better correlation than possible with a single system: (a) copper-silver eutectic braze to Kovar, and (b) Coast Metals Braze 52 (3B-4.5Si-0.15C-Ni), to columbium. The former system is a long established production braze system; the latter is a braze system which is more resistant to attack by alkali metals<sup>1</sup>. All correlation test ceramics were metalized with an Eitel-McCullough production paint, ( $\text{MoO}_3$ - $\text{MnO}_2$ - $\text{TiO}_2$ ), designated 20A. Standard Production bodies were used as the ceramic. These were Coors AD94 (94%  $\text{Al}_2\text{O}_3$ , 4%  $\text{SiO}_2$ , 1%  $\text{CaO}$ , 1%  $\text{MgO}$ , and Wesgo AL300 (97%  $\text{Al}_2\text{O}_3$ , 1.5%  $\text{SiO}_2$ , 1.5%  $\text{MgO}$ ).

A preliminary study was made to determine the extent of post brazing sample preparation that is necessary to adequately measure modulus of rupture bar brazed specimens. If grinding of all surfaces after brazing could be proven unnecessary, sample preparation time would be reduced considerably. For this series of tests the modulus of rupture test assemblies were brazed as indicated in Table V-2 using Kovar with both AD94 and AL300 aluminas. The brazed samples were divided into four categories: (1) minimum preparation with the excess metal trimmed sufficiently to permit the sample to fit into the test fixture, (2) samples trimmed of excess Kovar and hand ground to remove braze fillets, (3) samples trimmed of excess Kovar, hand ground to remove braze fillets, and surface ground on the support and bearing sides of the sample, and (4) maximum preparation with all sides surface ground flat and parallel.

The data in Table V-1 shows the modulus of rupture for the two alumina bodies evaluated. For comparison, the tensile strengths of these bodies as reported by the suppliers are listed at the bottom of the table. Tests of significant differences between means reveal that the mean of each M-of-R group are higher, with 95 percent confidence, than the tensile strengths reported by the manufacturer.

The analysis of variance shows that there is no significant difference between the M-of-R specimens as-received and

<sup>1</sup>Westinghouse Subcontract AF33(657)8954 Report WAED 62. 2E.

those submitted to the various heat treatments for each material. The alumina bodies are not degraded after subjecting them to typical thermal treatments associated with metalizing and brazing.

The modulus of rupture tests indicate that there is no significant difference between the strengths of the two alumina bodies. A ratio was established between M-of-R tests and tensile tests. Tensile strength is 0.69 times the modulus of rupture of the ceramic bodies.

Table V-3 shows the CLM-15 tensile and modulus of rupture data for brazed alumina to metal joints. Each ceramic and braze combination was compared for the corresponding M-of-R and tensile strength groups. In all four cases, the M-of-R groups had significantly higher means than the tensile strength groups. The ratio of the means of the CLM-15 tensile strength to the modulus of rupture for the brazed alumina bodies was 0.31 for the copper alloy and 0.21 for the nickel alloy.

An analysis of variance performed on the data (Table V-2) from sample groups which received different degrees of surface preparation indicate no significant difference. Sample surface preparation can be minimized in future tests.

Results of a comparison between drum peel and tab peel tests (Table V-4) show that there are no significant differences between ceramics and brazes on each test or between tests. This would indicate that both tests are performing their function nearly identically.

#### b. Metalizing Braze Seals - Alumina

Significant information was obtained from the study of tungsten-rare earth metalizing paints although these metalizings ultimately proved to have low adhesion values and were subject to solution by the nickel braze alloys.

The tungsten paints described at the bottom of Table V-6 were developed to capitalize on the inherent resistance of calcia, alumina and the rare earth oxides to attack by most alkali metals. Because these stable oxides have high melting and sintering temperatures, a more refractory metal component than molybdenum was considered to avoid the effects of over-sintering of the metal.

TABLE V-1. Ceramic Modulus of Rupture Test Data

Ceramic*	Condition	No. of Tests	Mean M-of- R (psi)	Standard Deviation M-of- R (psi)	Coefficient of Variation (percent)
AL300	As received	6	33, 400	1610	4. 8
AL300	Treatment 1	4	36, 400	1360	3. 7
	Treatment 2	4	42, 800	3820	9. 0
AD94	As received	5	42, 940	4080	9. 5
AD94	Treatment 1	4	46, 000	1700	3. 7
	Treatment 2	4	46, 200	1400	3. 0
Thermalox 998	As received	6	20, 600	1130	5. 5
<p>*See page 135 for composition.</p> <p>Treatment 1: Firing sequence same as sintering and brazing treatments for CuAg braze: 2600°F/Wet H<sub>2</sub>+N<sub>2</sub>, 1650°F/Wet H<sub>2</sub>+N<sub>2</sub>, then 1500°F/Wet H<sub>2</sub></p> <p>Treatment 2: Firing sequence same as sintering and brazing treatments for Alloy 52 Ni braze: 2600°F/Wet H<sub>2</sub>+N<sub>2</sub>, 1560°F/Dry H<sub>2</sub>, then 1850°F/Vacuum</p> <p>Tensile strength as reported by manufacturer.</p> <p>AL300 27000 psi AD94 26000 psi Thermalox 998 15700 psi (Reference: NAS3-4162)</p>					

TABLE V-2. Effect of Surface Preparation on Ceramic-Metal  
Modulus of Rupture Assemblies

Samples	No. of Tests	Mean M-of-R (psi)	Standard Deviation M-of-R (psi)	Coefficient of Variation (percent)
Preparation 1	4	20, 120	9, 400	46. 8
Preparation 2	4	13, 520	8, 300	61. 4
Preparation 3	3	23, 380	4, 300	18. 4
Preparation 4	3	24, 210	12, 120	50. 1
<p>Surface Preparation</p> <ol style="list-style-type: none"> <li>1. Trimmed only: Excess metal trimmed sufficiently for sample to fit test jig.</li> <li>2. Trimmed and cleaned: Metal trimmed and excess braze removed.</li> <li>3. Minimum grinding: Trimmed, cleaned and bearing surfaces ground smooth and flat.</li> <li>4. Maximum grinding: Trimmed, cleaned and all surfaces ground flat and square.</li> </ol> <p>All samples AD94 brazed to AL300 with 72 Ag-28Cu braze filler, nickel plated Kovar metal member, nickel plate on Eitel-McCullough 20A metalizing.</p> <p>(Reference NAS3-4162)</p>				

TABLE V-3. Correlation: CLM-15 Tensile Strength vs. Modulus of Rupture Data

	Ceramic	Braze System	CLM-15 TENSILE				MODULUS OF RUPTURE			
			No. of Tests	Mean Stress (psi)	Standard Deviation Stress (psi)	Coefficient of Variation (percent)	No. of Tests	Mean Modulus (psi)	Standard Deviation Modulus (psi)	Coefficient of Variation (percent)
	AL-300	CuAg	10	6,210	1.770	28.5	9	22,500	5,270	23.4
	AD-94	CuAg	9	9,290	1.730	18.6	9	26,180	11,080	42.3
	AL-300	52Ni	5	3,990	1.350	34	7	22,200	7,760	35.0
	AD-94	52Ni	5	6,775	1.460	21.5	4	30,150	7,030	23.3
Braze Systems:										
CuAg: 72 Ag-28Cu eutectic braze alloy, nickel plated kovar metal member, Ni plate on 20A metalizing.										
52Ni: 3B-4.5 Si-0.15C-bal. Ni braze alloy, iron plated Cb metal member, Fe barrier plate on 20A metalizing.										
Long time average for AD-94, Ni plated 20A metalizing Cu-Ag, Ni plated kovar is 11,400 psi.										
(Reference: NAS3-4162)										

TABLE V-4. Correlation: CLM-15 Drum Peel vs. Tab Peel Data

Ceramic	Braze System *	DRUM PEEL				TAB PEEL			
		No. of Tests	Mean (lb/in)	Standard Deviation (lb/in)	Coefficient of Variation (percent)	No. of Tests	Mean (lb/in)	Standard Deviation (lb/in)	Coefficient of Variation (percent)
AL300	CuAg	5	40.4	6.5	16.2	2	10.8	1.1	10.5
AD94	CuAg	5	51.0	2.4	4.7	7	39.5	21.0	53.1
AL300	52Ni	5	40.5	6.9	17.0	12	44.8	21.5	47.9
AD94	52Ni	5	40.0	12.2	30.5	7	57.1	27.2	47.6
<p>*See Table V-3 for description of braze system</p> <p>(Reference: NAS3-4162)</p>									

Initial tests with copper braze indicated the tungsten metalize paints to have promise (Second Quarterly Report WAED 64. 14E Table V-5). Subsequent less promising results with Coast Alloy 52 braze are shown in Table V-5. The final series of tests showed the paints to have insufficient adherence to high alumina ceramics. This is indicated by the sheared metalize, Figure V-6. The brittle sintered metalize did not withstand the stresses imposed by the electroplated iron-barrier layer. A cross-section of a W-12 paint on Ei-3-3 brazed with Ni base braze alloy (Coast Alloy 52) to a columbium metal member shows that shearing of the metalizing occurs at the tungsten to calcia-alumina glassy-phase interface. In this particular case, the shearing probably occurred during the polishing operation. A sample of 20A metalizing on AD94 (4% SiO<sub>2</sub>) ceramic with Coast Alloy 52 braze and a columbium metal member which received an identical brazing and polishing schedule showed no shearing. Obviously, further work with the silica-free metalizings must involve the promotion of better bonding between the tungsten and the non-metallic phases. Photomicrographs of these two systems are shown in Figures V-7 (a) and V-7 (b).

In general, increasing the percentage of non-metallics in the tungsten paints to 15% (W-11 through W-15) resulted in sufficient glassy-phase being produced (see Figure V-7 (b)); however, it may be noted that the tungsten metalizing is still somewhat porous. Apparently a high contact angle between the glassy-phase and the tungsten prevents complete penetration of the porous sintered tungsten. This explains why sintering temperatures of 3300°F or higher are necessary in spite of the fact that melting occurs at 2600°F in the CaO-Al<sub>2</sub>O<sub>3</sub> system. The metalizing system must rely on solid-state, self sintering of the tungsten to occur rather than non-reactive liquid-solid sintering of a calcia-alumina-tungsten system. It appears that further work on tungsten metalizing systems should involve contact angle studies of potential non-metallic metalizing additions on tungsten plaques, and detailed microscopic examination of the metalizing interface over a variety of processing conditions. The study of paints W-11 through W-15 has resolved the apparent conflict of results obtained for the tungsten-yttria type of paint at Eitel-McCullough, and by Stoddard and Cowan at the Los Alamos Scientific Laboratory. The Second Quarterly Report WAED 64. 14E, Table V-5 and work programmed during the third quarter shows that vacuum tight seals in all the systems W-11 through W-15 can be made using AD-99 ceramic, with iron barrier layer, and Coast Alloy 52

**TABLE V-5. Leak Test Results - Tungsten Series Paints  
Ceramic-Metal Brazed ASTM, CLM-15 As-  
semblies**

Metalize Paint	AD-99 Alumina		Ei3-3 Alumina
	Cb Washer	Kovar Washer	Cb(1%Zr) Washer
W-11M	LKR	LKR	LKR <sup>(a)</sup>
W-12M	VT	LKR	LKR
W-13M	VT	VT	LKR
W-14M	LKR	VT	LKR
W-15M	LKR	VT	LKR
<p><b>Legend:</b></p> <p><b>VT:</b> Leak rate less than <math>10^{-9}</math> Torr-liter per sec.</p> <p><b>LKR:</b> Leak rate greater than above</p> <p>All paints sintered 1/2-hour at 3045°F in forming gas (75%N<sub>2</sub>, 25%H<sub>2</sub>)(70°F dewpoint). See Table V-6 for metalizing paint formulations.</p> <p>All assemblies brazed with Coast Metals 52 braze (3B-4.5 Si-0.15C, Bal Ni): brazed at 1850°F without holding time at temperature.</p> <p>(a) Metallographic examination of similar samples showed that the nickel braze alloy penetrated the iron barrier and attacked the metalize.</p> <p align="right">(Reference: NAS3-4162)</p>			



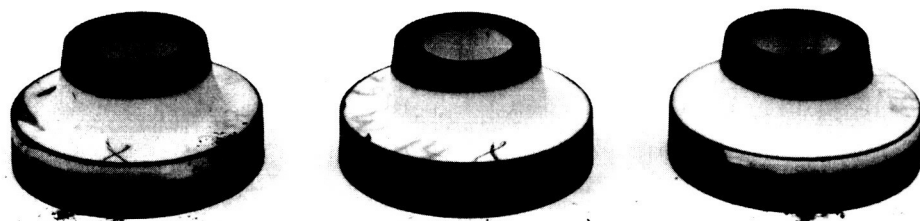


FIGURE V-6. Iron Plated Tungsten Metalize Paints on Alumina CLM-15 pieces. Note that the tungsten metalize has sheared off quite clean from the ceramic in some areas.

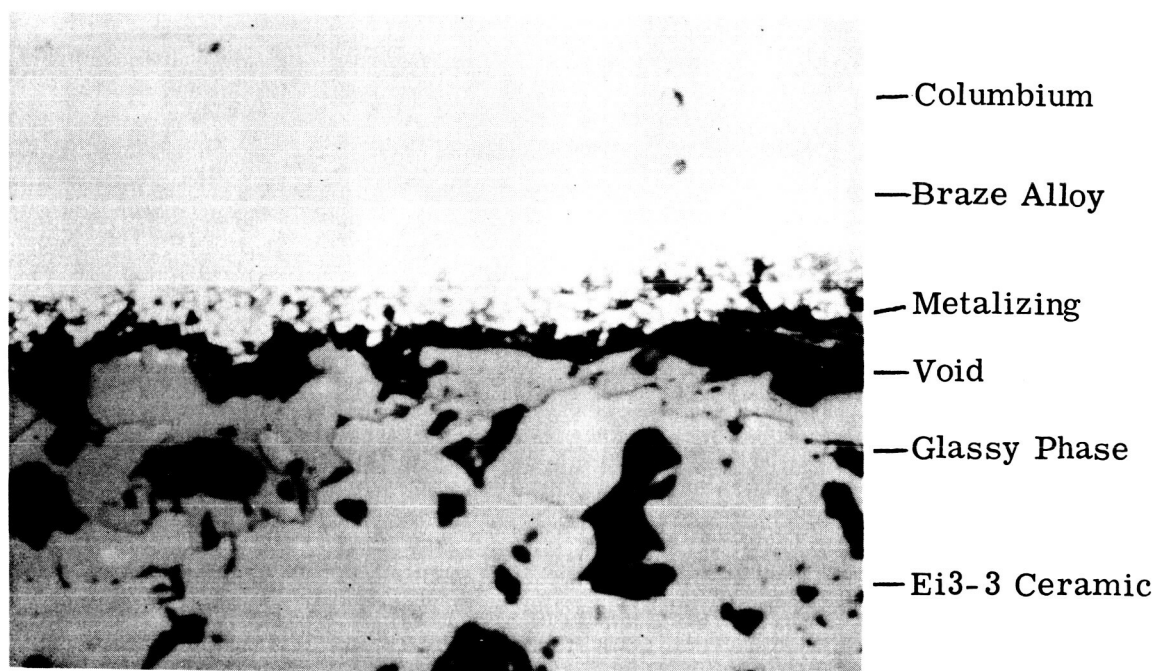


FIGURE V-7(a). W-12 Metalizing on Ei-3-3 Ceramic (600X)

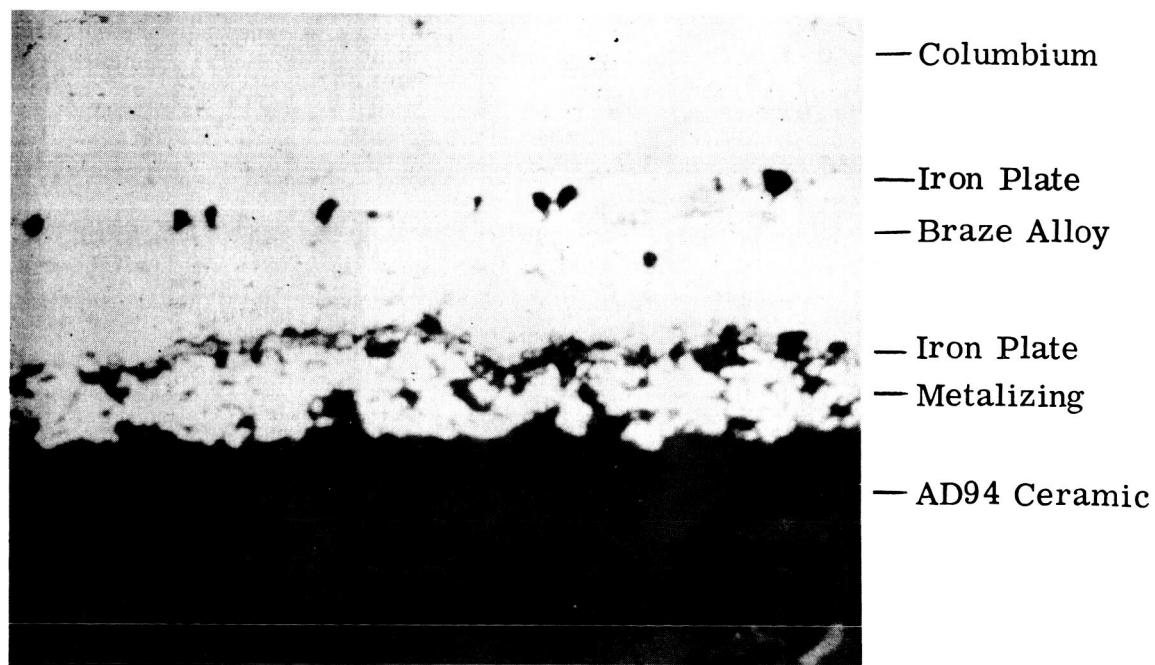


FIGURE V-7(b). 20A Metalizing on AD-94 Ceramic (600X)

braze to either columbium or Kovar metal members. The  $\text{SiO}_2$  (0.4%) present as the glassy-phase in the AD-99 is evidently sufficient to promote adequate bonding between the sintered tungsten sponge and the reacted non-metallic phases of the ceramic and the W-11 through W-15 series of paints. Recent work by Stoddard and Cowan shows about 0.1% silica to be present in their W- $\text{Y}_2\text{O}_3$  metalizing systems<sup>2</sup>.

At this time, therefore, it appears that silica free metalizing systems ( $\text{SiO}_2 < 0.03\%$ ) are only suitable for use in joints where stresses are at a minimum or are non-existent.

It should be noted that all of the nickel-base braze alloy samples (Alloy 52) on 20A metalizing using Al-300 or AD-94 ceramic and brazed to a columbium-1%Zr metal member in the correlation study were also leakers. These systems have been vacuum tight in the past. It is believed that the brazing cycle and a deficient iron barrier is the cause of the present difficulty. Specifically, the iron barrier layer is apt to become highly stressed if non-optimum plating conditions are used. This difficulty may be circumvented by applying the coating as a paint and firing this layer of iron or iron oxide onto the metalizing in dry hydrogen. The brazed Ei-3-3 ceramic pieces reported as leakers in Table V-5 were sectioned and studied metallographically to determine the cause of failure. Valuable information on the reason for metalize braze failures was observed. In numerous regions, the iron barrier plate over the Cb-1%Zr washer was penetrated by the nickel braze alloy and extensive solution of the Cb-1%Zr metal by the nickel followed. The metalizing layer was effectively destroyed opposite these regions of extensive solution, causing braze-ceramic interfaces of poor adherence (Figure V-8). The metallurgical structures indicated that solution of the Cb-1%Zr alloy by the nickel braze markedly lowers the melting point of the braze alloy and increases the activity of the braze alloy at the ambient brazing temperature.

Figure V-9 shows a crack in the braze alloy which occurred due to thermal stress in a region of high solution of the Cb-1%Zr by the nickel.

<sup>2</sup>"Tungsten Metalizing Alumina - Yttria Ceramics" presented at the 66th meeting of the American Ceramic Society, Chicago, Ill. April 22, 1964.

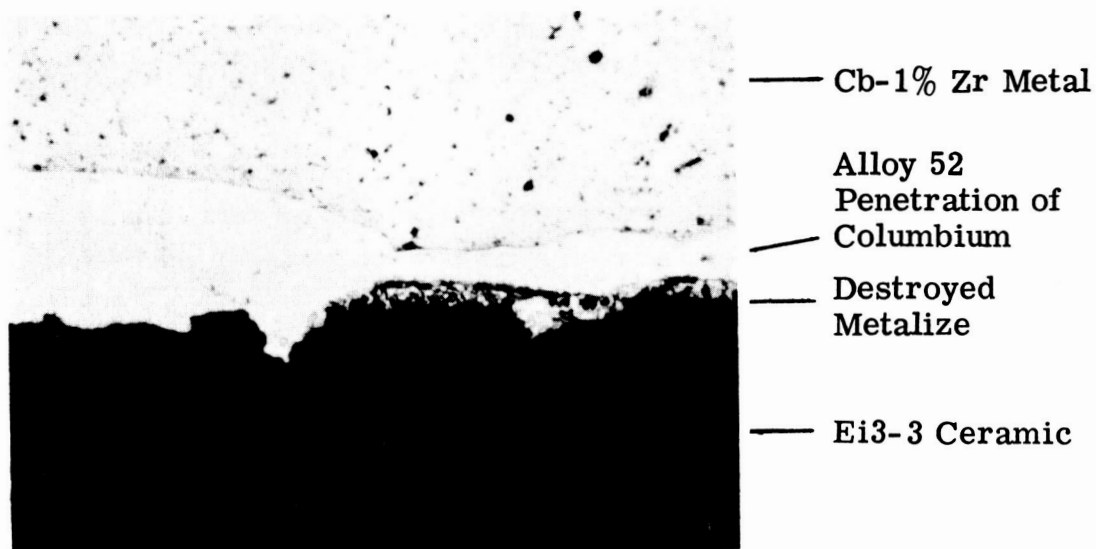
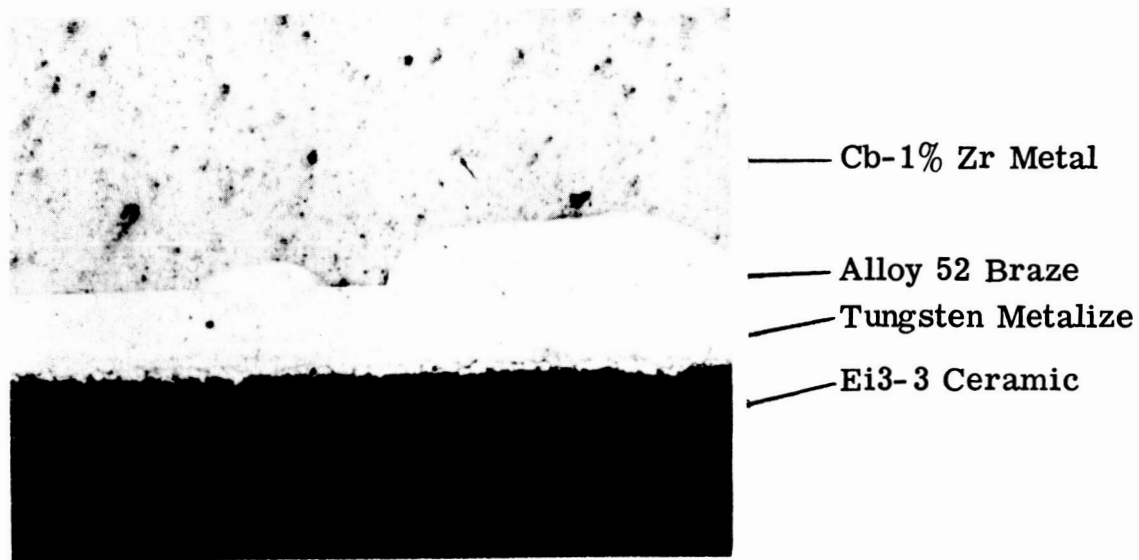


FIGURE V-8. Photomicrographs showing the solution of the columbium-1% zirconium and the attack on the tungsten metalize after penetration of the iron barrier by the nickel braze alloy. (200X)

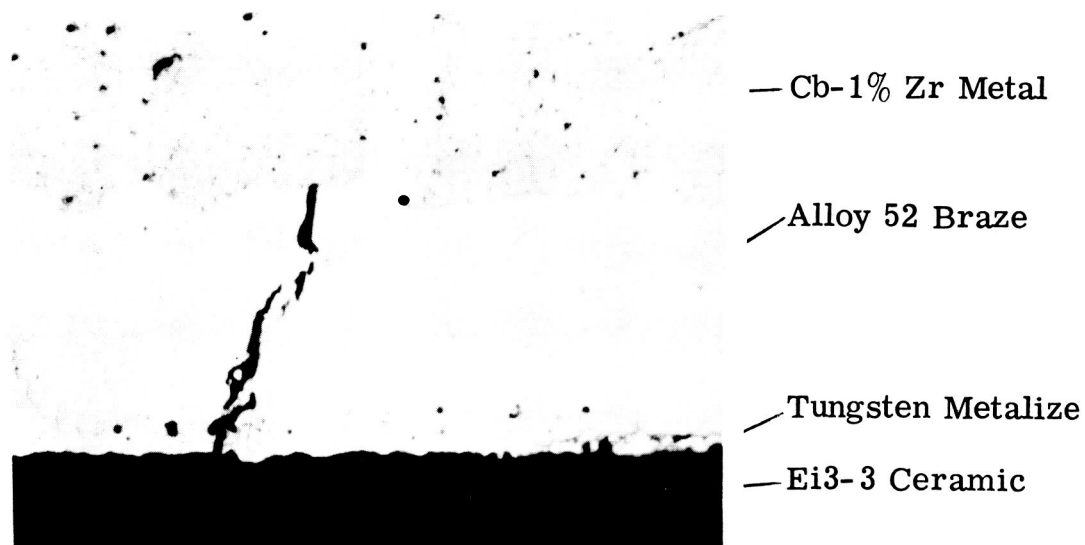


FIGURE V-9. Photomicrograph showing a crack in the braze region; such defects seem to be associated with excessive solution of the columbium-1% zirconium metal by the nickel braze material. (X200)

Although attack of the metalize and cracks in the braze layer are both undesirable effects, they are both indicative of reduced melting point and thermodynamic free energy. Conceivably, a more desirable brazing alloy can be formulated in the columbium-nickel system which will allow lower brazing temperature and lower thermal stress in the joint.

Two other approaches may be used to improve the characteristics of metalizing braze systems which utilize thermodynamically stable oxides in the metalizing layer: (1) use the more ductile molybdenum metal and control the degree of sintering by particle size control and (2) improve the iron barrier layer plating techniques to reduce or eliminate penetration by the nickel alloy during brazing.

#### c. Metalizing Braze Seals - Beryllia

A program to study the effect of sintering temperature on tungsten metalize coatings which were painted on 99.8% beryllia (Brush body Thermolox 998) was completed. The scratch hardness and electrical resistivity data are shown in Table V-6. The coatings did not develop the hardness and conductivity comparable with the standard 20A metalize until sintered at 3300°F. This sintering temperature is approximately 200°F higher than the normal firing temperature for the beryllia ceramic. The use of the high-sintering temperature caused some of the beryllia pieces to check and warp.

Tensile-test, and peel-test data derived from the CLM-15 beryllia samples are shown in Table V-7. The joints were weak because of poor adherence between the metalize paint and the ceramic. Two braze systems were used in this evaluation; copper-silver braze to nickel plated Kovar for the drum peel test samples, and copper braze to copper-nickel for the tensile test samples. Both braze systems are known to cause relatively low thermal stress and provide a reliable means for determining the adherence of metalized coatings.

The tensile test samples reported in Table V-7 were leak checked prior to destruction but the vacuum checks were inconclusive because the samples were checked and warped by the metalize sinter treatment. In spite of the checked appearance of the beryllia bodies, both samples brazed with W-13M paint and one sample with W-14M paint were leak tight. In

TABLE V-6. Sinter Test of Tungsten Metalize on Beryllia Bodies

BeO	Metalize Paint	SINTER TEMPERATURE FOR 1/2 HOUR *					
		2550°F		2920°F		3300 F	
		Hardness	Resistance (ohms)	Hardness	Resistance (ohms)	Hardness	Resistance (ohms)
Thermalox 998 BD 99.5	W-11M	1	> 20	2	5.0	3	0.3
	W-11M	1	> 20	2	12.0	4	0.1
Thermalox 998 BD 99.5	W-12M	1	> 20	3	0.6	3	0.1
	W-12M	1	> 20	4	0.1	4	0.2
Thermalox 998 BD99.5	W-13M	1	> 20	3	1.3	4	0.3
	W-13M	1	> 20	4	0.2	4	0.1
Thermalox 998 BD99.5	W-14M	1	> 20	3	0.5	4	0.1
	W-14M	1	> 20	3	0.6	3	0.1
Thermalox 998 BD99.5	W-15M	1	> 20	3	3.0	3	0.5
	W-15M	1	> 20	3	0.2	4	0.1
Ceramics:		Brush Thermalox 998 (Formerly F-1)    99.8 BeO-0.03Al <sub>2</sub> O <sub>3</sub> -0.01SiO <sub>2</sub> -0.20MgO-0.01CaO-0.005Na <sub>2</sub> O-0.01Fe <sub>2</sub> O <sub>3</sub> Coors BD 99.5    99.5 BeO-0.23Al <sub>2</sub> O <sub>3</sub> -0.16SiO <sub>2</sub> -0.07MgO-0.01CaO-0.03Na <sub>2</sub> O-0.01Fe <sub>2</sub> O <sub>3</sub>					
Paints:		W11M    85W - 15 Y <sub>2</sub> O <sub>3</sub> plus vehicle W12M    85W - 6 Al <sub>2</sub> O <sub>3</sub> - 9 CaCO <sub>3</sub> plus vehicle W13M    85W - 3.75 Y <sub>2</sub> O <sub>3</sub> - 3.75 Dy <sub>2</sub> O <sub>3</sub> - 3.75 Nd <sub>2</sub> O <sub>3</sub> - 3.75 Gd <sub>2</sub> O <sub>3</sub> plus vehicle W14M    95W - 2.5 Y <sub>2</sub> O <sub>3</sub> - 1 - Al <sub>2</sub> O <sub>3</sub> 1.5 CaCO <sub>3</sub> plus vehicle W15M    92W - 5.5 Y <sub>2</sub> O <sub>3</sub> - 0.5 MgO 2 - CaCO <sub>3</sub> plus vehicle					
Hardness:		1, very soft; 2, soft; 3, moderately hard; 4, hard as 20A by scratch test					
Resistance:		Electrical resistance in ohms between probes approximately 1 inch apart. A resistivity of less than 0.1 ohm is indicative of complete sintering.					

\*Furnace Atmosphere: 75% N<sub>2</sub> - 25% H<sub>2</sub>, 100°F Dewpoint.

**TABLE V-7. Evaluation of Metalize and Braze on  
99.8% Beryllia Bodies**

<b>Metalize Paint</b>	<b>Braze System</b>	<b>Tensile Strength (psi)</b>	<b>Drum Peel Test (lb)</b>
W-11M	CuAg		1.7
W-11M	Cu	850	
W-12M	CuAg		5.7*
W-12M	Cu	1,120	
W-13M	CuAg		2.6*
W-13M	Cu	2,000	
W-14M	CuAg		1.5
W-14M	Cu	1,200	
W-15M	CuAg		2.4*
W-15M	Cu	300*	

\*Single test value; all others are average of two tests.

**Braze System:**

**CuAg:** 72Ag-28Cu eutectic braze alloy, nickel-plated kovar metal member, and nickel plate on metalize.

**Cu:** copper braze; 70 Cu-30Ni metal member and copper plate on metalize

**Metalize Paint:** See Table V-6 for compositions.

(Reference: NAS3-4162)



general, the tungsten and rare earth oxide metalize paints with beryllia evaluated on this program exhibited low strengths and work has been discontinued in favor of the more promising active alloy sealing systems.

d. Active Metal Brazes

The active metal brazes which will be studied in this program are shown in Table V-8.

The active metal braze alloys were made by Battelle Memorial Institute by inert-electrode, arc melting. High-purity materials such as crystal-bar zirconium and titanium, electron-beam melted columbium, and Pechiney flake beryllium were used in all melts. Alloy buttons were comminuted using a diamond mortar.

To date, nine active alloys have been received from Battelle. Two brazing cycles on different alloys have been made.

The evaluation procedure is as follows: the dry pulverized braze alloy as received from Battelle is wetted with methacrylate lacquer. In the BeO modulus of rupture samples the braze is added directly to the interface region on both sides of the Cb-1%Zr metal member. The joint is closed by movement of the weighted top piece after the braze alloy melts. In the alumina ASTM CLM-15 samples the braze alloy is added to the lower interface; the upper interface is prepared by adding the braze alloy to the metal member outside the joint and allowing surface wetting reactions and capillary action to move the braze alloy through the joint.

Evaluation of BeO ceramic-metal joints will include vacuum leak determinations on cylinder geometries. The five most promising alloys will be selected based on joint integrity and modulus of rupture tests.

e. Thin Film Metalizing

Promising results were obtained with test joints prepared by using evaporated metal films to secure wettable ceramic surfaces. The use of evaporated coatings on ceramics with nickel-braze alloy resulted in seals which leaked due to attack of the braze material on the thin molybdenum through the barrier layer, but the use of evaporated coatings to promote ceramic wetting by active alloys is very encouraging.

TABLE V-8. Active Metal Braze Alloys

Order of Preference	Composition	Reported (b)		Remarks (a)	
		M. P. (°F)	Ductility		
1	6 Be-19Cb-75Zr	1920		V. T. (c) Cb/Al <sub>2</sub> O <sub>3</sub> , 6000 psi, good flow	
2	4 Be-68Ti-28V	2280		V. T. Cb/Al <sub>2</sub> O <sub>3</sub> , 4000 psi, fair flow	
3	16Ti-28V-56Zr	2250		V. T. Cb/BeO	
4	4Be-48Ti-48Zr	1920		V. T. Kovar/Al <sub>2</sub> O <sub>3</sub> , Cb/BeO, 4390 psi, good	
5	4Be-46Ti-4V-46Zr	1830		V. T. Cb/BeO, 1295 psi, good melt	
6	20Cb-30V-50Zr	2300	Very brittle	Partial melting, no adhesion at 2335°F	
7	65V-35Cb	3400	Ductile		
8	70Ti-30V	3000	Ductile		
9	15Cb-25V-60Zr	2335			
10	30Ti-20V-50Zr	2400	Brittle		
11	30Ti-30V-40Zr	2300	Brittle		
12	35Ti-35V-30Zr	2600	Brittle		
13	50Ti-20V-30Zr	2600	Slightly Ductile		
14	8Si-62Ti-30V	2400	Brittle		
(a) Reported on Westinghouse SPUR project, subcontract AF33(657)10922, Westinghouse Report WAED64. 22.					
(b) "Joining of Refractory Metals by Brazing and Diffusion Bonding" by W.R. Young and E.S. Jones					
(c) G. E. Report R62FPD32 under contract AF33(616)7484, December 1962.					
Vacuum tight measured by mass spectrometer.					

Relatively thick, evaporated molybdenum coatings were prepared to aid the wetting of alumina by active metal braze materials. A sectioned CLM-15 tensile test assembly which illustrates the additional braze flow obtainable is shown in Figure V-10. The bottom AD99 ceramic piece was evaporation metalized with less than one micron of titanium and less than one micron thick molybdenum; the other ceramic piece was not metalized. The 19Cb-75Zr-6Be braze alloy was placed on the outside of the Cb-1%Zr metal member. The assembly was brazed at 1910°F (no holding time) in a vacuum of better than  $5 \times 10^{-5}$  torr. The braze alloy moved through the joint forming a satisfactory fillet on the inside of the metalized ceramic. A similar sample had a tensile strength in excess of 10,000 psi.

Other alkali metal resistant metalizing compositions may show similar usefulness.

f. Electroformed Seals

Two samples of metalized AD94 ceramic were joined to a columbium washer by electroforming in a low-stress nickel sulphamate bath. Both seals were vacuum tight.

The first electroformed seal was designed as shown in Figure V-11. Difficulty was encountered in building up a nickel deposit of desirable thickness in the root region because of the limited throwing power of the plating bath. Although the nickel plate in the critical root region was only a few thousands thick, the seal was leak tight. The sample was tensile tested but proved to be very low in strength.

The second sample was designed to eliminate the necessity of plating nickel in a deep groove and is shown in Figure V-12. The ends of the AD94 alumina pieces were metalized and butted against the columbium washer. A small fillet of graphite powder was applied between the columbium washer and the metalized ceramic to assure a continuous electrical field at the joint. This sample was also leak tight.

Seals formed in this manner are too weak for use in load bearing structures.

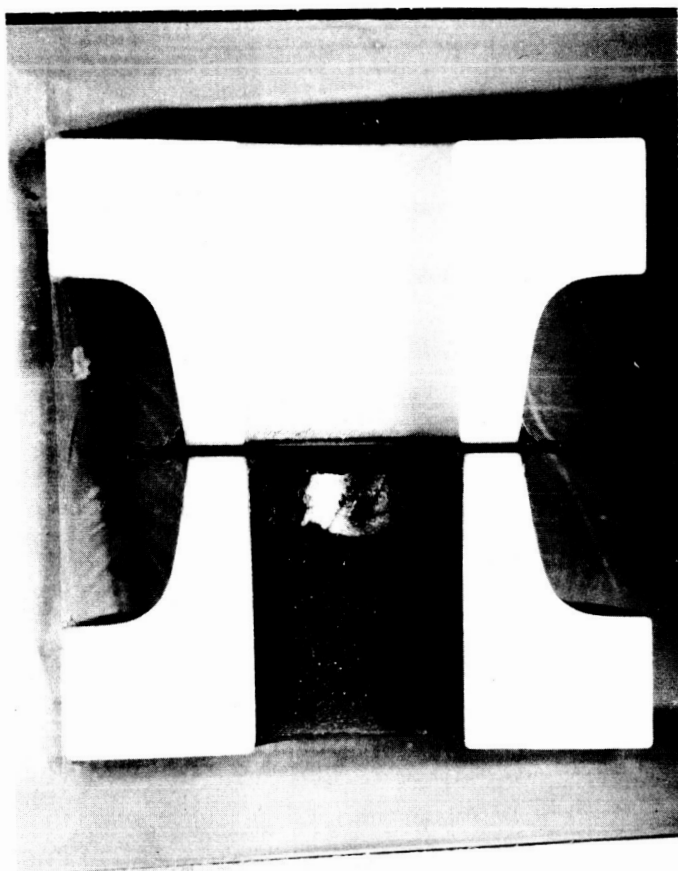


FIGURE V-10. Section Through a CLM-15 Test Sample With a Cb-Zr-Be Active Metal Braze Between AD-99 Ceramic and Cb-1Zr. The bottom sample was evaporation metalized. Superior wetting of this sample is indicated by the smooth inside fillets of braze metal not present on the upper unmetallized ceramic joint. (2X)

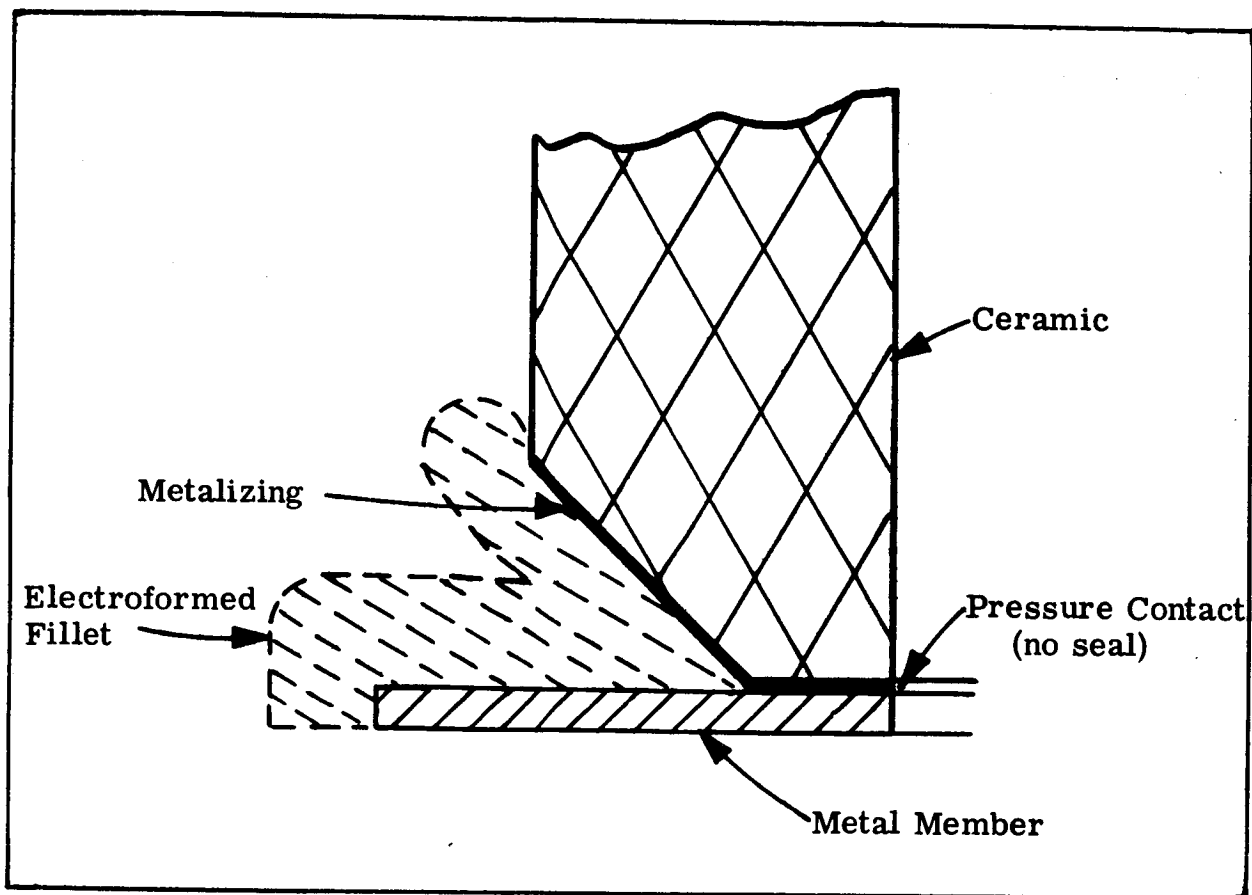


FIGURE V-11. Idealized Geometry of First Electroform Seal

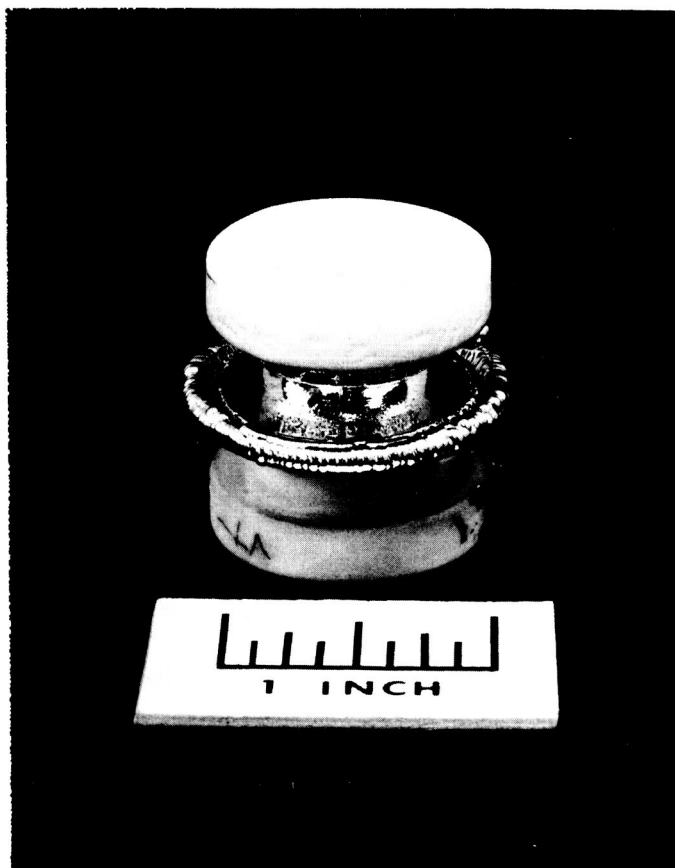


FIGURE V-12. Alumina to Columbiu-1% Zirconium Seal  
Joined by Electroforming a Sheath in a Sul-  
phamate Nickel Bath.

### 3. Potassium Exposure Testing

#### a. Preparation of Samples

The first capsule loading for 1600°F potassium vapor exposure will be carried out as outlined in the Second Quarterly Report WAED64. 14E with no significant changes. The vendor's analysis of the potassium is shown in Figure V-9. Five ceramic materials and one braze system will be tested. The distribution of samples is given in Table V-10. The ceramic M-of-R test samples all consist of 0.100 to 0.110 inch rectangular cross section bars except sapphire which is 0.100 inch circular cross section. AD99 is therefore represented with both round and rectangular bars to permit the necessary geometry correlation.

All samples prior to brazing or testing will be given an ultrasonic cleaning in detergent followed by a cleaning fire at 2600°F or over in 25% H<sub>2</sub>-75% N<sub>2</sub>, 100°F dewpoint gas.

All samples will be then identified by a notch code, weighed and stored in clean containers until loaded into capsules. The brazed ceramic-to-metal assemblies will be treated in a similar manner after the vacuum brazing operation and braze fillet removal on the M-of-R and tab-peel test geometries.

### 4. Conclusions

1. Correlation test data indicate the modulus of rupture and tab peel assemblies to be capable of resolving test variables as readily as the CLM-15 tensile test and drum peel test assemblies. The modulus of rupture bar has an added advantage in allowing both the ceramic and ceramic-to-metal seal to be evaluated separately. A tentative set of test comparison conversion factors has been determined which will be improved as additional data is compiled.
2. Work on tungsten base metalizing paints with thermodynamically stable secondary phases has shown such compositions to be excessively brittle after sintering.
3. The susceptibility of the thin, molybdenum film metalizing to solution by the nickel braze through imperfections in the iron barrier layer has redirected the interest in this approach toward the use of thin metalizing as

a wetting aid for active-alloy brazes to ceramic bodies.  
A test assembly, made in this manner, had unusually  
high strength.

TABLE V-9. Analysis of Potassium and NaK

Supplied by Mine Safety Research Appliance Corp.  
(High Purity Drum #278)

Potassium			
<u>Element</u>	<u>Analysis (ppm)</u>	<u>Element</u>	<u>Analysis (ppm)</u>
Ti	<5	Ni	<1
Fe	5	Mo	<5
B	<5	V	<1
Co	<5	Ca	4
Mn	<1	Ba	<3
Al	3	Sr	<1
Mg	<1	Be	<1
Sn	<1	Zr	<10
Cu	<1	Ag	<1
Pb	<1	N	<10*
Cr	<1	C	49*
Si	10	O	10*
Na	3		

\*Analysis by emission spectrograph except those marked by asterisk  
which were separated by mercury amalgamation prior to analysis.



TABLE V-10. Specimen Distribution For 1600°F Potassium Exposure Evaluation

Material	Designation	Capsule 1	Capsule 2	Capsule 3	Capsule 4	Capsule 5	Capsule 6	Capsule 7	Capsule 8 (a)
99.8% BeO	Brush Thermalox 998	5 Modulus of Rupture (M-of-R Bars)					2 M-of-R Bars		2 M-of-R Bars
100% Al <sub>2</sub> O <sub>3</sub>	Linde Sapphire		5 M-of-R Bars				2 M-of-R Bars		2 M-of-R Bars
99.8% Al <sub>2</sub> O <sub>3</sub>	GE Lucalox			5 M-of-R Bars			2 M-of-R Bars		2 M-of-R Bars
99.8% Al <sub>2</sub> O <sub>3</sub>	Wesgo Ei3-3				5 M-of-R Bars		2 M-of-R Bars		2 M-of-R Bars
99% Al <sub>2</sub> O <sub>3</sub>	Coors AD99					5 M-of-R Bars	2 M-of-R Bars		2 M-of-R Bars
Seal System Ei3-3 to -Cb-1Zr using braze 75 Zr - 19 Cb - 6 Be								5 M-of-R Assemblies, 2 Tab-Peel Test Assem- blies, 2 cylinders	
(a) Specimens in capsule 8 tested in vacuum environment (10 <sup>-5</sup> torr)									
All capsules maintained at temperature of 1600°F in vacuum of 10 <sup>-6</sup> torr for 500 hours.									
(Reference: NAS3-4162)									

## SECTION VI

### PROGRAM

#### A. OVERALL PROGRAM PLAN.

This program represents a 12-month effort ending the latter part of August 1964, with additional reporting and publication time. The first quarterly report (WAED 63. 16E) presented a summary of the suggested materials for use in advanced space electric power systems. It also discussed the gaps in the properties and identified the test program areas which were planned for filling these deficiencies. The second quarterly report (WAED 64. 14E) presented initial test results.

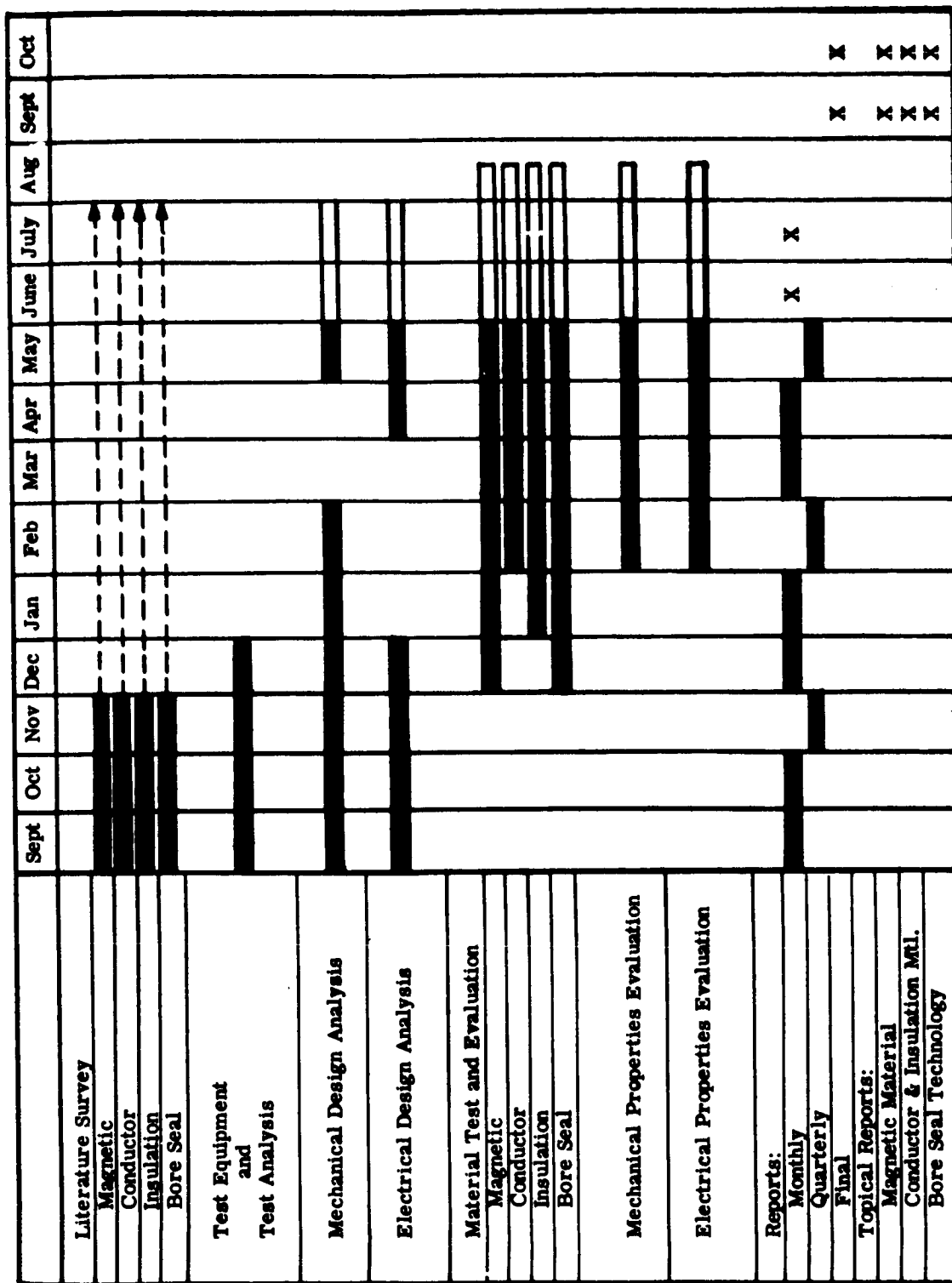
Figure VI-1 shows the program scheduling. The Westinghouse Aerospace Electrical Division is acting as the prime contractor and is being assisted by the Westinghouse Research and Development Center. The Eitel-McCullough Corporation is a subcontractor and is supporting the bore seal analysis.

#### B. FOURTH QUARTER PLAN.

This quarter's effort will conclude the test program. Three topical and final reports will be issued summarizing the work accomplished. The following summarizes the effort planned:

##### 1. Magnetic, Electrical Conductor, and Insulation Materials

Tests on all classes of materials will be completed. These will include aging, mechanical, electrical, magnetic and thermo-physical tests. The program will follow the detail test plan approved earlier.



☐ Program Plan  
 --> Supplementary Effort  
☒ Accomplishments (Indication of % Task Completion)

FIGURE VI-1. Program Plan - NASA Materials Study and Research Program

## 2. Bore Seal Materials

Alumina and beryllia active-metal seals to columbium - 1% zirconium and columbium D-43 alloy will be prepared and the evaluation of these seals before and after exposure to alkali metal vapors will be completed.

Ten active alloy brazes will be screened using alumina and beryllia. The best five will be selected and fabricated into modulus of rupture and leak-test assemblies.

From this group, three of the most promising will be chosen for alkali metal compatibility testing. Brazed samples will also be tested in an evacuated capsule to determine the effect of elevated temperatures on joint integrity.

# DISTRIBUTION LIST

<p>National Aeronautics &amp; Space Administration Washington 25, D. C. Attn: Walter C. Scott James J. Lynch (RN) George C. Deutsch (RR)</p> <p>National Aeronautics &amp; Space Administration Scientific &amp; Technical Information Facility Box 5700 Bethesda 14, Maryland Attn: NASA Representative</p> <p>National Aeronautics &amp; Space Administration Ames Research Center Moffet Field, California Attn: Librarian</p> <p>National Aeronautics &amp; Space Administration Goddard Space Flight Center Greenbelt, Maryland Attn: Librarian</p> <p>National Aeronautics &amp; Space Administration Langley Research Center Hampton, Virginia Attn: Librarian</p> <p>National Aeronautics &amp; Space Administration Lewis Research Center 21000 Brookpark Road Cleveland, Ohio 44135 Attn: Librarian</p> <p>Dr. Bernard Lubarsky (SPSD) MS 500-201 Roger Mather (NPTB) MS 500-309 G. M. Ault MS 105-1 R. A. Lindberg MS 500-309 John Dilly (SPSPS) MS 500-309 Norman T. Musial, Patent Counsel MS 77-1</p>	<p>T. A. Moss MS 500-309 Jesse H. Hall, MS 77-1 Anthony C. Hoffman MS 77-1 Richard L. Ashbrook MS 49-1 Charles S. Corcoran MS 500-201 Joseph T. Kohnik MS 21-5 Ernest A. Koutnik MS 500-201 John W. R. Creagh MS 500-309</p> <p>National Aeronautics &amp; Space Administration Manned Spacecraft Center Houston 1, Texas Attn: Librarian</p> <p>National Aeronautics &amp; Space Administration George C. Marshall Space Flight Center Huntsville, Alabama Attn: Librarian</p> <p>National Aeronautics &amp; Space Administration Jet Propulsion Laboratory 4800 Oak Grove Drive Pasadena 3, California Attn: Librarian</p> <p>National Aeronautics &amp; Space Administration Western Operations Office 150 Pico Boulevard Santa Monica, California Attn: John Keeler</p> <p>National Bureau of Standards Washington 25, D. C. Attn: Librarian</p>	<p>Aeronautical Systems Division Wright-Patterson Air Force Base, Ohio Attn: Charles Armbruster ASRPP-10 T. Cooper Librarian George M. Glenn Lester E. Schott (ASRMFP-3)</p> <p>Air Force Materials Laboratory Research and Technology Division Wright-Patterson Air Force Base, Ohio 45433 Attn: AFML (MANE, Mr. J. M. Kelble)</p> <p>Army Ordnance Frankford Arsenal Bridensburg Station Philadelphia 37, Pennsylvania Attn: Librarian</p> <p>Bureau of Mines Albany, Oregon Attn: Librarian</p> <p>Bureau of Ships Department of the Navy Washington 25, D. C. Attn: Librarian</p> <p>Bureau of Weapons Research &amp; Engineering Material Division Washington 25, D. C. Attn: Librarian</p> <p>U. S. Atomic Energy Commission P. O. Box 1102 East Hartford, Connecticut Attn: C. E. McColley CANEL Project Office</p>
---	--	--

<p>U. S. Atomic Energy Commission Technical Reports Library Washington 25, D. C. Attn: J. M. O'Leary</p> <p>U. S. Atomic Energy Commission Germantown, Maryland Attn: Col. E. L. Douthett, H. Rothen, Major Gordon Dicker, SNAP 50/SPUR Project Office Socrates Christoffer</p> <p>U. S. Atomic Energy Commission Technical Information Service Extension P. O. Box 62 Oak Ridge, Tennessee</p> <p>U. S. Atomic Energy Commission Washington 25, D. C. Attn: M. J. Whitman</p> <p>Argonne National Laboratory 9700 South Cross Avenue Argonne, Illinois Attn: Librarian</p> <p>Brookhaven National Laboratory Upton, Long Island, New York Attn: O. E. Weyer</p> <p>Oak Ridge National Laboratory Oak Ridge, Tennessee Attn: W. C. Thurber Dr. A. J. Miller Librarian</p> <p>Office of Naval Research Power Division Washington 25, D. C. Attn: Librarian</p>	<p>U. S. Naval Research Laboratory Washington 25, D. C. Attn: Librarian</p> <p>Advanced Technology Laboratories Division of American Standard 360 Whisman Road Mountain View, California Attn: Librarian</p> <p>Aerojet-General Corporation P. O. Box 296 Azusa, California Attn: Librarian</p> <p>Aerojet General Nucleonics P. O. Box 77 San Ramon, California Attn: Librarian</p> <p>Aerovox Corporation 740 Belleville Avenue New Bedford, Massachusetts Attn: Librarian</p> <p>Airborne Accessories Corporation 1414 Chestnut Avenue Hillside 5, New Jersey Attn: Librarian</p> <p>AiResearch Manufacturing Company Sky Harbor Airport 402 South 35th Street Phoenix, Arizona Attn: Librarian E. A. Kovacevich</p> <p>AiResearch Manufacturing Company 9851-9951 Sepulveda Boulevard Los Angeles 45, California Attn: Librarian</p>	<p>Allen Bradley Company 136 West Greenfield Avenue Milwaukee 4, Wisconsin Attn: Librarian</p> <p>Allis-Chalmers Manufacturing Company 1126 South 70th Street Milwaukee, Wisconsin Attn: Librarian</p> <p>Allis-Chalmers Manufacturing Company West Allis, Wisconsin Attn: Librarian</p> <p>Allis-Chalmers Atomic Energy Division Milwaukee, Wisconsin Attn: Librarian</p> <p>Allison-General Motors Energy Conversion Division Indianapolis, Indiana Attn: Librarian</p> <p>American Machine &amp; Foundry Company Alexandria Division 1025 North Royal Street Alexandria, Virginia Attn: Librarian</p> <p>American Society of Metals Novelty, Ohio Attn: Librarian</p> <p>AMF Atomics 140 Greenwich Avenue Greenwich, Connecticut Attn: Librarian</p> <p>The Anaconda Company Crane Street Waterbury, Connecticut Attn: Librarian</p>
---	--	---

<p>Armour Research Foundation 10 W. 35th Street Chicago 16, Illinois Attn: Librarian</p> <p>Arrow-Hart and Hegeman Electric Company 103 Hawthorn Street Hartford 6, Connecticut Attn: Librarian</p> <p>Atomics International 8900 DeSoto Avenue Canoga Park, California Attn: Librarian</p> <p>AVCO Research and Advanced Development Dept. 201 Lowell Street Wilmington, Massachusetts Attn: Librarian</p> <p>Babcock and Wilcox Company Research Center Alliance, Ohio Attn: Librarian</p> <p>Battelle Memorial Institute 505 King Avenue Columbus, Ohio Attn: Librarian</p> <p>Bell Telephone Laboratories Mountain Avenue Murray Hill, New Jersey Attn: J. F. Schaff</p> <p>Bendix Aviation Corporation Red Bank Division Highway 35 Eatontown, New Jersey Attn: Librarian</p>	<p>The Bendix Corporation Research Laboratories Division Southfield, Detroit 1, Michigan Attn: Librarian</p> <p>Bodine Electric Company 2500 W. Bradley Place Chicago 18, Illinois Attn: Librarian</p> <p>The Boeing Company Seattle, Washington Attn: Librarian</p> <p>Bourns, Incorporated Instrument Division 6135 Magnolia Avenue Riverside, California Attn: Librarian</p> <p>Brush Beryllium Company Cleveland, Ohio Attn: Librarian</p> <p>Carborundum Company Niagara Falls, New York Attn: Librarian</p> <p>Chance Vought Aircraft, Incorporated P. O. Box 5907 Dallas 22, Texas Attn: Librarian</p> <p>Climax Molybdenum Company of Michigan Detroit, Michigan Attn: Librarian</p> <p>Collins Radio Company 5225 C Avenue N. E. Cedar Rapids, Iowa Attn: Librarian</p>	<p>Convair Astronautics 5001 Kerny Villa Road San Diego 11, California Attn: Librarian</p> <p>Cook Electric Company 6401 W. Oakton Street Morton Grove, Illinois Attn: Librarian</p> <p>Cornell Dubilier Electronics Division of Federal Pacific Electric 921 Providence Highway Norwood, Massachusetts Attn: Librarian</p> <p>Crucible Steel Company of America Pittsburgh, Pennsylvania Attn: Librarian</p> <p>Curtiss-Wright Corporation Research Division Tuehanna, Pennsylvania Attn: Librarian</p> <p>Cutler-Hammer 1391 W. St. Paul Avenue Milwaukee 1, Wisconsin Attn: Librarian</p> <p>Dartmouth College Hanover, New Hampshire Attn: Librarian</p> <p>Daystrom, Incorporated 430 Mountain Avenue Murray Hill, New Jersey Attn: Librarian</p> <p>Delco Division General Motors Corporation 700 E. Firmin Street Kokomo, Indiana Attn: Librarian</p>
--	--	--

<p>Douglas Aircraft Company, Inc. Missile &amp; Space Systems Division 300 Ocean Park Boulevard Santa Monica, California Attn: Librarian</p> <p>E. I. duPont de Nemours &amp; Company, Inc. Wilmington 98, Delaware Attn: Librarian E. M. Mahla Lee J. Barron Hugh Hix</p> <p>Egerton Germeshausen &amp; Grier, Inc. Santa Barbara Airport Goleta, California Attn: Librarian</p> <p>T. A. Edison Industries Lakeside Avenue West Orange, New Jersey Attn: Librarian</p> <p>Electro-Optical Systems, Incorporated Advanced Power Systems Division Pasadena, California Attn: Librarian</p> <p>Emerson Electric Manufacturing Company Electronics &amp; Avionics Division 8100 Florissant Avenue St. Louis 36, Missouri Attn: Librarian</p> <p>Fairchild Controls Corporation 225 Park Avenue Hicksville, Long Island, New York Attn: Librarian</p> <p>Fansteel Metallurgical Corporation North Chicago, Illinois Attn: Librarian</p>	<p>Firth Sterling, Incorporated McKeesport, Pennsylvania Attn: Librarian</p> <p>Ford Motor Company Aeronutronics Newport Beach, California Attn: Librarian</p> <p>General Atomic John Jay Hopkins Laboratory P. O. Box 608 San Diego 12, California Attn: Librarian</p> <p>General Dynamics Corporation Stromberg-Carlson Division 100 Carlson Road Rochester, New York Attn: Librarian</p> <p>General Dynamics/Fort Worth P. O. Box 748 Fort Worth, Texas Attn: Librarian</p> <p>General Electric Company Atomic Power Equipment Division P. O. Box 1131 San Jose, California</p> <p>General Electric Company Chemical &amp; Materials Engineering Laboratory Advanced Technology Laboratories Schenectady, New York Attn: Librarian</p> <p>General Electric Company Missile &amp; Space Vehicle Department 3198 Chestnut Street Philadelphia 4, Pennsylvania Attn: Librarian</p>	<p>General Electric Company Direct Current Motor and Generator Department 3001 East Lake Road Erie, Pennsylvania Attn: J. T. Duane Attn: Librarian</p> <p>General Electric Company Vallecitos Atomic Laboratory Pleasanton, California Attn: Librarian</p> <p>General Electric Company Missile and Space Division Cincinnati, Ohio Attn: Dr. J. W. Semmel Attn: Librarian</p> <p>General Electric Company Specialty Control Department P. O. Box 812 Waynesboro, Virginia Attn: Librarian</p> <p>General Motors Corporation Allison Division Indianapolis 6, Indiana Attn: Librarian</p> <p>Giannini Controls 1600 South Mountain Avenue Duarte, California Attn: Librarian</p> <p>Hamilton Standard Division of United Aircraft Corporation Windsor Locks, Connecticut Attn: Librarian</p> <p>Hartman Electric Manufacturing Company 175 N. Diamond Street Mansfield, Ohio Attn: Librarian</p>
--	--	---



<p>High Voltage Engineering Corporation Burlington, Massachusetts Attn: Librarian</p> <p>Hughes Aircraft Company Engineering Division Culver City, California Attn: Librarian</p> <p>Ilkon Corporation Natick Industrial Center Natick, Massachusetts Attn: Librarian Dr. Seigo Matsoda</p> <p>International Business Machine Corporation State Highway 17-C Owego, New York Attn: Librarian</p> <p>International Resistance Company 401 N. Broad Street Philadelphia 8, Pennsylvania Attn: Librarian</p> <p>International Telephone &amp; Telegraph Federal Laboratories 500 Washington Avenue Nutley 10, New Jersey Attn: Dr. A. M. Levine, Missile &amp; Space Systems</p> <p>Kaman Nuclear Division Kaman Aircraft Corporation Colorado Springs, Colorado Attn: Librarian</p> <p>Kennametal, Incorporated Latrobe, Pennsylvania Attn: Librarian</p> <p>Kodak Research Labs 343 State Street Rochester, New York Attn: Librarian</p>	<p>Latrobe Steel Company Latrobe, Pennsylvania Attn: Librarian</p> <p>Lear Siegler, Incorporated Astronics Division 3171 S. Bundy Drive Santa Monica, California</p> <p>Lear Siegler, Incorporated Power Equipment Division P. O. Box 6719 Cleveland, Ohio Attn: Librarian</p> <p>Leeds and Northrup 4970 Stenton Avenue Philadelphia, Pennsylvania Attn: Librarian</p> <p>Leland Airborne Products Division of AMF P. O. Box 128 Vandalia, Ohio Attn: Librarian</p> <p>Lessonia Moos Laboratories Lake Success Park, Community Drive Great Neck, Long Island, New York Attn: Librarian</p> <p>Ling-Tempo-Vought, Incorporated P. O. Box 5003 Dallas 22, Texas Attn: Librarian</p> <p>Litton Industries, Incorporated 336 N. Foothill Road Beverly Hills, California Attn: Librarian</p> <p>Lockheed-Georgia Company Division of Lockheed Aircraft Company Marietta, Georgia Attn: Librarian</p>	<p>Lockheed Missiles and Space Division Lockheed Aircraft Corporation Sunnyvale, California Attn: Librarian</p> <p>Los Alamos Scientific Laboratory University of California Los Alamos, New Mexico Attn: Librarian</p> <p>ManLabs, Incorporated 21 Erie Street Cambridge 39, Massachusetts Attn: Librarian</p> <p>Mallory Controls Company P. R. Mallory &amp; Company, Incorporated 555 Hoke Avenue Frankfort, Indiana Attn: Librarian</p> <p>Marquardt Aircraft Company P. O. Box 2013 Van Nuys, California Attn: Librarian</p> <p>The Martin Company Baltimore 3, Maryland Attn: Librarian</p> <p>The Martin Company Nuclear Division P. O. Box 5042 Baltimore 20, Maryland Attn: Librarian</p> <p>Martin Marietta Corporation Metals Technology Laboratory Wheeling, Illinois</p> <p>Massachusetts Institute of Technology Cambridge 39, Massachusetts Attn: Librarian</p>
---	--	---

<p>Materials Research Corporation Orangeburg, New York Attn: Librarian</p> <p>McDonnell Aircraft St. Louis, Missouri Attn: Librarian</p> <p>Melpar, Incorporated Sub. Westinghouse Air Brake Company 3000 Arlington Boulevard Falls Church, Virginia Attn: Librarian</p> <p>Michigan State University East Lansing, Michigan Attn: Librarian</p> <p>Minneapolis-Honeywell 2747 Fourth Avenue S. Minneapolis 8, Minnesota Attn: Librarian</p> <p>Minnesota Mining &amp; Manufacturing Company Electric Products Division 2501 Hudson Road St. Paul 19, Minnesota Attn: Librarian</p> <p>Motorola, Incorporated Western Military Electronics Center P. O. Box 1417 Scottsdale, Arizona Attn: Librarian</p> <p>MSA Research Corporation Callery, Pennsylvania Attn: Librarian</p> <p>New Hampshire University Durham, New Hampshire Attn: Librarian</p>	<p>National Research Corporation 405 Industrial Place Newton, Massachusetts Attn: Librarian</p> <p>New Mexico University Albuquerque, New Mexico Attn: Librarian</p> <p>North American Aviation, Inc. Atomics International Division P. O. Box 309 Canoga Park, California Attn: Librarian Dr. R. L. McKisson</p> <p>North American Aviation Los Angeles Division Los Angeles 9, California Attn: Librarian</p> <p>Norton Company Worcester, Massachusetts Attn: Librarian</p> <p>Nuclear Metals, Incorporated West Concord, Massachusetts Attn: Librarian</p> <p>Nuclide Analysis Associates P. O. Box 752 State College, Pennsylvania</p> <p>Ohmite Manufacturing Company 3601 Howard Street Skokie, Illinois Attn: Librarian</p> <p>Pennsylvania University 3440 Woodland Avenue Philadelphia, Pennsylvania Attn: Librarian</p>	<p>Pesco Products Division Borg-Warner Corporation 24700 N. Miles Road Bedford, Ohio Attn: Librarian</p> <p>Pratt &amp; Whitney Aircraft 400 Main Street East Hartford 8, Connecticut Attn: Librarian</p> <p>Pratt &amp; Whitney Aircraft CANEL P. O. Box 611 Middletown, Connecticut Attn: Librarian</p> <p>Radio Corporation of America Front &amp; Cooper Street Camden, New Jersey Attn: F. S. Leroy</p> <p>Radio Corporation of America Defense Electronic Products Front &amp; Cooper Streets Camden 2, New Jersey Attn: Librarian</p> <p>Radio Corporation of America Findlay, Ohio Attn: Librarian</p> <p>Radio Corporation of America Semiconductor &amp; Materials Division U. S. Route 202 Somerville, New Jersey Attn: Librarian</p> <p>Raytheon Company Spring Street Lexington 73, Massachusetts Attn: Librarian</p>
--	--	--

<p>Reliance Electric &amp; Engineering Company 24701 Euclid Avenue Cleveland 17, Ohio Attn: Librarian</p> <p>Republic Aviation Corporation Farmingdale, Long Island, New York Attn: Librarian</p> <p>Rocketdyne Canoga Park, California Attn: Librarian</p> <p>Sangamo Electric Company 1301 N. Eleventh Street Springfield, Illinois Attn: Librarian</p> <p>Sigma Instruments, Incorporated 180 Pearl Street South Braintree 85, Massachusetts Attn: Librarian</p> <p>Solar 2200 Pacific Highway San Diego 12, California Attn: Librarian</p> <p>Sorenson Division Raytheon Company Richards Avenue South Norwalk, Connecticut Attn: Librarian</p> <p>Southern Regional Research Lab. New Orleans, Louisiana Attn: Librarian</p> <p>Southwest Research Institute 8500 Culebra Road San Antonio 6, Texas Attn: Librarian</p>	<p>Sperry Rand Corporation Electric Products Division 1815 Locust Street St. Louis 3, Missouri Attn: Librarian</p> <p>Sperry Rand Corporation Ford Instrument Company 31-10 Thomson Avenue Long Island City, New York Attn: Librarian</p> <p>Sprague Engineering Corporation 19320 S. Vermont Gardena, California Attn: Librarian</p> <p>Sprague Electric Company 125 Marshall Street North Adams, Massachusetts Attn: Librarian</p> <p>Square D. Company 4045 North Richards Street Milwaukee 12, Wisconsin Attn: Librarian</p> <p>Standford Research Institute Menlo Park, California Attn: Librarian</p> <p>Superior Electric Company 383 Middle Street Bristol, Connecticut Attn: Librarian</p> <p>Superior Tube Company Mearlstown, Pennsylvania Attn: Mr. A. Board</p> <p>Sylvania Electric Products, Inc. Chem. &amp; Metallurgical Toledo, Pennsylvania Attn: Librarian</p>	<p>Sylvania Electric Products, Incorporated General Telephone &amp; Electronics Corporation 12 Second Avenue Warren, Pennsylvania Attn: Librarian</p> <p>Texas Instruments, Incorporated Apparatus Division 6000 Lemmon Avenue Dallas, Texas Attn: Librarian</p> <p>Texas Instruments, Incorporated 6000 Lemmon Avenue Dallas 9, Texas</p> <p>Thompson Ramo Wooldridge, Inc. Caldwell Res Center 23555 Euclid Avenue Cleveland 17, Ohio Attn: Librarian G. J. Guarnieri</p> <p>Thompson Ramo Wooldridge, Incorporated TAPCO Division 23555 Euclid Avenue Cleveland 17, Ohio Attn: Librarian</p> <p>Thompson Ramo Wooldridge, Inc. New Devices Laboratories 7209 Platt Avenue Cleveland 4, Ohio Attn: Librarian</p> <p>Union Carbide Corporation Parma Research Center Technical Information Service P. O. Box 6116 Cleveland, Ohio 44101</p> <p>Union Carbide Metals Niagara Falls, New York Attn: Librarian</p>
--	---	--

<p>Union Carbide Nuclear Company P. O. Box X Oak Ridge, Tennessee Attn: X-10 Laboratory Records Dept.</p> <p>United Nuclear Corporation Five New Street White Plains, New York Attn: Librarian</p> <p>University of Michigan Department of Chemical &amp; Metallurgical Engineering Ann Arbor, Michigan Attn: Librarian</p> <p>Vought Astronautics P. O. Box 5907 Dallas 22, Texas Attn: Librarian</p>	<p>Wah Chang Corporation Albany, Oregon Attn: Librarian</p> <p>Western Electric Company 222 Broadway New York 38, New York Attn: Librarian</p> <p>Western Electric Manufacturing Association 3600 Wilshire Boulevard Los Angeles 5, California Attn: Librarian</p> <p>Westinghouse Electric Corporation Astronuclear Laboratory P. O. Box 10864 Pittsburgh 36, Pennsylvania Attn: Librarian R. T. Begley</p>	<p>Westinghouse Electric Corporation Aerospace Electrical Division Lima, Ohio Attn: Librarian</p> <p>Westinghouse Electric Corporation Central Research Laboratory Pittsburgh 35, Pennsylvania</p> <p>Westinghouse Electric Corporation Research &amp; Development Laboratory Pittsburgh 35, Pennsylvania</p> <p>Wolverine Tube Division Calumet &amp; Hecla, Incorporated 17200 Southfield Road Allen Park, Michigan Attn: Mr. Eugene F. Hill</p>
--	--	--